"Synthesis, conjugation, and biological evaluation of new *N*-functionalized tubugis"

Dissertation

Zur Erlangung des Doktorgrades

der Naturwissenschaften (Dr. rer. nat.)

der

Naturwissenschaftlichen Fakultät II Chemie,

Physik und Mathematik

der Martin-Luther-Universität Halle-Wittenberg

vorgelegt von

Frau M.Sc. Dayma Llanes Martínez

Halle (Saale), 2023

The work described in this dissertation has been developed at the Leibniz Institute of Plant Biochemistry (IPB) in cooperation with Martin-Luther Halle-Wittenberg University.

Supervisor and thesis editor: Prof. Dr. Ludger A. Wessjohann

Co-supervisor: Dr. Robert Rennert

International co-supervisor: Prof. Dr. Daniel García Rivera

1st Reviewer: Prof. Dr. Ludger A. Wessjohann (IPB-Halle)

2nd Reviewer: Prof. Dr. Goran Kaluderovic

Date of Public Defense: 21.11.2023

Declaration

"I declare that I have completed this dissertation without unauthorized help of a second party and only with the assistance acknowledged therein. I have appropriately acknowledged and referenced all text passages that are derived literally from or based on the content of published or unpublished work of other authors."

_____   _____
            Date   Dayma Llanes Martínez

"There is a single light of science, and to brighten it anywhere is to brighten it everywhere."

Isaac Asimov

ABSTRACT

Tubulysins are a family of antimitotic compounds discovered in the present century, which have shown a remarkable impact on the development of modern strategies against cancer. The greatest interest in these natural products relies on their potent cytotoxicity, which is superior to most available antimitotics. Tubulysins are also known for their challenging synthesis and high resistance to structural modifications; aspects with significant consequences to their applications. Today, tremendous effort has been devoted to finding new synthetic methods that enable access to tubulysins in an efficient and reproducible manner. This thesis focuses on the development of solid-phase synthesis and biological study of novel analogs of tubulysins called "tubugis". With a high resemblance to their natural counterparts, tubugis can be constructed in a more straightforward and efficient manner. Tubugis are known to reproduce the notable anticancer activity of tubulysins while showing higher stability, thus being considered a great promise in anticancer-based applications.

The first chapter of the present document describes the state-of-the-art of chemical and biological features of tubulysins and their synthetic analogs. Here, special attention has been directed to the emergence of targeted-drug delivery strategies in anticancer therapies involving tubulysins as payloads. Moreover, the evolution of synthetic methods towards natural tubulysins via multicomponent reactions is presented and analyzed, highlighting how multicomponent reactions have played a determinant role. In the second chapter, a solid-phase approach including an on-resin Ugi 4-component reaction was developed for the construction of tubugis. A series of on-resin protocol innovations were implemented to ensure a high resin loading in combination with simple synthetic setups that enabled the delivery of the tubugi in a notable overall yield, with a single purification step. One of the challenges for tubulysins in targeted-delivery techniques is the assessment of a suitable linker that enables conjugation without losing anticancer activity. In the third chapter, the solid-phase and multicomponent methods developed before were used for the introduction of diverse functionalities at the *N-*

tertiary amide residue. The scope of the synthesis includes the incorporation of bio-relevant molecules such as lipids, PEGylated chains, fluorescent labels, and steroids. The aim was to develop a new site for future conjugation and assess the most suitable linkable residues including carboxylic acids, amino groups, and thiols.
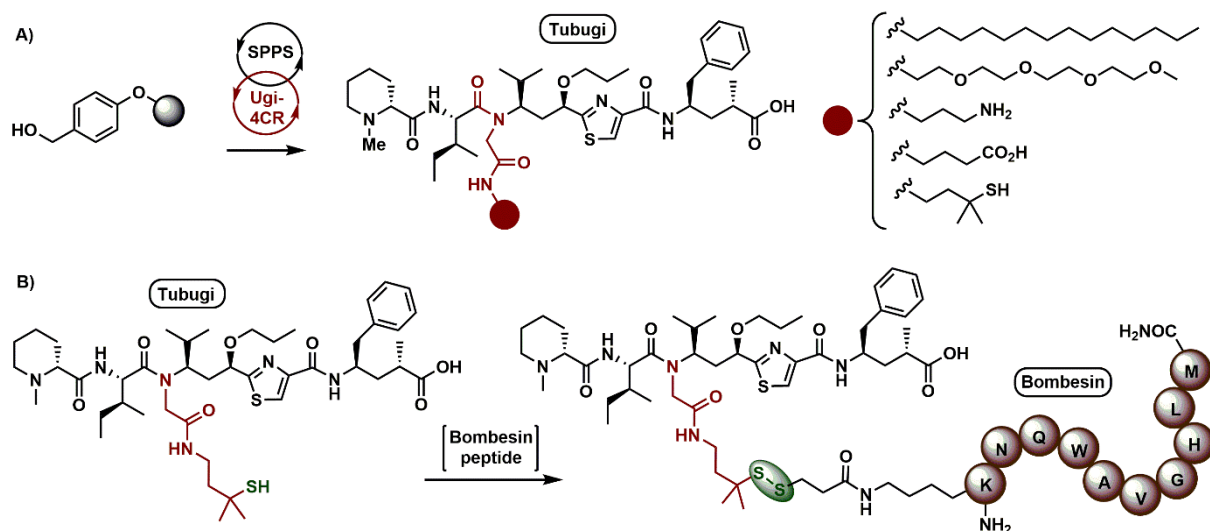
Graphical Abstract. A) Solid-phase synthesis and derivatization of tubugis (Chapters 2 and 3). **B)** Design and synthesis of Bombesin-tubugi conjugates (Chapter 4).

Peptides can offer the versatility needed for a successful oncology drug discovery approach. Peptide–drug conjugates (PDCs) are emerging targeted therapeutics that present increased tumor penetration and selectivity. The fourth chapter describes the design and synthesis of novel PDCs based on the conjugation of the specially-functionalized tubugis to bombesin, a targeting peptide with applications in specific cancer imaging and treatment. Using disulfide-based linkages, chemistry with proven stability, and selective cleavage properties, three different Bombesin-tubugi conjugates were obtained. The cell proliferation profiles of the PDCs, investigated by in vitro experiments, showed notable selectivity and high cytotoxic activity, which converts them into motivating candidates for further anticancer studies.

ZUSAMMENFASSUNG

Tubulysine sind eine Familie von antimitotischen Verbindungen, die in diesem Jahrhundert entdeckt wurden und einen bemerkenswerten Einfluss auf die Entwicklung moderner Strategien gegen Krebs haben. Von Interesse ist hierbei die potente Zytotoxizität dieser Naturstoffe, welche den meisten verfügbaren Antimitotika überlegen ist. Jedoch ist sowohl die Synthese der Tubulysine als auch ihre strukturelle Modifikation herausfordernd, was erhebliche Konsequenzen für ihre Anwendungen hat. So wurden enorme Anstrengungen unternommen, um neue Synthesemethoden zu finden, die einen effizienten und reproduzierbaren Zugang zu Tubulysinen ermöglichen. Diese Dissertation konzentriert sich auf die Entwicklung einer Festphasensynthese neuartiger Tubulysin-Analoga. Auch wird das Design und die biologische Charakterisierung dieser sog. „Tubugis" behandelt. Tubugis weisen eine hohe Ähnlichkeit zu ihren natürlichen Gegenstücken auf, können aber einfacher und effizienter konstruiert werden. Auch sind sie dafür bekannt, die außergewöhnliche Antikrebsaktivität von Tubulysinen zu reproduzieren, während sie eine höhere Stabilität aufweisen. Somit stellen sie vielversprechede Kandidaten für Krebstherapie dar.

Das erste Kapitel dieser Arneit beschreibt den Stand der Technik und die chemisch / biologischen Eigenschaften von Tubulysinen, sowie ihrer synthetischen Analoga. Besonderes Augenmerk wird hierbei auf das Aufkommen von *targeted drug delivery*-Strategien mit Tubulysinen als Nutzlast für Antikrebstherapien gelegt. Darüber hinaus wird die prominente Rolle von Mehrkomponentenreaktionen für die Entwicklung von Synthesemethoden hin zu natürlichen Tubulysinen vorgestellt und analysiert. Im zweiten Kapitel wird die entwickelte Synthese mittels der Ugi-4-Komponenten-Reaktion von Tubugis auf der Festphase behandelt. Hierbei sorgten Reihe von innovativen und simplifizierten Protokollen für eine hohe Beladung der Festphase und eine bemerkenswert hohe Gesamtausbeute nach nur einem einzigen Aufreinigungsschritt.

Eine der Herausforderungen bei zielgerichteten Verabreichungstechniken von Tubulysinen ist die Identifizierung einer geeigneten Position für die Vehikelkonjugation, welche die Antikrebsaktivität konserviert. Im dritten Kapitel werden die Verwendung der zuvor entwickelten Festphasen- und Mehrkomponentenmethoden zur Einführung diverser Funktionalitäten am N-tertiären Amidrest beschrieben. Der Umfang der Synthese umfasst z. B. den Einbau biorelevanter Moleküle wie Lipide, PEGylierte Ketten, fluoreszierende Markierungen und Steroiden. Zur Identifizierung der Position für eine zukünftige Konjugation, wurden auch Funktionalitäten wie Carbonsäuren, Aminogruppen und Thiole eingeführt.
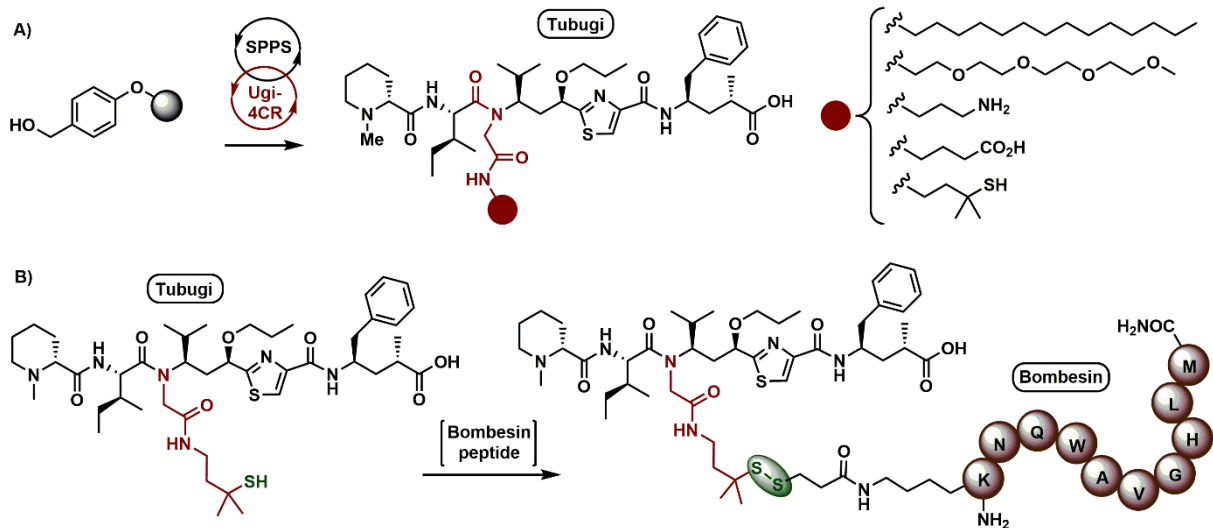
Grafische Zusammenfassung. A) Festphasensynthese und Derivatisierung von Tubugis (Kapitel 2 und 3). **B)** Design und Synthese von Bombesin-Tubugi-Konjugaten (Kapitel 4).

Peptidstrukturen, sowie ihre standartisierte Assemblierung, bieten die Vielseitigkeit, welche für eine erfolgreiche Entwicklung von Wirkstoffen in der Onkologie erforderlich ist. Der Einsatz von Peptid-Wirkstoff-Konjugate (PDCs) stellt einen aufstrebenden Therapieansatz dar, der von erhöhter Tumorpenetration und -selektivität profitiert. Das vierte Kapitel beschreibt das Design und die Synthese neuartiger PDCs basierend auf der Konjugation des neu entwickelten und speziell funktionalisierten Tubugis an Bombesin – ein zielgerichtetes Peptid mit Anwendungen in der spezifischen Krebsbildgebung und -behandlung. Es konnten drei verschiedene Bombesin-Tubugi-Konjugate mittels Disulfidbindungen, einer Chemie mit nachgewiesener

Stabilität und selektiven Spaltungseigenschaften, hergestellt werden. In In-vitro-Experimenten wurden abschließend Zellproliferationsprofile der PDCs untersucht. Hier zeigte sich eine bemerkenswerte Selektivität und eine hohe zytotoxische Aktivität, was sie zu erfolgversprechenden Kandidaten für weitere Antikrebsstudien macht.

Table of contents

LIST OF ABBREVIATIONS

Alloc	allyloxycarbonyl	NMR	nuclear magnetic resonance
Ab	antibody	mAb	monoclonal antibodies
ADCs	antibody-drug conjugates	MCR	multicomponent reaction
Ac	acetate	MTAs	microtubule-targeting agents
AcOH	acetic acid	PDCs	peptide-drug conjugates
Boc	*tert*-butoxycarbonyl	PABC	p-aminobenzyl carbamate
BB	building block	PABQ	p-aminobenzyl quaternary ammonium
BnR	bombesin peptide receptor	^{n}Pr	n-propyl
calcd.	calculated	Ph	phenyl
DMSO	dimethyl sulfoxide	PyAOP	(7-azabenzotriazol-1-yloxy) tripyrrolidinophosphonium hexafluorophosphate
DIPEA	diisopropylethylamine	PyBOP	benzotriazol-1-yl-oxytripyrrolidinophosphonium hexafluorophosphate
DMAP	4-(dimethylamino)-pyridin	PC-3	human prostate cancer cell line
DMF	dimethylformamide	RP-HPLC	reserved-phase high-performance liquid chromatography
DCM	dichloromethane	R*f*	retention factor
equiv	equivalent	RT	room temperature
ESI-MS	electrospray ionization mass spectrometry	SPPS	solid-phase peptide synthesis
EtOAc	ethyl acetate	Su	succinimide
FDA	Food and Drug Administration	*t*Bu	*tert*-butyl
FA	formic acid	TBS	*tert*-butyldimetylsilane
Fmoc	fluorenylmethyloxycarbonyl	TFA	trifluoroacetic acid
GRPR	gastrin-releasing peptide receptor	T-47D	human breast cancer cell line
HPLC	high performance liquid cromatography	THF	tetrahydrofuran
HOBt	1-hydroxibenzotriazole	TIS	triisopropylsilane
HR-MS	high-resolution mass spectrometry	TBAF	tetrabutyl ammonium fluoride
HCT-116	human colon cancer cell line	TLC	thin-layer chromatography
IR	infrared	TMSE	trimetylsililethanol
Me	methyl	Trt	triphenylmethyl
MDA-MB-231	Triple-Negative Breast Cancer (TNBC)	Tup	tubuphenylalanine
Mep	methylpipecolic acid	Tuv	tubuvaline
MPEG	methyl polyethylene glycol	Ugi-4CR	Ugi 4-component reaction

Chapter 1

Tubulysins and their synthetic analogs: Biological significance in anticancer therapies, methods of synthesis and derivatization
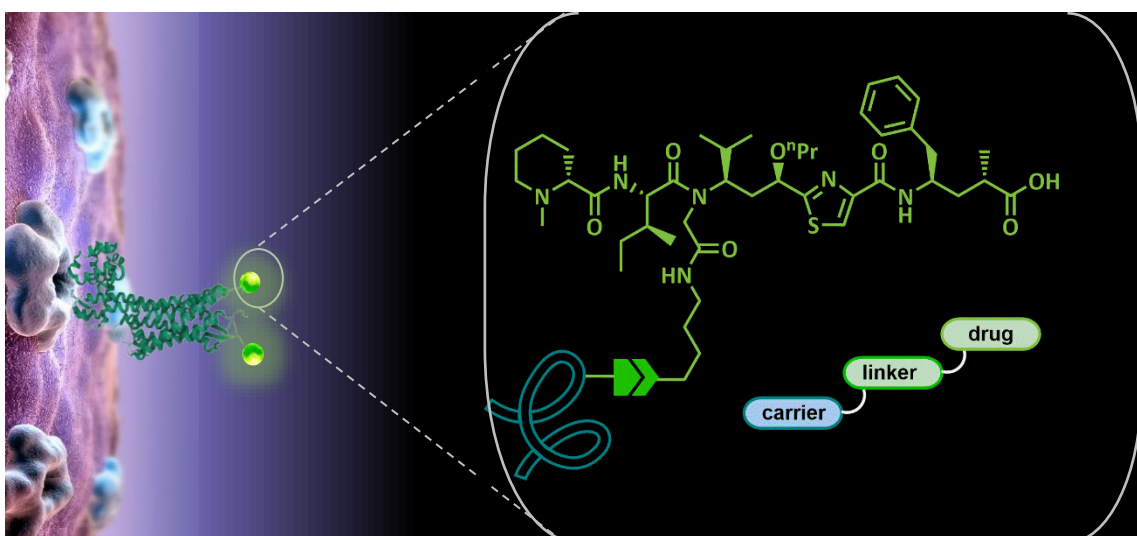
Chapter content

- Introduction to targeted-delivery therapies against cancer
- Peptide-drug conjugates
- Targeting in Peptide-drug conjugates
- Microtubule-targeting agents as cytotoxic drugs
- Linker chemistries. Applications in tubulysin conjugation
- Synthetic strategies to achieve tubulysins
- Solid-phase synthesis of tubulysins
- Multicomponent reactions in tubulysin synthesis
- Final considerations and outlook of the present thesis

1.1. Introduction to targeted-delivery therapies against cancer

According to the World Health Organization, cancer-related deaths are estimated to increase by over 13 million yearly until 2030.[1] Consequently, research devoted to the development of new and more effective anticancer therapies is imperative. The alternatives we have today to fight cancer include surgical intervention, chemotherapy, immuno therapy, radiation therapy, or a combination of these options. Although these methods are constantly being improved, they are not exempt from the undesirable side effects that are often responsible for the high mortality rate. Conventional anti-cancer drugs suffer from being non-selective and causing damage to healthy cells.[2] Typically, treatments are based on the administration of high doses of drugs because of poor bio-accessibility to tumor tissues, a condition that may lead to increased toxicity and multidrug resistance.[2]

Successful cancer treatments can be defined as selective killing of cancer cells while healthy cells are not affected. This selectivity is very challenging due to the high similarity between healthy and diseased cells. Tumor cells overexpress cell surface receptors, which are considered tumor biomarkers, and for this reason, they are of high interest in cancer targeting.[3] Antibodies, because of the ability to specifically bind receptors, in this case, such highly expressed in tumor cells, possibly constitute a pioneering alternative in targeted therapy.[4] With the developments and improvements in monoclonal antibodies (mAbs) in the '80s, several candidates reached clinical approval to be used as anticancer drugs; although with notably low efficacy.[5] Soon after, it was envisioned that the insufficient potency of naked mAbs can be circumvented by arming them with potent cytotoxics.[4] Antibody-drug conjugates (ADCs) can be considered as a merger of two earlier approaches against cancer and are today of great promise. The combination of these two models is expected two overcome the individual shortcomings.

In ADCs, mAbs would play the role of vehicles that will specifically target cancer cells and deliver the highly potent payloads responsible for cell death. So far, nine ADCs have received approval from the US Food and Drug Administration and the European Medicines Agency (e.g. Brentuximab vedotin,[6] ADC fully approved in 2015, Figure 1.1 A), and another 80 ADCs are in clinical development.[7] These facts make ADCs front runners in the anticancer drug pipeline. Unfortunately, along with the great versatility that ADCs show, they also have serious limitations. Most monoclonal antibodies are known for their low propensity to penetrate tumors because of their high molecular weight (approximately 150 kDa), making them too big to diffuse efficiently into malignant tissue.[8] Moreover, monoclonal antibodies can be immunogenic, even when they have been humanized, and tend to aggregate in excretory organs such as the liver and, [9] last but not least; the generation of monoclonal antibodies is expensive, time-consuming, and non-selective payload conjugation can reduce product homogeneity.[9]
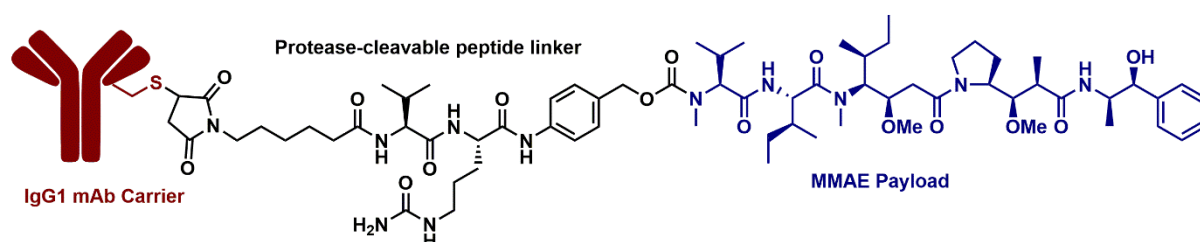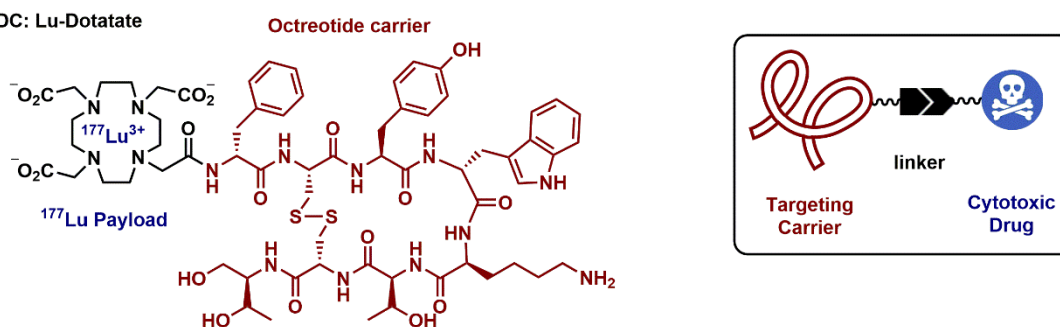
Figure 1.1. **A)** Structure of Brentuximab vedotin, one of the first FDA-approved ADCs. **B)** Structure of ^{177}Lu-DOTATATE, the first FDA-approved by PDC in 2018. MMAE: Monomethyl auristatin E.

1.2. Peptide-drug conjugates

The limitations of ADCs can be overcome by using peptide-drug conjugates (PDCs), which are a class of targeted therapeutics with similar construction to ADCs only differing on the targeting device. At present, there are only two PDCs on the market but many more are in various phases of clinical trials.[8] ^{177}Lu-DOTATATE is the name of the first PDC used in a therapeutic setting, approved by the FDA in January 2018 (Figure 1.1 B).[10]

The low appearance of PDCs on the market has been markedly influenced by the limitations of peptides in pharmacological properties.[11] Great efforts have been directed to combat these deficiencies and currently several methods can be used to advance these properties of peptides. Strategic formulation and chemical modifications (e.g., methylation, cyclization, and introduction of non-proteinogenic amino acids) have played a crucial role and today are successfully used for enhancing cell permeability, enzymatic stability, and reducing renal clearance.[11] Even though PDCs are much less present in clinical trials as compared to ADCs, they provide exquisite versatility that can aid the design of privileged targeted therapeutics. The relatively small size of a peptide (up to 40 amino acids, 500-5000 Da) leads to enhanced penetration into solid tissues resulting in better anti-tumor effects.[12] Additionally, the well-established, less time-consuming methods for peptide synthesis are a tremendous advantage in PDCs regarding regulatory demands for registration and further drug manufacture. These benefits together with the low immunogenicity make PDCs very promising anticancer therapeutics.

1.2.1. Targeting in peptide-drug conjugates

A targeting peptide is chosen, analogous to mAbs, for its specific binding capabilities to receptors overexpressed at the tumor cell membrane. Many natural peptides and their synthetic analogs have been explored in the development of PDC agents (Table 1.1). Among the most recurrent peptide receptors, are the family of Somatostatin receptors. Somatostatin (also known

as growth hormone-inhibiting hormone, GHIH) is a peptide that regulates multiple endocrine functions, exhibiting many effects in growth suppression and cell differentiation.[8] Their analogs Octreotide, Lanreotide, and Pasireotide have been clinically applied in the treatment of several cancers including pancreatic and vasoactive cancers.[13] Various analogs of Somatostatin have been applied for targeting and intracellular delivery of cytotoxics, specially radiotherapeutic agents, where the mentioned FDA-approved ^{177}Lu-DOTATATE constitutes a very inspiring achievement.[10]

Table 1.1. Overview of some peptide-binding receptors, tumor expression, and corresponding targeting peptides.

Binding receptor	Tumor expression	Targeting peptide
Integrins (a5b1, a8b1 and aIIbb3)	Glioblastoma cells and ovarian cancer cells	**RGD** (arginine, glycine, aspartic acid)
GnRH-R	Ovarian, breast, prostate, lung cancer	**GnRH** (gonadotropin-releasing hormone)
SSTR1-5 (somatostatin receptor)	Small cell lung, neuroendocrine tumor, prostate cancer, breast cancer, colorectal carcinoma, gastric cancer, hepatocellular carcinoma	**SST** (somatostatin)
EGFR: HER1, HER2, HER3, HER4	Lung, breast, bladder, and ovarian cancers	**EGF** (epidermal growth factor)
Bn receptors (GRPR)	Lung, prostate, breast, pancreatic, head/neck, colon, uterine, ovarian, renal cell, glioblastomas, neuroblastomas, gastrointestinal carcinoids, intestinal carcinoids, and bronchial carcinoids	Bombesin peptide
NPY-R (hY1R)	Breast cancer, Ewing sarcoma	Neuropeptide Y

Another widely used peptide carrier is the tripeptide Arginine-Glycine-Aspartic acid (RGD), identified to bind integrins, membrane-bound receptors that mediate cell adhesion, migration, and proliferation.[14] Since these processes are highly relevant in carcinogenesis and their overexpression in various tumor cell is documented, integrins are considered important anti-cancer targets.[15] Numerous variants of cyclic RGD peptides, such as c(RGDfK), have shown high affinity to integrin receptors, finding considerable attention in the development of PDCs with notable tumor-tissue permeability.[15][16]

The human Y1 receptor (hY1R) is one of four members of the neuropeptide Y (NPY) receptor family. Interestingly, while NPY acts as a neurotransmitter regulating homeostasis and anxiety, hY1R was found to be present in certain tumor tissues, including ovarian, adrenal cortical, Ewing sarcoma, and testicular, among others.[9] The fast and recyclable mechanism of internalization involving Y-receptors is generally known to be especially suitable to deliver certain payloads in intracellular compartments.[17] Consequently, many studies have revealed the use of NPY analogs with potent and highly specific affinity to hY1R, in the development of PDCs. Very recently the conjugation of super potent synthetic analogs of tubulysins to a NPY derivative was reported with notable anticancer potency.[18]

The bombesin peptide receptor (BnRs) family, in correspondence with their natural ligands, forms a diverse system with important repercussions in cancer research.[19] Although they can be classified in three different subgroups, the high binding affinity of all of them to the bombesin peptide encompasses them into one single family. Bombesin is a natural peptide (Sequence: Pyr-QRLGNQWAVGHLM-NH$_2$) first isolated from the skin of the Bombina bombina frog in 1972.[20] Amon all BnRs, the gastrin-releasing peptide receptors (GRPR), are of the greatest interest because of their overexpression in a vast number of cancer cells including those of the highest recurrence (Table 1.1).[19] Accordingly, bombesin peptide has been recognized as relevant in the development of PDCs for tumor diagnostics, radionuclide therapy, and drug delivery, with promising results in clinical studies.[9]

1.3. Linker chemistry in the design of drugs-conjugates

In targeted delivery-based anticancer therapies, the high specificity of the carrier in combination with the high cytotoxicity of the drug are decisive. Additionally, another key structural feature constitutes the linker moiety that allows the connection of both entities.[21] The chemistry involved in the linkage has been recognized to be crucial in modulating pharmacokinetics and therapeutic indexes of novel ADCs and PDCs.[22] The challenge in

developing a successful linker has been to create a stable but conditionally cleavable connection between the carrier and the drug. Over the last decade, linkers have experienced significant optimization, mostly aiming at reducing the premature release of the payload, and tuning specific properties such as reactivity and solubility.[23] Here, the best choices have been directed to linkers with releasing mechanisms mediated by enzymes, change in pH, or reductive environment (Figure 1.2).
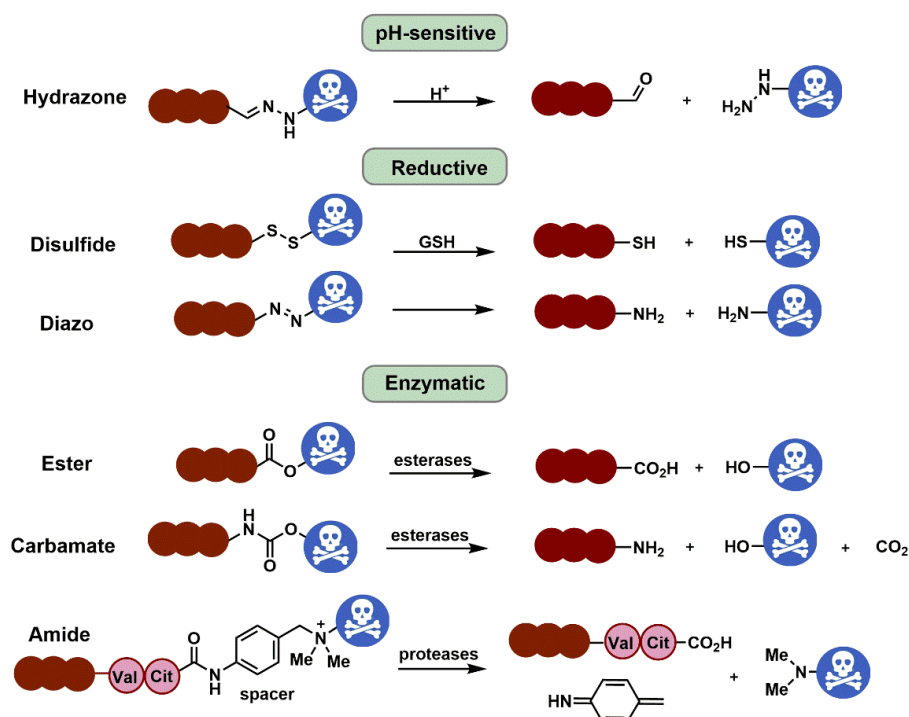
Figure 1.2. Different linkers chemistries depending on the release mechanism (pH-sensitive, reductive, or enzymatic).

The significant difference in the pH value of the tumor cell versus healthy tissue constitutes a traditional alternative for the selective delivery of cytotoxins. The most common acid-sensitive linker is the hydrazone bond, which is chemically stable in a neutral environment but easily hydrolyzable under weak acidic conditions.[24] Although this technology has been successfully applied in FDA-approved ADCs, recently the field has significantly moved to other alternatives.[25] Disulfide bond-based linkages also appear as a highly recurrent approach in conjugation chemistry.[26][27] The excellent reversible properties of disulfides stand out among

the several advantages in comparison with other linkers, as they can be easily and chemo-selectively interconnected.[28][29] Most importantly, the resulting disulfide bond (if is sterically hindered, e.g. due to the presence of geminal methyl groups), can offer sufficient stability during circulation in the bloodstream, while allowing efficient and selective cleavage inside the target cell due to the higher concentration of glutathione.[28][30] However, thiol groups are rarely present in cytotoxic agents, and therefore they must be introduced by synthetic manipulations that often have a negative influence on the potency.[29]

It is possible that the linker chemistries that have gained more popularity in conjugation are those with releasing mechanisms that are regulated by enzymes.[25] Several amino acid combinations, such as Ala-Ala-Asn, Val-Cit, Val-Al, etc have been identified to be stable in serum but are hydrolyzed intracellularly by proteases. The highly controlled release here is guaranteed considering that a special class of enzymes, particularly cathepsins, are overexpressed in tumor cells. Moreover, peptide-based linkers combined with p-aminobenzyl spacers, allow the traceless delivery of the drug, a technologically advanced mechanism with proven superiority among many different linker chemistries.[31]

1.4. Microtubule-targeting agents as cytotoxic drugs

In general, the cytotoxic component, also named payload, warhead, chemotherapeutic, or anticancer agent constitutes the heart of a drug-conjugate. The targeting carrier contributes to the tumor specificity, the linker enables the union and the selective delivery but it is the cytotoxic agent who fulfills the fundamental purpose to kill the tumor cell. This cytotoxic action needs to be executed intracellularly at very low concentrations due to the low distribution achieved after intravenous administrations and targeting. Therefore, to be chosen as suitable payloads, the drug must display super potent cytotoxicity, possessing half inhibitory concentrations (IC_{50}) in the very low nanomolar to picomolar range. A very limited number of cytotoxic drugs can reach this requirement and they can be classified as DNA-damaging or

microtubule inhibitors, with the last ones being the payloads with the highest presence in clinically approved ADCs.
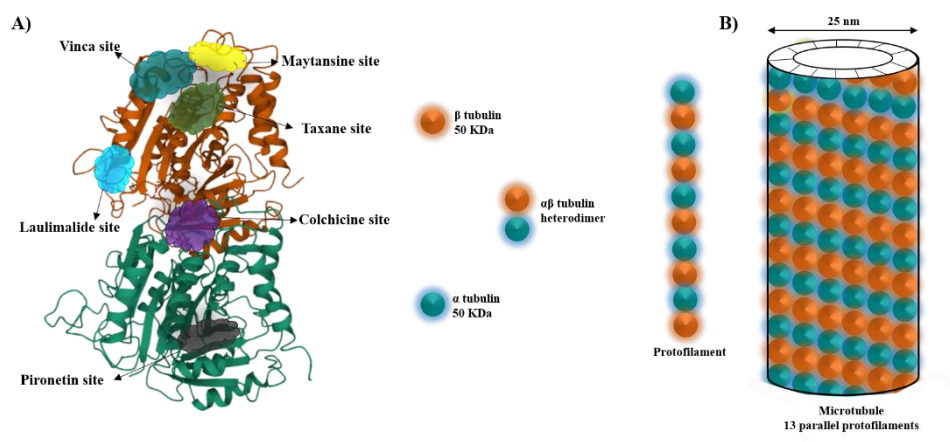

Figure 1.3. **A)** Six binding sites of microtubule-targets on tubulin (α-tubulin green and β-tubulin brown). **B)** Structure of a microtubule consisting of a stiff hollow tube formed from 13 protofilaments aligned in parallel.

Microtubules are the biggest element of the cytoskeleton in eukaryotic cells. They are long, filamentous, cylindrical polymeric assembled from 13 parallel circular oriented protofilaments (Figure 1.3). Each protofilament is formed by heterodimers that align in a head-to-tail manner and then fold into a tube. Microtubules are present in several basic cellular functions like cell signaling, transport of vesicles, cell motility and cytoplasmic streaming, maintenance of cell morphology, but especially in cell division and mitosis. Their participation in cell division makes microtubules one of the most important spots for cancer treatment but also an essential target for the discovery and development of new anticancer drugs.

A great number of microtubule-targeting agents (MTAs) have been isolated from a wide variety of organisms during the last three decades showing prominent cytotoxic activity. These MTAs bind the tubulin heterodimer and disrupt the dynamics and structure of the microtubule, consequently inducing cell death. So far only six MTA-binding sites have been described on tubulin, five of them located on β-tubulin, called: Vinca, Colchicine, Maytansine, Taxane, and Laulimalide, and only one binding site in α-tubulin, known as Pironetin site (Figure 1.3).

Notably, the most active MTAs are those inhibiting the Vinca domain, a crucial site located in the interface formed between two tubulin heterodimers. The best known members of this group are the dolastatins and related tubulysin families, extremely cytotoxic natural products (Figure 1.4).
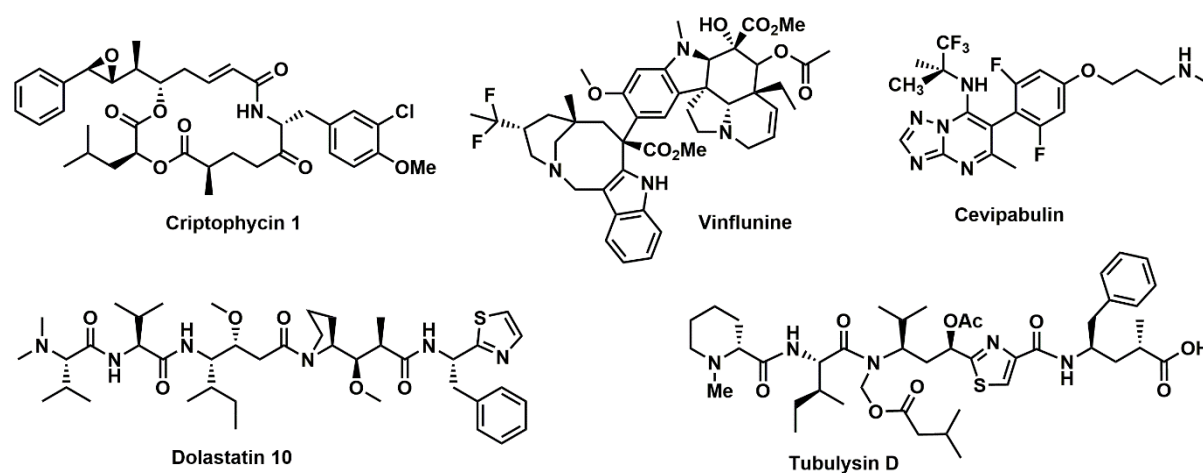

Figure 1.4. Chemical structure of some vinca-site binding natural products.

Dolastatins consist of natural pentapeptides, isolated from the sea hare *Dolabella auricularia* in 1993.[32] Synthetic analogs of Dolastatins called Auristatins, designed for clinical developments are pioneers (Figure 1.1 A) and the most recurrent payloads in ADCs.[33][21] On the other hand, tubulysins were isolated by Höfle's group in 2000 from strains of the myxobacteria *Archangium gephyra* and *Angiococcus disciformis*.[34] Tubulysins are antimitotic drugs that disrupt the microtubule spindle and induce apoptosis showing growth inhibition (GI_{50}) values ranging from nanomolar to picomolar concentrations.[34] Amazingly, this family is, for a variety of cancers, 20 to 1000-fold more potent than the anticancer drugs Epothilones, Vinblastine, and Taxol as cell growth inhibitors.[35] Together with the high cytotoxicity due to inhibiting cell proliferation, tubulysins also show strong angiogenesis effects and exhibit antivascular properties in vitro and in vivo.[36] The combination of antiproliferative and antiangiogenic properties makes this family a remarkable leader as payloads for targeted deliveries therapies.[36]

1.5. Strategies for tubulysins conjugation

Despite the impressive antiproliferative efficacy of tubulysins, their application in the latest conjugation strategies is limited in most part due to their difficult synthesis and lack of suitable residues for functionalization.[37][9] For this family, the options are very limited; despite its resemblance with other inhibitors of tubulin polymerization, like Auristatins, they show higher resistance to structural modifications.[38,39] Nevertheless, some important alternatives have shown success for the functionalization and conjugation of this cytotoxic family, beyond the challenges of its inflexible modification.
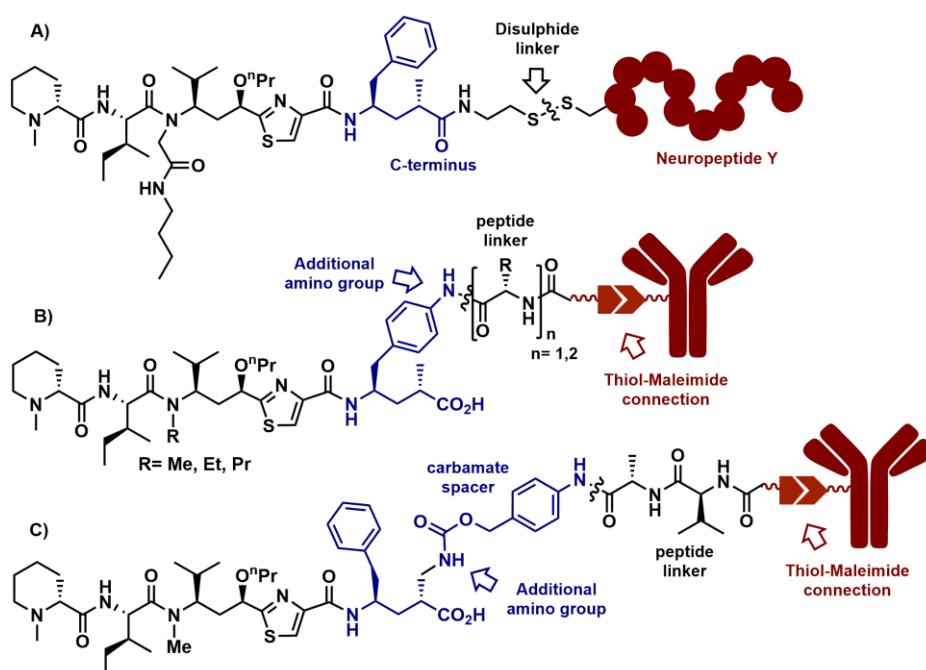
Figure 1.5. Tubulysins functionalization and conjugation through its Tup residue.

The Tubuphenylalanine (Tup) residue (Figure 1.5 A, B, and C in blue), has been the most frequent target in tubulysin conjugations, allowing the implementation of a variety of different functionalization and chemistries. The earliest examples have been based on the linkage of the carboxylic acid of the Tup residue (*C*-terminus) in conjugations to vitamins, polymers, and peptides, most of the cases through an amide or more recently *via* a hydrazone moiety.[18,40–42] Worth highlighting, the only example in the conjugation of a Ugi-derived tubulysins has been

also achieved by combining the *C*-terminus in a disulfide-base linkage for the construction of a PDC (Figure 1.5 A).[18] Important achievements are also reached through the insertion of an amino group at the *para* position of the phenyl group of the Tup residue (Figure 1.5 B). This strategy provides the suitable functionality needed for conjugation and fortunately, the released drug maintains the desired nanomolar activity.[43] Different dipeptides or single amino acid-based linkers such as Lys,[44] Gly,[45] Val-Ala[46], and Val-Cit,[47] attached *via* amide bond to the corresponding amino group proved to be capable of selectively releasing the tubulysin payload. On the other hand, it has been proposed recently that introducing an amino group at the methyl group of Tup, also does not have a detrimental impact on the cytotoxicity.[46] Consequently, Nicolaou and co-workers also designed promising ADCs where these amino-containing tubulysins were attached via a Val-Ala peptide linkage (Figure 1.5 C).[46]
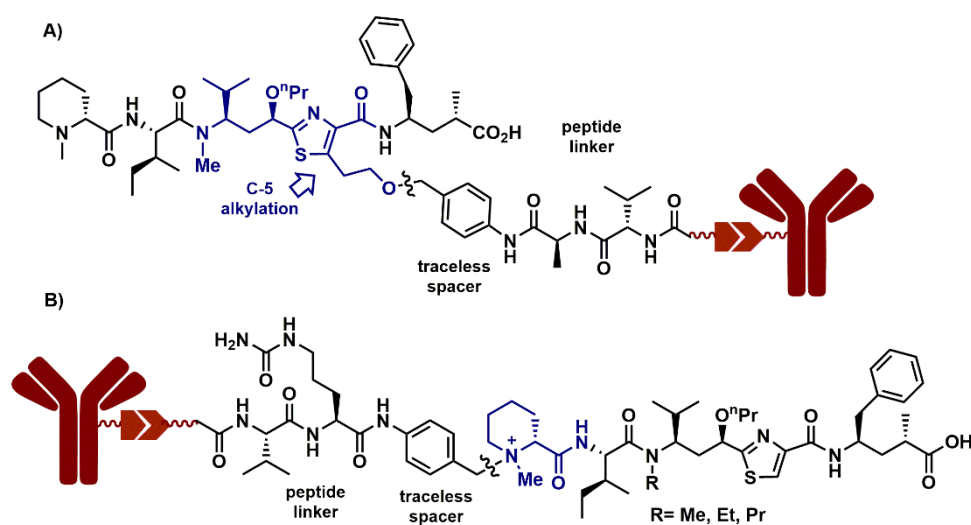
Figure 1.6. Tubulysins functionalization and conjugation though: **A)** Tuv residue and **B)** Mep residue.

Modifications seeking linkable functionalization at the tubuvaline (Tuv) residue (Figure 1.6 A in blue) have been rarely considered, as it constitutes the most synthetic challenging building unit. Interestingly, it was shown also by Nicolaous's group, that by introducing specific modifications at the C-5 position of the thiazole ring, the biological activity is increased (Figure

1.6 A).[46] Later, they also proved that using p-aminobenzyl spacer at this site in combination with peptide linkers a non-precedent tubulysin conjugate can be obtained.[46]

Linking tertiary amines, a common functional group present in many natural products including anticancer agents, has been historically considered a "forbidden challenge".[48] However, the development of self-immolative quaternary ammonium (PABQ) linker for tertiary amines, constitutes a revolutionary achievement and today it is one of the most applied linkers due to the improved pharmacokinetic and therapeutic efficacy of the conjugates.[49][50] In tubulysins, placing a PABQ linker at the Mep residue has offered an outbreak of applications, and thanks to its traceless manner, no additional modification or functionalization of the natural structure is therefore required (Figure 1.6 B).

1.6. Synthetic strategies to achieve tubulysins

Tubulysins are endowed with a tetrapeptide skeleton including, from the *N*- to *C*-terminus, the residues: *N*-methyl-D-pipecolic acid (Mep), L-isoleucine (Ile), and the very uncommon tubuvaline (Tuv) and either tubuphenylalanine (Tup) or tubutyrosine (Tut).
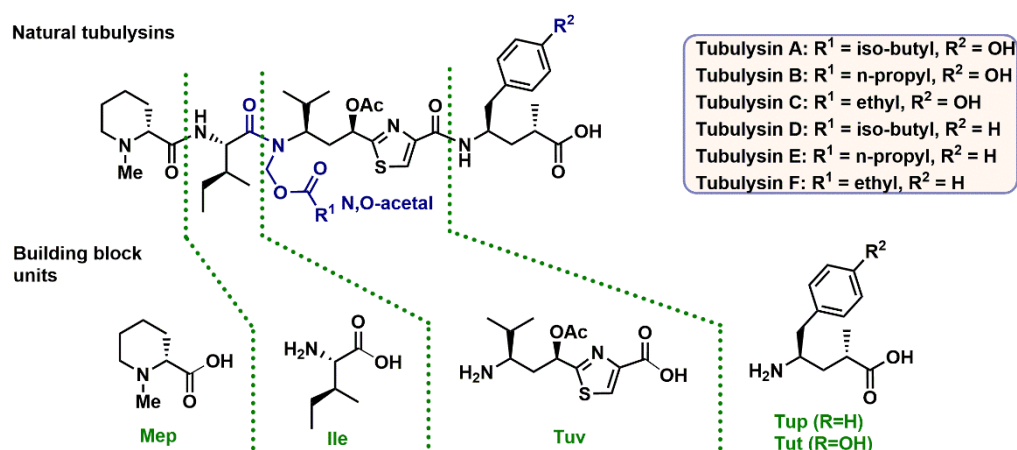

Figure 1.7. Structure of natural tubulysins and building blocks contained.

Unfortunately, despite the peptide nature, tubulysins are known for their troublesome synthesis. Since the beginning of this century and until today, there have been tremendous efforts in the synthesis of members of the family since isolation from natural sources is limited to low

yield.[35,51–56] In tubulysins only two amino acid fragments can be considered synthetically simple, Ile occurs naturally and Mep can be obtained in one step from D-Pipecolic acid, and is commercially available. The *C*-terminal, Tup or Tut, and the central residue, Tuv, are considered very uncommon and synthetically challenging. The presence of and *N,O*-acetal at the Tuv residue makes the synthesis even more complex since this fragment is not compatible with most protecting-group strategies.[35][36] The earliest attempts in the synthesis of tubulysins were dedicated to the development of enantioselective processes for the synthesis of these complex residues and therefore today, they can be obtained through very straightforward methods even at gram scale.[36][57][58][51] The final assembly by peptide bond formation is also tricky considering the sterical hindrance of the four residues. Since 2006, with the first synthesis of Tubulysin D, U, and V, most synthetic strategies involve solution-phase protocols characterized by low yield and difficult reproducibility.[35][54] Apart from the protecting group strategy and the incorporation or not of the *N,O*-acetal moiety, clear differences have been related to the strategic order in which the building blocks are incorporated.

The first total synthesis of Tubulysin D (the most active member of the series) by Ellman and co-workers, starts with the key assembly of the central part Ile-Tuv together with the incorporation of the *N,O*-acetal (Scheme 1.1 A).[35] Later, the Mep residue is introduced and finally, the *C*-terminus is constructed with the coupling of Tup. Following similar strategies, plenty of analogs of tubulysins have been synthesized but replacing the complex *N,O*-acetal residue by simple alkyl chains. In a more convergent synthesis, Wessjohann/Dömling and co-workers, reported in the same year the first total synthesis of Tubulysins U and V, both natural Tubulysins lacking the complex *N,O*-acetal.[54] As described in scheme 1.1 B, here the peptide backbone was assembled in a convergent manner based on the final assembly of the dipeptides Mep-Ile and Tuv-Tup synthesized in advance.
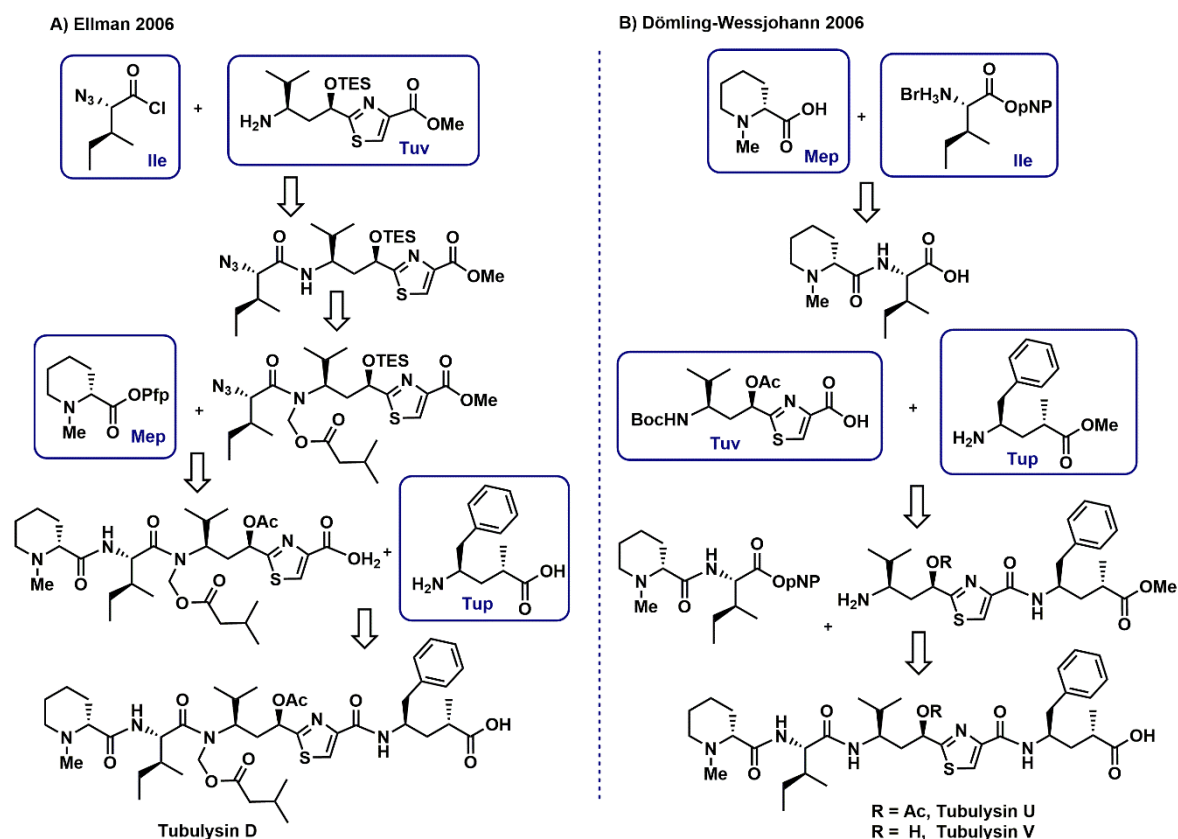
Scheme 1.1. Different strategies for building block assembly. **A)** First total synthesis of Tubulysin D. **B)** First total synthesis of Tubulysins U and V.

1.6.1. Solid-phase syntheses of tubulysins

Undoubtedly, solid-phase methods are prevalent for the construction of peptidic compounds, and for many years, traditional total synthesis of natural peptides has been translated from solution-phase to solid-phase.[59] The higher conversion, reproducibility, speed, and operational simplicity make these protocols highly advantageous.[60] Although the synthesis of tubulysins has been conducted vastly in solution, recent reports by Toader's group, make use of solid-phase synthesis, thus opening a new avenue of opportunities for the synthesis and derivatization of these potent compounds.[61][44] As shown in scheme 1.2, the strategy proposed is based on the assembly of Fmoc-*N*-protected building units (except Mep which is introduced *N*-methylated) using standard solid-phase protocols in Trityl resin.
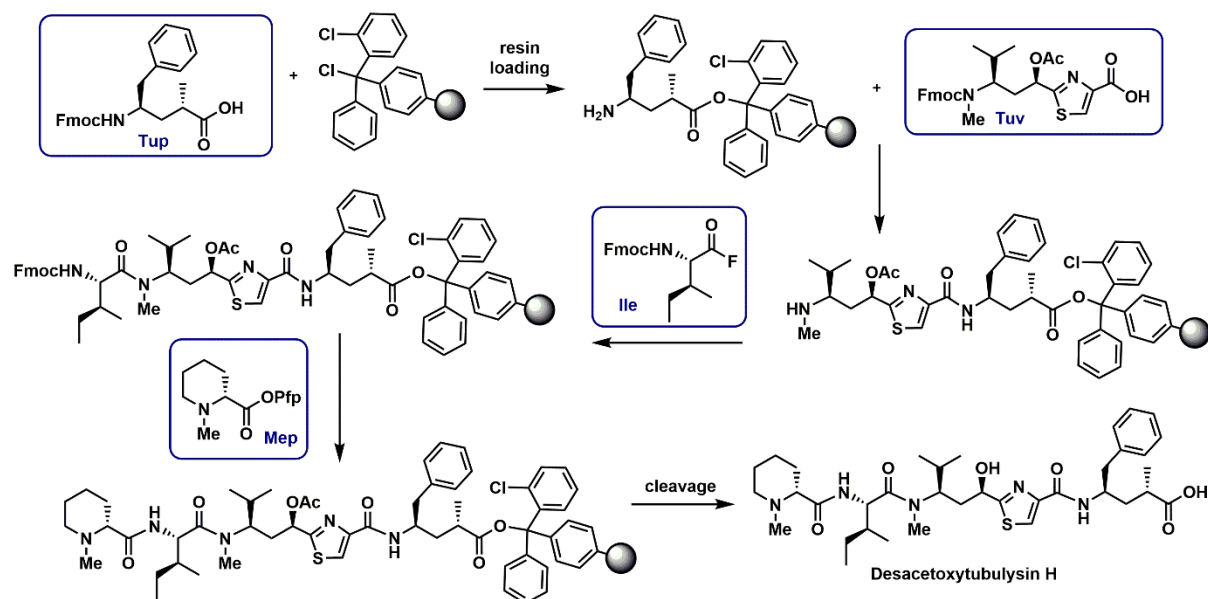
Scheme 1.2. Solid-phase synthesis of Desacetoxytubulysin H.

Different from the solution-phase methods where the construction of the central part is first and the Tup unit is incorporated at the end of the synthesis, in solid-phase methods the *C*-terminus is first incorporated. As pointed out, the successful coupling of the first amino acid to the resin is considered a key step in an on-resin methodology, as it will determine the synthetic scale and the final amount of peptide to obtain. Considering that the first two building units are very precious, they were incorporated using special protocols as to not waste material, a common drawback in solid-phase methods. Due to the availability of the next two residues, Ile and Mep, they are coupled using several-fold excess and repetitive cycles to ensure total conversion. This is a clear advantage of solid-phase protocols, as the *N*-alkylated amide, is the most demanding peptide bond on the whole synthesis and therefore one of the bottlenecks of traditional protocols in solution. It is worth mentioning that beyond the rapid access offered by these protocols, the possibility to have this highly cytotoxic compound attached to a solid support during the synthesis reduce considerably the risk of contact, making the synthesis much safer.

1.7. Multicomponent reactions in tubulysin synthesis

Multicomponent reactions (MCRs) are defined as synthetic processes where three or more compounds react to give a product that incorporates most of the atoms of the starting materials.[62] MCRs offer a range of opportunities over the more traditional multistep synthesis as they are often easier to carry out and allow the generation of high molecular complexity. These futures make MCRs very interesting processes in all areas of synthetic chemistry with remarkable applications in drug discovery and development. Among all MCRs, those involving isocyanides have dominated the interest of the chemical community.[62] Here, Passerini three-component reaction and Ugi four-component reaction, constitute the most commonly used, with enormous participation in the construction of peptidic and heterocyclic scaffolds.[63][64][65] Interestingly, both multicomponent methods, since the very beginning have been closely related with the synthesis of tubulysins offering interesting contributions for the assembly of either the building units or the final peptide scaffold.
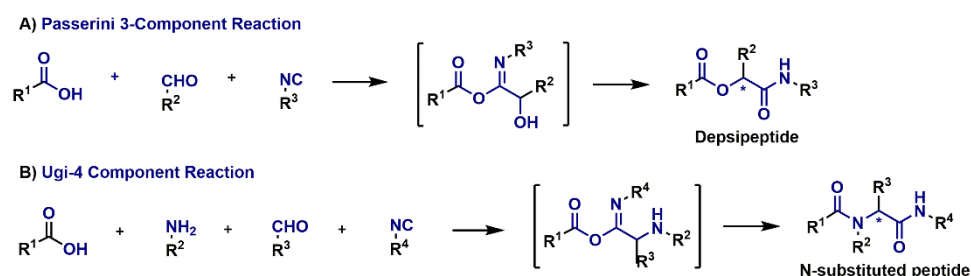
Scheme 1.3. **A)** Passerini three-component reaction and **B)** Ugi four-component reaction.

1.7.1. Passerini reaction in tubulysin synthesis

The condensation between an isocyanide, carboxylic acid, and aldehyde in the formation of α-acyloxycarboxamides is known as Passerini three-component reaction (P-3CR). The ability to fuse advanced intermediates in the formation of complex structures with this reaction was a key step in the first total synthesis of Tubulysin U and Tubulysin V.[54] Here, the authors took advantage of a newly discovered variant and obtained impressively and straightforwardly the

Tubuvaline building block, considered the most complex fragment in tubulysins. This three-component reaction permits the assembly in one pot of hydroxymethyl thiazoles. Therefore, when combining Boc-homovaline aldehyde, Schöllkopf isonitrile (available in one single step from isocyanoacetic ester and DMF), and thioacetic acid, the complex structure is formed in a 3:1 mixture of diastereomers that favor the natural one (Scheme 1.4).
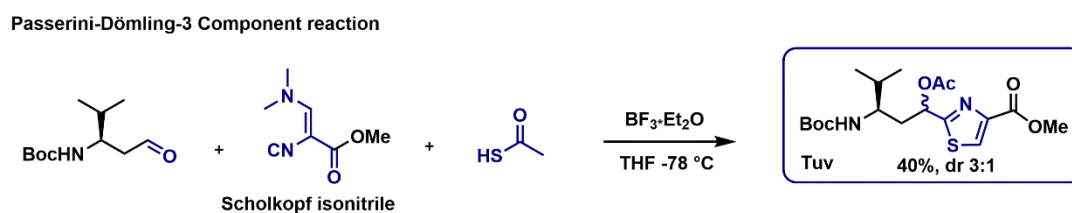
Scheme 1.4. Multicomponent synthesis of Tuv by Passerini-Dömling reaction.

Very recently, Dömling has extended the role of Passerini reaction in the synthesis of tubulysins to higher levels of straightforwardness (Scheme 1.5).[66] Using a catalyzed-version of the Passerini reaction, they were able to construct, an advanced intermediate that after two simple transformations generate the Tuv along with the Mep-Ile attached, and all in one pot.
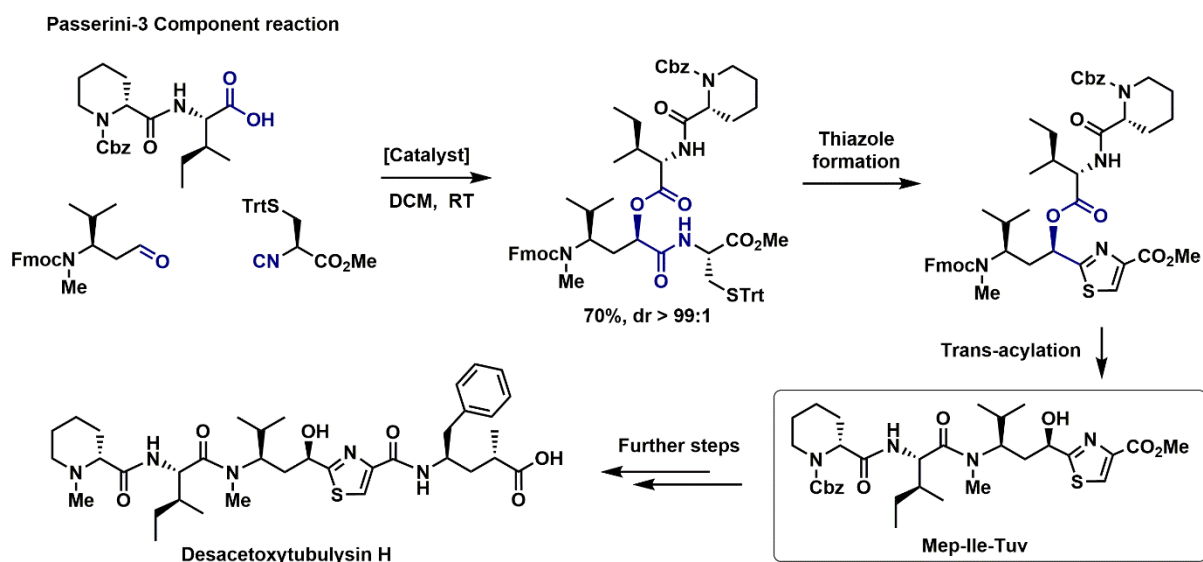

Scheme 1.5. Multicomponent-assisted synthesis of Mep-Ile-Tuv.

The prominence of the multicomponent process relies not only on the facile combination of the simple and accessible starting materials but also on the diastereoselective manner in which it

is executed. Undoubtedly, this approach constitutes a very elegant approach and demonstrates the high levels of diversity and complexity that MCRs offer.

1.7.2. Ugi reaction in tubulysin synthesis

The condensation of an amine, a carbonyl compound, a carboxylic acid, and an isocyanide to address the formation of an α-amino acylamide is known as the Ugi-4 component reaction. Although Ugi-4CR can be seen as a variation of the Passerini reaction, in which the carbonyl component is substituted by an *in situ* formed imine (or rather iminium), it rapidly became very popular MCR because of its numerous applications. Beyond its value in combinatorial and heterocyclic chemistry, the Ugi-4CR in recent times gained increased recognition in the synthesis and derivatization of peptides in solid-phase protocols. [59]
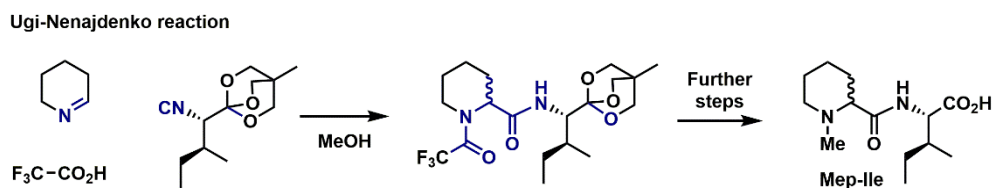
Scheme 1.6. Multicomponent synthesis of Mep-Ile by Ugi-Nenajdenko reaction.

The participation of Ugi-4CR also stands out in the development of synthetic methods for the synthesis of tubulysins. In 2011, Wessjohann and co-workers showed that the cautious combination of different components in an MCR can generate very diverse and ingenious tubulysin-related substrates.[67] As shown in scheme 1.6, using trifluoroacetic acid, a cyclic imine, and an isoleucine-derived Nenjadenko isocyanide, it was possible to generate the uncommon pipecolic acid already coupled to the isoleucine residue. This method exhibited notable distinction, although this fragment can be alternatively synthesized utilizing the more conventional peptide coupling chemistry.
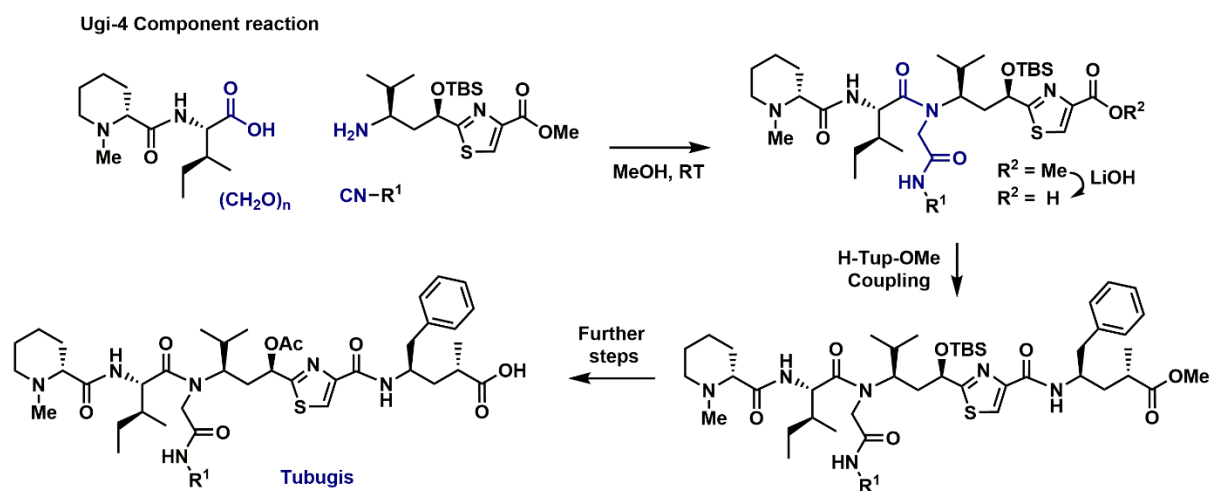
Scheme 1.7. Multicomponent synthesis of tubugis, Ugi-derived analogs of tubulysins.

The use of the Ugi-4CR in the construction of the tertiary amide of the tubulysins is unequivocally a tremendous achievement.[67] As shown in scheme 1.7, the combination of Mep-Ile with Tuv by executing the multicomponent process generates the desired coupling along with a retro amide that replaces the problematic *N,O*-acetal. These Ugi-derived tubulysins so-called "tubugis" are remarkably stable under physiological conditions (which cannot be said of natural tubulysins) and maintain the picomolar cytotoxic activity. Nowadays, tubugis have evidenced increased attention, and in similarity to other tubulysins, they are playing an important role in the development of new strategies in anticancer therapies.

1.8. Final considerations and outlook of the present thesis

Undoubtedly, the targeted delivery of potent cytotoxic molecules is striking within modern strategies in the war against cancer. Despite being one of the last drugs to enter into the field, tubulysins and their synthetic analogs are among those of greatest promise because of their remarkable cytotoxicity. Unfortunately, because of their high complexity, the development of tubulysin has often relied on multistep solution-phase protocols that feature moderate to low yields. Therefore, most synthetic analogs consist of simplified structures, especially at the complex tertiary amide residue. A forthright alternative has consisted in the construction of this tertiary amide by the execution of a Ugi reaction. These so-called "tubugis" have shown

impressive results in anticancer studies, which makes them very interesting candidates to be applied in targeted delivery strategies.

Since solid-phase synthesis has become not only a platform for feasible derivatization but also large-scale synthesis of bio-relevant molecules, the first general objective of the present thesis constitutes:

Chapter 2: Development of an on-resin strategy for the synthesis of tubugis based on a series of resin-loading innovations and the execution of an organo-catalyzed Ugi reaction.

As described in epigraph 1.3, tubulysins are also known for their resistance to structural changes that permit suitable derivatization and conjugation. Since multicomponent reactions are recognized as superior synthetic protocols featuring great levels of structural diversity, here we took advantage of the Ugi 4-component, and the second general objective is presented as:

Chapter 3: Introduction of a series of modifications at the *N*-tertiary amide residue featuring at structure-activity relationships and potential sites further conjugation.

Together with antibodies, in pharmaceutical discovery research, peptide-drug conjugates (PDCs) are experiencing a high progression. Among all the targeting peptides studied so far, bombesin peptide constitutes one of the candidates with excellent cancer receptor specificity, with similar applications in tumor imaging, although very discrete in conjugation techniques. Therefore, here it was also chosen as component of the third general objective:

Chapter 4: Design and synthesis of novel PDC based on the combination of bombesin analog with an *N*-functionalized tubugis.

Chapter 2

Development of a solid-phase methodology for the synthesis of Ugi-derived analogs of tubulysins
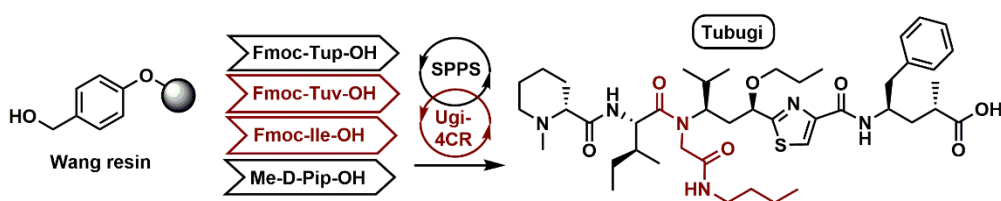
Abstract

The increased interest of the pharmaceutical industry in ADCs and PDCs payloads has required the development of synthetic protocols that produce them at a large scale and in a highly reproducible manner. Although tubulysins are considering complex molecules, synthetic analogs such as tubugis are privileged as they are constructed involving high-standard multicomponent reactions. Here, a solid-phase approach including on-resin Ugi 4-component reactions was developed for the synthesis of tubugis. A series of on-resin innovations were implemented to ensure a high resin loading in combination with simple synthetic setups that enabled the delivery of the tubugis in high overall yield with only one purification step.

2.1. Introduction

Among the potent antimitotic agents known so far, tubulysins are lead compounds for the development of tumor-targeted therapeutics (Figure 2.1 A).[68][36] However, the availability of such compounds is still limited due to the low-to-moderate yields of the solution-phase procedures and the several purification steps required. A family of synthetic analogs of tubulysins that reproduce the high cytotoxicity have the tertiary amide generated by a Ugi-4 component reaction (Figure 2.1 B).[67] These so-called "tubugis" have been synthesized following similar strategies as to the natural tubulysins in solution phase synthesis but including an Ugi-4CR to couple the Mep-Ile-OH fragment as carboxylic acid component and H-Tuv-OEt as amine component.[67] However, the Ugi reaction-based fragment coupling can be inefficient and difficult to scale up.
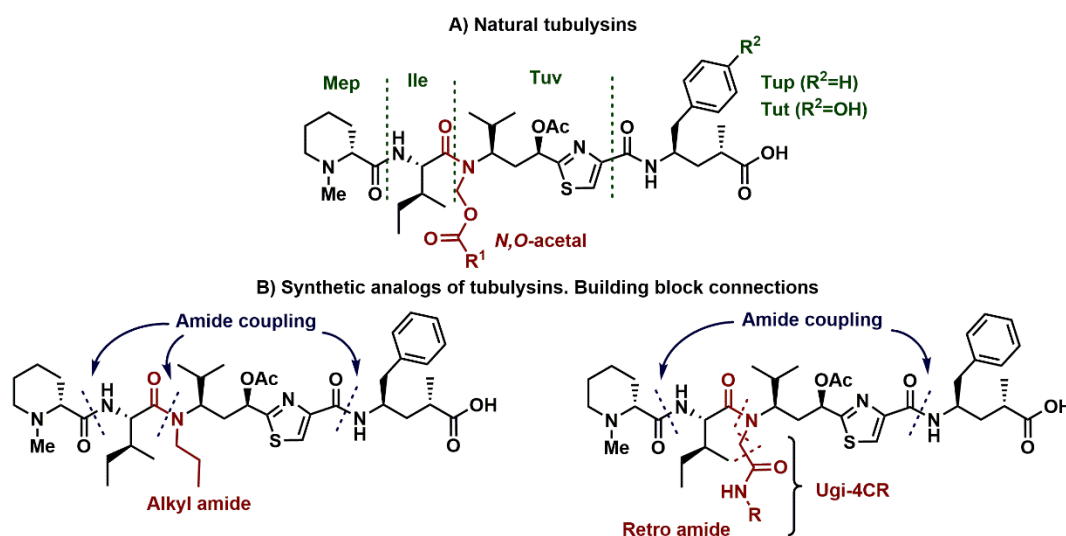

Figure 2.1. A) Natural tubulysins and the building blocks that construct them. **B)** Synthetic tubulysins replacing the *N,O*-acetal residue by simpler alkyl chains or the "retro amide" moiety of the Ugi-4CR.

Herein we describe a novel on-resin methodology that significantly improves the access to tubugis. To achieve this goal, we designed a series of innovations leading to a new protocol that sequentially assembles complete tubugi on-resin and requires only one final purification step. We first aimed to synthesize the most active tubugi obtained so far, although replacing

the OAc protecting group present in building block Tubuvaline (Tuv) with an n-propyl ether. The decision was based on the now proven fact the acetyl protecting group in Tuv has detrimental consequences on the activity in tubulysins due to enzyme-mediated deacetylation.[45]

2.2. Synthesis of building blocks

The on-resin synthesis of tubugis requires the combination of its amino acid residues following the standard strategy used in solid-phase peptide synthesis, which relies on the temporary protection of the amino group as Fmoc carbamate. As shown in figure 2.1, listing from the *C*- to the *N*-terminus, the more complex building blocks, tubuphenylalanine (Tup) and tubuvaline (Tuv) are found first. Both are commonly produced by many steps in solution-phase, nevertheless, several straightforward reports permit their synthesis in gram scale.[36] The third building block is L-isoleucine (Ile), which is assembled in tubugis by the execution of an Ugi-4CR. L-isoleucine can be acquired Fmoc protected as it is a standard building unit in peptide chemistry. Likewise, in Ugi-4CR, two additional components are needed, paraformaldehyde and n-butyl isocyanide, both readily available commercially. Finally, the last amino acid residue, *N*-methyl-D-pipecolic acid (Mep) can be obtained in one step by methylation of the D-pipecolic acid and used without any further modification.

2.2.1. Synthesis of Fmoc-Tup-OH

In the literature, more than a dozen strategies have been reported to accomplish the synthesis of tubuphenylalanine and its relatives. In our group, this unit has been commonly obtained based on a Wittig reaction and hydrogenation of a menthol ester as key steps.[69] Initially, the key intermediate **5** was envisioned to be obtained by executing first a Wittig reaction by combining Boc-Phenylalaninal **4** with the ylide **6,** and later the introduction of (-)-menthol (Scheme 2.1 B, blue). However, coupling (-)-menthol to the advanced intermediate **8** never

resulted in a conversion higher than 40%. Therefore, a more convergent strategy was envisioned resting on the execution of the Wittig reaction between Boc-phenylalaninal **4** and ylide **3** having the menthol already incorporated (Scheme 2.1 B, black).[58]
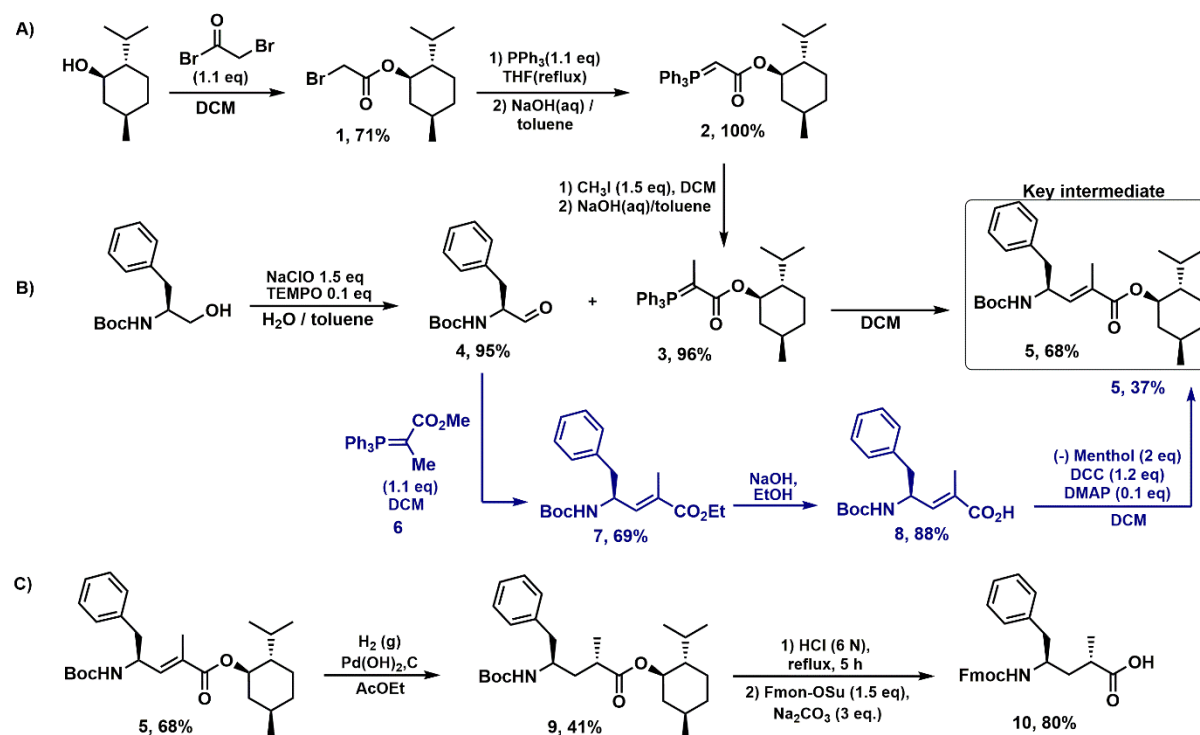

Scheme 2.1. A) Synthesis of menthol-containing ylide 3. **B)** Synthesis of the key intermediate by Wittig reaction using menthol-containing ylide 3 or Wittig reaction and later menthol-coupling (in blue). **C)** Global protecting group removal and Fmoc group introduction. In parenthesis the number of the compound is followed by the yield obtained.

As depicted in scheme 2.1, the intended synthesis started with the acylation reaction between bromoacetyl bromide and (-)-menthol affording compound **1** in 71% yield. Following, the reaction with triphenylphosphine and later treatment with base yield the corresponding ylide **2**. This ylide is subjected to a tandem procedure consisting of methylation and further treatment with NaOH (aq) to generate the ylide **3** substrate of the Wittig reaction (Scheme 2.1 B, black). Boc-Phenylalaninal, a second substrate of the Wittig reaction, is obtained by TEMPO/NaClO oxidation in 95% yield starting from Boc-Phenylalaninol as previously reported. Thus, the combination of these two building blocks afforded the key intermediate **5** in 68% yield.

Remarkably, the simplicity and efficiency in the synthesis of the precursors and the convergent manner of this new strategy gave this valuable intermediate in multigram scale. Subsequently, compound **5** is hydrogenated and subjected to purification by a chromatographic column of the diastereomeric mixture to afford the desired compound **9** in a satisfactory 41% yield. The simultaneous removal of the menthol ester and Boc protecting group is performed by one-pot acid hydrolysis refluxing **9** in HCl (6N). Final Fmoc protection following standard conditions afforded the desired compound Fmoc-Tup-OH (**10**) in 80% yield.

2.2.2. Synthesis of Fmoc-Tuv(O^{n}Pr)-OH

The synthesis of Fmoc-Tuv(O^{n}Pr)-OH was facilitated by the acquisition of the very advanced intermediate **11** from a commercial source, that was subjected only to remove the protecting groups and introduce the desired Fmoc carbamate (Scheme 2.2).
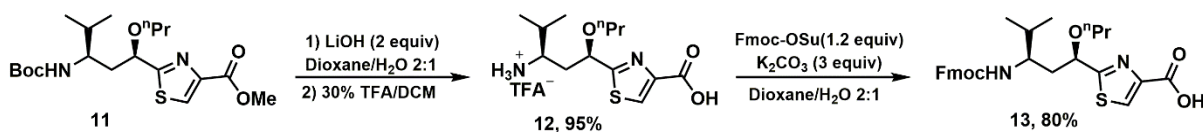

Scheme 2.2. Synthesis of Fmoc-Tuv(O^{n}Pr)-OH starting from Boc-Tuv(O^{n}Pr)-OEt.

Treating **11** with LiOH in dioxane/water 2:1 (*v/v*) quantitatively afforded the carboxylic acid after acid workup. The removal of Boc protecting group to obtain compound **12** was accomplished using 30% TFA in DCM, and the product obtained after removing the volatiles and without any further purification was directly subjected to the Fmoc protection to afford the desired building block **13** in 80% global yield.

2.2.3. Synthesis of *N*-methyl-D-pipecolic acid

The synthesis of *N*-Me-D-Pip-OH is performed in a quantitative one-step procedure (Scheme 2.3). As shown, the reductive amination of D-Pip-OH with 37% formalin solution and hydrogen, catalyzed by 10% palladium over carbon in dry methanol afford **14** as a grey solid.
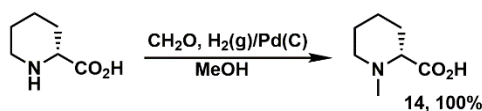
Scheme 2.3. Synthesis of *N*-Me-D-Pip-OH by methylation of H-D-Pip-OH.

2.3. On-resin assembly of building blocks
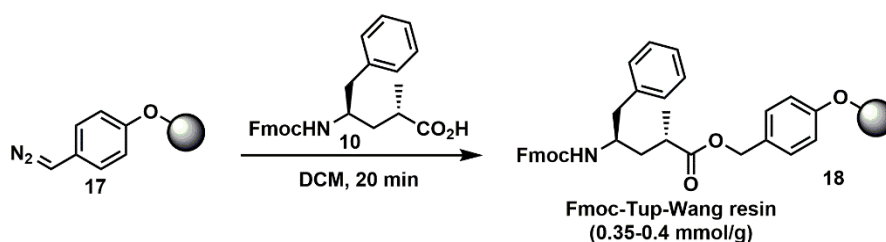
2.3.1. Resin loading of Fmoc-Tup-OH

The first crucial step in the on-resin methodology deals with the way of attaching Fmoc-Tup-OH to the solid support, considering that this is one of the most valuable building blocks. For a future scalable purpose, in general, it is required to functionalize the resin with a relatively high loading without using several-fold excess of the costly Fmoc-Tup-OH. Consequently, typical ways of functionalizing Trityl and Wang resins were not appropriate in this case. We envisioned that the direct coupling of a carboxylic acid to a diazo compound could be nearly quantitative, without using an excess of the building block. For this, a diazo-Wang resin was obtained in only three steps combining procedures reported in the literature (Scheme 2.4 A).[70] Initially, Wang resin was transformed into oxo-Wang resin **15** using Dess-Martin periodinane in DCM for 2 h. After thoroughly washing the resin, it is dried under high vacuum overnight. The IR signal at 1696 cm^{-1} (Scheme 2.4 B) supports the formation of oxo-Wang resin **15**. As reported in the literature, hydrazine **16** is formed by adding 2 equiv of 2,4,6-triisopropylbenzenesulfonyl hydrazide in dioxane and shaking the reaction mixture for 12 h.[70] The formation of the diazo moiety was accomplished by introducing some variation to the reported method. Due to the swelling deficiencies and possible instability of the diazo compound in water, the solution of KOH in THF/water 2:1 was not considered. Instead, 1,1,3,3-Tetramethylguanidin in DMF, inspired by the work of Pedro et al. in the synthesis of diazo compounds, proved to be sufficiently efficient to afford the desired diazo-Wang resin **17** as deep red beads after 5 min reaction at 90 ºC.[71] The analysis by IR verified the formation of

the desired diazo group by the appearance of its characteristic signal at 2055 cm^{-1} (Scheme 2.4B, right).
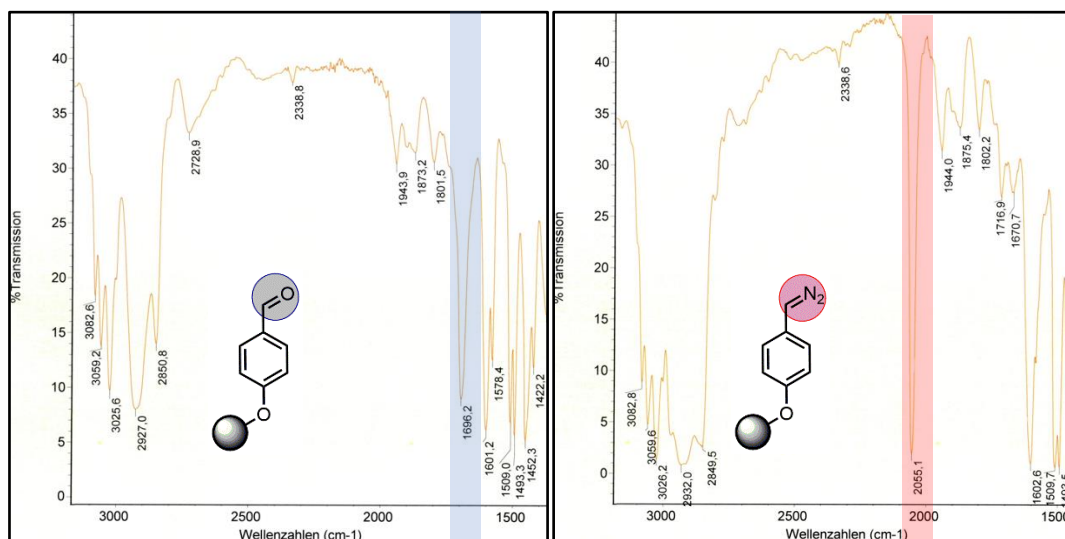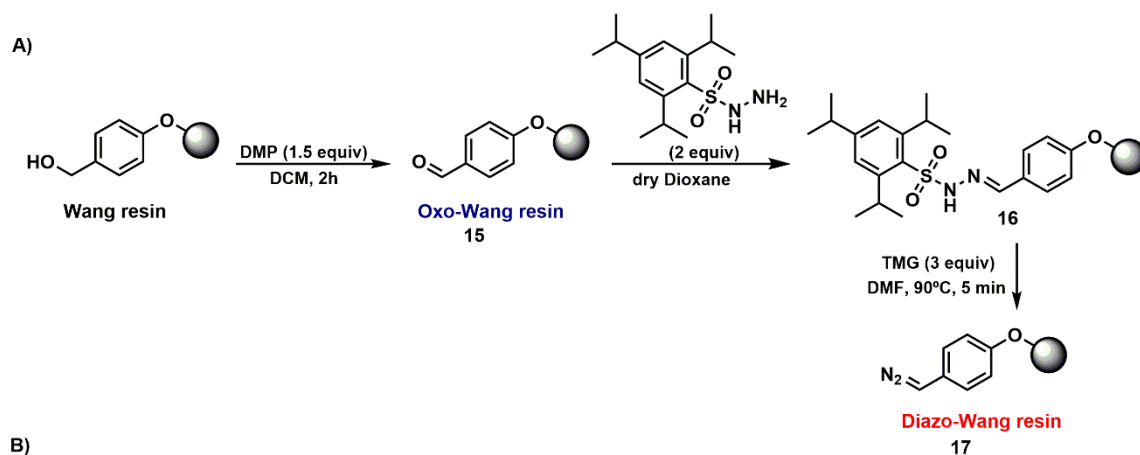
Scheme 2.4. A) Synthesis of Diazo-Wang resin starting from Alcohol-Wang resin in three steps. **B)** Infrared spectra of Oxo-Wang resin, 1696 cm^{-1} (left spectrum) and Diazo-wang resin, 2055 cm^{-1} (right spectrum). TMG: 1,1,3,3-Tetramethylguanidine.

To assess the global efficiency of the method, the final loading is determined. Thus, a fraction of the resin **17** (50 mg) is treated with a solution of Fmoc-Phe-OH (9.8 mg, 0.025 mmol, assuming an expected resin loading = 0.5 mmol/g), observing within less than 20 min, the disappearance of the red color and N$_2$ (g) generation. By the absorbance of the dibenzofulvene at 301 nm, after the removal using 20% piperidine in DMF, a final loading from 0.35 to 0.4 mmol/g was obtained, which is in correspondence with the value in commercial resins.

Scheme 2.5. Loading of Fmoc-Tup-OH on the Diazo-Wang resin.

With a procedure at hand that quantitatively attaches amino acids to the resin, we had a result very appropriate for the coupling of the valuable Fmoc-Tup-OH. With it is ensured that only the amount of the building block consumed that finally gets attached to the resin. Therefore, the reaction of the diazo-Wang (1 g) resin with Fmoc-Tup-OH, using only 1.2 equiv (according to an expected loading of 0.35-0.40 mmol/g) yielded the desired Fmoc-Tup-Wang resin (1.05 g, 0.35 mmol/g). Only a slight excess of the Tup building unit was not bound to the resin and it was possible to recover it by simply washing the resin with dichloromethane.

2.3.2. On resin Tuv-Tup coupling

The removal of Fmoc protecting groups is standardly accomplished by the treatment with 20% piperidine in DMF. Even when this reaction is finished within a few minutes, to ensure total transformation, commonly two washes of 10 min are used. However, because of the risk of intramolecular lactamization, once the amino group is free, here the Fmoc was deprotected by two treatments of 5 min.
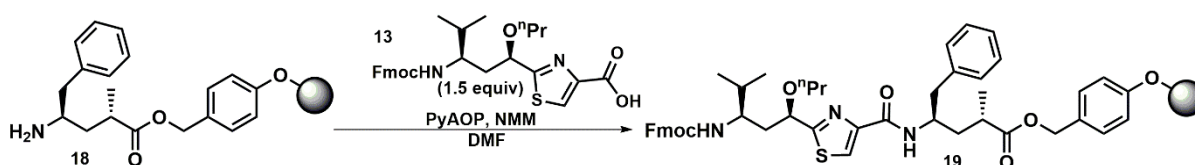
**Scheme 2.6.** Coupling of Fmoc-Tuv(O^{n}Pr)-OH to H-Tup-Wang resin.

The coupling of the second and also complex building unit (Fmoc-Tuv(O^{n}Pr)-OH) was planned to be accomplished using an amount that ensures the total coupling but doesn't require 3 to 5-fold excesses as usually needed in standard procedures. In our experience, with only 1.5 equiv

of Fmoc-Tuv(O^{n}Pr)-OH, using PyAOP/NMM as an activating mixture in DMF and increasing the reaction time up to 6 h, it was possible to quantitatively achieve the Tuv-Tup coupling (Scheme 2.6). This was verified by the Kaiser test in combination with ESI-MS after mini cleavage.

2.3.3. Aminocatalysis-mediated Ugi-4CR for the simultaneous Ile coupling and tertiary amide formation

The sterically hindered and complex tertiary amide in tubulysins considerably restricts the tetrapeptide assemblage. The introduction of the Ugi-4CR in the synthetic design of tubugis generates the formation of the *N*-substitution and the amide coupling in one single step and, even with structural changes, this reproduced the potent anticancer activity of tubulysins. Nonetheless, the solution-phase procedure, characterized by low global yield and difficult handling, has served to create only a few examples of the promising tubugis. Here we thought, that the execution of the multi-component process via on-resin organocatalysis-mediated reaction would improve straightforwardness and higher conversion, as proven for some other challenging synthesis in our group.[72][73]

The synthetic protocol started with an initial trans-imination step using paraformaldehyde and catalyzed by pyrrolidine in a mixture of tetrahydrofuran/methanol 2:1 (*v/v*) for 30 min to obtain the imine **20** (Scheme 2.7). After washing the resin-bound imino-peptide, the subsequent Ugi-4CR reaction is performed with 4 equivalents of the n-butyl isocyanide and 4 equivalents of Fmoc-Ile-OH in the same solvent mixture tetrahydrofuran/methanol 2:1 (*v/v*).
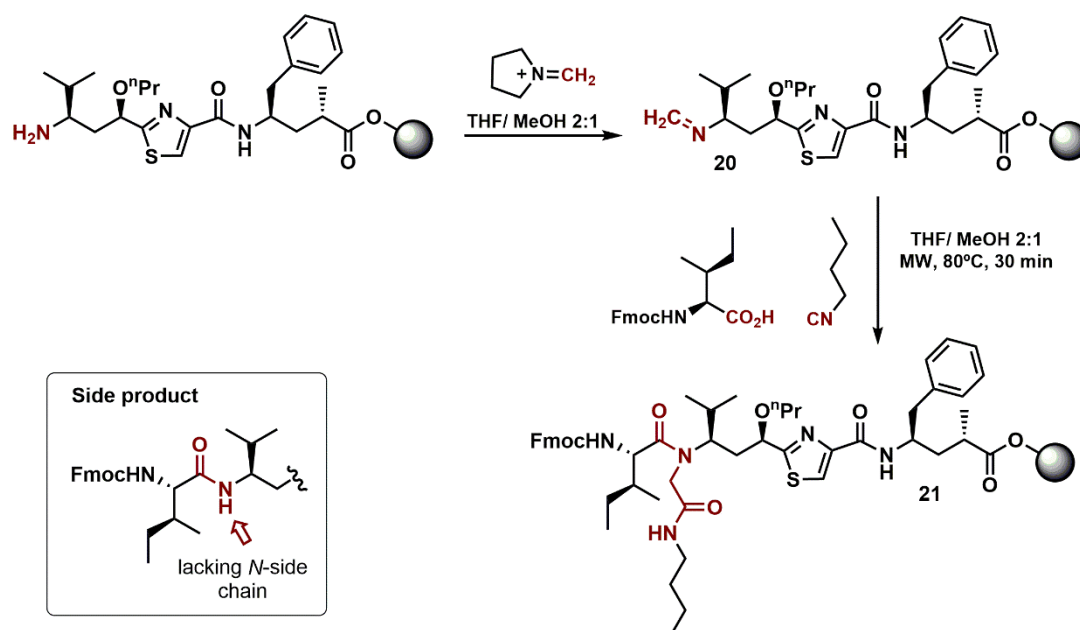
Scheme 2.7. On-resin Ugi procedure in two steps. 1) organocatalytic transamination using paraformaldehyde and pyrrolidine. 2) Microwave-assisted Ugi reaction.

The ready and cheap access to both building blocks involved in the next steps allows for the use of large excesses, one of the key aspects of high conversion in solid-phase protocols. After screening several experimental conditions, it was concluded that the optimal transformation was obtained at 80ºC in microwave for 45 min. Analysis by high-performance liquid chromatography (RP-HPLC) and ESI-MS, after mini-cleavages, showed complete consumption of the peptide precursor in most of the attempts. In cases of remaining starting material, the second cycle of imine formation and Ugi reaction unequivocally lead to full conversion. It is worth mentioning that besides the desired product, the formation of a side-product in about 5-10% was commonly observed. This consisted of the direct coupling of Ile without having the *N*-substitution (Scheme 2.7), as mentioned in previous reports. Nevertheless, it can be remarked that the higher conversion and benefits of the solid-phase performance of the Ugi-4CR constitute one of the key elements contributing to the robustness of the new methodology proposed.

2.3.4. *N*-Me-D-Pip-OH coupling and final cleavage

The assembly of the last building block is performed following standard coupling conditions (Scheme 2.8), using several fold-excess due to feasible access from a commercial source. Consequently, 4 equiv *N*-Me-D-Pip-OH are mixed with 4 equiv of PyBOP and 8 equiv of NMM, in DMF for 4 min, and later added to the resin for 4 h, achieving the desired coupling quantitatively.
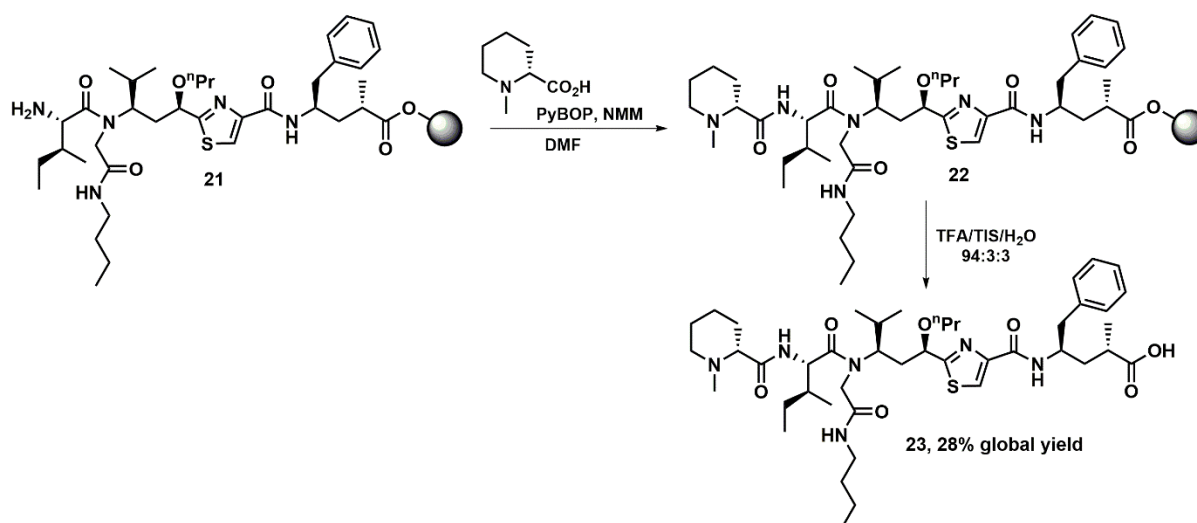
Scheme 2.8. Coupling of the *N*-Me-D-Pip-OH and final cleavage.

Final cleavage using the standard cocktail TFA/TIS/H_2O (94:3:3, *v/v/v*) afforded the crude peptide mixture. Instead of precipitation with diethyl ether and lyophilization, the solvent was evaporated in a high vacuum and immediately proceeded to RP-HPLC analysis and purification, avoiding any unnecessary handling of the highly toxic compound. Analysis of the crude by analytic RP-HPLC (Figure 2.2 A) showed the formation of the desired Tubugi **23** (Scheme 2.8) indicated by HR-MS (Figure 2.2 B) as a major component. Some minor impurities were also detected due to deletion sequences and mostly the product of direct coupling of the Ile residue over Tuv, the usual side product of on-resin-Ugi reactions. Purification by preparative RP-HPLC using a gradient Acetonitrile/H_2O (with 0.1% Formic

acid) and final lyophilization afforded 8.1 mg of the pure Tubugi **23,** corresponding to 28% global yield.
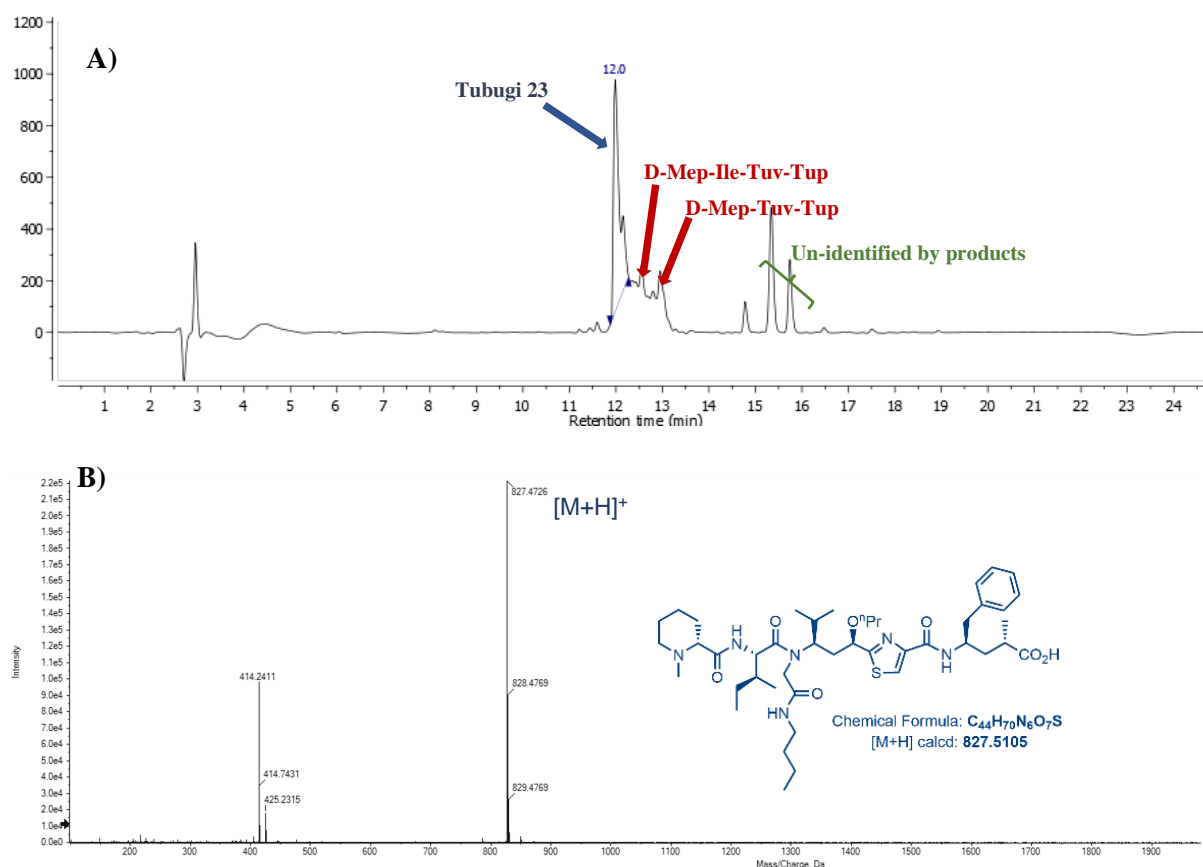

Figure 2.2. A) RP-HPLC trace of crude Tubugi **23** after cleavage from resin. B) HR-MS of Tubugi **23.**

The ^{1}H-NMR, as depicted in figure 2.3, shows the presence of many broad sets of signals (mainly in the central part where alpha protons appear) due to the occurrence of a mixture of conformers, a phenomenon commonly observed in peptoids. However, in the zone of higher frequencies, it is possible to assess the characteristic signal of the C-H (8.13 ppm) in the thiazole ring along with two signals corresponding to NH (8.00 ppm and 7.81 ppm) from peptide bonds. The third NH signal, also expected in this zone, must be included among the aromatic protons of Tup observed in 7.21 ppm, as they integrate six protons instead of five.
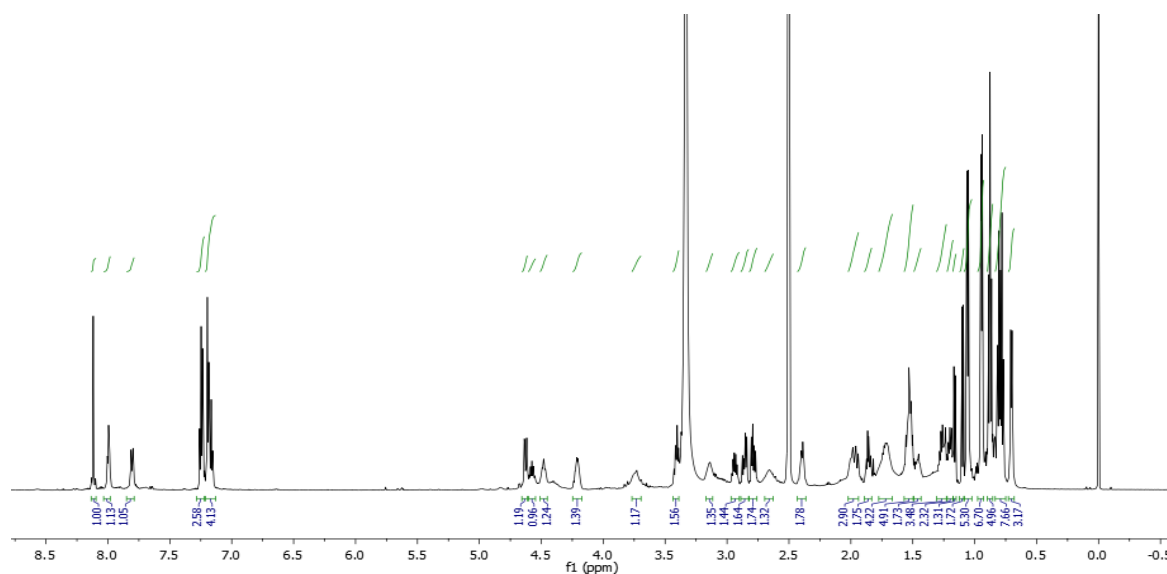
Figure 2.3. ^{1}H-NMR spectrum of pure Tubugi **23.**

When compared with the previous synthetic protocol, there is no doubt that the approach developed here constitutes a superior strategy. First, the 28% global yield obtained stands over the poor 8% obtained in the tedious solution-phase method. The straightforwardness and easy implementation of its solid-phase manner, make the total synthesis a very achievable and reproducible alternative. Undeniably, these benefits open new opportunities for the creation and derivatization of new tubugis, which will boost their application in anticancer research.

Evaluation of anticancer activities

The cytotoxic and antiproliferative activity, respectively, of Tubugi **23** was tested against two human cancer cell lines, namely prostate adenocarcinoma PC-3 cells and colorectal carcinoma HCT-116 cells. For this purpose, *in vitro* cell viability and cytotoxicity assays were conducted using resazurin reagent and fluorometric read-out after 48 h treatment of the cells with Tubugi **23**. The dilution of the samples to concentrations in the pico- and nanomolar range allowed the measurement of dose-response curves and the determination of IC_{50} values, as indicated in figure 2.4. As expected, Tubugi **23** showed a very potent cytostatic and antiproliferative effect on both tested human cancer cell lines, with IC_{50} values in the sub-nanomolar range that resembles the parent Tubugi derivative synthesized in the previous report.
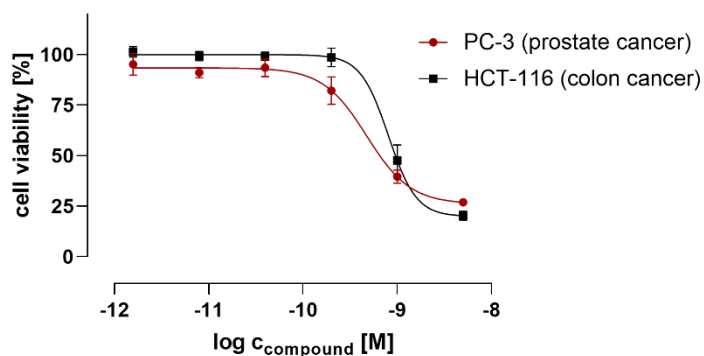
PC-3 (prostate cancer):   0.47 nM (95% CI: 0.38 - 0.58 nM)
HCT-116 (colon cancer):   0.81 nM (95% CI: 0.70 - 0.93 nM)

Figure **2.4**. Impact of Tubugi **23** on the in vitro cell viability of human PC-3 prostate and HCT-116 colon cancer cell, as determined by resazurin-based fluorometric assay after 48 h treatment of the cells.

2.4. Conclusions

We have proven that solid-phase methodology represents a significant advance in the synthetic process toward tubugis, improving the simplicity and overall efficiency. According to the requirements of the Fmoc solid-phase strategy, all building blocks required were synthesized in gram scale following standard protocols. As a key step in solid-phase methods, the loading of the first building block was executed with an innovative diazo resin that enables the incorporation of the valuable Tup unit in a quantitative and no-waste manner. Moreover, the execution of the organocatalysis-assisted Ugi-4 component reaction on-resin allowed conversion rates much higher than those obtained following solution-phase methods. The highly reproducible and operationally simpler solid-phase assembly afforded the desired tubugis in a single purification step in a notable 28% global yield.

2.5. Experimental Section

2.5.1. General Information

All starting materials were purchased from commercial sources and used without further purification. ^{1}H-NMR and ^{13}C-NMR spectra were recorded either in a Varian Mercury 400 NMR spectrometer at 399.94 MHz and 100.57 MHz, respectively or in an Agilent (Varian) VNMRS 600 NMR spectrometer at 599.83 MHz and 150.83 MHz, respectively. Chemical shifts (δ) are reported in ppm relative to the TMS (^{1}H NMR) and the solvent signal (^{13}C NMR). High-resolution mass spectra were obtained in a TripleTOF 6600-1 mass spectrometer (Sciex) equipped with an ESI-DuoSpray-Ion-Source (it operated in positive ion mode) and was controlled by Analyst 1.7.1 TF software (Sciex). The ESI source operation parameters were as follows: ion spray voltage: 5,500 V, nebulizing gas: 60 p.s.i., source temperature: 450 °C, drying gas: 70 p.s.i., curtain gas: 35 p.s.i. Data acquisition was performed in the MS1-TOF mode, scanned from 100 to 1500 Da with an accumulation time of 50 ms. IR spectra were obtained on a Thermo Nicolet 5700 FT-IR spectrometer. Column chromatography was carried out using Merck silica gel 60 (0.015-0.040 nm) and analytical thin layer chromatography (TLC) was performed on Merck silica gel 60 F254 aluminum sheets. Analytical RP-HPLC analysis was performed with an Agilent 1100 system in a reverse-phase C18 column (4.6 × 150 mm, 5 μm) with a PDA detector. A linear gradient from 5% to 100% of solvent B in solvent A over 20 min at a flow rate of 0.8 mL/min was used. The preparative purification was performed on Knauer 1001 system with UV detector K-2501. Separation was achieved using an RP C18 column (25 × 250 mm, 25 μm). A linear gradient from 30% to 50% of solvent B in solvent A over 20 min at a flow rate of 5 mL/min was used. Detection was accomplished at 210 nm. Solvent A: 0.1% (*v/v*) formic acid (FA) in water. Solvent B: 0.1% (*v/v*) FA in acetonitrile.

2.5.2. Synthesis of building block units

2.5.2.1. Synthesis of Fmoc-Tup-OH
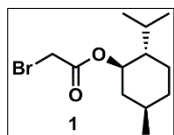
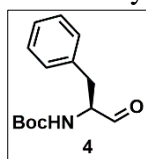 Bromoacetyl bromide (3 mL, 33 mmol) is slowly added to a solution of menthol (4.7 g, 30 mmol) and DIPEA (6.2 mL, 35 mmol) in dry THF (30 mL) at 0 °C. The reaction was let to reach RT and stirred for an additional 3 h. Then, the reaction mixture was quenched with an HCl (1 N), diluted with AcOEt (50 mL), washed with brine, dried over anhydrous (anh). Na_2SO_4 and evaporated at reduced pressure. The crude was purified by column chromatography (hexane/AcOEt 30:1) to afford **1** (5.9 g, 71%) as a colorless oil. Rf = 0.4 (hexane/AcOEt 30:1).
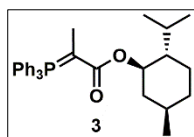
 A solution of **1** (5.0 g, 18 mmol) in THF (50 mL) refluxed in the presence of PPh$_3$ (4.7 g, 18 mmol) until completion as indicated by TLC (around 3 h). Then, the solvent was evaporated at reduced pressure and the resulting crude solid was triturated with a mixture of hexane/Et$_2$O 7:3 (*v/v*). After filtering and drying, the resulting phosphonium salt is suspended in toluene (150 mL). A solution of 0.4 N NaOH (25 mL) is added dropwise and the reaction mixture was stirred for 3 h. The organic layer was separated, washed with brine, dried over anh. Na_2SO_4, and concentrated at reduced pressure to afford the ylide **2** (8.25 g, 100%) as a white foam. Rf = 0.7 (CHCl$_3$/MeOH 2:1). To the ylide **2** (7.8 g, 17 mmol) dissolved in DCM (60 mL), MeI (1.6 mL, 23 mmol) is slowly added at 0 °C. The reaction was let to reach RT and stirred overnight. Then, the solvent was evaporated and the resulting solid is suspended in toluene and treated with 0.4 N solution of NaOH as indicated above to give **3** (7.7 g, 96%) pure as a yellow foam. Rf = 0.6 CHCl$_3$/MeOH 3:1).

Boc-Phenylalaninol (2.5 g, 10 mmol) is mixed with Dess-Martin periodinane (6.4 g, 15 mmol) in DCM (80 mL) at 0 °C. After stirring for 15 min at this temperature, the reaction mixture was allowed to reach RT and stirred overnight. The reaction is diluted

with $CHCl_3$ (50 mL) and washed with $NaHCO_3$ sat. soln. and brine. The organic layer is separated, dried over anh. Na_2SO_4, and concentrated at reduced pressure. The crude was purified by column chromatography (hexane/AcOEt 8:1) to afford **4** (2.4 g, 95%) as a white foam; R*f* = 0.6 (hexane/AcOEt 4:1).
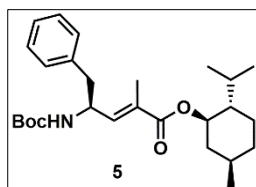
Boc-Phenylalaninal (2.0 g, 8 mmol) is mixed with **3** (5.7 g, 12 mmol) in DCM (50 mL) at 0 °C. After stirring for 15 min at this temperature, the reaction mixture was allowed to reach RT and stirred for 8 h. The reaction was quenched with a 1 N $NaHSO_4$ and diluted with $CHCl_3$ (50 mL). The organic layer was separated, washed with brine, dried over anh. Na_2SO_4, and concentrated at reduced pressure. The crude was purified by column chromatography (hexane/AcOEt 4:1) to afford **5** (2.4 g, 68%) as a white foam; R*f* = 0.5 (hexane/AcOEt 2:1).
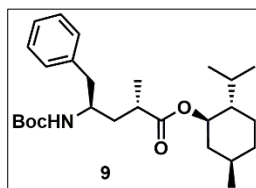

Compound 5 (2.1 g, 4.7 mmol) is dissolved in EtOAc (20 mL), mixed with a catalytic amount of 10% Pd/C, and stirred under a hydrogen atmosphere overnight. The reaction mixture is filtered through celite and concentrated under reduced pressure in a rotary evaporator. By column chromatography (hexane/AcOEt 4:1) the two diastereomers were separated, affording the desired compound Boc-protected Tup ester **9** (0.86 g, 41%) as white solid. Rf = 0.6 (hexane/AcOEt 4:1).
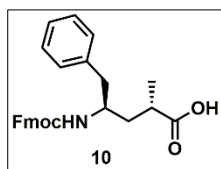
The removal of the menthyl ester and Boc protecting group was achieved by refluxing **9** (0.8 g, 1.8 mmol) in HCl (20 mL, 6N) for 4 h. After cooling the mixture to room temperature, it was extracted with AcOEt (15 mL) to remove the remaining menthol and the water layer was evaporated under high vacuum to afford H-Tup-OH (0.4 g, 100%) used in the next step without further purification. H-Tup-OH (0.4 g, 1.8 mmol) is dissolved in of dioxane/water 2:1 (20 mL), Fmoc-OSu (0.91 g, 2.7 mmol) and K_2CO_3 (0.75 g, 5.4 mmol) were added and the reaction mixture was stirred overnight. The

crude mixture is diluted with 30 mL of water, the remaining Fmoc-OSu is extracted with Et_2O (2×15 mL) and disposed of. The aqueous layer is acidified until pH 3 and extracted with AcOEt (2×20 mL). The organic layers were collected, dried over Na_2SO_4 (anh.) and evaporated under reduced pressure in a rotary evaporator to afford after column chromatography (DCM/MeOH 20:1) the pure Fmoc-Tup-OH (0.62 g, 80%) as a white amorphous solid. $R_f = 0.50$ (DCM/MeOH 20:1). ^1H NMR (400 MHz, DMSO-d_6) δ 9.78 (s, 1H), 7.97 (s, 2H), 7.82 (d, $J = 2.2$ Hz, 1H), 7.74 (s, 1H), 7.71 (dd, $J = 8.1, 1.9$ Hz, 1H), 7.45 (d, $J = 7.2$ Hz, 1H), 7.24 (t, $J = 7.7$ Hz, 1H), 7.01 – 6.91 (m, 1H), 6.43 (s, 1H), 6.35 (s, 1H), 4.31 (dd, $J = 7.8, 5.1$ Hz, 1H), 4.17 – 4.12 (m, 1H), 3.17 – 3.08 (m, 1H), 2.83 (dd, $J = 12.4, 5.1$ Hz, 1H), 2.59 (s, 1H), 2.30 (t, $J = 7.4$ Hz, 2H), 1.71 – 1.56 (m, 3H), 1.55 – 1.42 (m, 1H), 1.39 – 1.30 (m, 2H). ^{13}C NMR (101 MHz, DMSO-d_6) δ 172.7, 171.0, 162.7, 147.5, 138.4, 128.7, 127.7, 127.5, 125.1, 121.9, 121.1, 119.9, 115.7, 61.0, 59.2, 55.4, 4.13, 35.8, 28.2, 28.1, 25.2, 25.2.

2.5.2.2. Synthesis of Fmoc-Tuv(O^{n}Pr)-OH
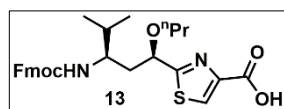
Boc-Tuv(O^{n}Pr)-OEt (**11**, 1.53 g, 3.7 mmol) was subjected to removing the methyl ester group by dissolving it in dioxane/water (30 mL, 2:1 *v/v*), adding LiOH (0.27 g, 11.1 mmol), and left stirring for 2 h. The mixture is acidified until pH 3 and extracted with AcOEt (2×20 mL). Organic layers were collected, dried over Na_2SO_4 (anh.), and evaporated under reduced pressure in a rotary evaporator. The product obtained was dissolved in 30% TFA/DCM (30 mL) and after 2 h of stirring no starting material was detected by thin-layer chromatography and the reaction product is concentrated under reduced pressure in a rotary evaporator and then placed under high vacuum. The resulting product **12** is dissolved in 20 mL of dioxane/water 2:1, Fmoc-OSu (1.9 g, 5.6 mmol), and K_2CO_3 (1.5 g, 11.1 mmol) are added and the reaction mixture is left stirring overnight. The mixture is diluted with 30 mL of water, the remaining Fmoc-OSu is extracted with Et_2O (2×15

mL) and disposed of. The aqueous layer is acidified until pH 3 and extracted with AcOEt (2×20 mL). Organic layers were collected, dried over Na_2SO_4 (anh.), and evaporated under reduced pressure in a rotary evaporator to afford after column chromatography (DCM/MeOH 20:1) the pure Fmoc-Tuv(O^{n}Pr)-OH **13** (1.13 g, 80%) as a white amorphous solid. $R_f = 0.55$ (DCM/MeOH). ^{1}H NMR (400 MHz, CDCl$_3$) δ 8.21 (s, 1H), 7.75 (d, J = 7.5 Hz, 2H), 7.64 (t, J = 7.0 Hz, 2H), 7.42 – 7.36 (m, 2H), 7.32 – 7.27 (m, 2H), 5.29 (s, 1H), 4.84 (d, J = 11.2 Hz, 1H), 4.45 (dd, J = 10.6, 7.1 Hz, 1H), 4.40 – 4.32 (m, 1H), 4.22 (t, J = 7.0 Hz, 1H), 3.97 – 3.85 (m, 1H), 3.47 (q, J = 7.3, 6.6 Hz, 2H), 2.64 (s, 2H), 1.85 (s, 1H), 1.85 – 1.75 (m, 2H), 1.63 (q, J = 6.9 Hz, 2H), 1.44 (s, 1H), 0.97 – 0.84 (m, 9H). ^{13}C NMR (101 MHz, cdcl$_3$) δ 156.4, 144.0, 144.0, 141.3, 141.3, 127.6, 127.0, 125.2, 125.0, 119.9, 73.3, 67.0, 66.4, 53.4, 52.6, 47.4, 40.1, 32.7, 28.4, 25.3, 23.0, 18.7, 17.94, 10.6, 10.5.

2.5.2.3. Synthesis of *N*-Me-D-Pip-OH
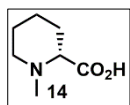
The synthesis of *N*-Me-D-Pip-OH, obtained in a quantitative one-step procedure is shown in scheme 2.3. This building block was synthesized by reductive amination of D-Pip-OH (1.2 g, 9 mmol) with 37% formalin solution (0.77 mL, 10 mmol) and hydrogen, catalyzed by 10% palladium over carbon in dry methanol. The pure compound is obtained after palladium catalyst removal by filtering the reaction crude through celite and evaporating the solvent to obtain 1.31 g of **14** as a light grey solid. 1H NMR (400 MHz, Methanol-d4) δ = 3.42 (dd, J = 12.4, 4.0 Hz, 1H), 3.35 (dd, J = 11.6, 3.4 Hz, 1H), 3.31 (p, J = 1.7 Hz, 1H), 2.99 (td, J = 12.4, 3.3 Hz, 1H), 2.86 (s, 3H), 2.27 – 2.19 (m, 1H), 1.90 – 1.81 (m, 2H), 1.79 – 1.68 (m, 2H), 1.60 – 1.49 (m, 1H). 13C NMR (101 MHz, Methanol-d4) δ = 173.5, 70.3, 55.2, 43.1, 29.5, 24.1, 22.7.

2.5.2.4. Preparation of Fmoc-Tup-Wang resin
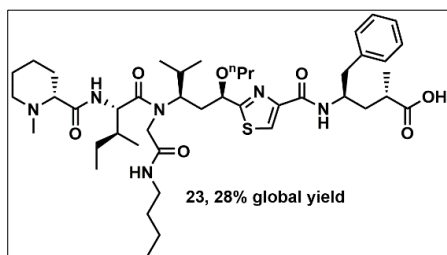

Fmoc-Tup-Wang resin
(0.35-0.4 mmol/g)
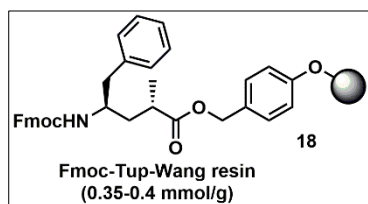
In a fritted-syringe, Wang resin (1 g, 1 mmol) is swelled with DCM (10 mL) for 10 min, DMP (0.63 g, 1.5 mmol) is added, the suspension is shaken for 3 h and then thoroughly washed with DMF (3×1), DCM (2×1 min) and finally with dry dioxane (1 min). The resin **15** is mixed with 2,4,6-triisopropylbenzenesulfonylhydrazide (0.6 g, 2 mmol) in dry dioxane (15 mL) and left shaking for 24 h. The suspension is filtered and the resin is washed sequentially with dioxane (2×1 min), DCM (2×1 min), and finally Et$_2$O (1×1 min). The hydrazine-bound resin **16** is transferred to a glass tube, DMF is added and the system is stirred for 3 min. The glass tube is immersed in an oil bad at 90ºC, tetramethyl guanidinium (0.35 mL, 3 mmol), the mixture is stirred for only 7 min to afford a deep red diazo-Wang resin **17** (IR 2055 cm^{-1}, Scheme 2.4 B), as reported in the literature. The reaction mixture is transferred to a fritted syringe, filtered, and sequentially washed with DMF (3×1), DCM (2×1 min). Fmoc-Tup-OH **10** (172 mg, 0.4 mmol) dissolved in DCM (10 mL) is added and the suspension is shaken until completion (around 20 min) checked by the complete disappearance of the deep red color and the ceasing of the N$_2$(g) bubbling. The suspension is filtered (conserving the remained Fmoc-Tup-OH) and the resin is washed with DMF (3×1) and DCM (2×1 min) affording the Fmoc-Tup-Wang resin **18** (1.1 g, 0.3 mol/g) as a light-yellow resin. Loading is determined by mixing the resulting resin (around 10 mg) in an Eppendorf tube with 20% piperidine/DMF (1 mL), stirring for 20 min, and centrifuging. 100 µL were transferred to a tube containing 10 mL DMF and mixed. The absorbance of 2 mL aliquots of the above solution and a reference (same composition solution but without the peptide) is measured at 310 nm and repeated 2 times. Loading = [101× (Absorbance)]/ [7.8 × (weight in mg)]. The procedure was repeated at 2 g and 5 g scales with similar success.

2.5.3. Synthesis of Ugi-modified tubulysin analogs

2.5.3.1. General methods for Solid-Phase Peptide Synthesis

Tubugi derivatives were synthesized manually on Fmoc-Tup-Wang resin **18** (0.1 g, 0.3 mmol/g) by a stepwise Fmoc/*t*Bu strategy. *Swelling*: The resin is swelled for 20 min in DCM. *Fmoc removal*: The resin is treated with a solution of 20% piperidine in DMF (2×10 min), then washed with DCM (3×1 min) and DMF (2×1 min). *PyBOP/NMM coupling*: Fmoc protected amino acid (4.0 equiv) and PyBOP (4.0 equiv) is dissolved in DMF, then NMM (8 equiv) is added. The mixture is pre-activated for 5 min, added to the resin, and stirred at room temperature until completion as indicated by the Kaiser test. In the case of Fmoc-Tuv(OR)-OH, 1.5 equiv were used in addition to PyBOP (1.5 equiv) and NMM (3 equiv), and the reaction mixture was left stirring for 6 h. The resin is washed with DCM (3×1 min) and DMF (2×1 min). *Aminocatalysis-mediated Ugi reaction*: The free *N*-terminal resin-bound peptide is subjected to imine formation by treating the resin beads with a suspension of paraformaldehyde (4 equiv) and pyrrolidine (4 equiv) in THF/MeOH (1:1) for 30 min. The excess of reagents is removed by washing the beads with THF (3×1min). The resin is transferred to a 5 mL microwave tube and a solution of the Fmoc-protected amino acid (4 equiv) in 1 mL of THF/MeOH (1:1) and of the isocyanide (4.0 equiv) in 1 mL of THF/MeOH (1:1) are added to the resin and the mixture is stirred in microwave at 80 ºC for 30 min. Completion is indicated by ESI-MS and RP-HPLC monitoring after mini-cleavages and if necessary, the reaction is performed again. Finally, the resin is washed with DCM (3×1 min) and DMF (2×1 min). *Cleavage*: The resin is treated with the cocktail TFA/TIS/H$_2$O (95:2.5:2.5). The filtrate is concentrated at reduced pressure until dryness, mixed within acetonitrile/water 1:2 (*v/v*), and lyophilized.

2.5.3.2. Synthesis of Tubugi 23

Starting from Fmoc-Tup-Wang resin **18** (100 mg, 0.03 mmol), Fmoc-Tuv(O^{n}Pr)-OH **13** (26.1 mg, 0.045 mmol) is coupled following the general method given above. After removing the Fmoc protecting group, an aminocatalysis-mediated Ugi reaction is performed using Fmoc-Ile-OH (41 mg, 0.12 mmol), paraformaldehyde (3.6 mg, 0.12 mmol), and *n*-butylisocyanide (10 mg, 0.12 mmol) as described above. RP-HPLC analysis after mini-cleavage showed that after performing the reaction two times, a total transformation of the starting material gave mainly the Ugi product but also the undesired product of direct coupling in about 5%. Then, the Fmoc protecting group is removed and *N*-Me-D-Pip-OH (17 mg, 0.12 mmol) is coupled using PyBOP (63 mg, 0.12 mmol) and NMM (27 μL, 0.12 mmol) in DMF for 2 h. The crude peptide is finally cleaved from the resin and purified by preparative RP-HPLC to afford the pure Tubugi **23** (7.0 mg, 28%) as a white amorphous solid. R_t = 12.2 min. HR-MS *m/z*: 827.5123 [M+H]$^+$, calcd. for C$_{44}$H$_{71}$N$_6$O$_7$S: 827.5105.

### 2.5.4. *In vitro* Cell Viability Assay

The prostate cancer cell line PC-3 was cultured in RPMI 1640 medium supplemented with 10% heat-inactivated FCS and 2 mM L-glutamine. HCT-116 colorectal cancer cell was cultured in DMEM supplemented with 10% not heat-inactivated FCS and 2 mM L-glutamine. All cells were routinely cultured in T-75 flasks in a humidified atmosphere with 5% CO2 at 37°C to reach subconfluency (~ 70-80%) prior to subsequent sub-culturing or assay usage. The adherent cells were rinsed with PBS and detached using trypsin/EDTA (0.05% in PBS) prior to cell passaging and seeding. Both human cancer cell lines were purchased from ATCC (Manassas, USA). Media and supplements for cell culturing were purchased from Capricorn

Scientific GmbH (Ebsdorfergrund, Germany). All cell culture plastics were purchased from TPP (Trasadingen, Switzerland) and Greiner Bio-One GmbH (Frickenhausen, Germany), respectively.

Anti-proliferative and cytotoxic effects, respectively, of the tubulysin derivatives, were investigated using a fluorometric resazurin-based cell viability assay. Resazurin, purchased from Sigma-Aldrich (Taufkirchen, Germany), was prepared as 50X (2.5 mM) stock solution in sterile filtered aqua bidest. and stored at 4°C under light protection. To assay the test items, human prostate PC-3 and colorectal HCT-116 cancer cells were seeded in low densities into 96-well plates (4,000 – 6,000 cells per well; seeding confluency ~ 10%), and were allowed to adhere for 24 h. Subsequently, the compounds – diluted to appropriate concentration series covering the pico- and nanomolar range using the respective culture media – were added to the cells (100 µL/96-well) for a 48 h treatment under standard growth conditions. For control measures, cells were treated in parallel with 0.5% (*v/v*) DMSO (negative control, representing the DMSO content of the highest test item concentration; Duchefa Biochemie, Haarlem, The Netherlands) and 100 µM digitonin (positive control, for data normalization set to 0% cell viability; Sigma-Aldrich, Taufkirchen, Germany), both in standard growth medium. After 48 h cell treatment, the incubation medium was discarded, and cells were rinsed once with PBS (100 µL/96-well). A 1X (50 µM) resazurin working solution was prepared freshly in basal culture medium, added to the treated cells (100 µL/96-well) that were subsequently incubated for further 2 h under standard growth conditions. Each data point was determined in technical triplicates and at least 3-4 biological replicates. The conversion of resazurin to resorufin by the remaining portion of viable, metabolically active cells was fluorometrically measured (exc.: 540 nm/em.: 590 nm) using a SpectraMax M5 multiwell plate reader (Molecular Devices, San Jose, USA). For non-linear regression analyses of the data GraphPad Prism 8.0.2 software was used to calculate IC_{50} values.

Chapter 3

Introducing *N*-modifications at the internal tertiary amide residue, structure-activity relationships and exploring a new site for potential conjugation
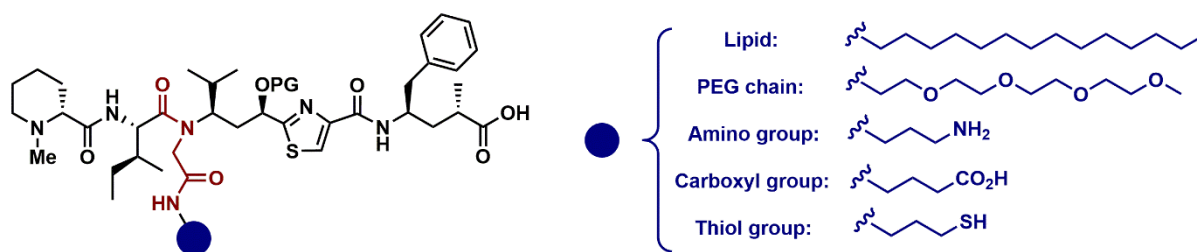

Abstract

One of the challenges in targeted delivery of tubulysins consists in designing a suitable linkage that enables conjugation without losing the toxin's anticancer activity after release. Here we took advantage of the solid-phase methodology and the multicomponent reaction to develop new analogs. Our aim was to mimic natural tubulysins using a tubugi skeleton bearing diverse functionalities at the *N*-tertiary amide residue, including linker moieties like carboxylic acids, amino groups, and thiols. The scope of the synthesis includes the incorporation of bio-chemically relevant molecules such as lipids and steroids, PEGylated chains, and fluorescent labels. The influence of the substituents on the bioactivity is evaluated, showing that thiols and long alkyl chains, i.e., more lipophilic side chains, reduce activity.

3.1. Introduction

Natural tubulysins differ considerably from synthetic tubugis in the tertiary amide that connects Ile and Tuv residues. In naturally occurring tubulysins, the *N*-tertiary amide contains a complex *N,O*-acetal moiety with an alkyl chain that varies from ethyl to n-propyl or isobutyl, among others. Interestingly, despite the highly conserved structure of tubulysins and its "resistance" to most modifications, which cause strong activity losses, many successful variations have been introduced at this position.[74]

Scheme 3.1. On-resin *N*-side chain (tertiary amide) derivatization using different isocyanides in the Ugi-4CR.

Synthetic tubulysins comprising a *N*-tertiary amide with simple methyl, ethyl, or propyl alkyl chains maintain the potent cytotoxic activity and allow to gain stability along with synthetic simplicity.[43][75][40] In addition, Zanda and co-workers discovered that modulating the hydrophobicity with more complex alkyl chains can lead to the creation of super potent cytotoxic activities.[74] The nature of this tertiary amide and how it is constructed also represent the distinction between tubugis versus other tubulysin derivatives. Interestingly, despite the straightforward functionalization that the Ugi-4CR offers; so far only few examples of tubugis have been synthesized.[67]

3.2. Synthesis and cytotoxic activity of tubugis with hydrophobic residues at the *N*-side chain

The straightforward manner of the on-resin multicomponent protocol, discussed in Chapter 2, permits the synthesis of a large set of different analogs. Firstly, we aimed to explore dissimilar functionalities using synthetic isocyanides responsible for functional group diversification at the side chain (Scheme 3.1). As stated above, the hydrophobicity of the side chain plays an important role in the cytotoxic activity. Therefore, here we initially proposed to evaluate the influence of lipids and a steroid, as well as PEG, located at the retro amide residue of the Ugi reaction, on the cytotoxicity.

3.2.1. Synthesis and cytotoxic activity of lipid-tubugi conjugates
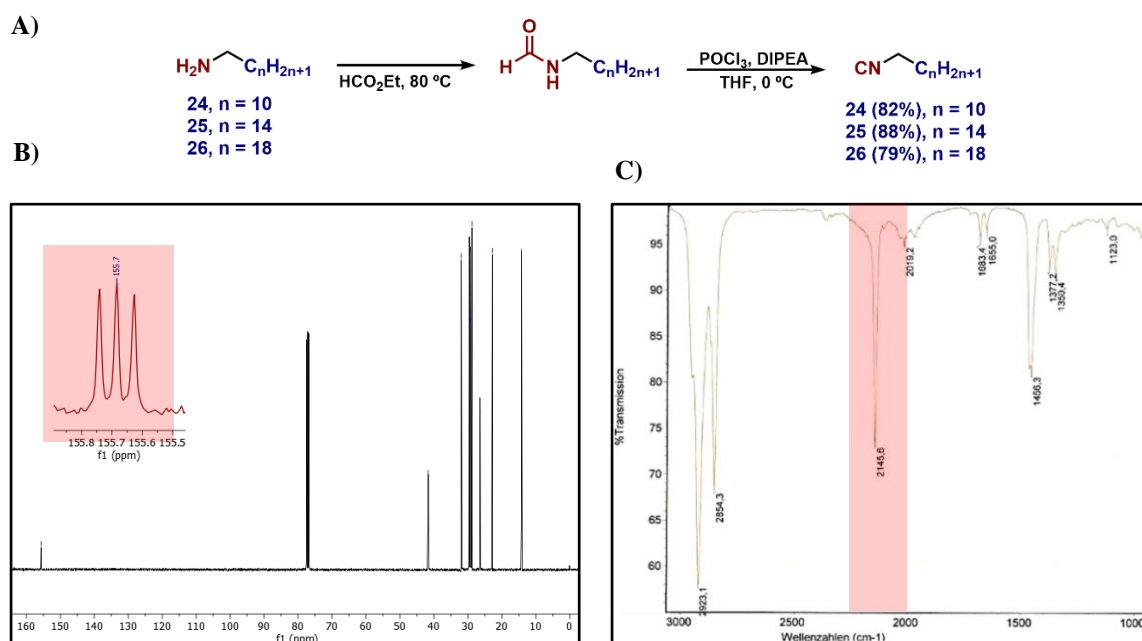
Scheme 3.2. A) Synthesis of lipid isocyanides **24**, **25** and, **26** by formylation/dehydration of lipid amines. **B)** ^{13}C-NMR spectrum of **24**. **C)** IR spectrum of **24**, with the isonitrile signals highlighted.

Isocyanides are a special class of organic compounds which usually can be synthesized by simple transformation of amines. As depicted in scheme 3.2, following the formylation/dehydration method, different lipid amines were converted into lipid isocyanides, with global yields of around 80%.

Analytical data that unequivocally corroborate the formation of the isocyanide functional group are ^{13}C-NMR in combination with infrared (IR) spectroscopy. As shown in scheme 3.2 B, in the downfield zone of the ^{13}C-NMR spectrum and close to 155 ppm, appears a classic 1:1:1 triplet corresponding to the carbon atom of the isocyanide group and its coupling with nitrogen (spin=1). Furthermore, the characteristic signal in IR confirms the presence of an isocyanide through the carbon-nitrogen triple bond signal around 2100 cm^{-1}.
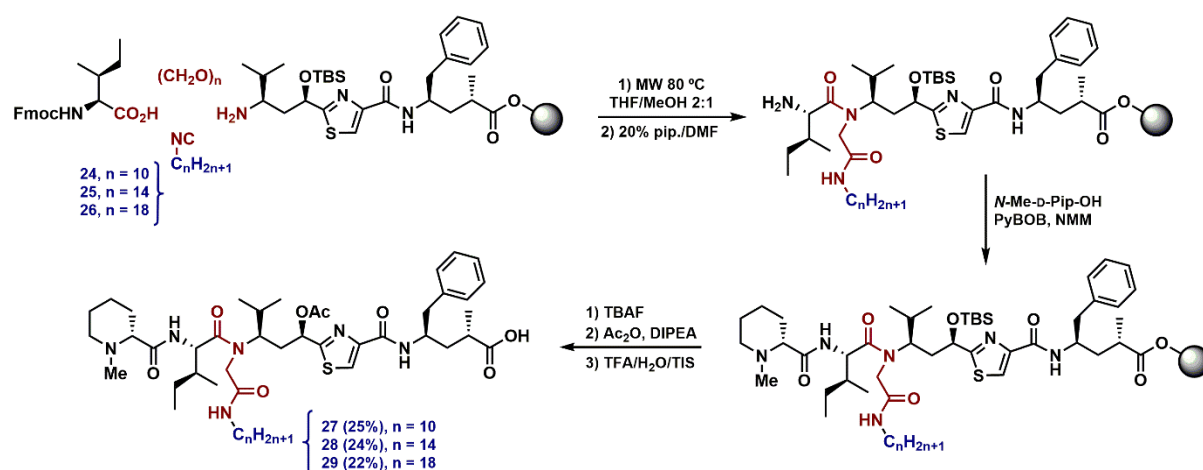
Scheme 3.3. On-resin synthesis of the tubugis **27**, **28**, and **29**, containing a *N*-lipid side chain of various lengths.

The insertion of the isocyanides in the on-resin multicomponent protocol was performed once the fragments Tuv-Tup are already assembled, as detailed in the previous chapter. In this family, a Tuv building unit containing the hydroxyl group temporarily protected as tert-butyldimethylsilyl (TBS) ether was used, to be later transformed into the natural acetyl group (or alternatively an alkyl group). As described, initially the paraformaldehyde is mixed with pyrrolidine in THF/MeOH 2:1 (*v/v*), and the obtained suspension is added to the Tuv-Tup-resin with unprotected amino groups (Scheme 3.3). The mixture is stirred for 30 min and then washed two times with THF/MeOH 2:1 (*v/v*). Excess of Fmoc-Ile-OH (4 equiv) and the isocyanide (8 equiv), dissolved in THF/MeOH 2:1 (1 m|L, *v/v*) are sequentially added and the mixture is allowed to react for 30 min at 80 ºC under microwave heating. After repeating the

process one more time, no starting material was detected according to RP-HPPLC analysis in combination with ESI-MS (after mini-cleavage). Then, as shown in scheme 3.3, the Fmoc protecting group is removed and *N*-Me-D-Pip-OH is coupled, following the conditions already discussed. The removal of the TBS protecting group was done by treating the resin with a solution of tetrabutyl ammonium fluoride (TBAF) in THF (containing 10% of phosphate buffer, pH 7.4, 0.1 M) overnight at room temperature. Further acetylation is executed using acetic anhydride (10 equiv) and DIPEA (10 equiv) in the presence of a catalytic amount of 4-(dimethylamino)-pyridine (DMAP). Final cleavage and purification by HPLC afforded the series of lipid-tubugis **27-29**, corresponding to the lipid isocyanides **24**, **25**, and **26**, resp.

Evaluation of anticancer activities

The cytotoxic and antiproliferative activities of all tubugi derivatives obtained was tested against two human cancer cell lines, prostate adenocarcinoma PC-3 cells and colorectal carcinoma HCT-116 cells.

Derivatization	Cpd	HCT-116	PC-3
⟿⟍⟋⟍	23	0.81 nM (95% CI: 0.70 - 0.93 nM)	0.46 nM (95% CI: 0.37 - 0.56 nM)
⟿⟍⟋⟍⟋⟍	27	20.9 nM (95% CI: 17.0 - 25.4 nM)	16.3 nM (95% CI: 12.8 - 20.1 nM)
⟿⟍⟋⟍⟋⟍⟋	28	13.9 nM (95% CI: 12.7 - 15.1 nM)	5.3 nM (95% CI: 4.3 - 6.4 nM)
⟿⟍⟋⟍⟋⟍⟋⟍	29	3.6 nM (95% CI: 3.3 - 3.9 nM)	1.1 nM (95% CI: 0.94 - 1.3 nM)
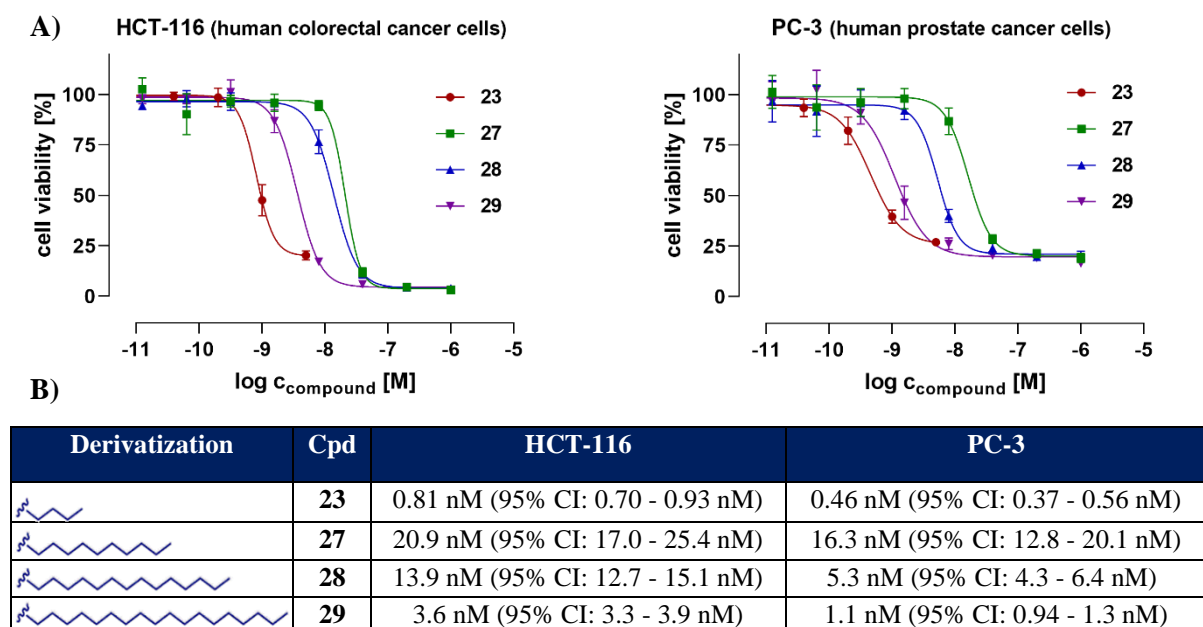
Figure 3.1. Cell-based biological testing of tubugi derivatives with *N*-side chains of various lengths. **A)** Cell viability of human HCT-116 colon and PC-3 prostate cancer cell, as determined by resazurin-based fluorometric assay after 48 h treatment with **23**, **27-29**. **B)** Calculated IC_{50} values of the tubugis **23**, **27-29**.

In vitro cell viability and cytotoxicity assays were conducted using resazurin reagent and fluorometric read-out after 48 h treatment of the cells with the tubugis. The dilution of the samples to concentrations in the pico- and nanomolar range allowed the measurement of dose-response curves and the determination of IC_{50} values, as indicated below.

The first series of tubugis with hydrophobic residues at the *N*-side chain exhibited potent cytostatic and antiproliferative effects on both tested human cancer cell lines, but interestingly none of the derivatives was more active than the short chain tubugi **23**. As shown in figure 3.1, with increasing the length of the lipid from C10, C14, and C18, there was a clear rise in potency. This result confirmed that hydrophobicity plays a crucial role and can enhance the biological activity of tubulysin derivatives, as previously stated by Zanda and coworkers. However, this seems to be a secondary effect, as short chains work better. The reasons for such counter-effects can only be speculated. E.g., secondary effects positively correlated with chain length can be better cell membrane penetration or physicochemical concentration, while shorter chains allow for better active site entrance.

3.2.2. Synthesis and cytotoxic activity of a PEG-tubugi conjugate

Aqueous solubility and cell membrane penetration potency are two important properties of biomolecules that can be substantially modulated by introducing PEGylated chains.[76][77] Due to the poor solubility of tubulysins in aqueous media, we thought that the incorporation of an O-methyl PEG (MPEG) at the *N*-side chain could be beneficial with respect to the molecules' solubility without too much impeding cellular uptake.

As described above, as educt for the solid phase peptide synthesis an isocyanide-MPEG needed to be obtained and used further as a substrate in the multi-component process. Amino-containing MPEG is commercially accessible, and as shown in scheme 3.4 A, it can be transformed into an isocyanide following the sequential formylation and dehydration process.

As depicted in scheme 3.4 B, the Ugi reaction was executed on resin-bound Tuv-Tup, using MPEG-isocyanide (8 equiv), paraformaldehyde (5 equiv), and Fmoc-Ile-OH (4 equiv) following the standard procedure with MW heating tot 80 °C for 30 min. To ensure total transformation, the whole process of imine formation and Ugi reaction was repeated one more time. After Fmoc deprotection *N*-Me-D-Pip-OH was coupled. Finally, the cleavage and following RP-HPLC purification provided the desired pure MPEG-tubugi **31** (see experimental part 3.5.5.4).
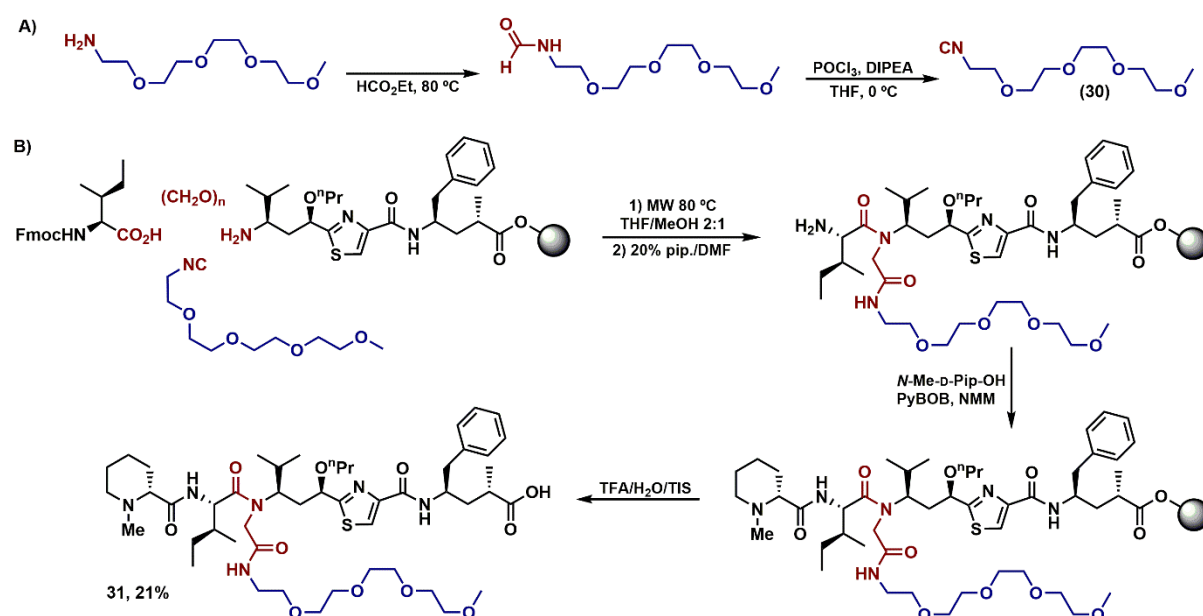
Scheme 3.4. A) Synthesis of isocyanide **30** by formylation/dehydration of a MPEG amine (specifically *O*-methyl-tetraethylenglycol amine). **B)** On-resin synthesis of *N*-side chain MPEGylated Tubugi **31**.

Evaluation of the anticancer activity

This compound represents the first example of combining a PEG chain with tubulysins, and unquestionably highlights the potential of the easy derivatization enabled by the on-resin multi-component process. As depicted in figure 3.2, the MPEGylated Tubugi **31** showed an IC_{50} value in the nanomolar range, a value relatively similar to that of lipid-tubugis with side chains of similar length, but with better water solubility.

A)

B)

Derivatization	Cpd	HCT-116	PC-3
	31	23.9 nM (95% CI: 21.4 - 26.7 nM)	13.4 nM (95% CI: 11.4 - 15.7 nM)
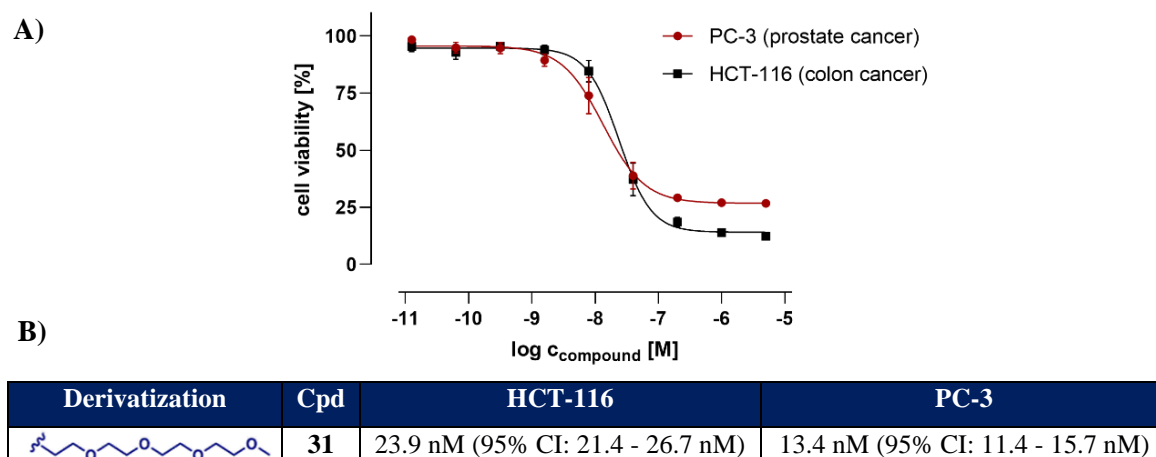
Figure 3.2. Cell-based biological testing of Tubugi **31**. **A)** Cell viability of human HCT-116 colon and PC-3 prostate cancer cells, as determined by resazurin-based fluorometric assay after 48 h treatment of the cells with the MPEGylated Tubugi **31**. **B)** Calculated IC_{50} value.

3.2.3. Synthesis and cytotoxic activity of a steroid-tubugi and fluorescently labeled tubugi

At this stage, we decided to go beyond direct functionalization of the *N*-side chain offered by the bio-relevant isocyanides previously synthesized. Taking advantage of the easy derivatization, if using an isocyanide bearing a standard linker moiety such as an amino group (initially protected to withstand the Ugi coupling), the possibilities of chemical tubugi diversification can be considerably increased by standard methods of coupling and derivatization. As shown in scheme 3.5, the allyl (3-isocyanopropyl) carbamate permits the synthesis of the on-resin intermediate bearing an amino group after the selective removal of the Alloc carbamate. The presence of a primary amino group at the *N*-side chain then should allow the incorporation of dissimilar functionalities commonly used in conjugation chemistry. In the context of evaluating the hydrophobicity of residues at these positions, here we aimed at creating a bio-conjugate combining a steroid with the on-resin tubugi (Scheme 3.5). Cholic acid was considered to be a privileged choice for the steroid. First, due to its carboxylic acid at the side chain allows easy attachment to an amino group by simple amide coupling. Second, the presence of multiple hydroxyl groups in cholic acid may offer an important balance of

hydrophobicity/polarity and therefore improved solubility in aqueous media in comparison with other steroids. Thus, the coupling of cholic acid (5 equiv) was done using the standard condition of solid-phase peptide coupling, in this case by DIC (5 equiv) and HOBt (5 equiv) in DMF as solvent. The final cleavage and purification using RP-HPLC afforded the steroid-tubugi conjugate **32** with a notable 23 % yield.
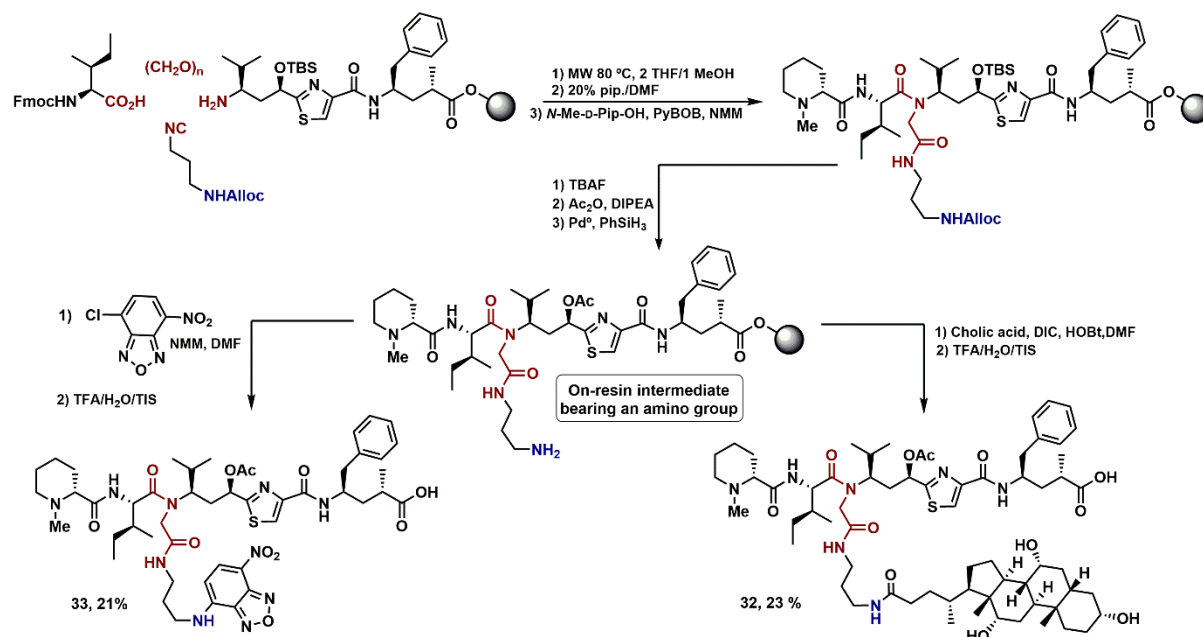
Scheme 3.5. On-resin synthesis of an *N*-side chain amino-containing tubugi. Synthesis of the steroid-Tubugi **32** and fluorescently labeled Tubugi **33.**

On the other hand, the covalent attachment of fluorescent tags can offer insights into cellular uptake and distribution mechanisms. Especially when using super potent candidates of anticancer agents like tubulysins, this knowledge is crucial considering the poor cancer cell selectivity of naked tubulysins on the one hand and very high cytotoxicity on the other hand. According to this, we thought that the chemical strategy presented here could be especially suitable for the introduction of fluorescent labels in tubulysins, allowing us to perform studies without precedent in literature. 4-Cloro-7-nitro-benzofurazan (Cl-NBD) was chosen as the best candidate considering its small size that should not significantly influence the pharmacological properties of the tubulysins. Additionally, NBD is exited in a non-UV wavelength (467 nm)

and its fluorescence emission at 540 nm is also appropriate considering the requirements of cell-based experiments.[78] The amino group-containing on-resin tubugi intermediate thus can be used as a substrate for direct on-resin labeling. The reaction is executed by mixing the resin-bound tubugi with a solution of Cl-NBD (5 equiv) and NMM (8 equiv) in DMF, and shaking the suspension overnight, obtaining Tubugi **33** after cleavage.

It is worthwhile to highlight that this strategy allows the introduction of the fluorescent label at the most variable residue of the family (the tertiary amide), maintaining the rest of the residues unaltered. Of course, a dye label can also be introduced directly as isocyanide, but this approach is more flexible as no extra indvidual synthesis of isocyanide dyes and the corresponding tubugis is required.

Evaluation of anticancer activities

The antiproliferative activity of the Tubugi **32** and Tubugi **33** is shown in figure 3.3. Also, for these two compounds, strong cytotoxic activity in the lower nanomolar range was detected. Especially in the case of NBD-labeled Tubugi **33**, the similarity of its IC_{50} values in both cancer cell lines compared well with the rest of the tubugi family may allow the results of the internalization studies using Tubugi **33** to be translated to the rest of the synthesized derivatives.

A)

B)

C)

Derivatization	Cpd	HCT-116	PC-3
NBD	33	50.5 nM (95% CI: 43.2 - 60.3 nM)	11.6 nM (95% CI: 8.7 - 16.0 nM)
Cholic tubugi	32	156.0 nM (95% CI: 139.7 - 174.0 nM)	99.8 nM (95% CI: 75.0 - 141.9 nM)
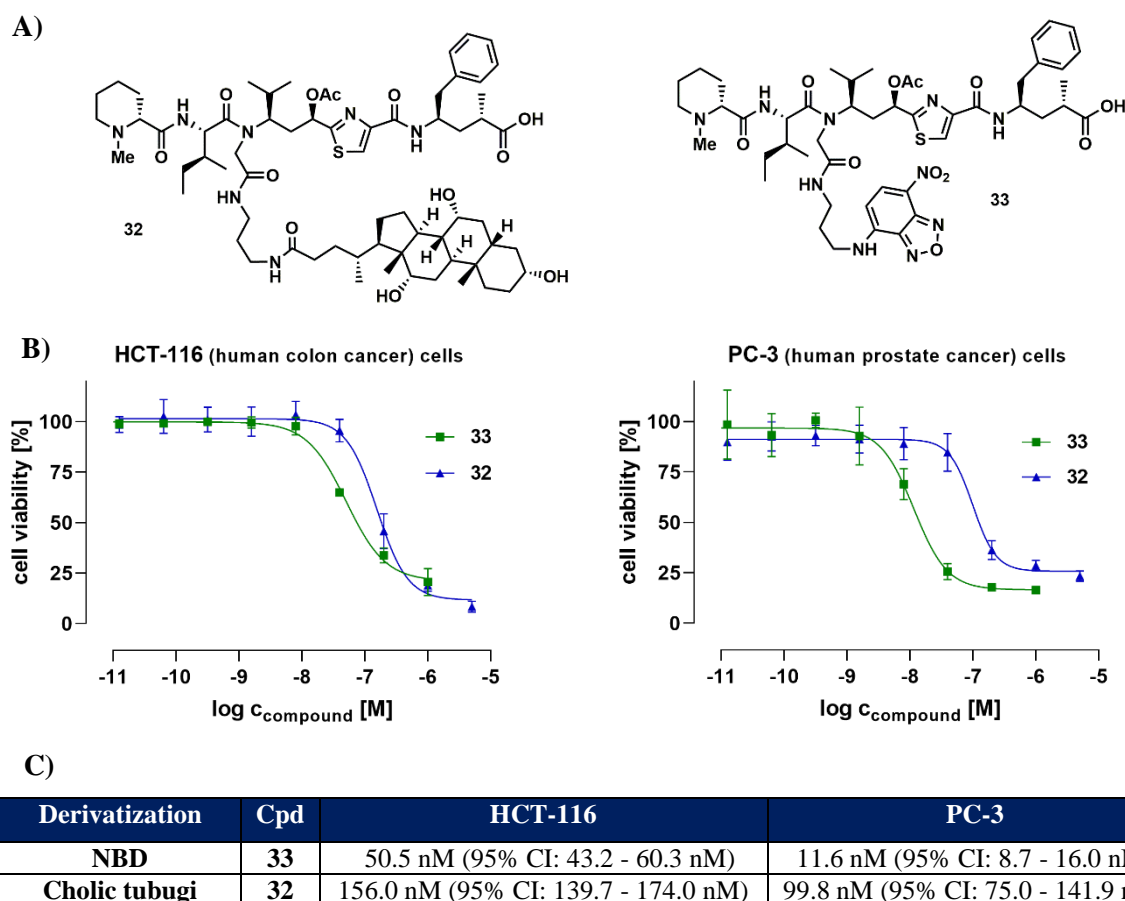
Figure 3.3. A) Structure of the steroid- and NBD-bearing Tubugis **32** and **33**, respectively. **B)** Cell-based biological testing of Tubugis **32** and **33**. Cell viability of human HCT-116 colon and PC-3 prostate cancer cells, as determined by resazurin-based fluorometric assay after 48 h treatment of the cells. **C)** Calculated IC_{50} values.

3.2.3.1. Cell internalization study – flow cytometric analysis of Tubugi 33

The internalization of the fluorescently labeled Tubugi **33** inside the cancer cells was investigated by fluorescence microscopy and flow cytometry. Initially, fluorescence spectra were recorded to determine optimized excitation and emission wavelengths of Tubugi **33** (λexc = 464 nm / λem = 537 nm). The cellular internalization of Tubugi **33** was further analyzed in more detail by conducting flow cytometric analyses. In this sense, experiments varying the duration and Tubugi **33** concentration as well as the temperature of and during the cells treatment were executed.

To investigate the time-dependency of the tubugi internalization, PC-3 cancer cells were treated with 5 µM of Tubugi **33** at 37 °C for 1 min, 1 h, 2 h, and 3 h (the 1 min treatment is virtually representing a "treated but no internalization" control, as confirmed by the aforementioned fluorescence microscopic study). As soon as the desired incubation time was finished, the incubation medium was discarded, and the cells were washed once with the basal cell medium RPMI 1640 without any supplements and without phenol red. Afterwards, the cells were detached from the 24-well plate using trypsin/EDTA (0.05% in PBS), and carefully resuspended in ice-cold RPMI 1640 complete medium, including 10% FCS to stop the trypsin activity. All samples were hold on ice until measurement. Directly prior to the flow cytometric measurement, each sample was mixed with ice-cold trypan blue solution (in RPMI 1640 basal medium; final concentration of 0.1% *v/v* per sample) to quench NBD fluorescence of non-internalized Tubugi **33** that might remain unspecifically have bound to the outer surface of the cell membrane.

The results of these flow cytometric analyses are shown in figure 3.5. The maximal internalization of Tubugi **33** in the PC-3 prostate cancer cells was reached already after 1 h of incubation, while longer incubation times – namely 2 h and 3 h – further improved the incubation just to a minor extent (Figure 3.5 A).

To study the concentration-dependent internalization, PC-3 cells were treated at 37 °C with Tubugi **33** at different concentrations 1 µM, 5 µM, and 10 µM. The results were measured after 1 min and 1 h of incubation. Also here, 1 min is virtually representing a "treated but no internalization" control, 1 h incubation time was chosen based on the results discussed above. After finalizing the incubation time, the cancer cells were treated as mentioned above. As shown in figure 3.5 B, the cellular internalization of Tubugi **33** is concentration-dependent, with the higher internalization the higher the concentration. Whereby a treatment with 5 µM of Tubugi **33** was nearby as effective as a treatment with 10 µM.

A)

B)

Figure 3.4. Fluorescence microphotographs of PC-3 cells treated with 10 µM of Tubugi **33**, **A)** after 1 min, and **B)** after 1 h of incubation. Fluorescent signals of the NBD-labeled Tubugi **33** are shown in green, the cell nuclei were stained using Hoechst 33342 dye and appear in blue. Scale bars are 40 nm.

In temperature-depending internalization experiments, PC-3 cancer cells were treated with 5 µM of Tubugi **33** for 1 h at 4 $^{\circ}$C and 37°C, respectively. As shown in figure 3.5 C, the cellular internalization of Tubugi **33** at 4°C was within an incubation time of 1 h only slightly increased compared to the "treated but no internalization" control with only 1 min incubation.

Figure 3.5. Flow cytometric analyses of Tubugi **33** using PC-3 cancer cell, **A)** at different incubation times, on **B)** at different concentrations, and **C)** at different temperatures.

The observation of temperature-dependency can, beyond the usual physicochemical rate increase, also indicates an active, energy-dependent internalization mechanism such as endocytosis, which if present then most likely is also relevant for other tubugi derivatives. Hence, both the fluorescence microscopic inspection (Figure 3.4 B) and the flow cytometric study (Figure 3.5 C) support the hypothesis that an active cellular internalization process, most likely an endocytotic pathway, may be undergone by Tubugi **33**.

3.3. Synthesis and cytotoxic activity of tubugis with polar residues at the *N*-side chain

Tubulysins have taken slower to be applied as payload in targeted delivery therapies in comparison with other less potent antimitotic compounds, not only because of their difficult synthesis but probably also because of challenging functionalization that allows its linkage to the carrier.[21] In tubulysins, the options are very limited, although there have been some important contributions (discussed in epigraph 1.5). However, most of the described and tested functionalizations, unfortunately, compromise the antiproliferative efficacy of the tubulysin derivatives.[48][49] While this is desired as long as bound to a targeting moiety, it is undesired after release or internalization into the (cancer) cell.

Therefore, the *N*-tertiary amide residue was further evaluated for an introduction of functionalizations that permit the linkage to a carrier molecule but do not inflict too much on activity after release. The challenge was the development of such linkages that can be cleaved under the specific intracellular conditions after cellular internalization of the molecule. Consequently, it was our next goal to synthesize a small library of isocyanides functionalized with carboxylic acids, amino groups, and thiol groups, respectively. Exploring the anticancer activities of the different functionalized tubugis was expected to decipher the best candidates to be considered as payloads in targeted-delivery technologies.

3.3.1. Synthesis and cytotoxic activity of tubugis with an amino group at the *N*-side chain

The use of amino groups for the attachment of a drug payload to carrier molecule is maybe the chemical option most often used in targeted drug delivery approaches, obviously because of its abundance in natural compounds, including cytotoxic drugs.[50][49] Amino groups in combination with lipids also are known to enhance human membrane penetration even better than lipids alone. Secondary and primary amino group-containing drugs are commonly connected via a p-amino benzyl carbamate (PABC) and a peptide as a spacer.[23] Also, the direct attachment to an amino acid or dipeptide, representing a known cleavage site for cellular proteases, via an amide bond is another common approach (epigraph 1.5). Remarkably, tertiary amine-containing drugs can be also connected to carrier molecules, due to the recent development of self immolative p-aminobenzyl quaternary ammonium (PABQ) linkers that constitute an important solution for the targeted and traceless delivery of tubulysins.[49] At this point, we hypothesized that introducing an amino group to the *N*-side chain of tubugis would be advantageous considering the plethora of advances in terms of compatible linkers, connectors and spacers already existent for this functional group.

For that purpose, a series of amino-protected isocyanides **34-38** was synthesized to be used in the multicomponent synthetic procedure, similar to the one described in scheme 3.2 A. The obtention of isocyanides bearing orthogonally protected amino groups (see experimental part 3.5.2) required three steps starting from commercially available diamines, yielding the desired isocyanides in around 65% global yield. As shown in scheme 3.6, five different isocyanides were conceived to be incorporated into the final tubugi derivatives. Importantly, the lipid-isocyanides **36**, **37**, and **38** allow the introduction of an amino group while, at the same time, balancing the polarity of the final tubugi derivatives with the hydrophobic hydrocarbon spacer

of 8, 10 or 12 carbon atoms, respectively. For that reason, the final tubugis **36**-**38**, obtained after resin cleavage and purification, were assumed as promising payload candidates.
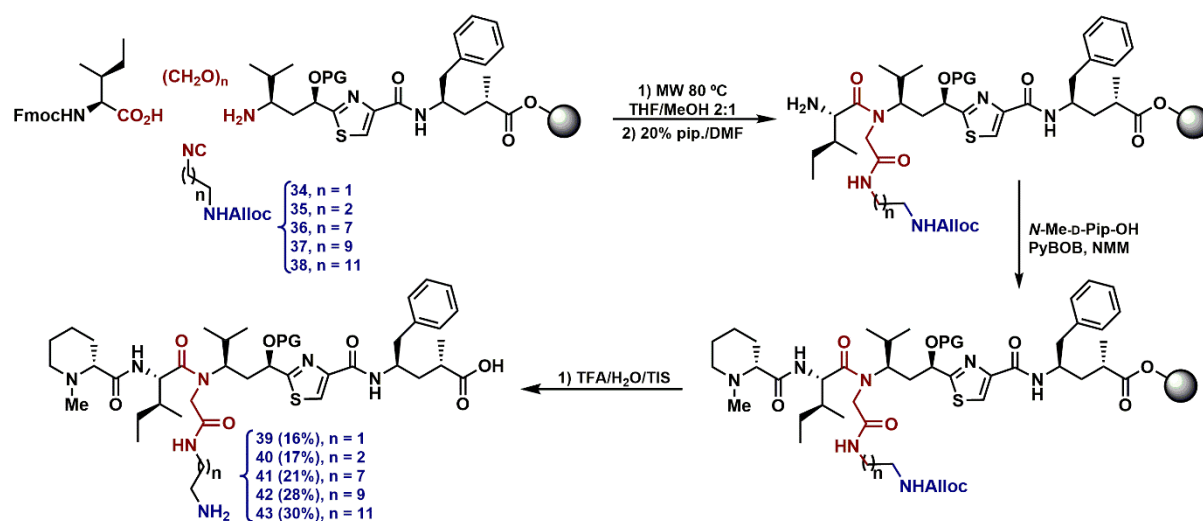
Scheme 3.6. On-resin synthesis of tubugis **39**-**43** containing amino groups located at the *N*-side chain.

Evaluation of anticancer activities

Opposite to the effect of introducing hydrophobic residues, polar and ionizable functional groups such as amino groups are known to disturb the anticancer activity. As shown in figure 3.6 the IC_{50} values obtained for tubugis **39** and **40** are far higher, indicating lower activity, in comparison with the series of tubugis modified with hydrophobic residues alone (compare Figure 3.1). A result that guided us to synthesize the analogs **41**-**43**, where the terminal amino group is introduced well separated from the tubugi skeleton using longer lipid chains. Thus in this case the combined lipid plus amino group was not beneficial, or if cell penetration was better, it did not perform well at the active site.

It was observed that a longer hydrocarbon spacer between the tubugi backbone and the amino group has a positive effect on the anticancer activity, what is, generally, in good accordance with the results of tubugi derivatives **27-29** containing the non-functionalized lipid chains (compare Figure 3.1). Here again, the analog with the longest chain length, namely Tubugi **43**, was found to be the most active one amongst the derivatives with longer, terminally

functionalized lipid chains. Again, the chain length – activity relationship is not linear, following similar trends as for alkyl chains alone, albeit with different curve-peaks and lower activities in general.
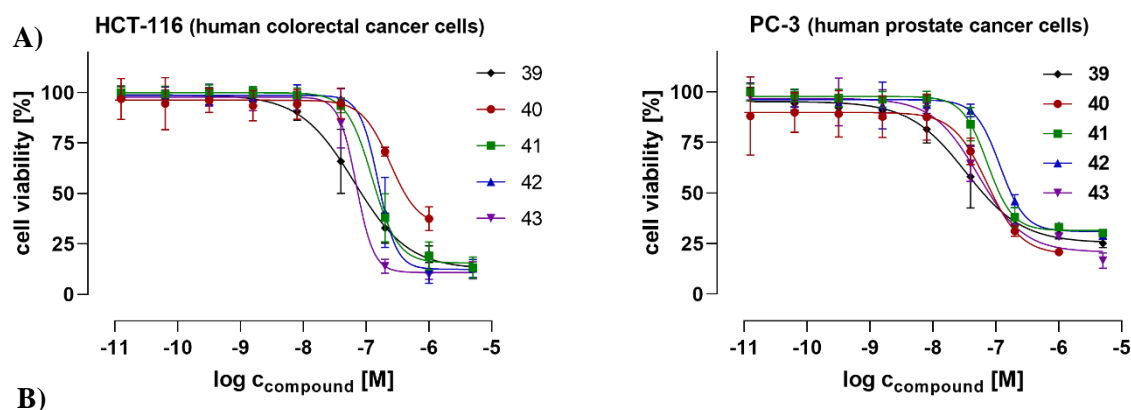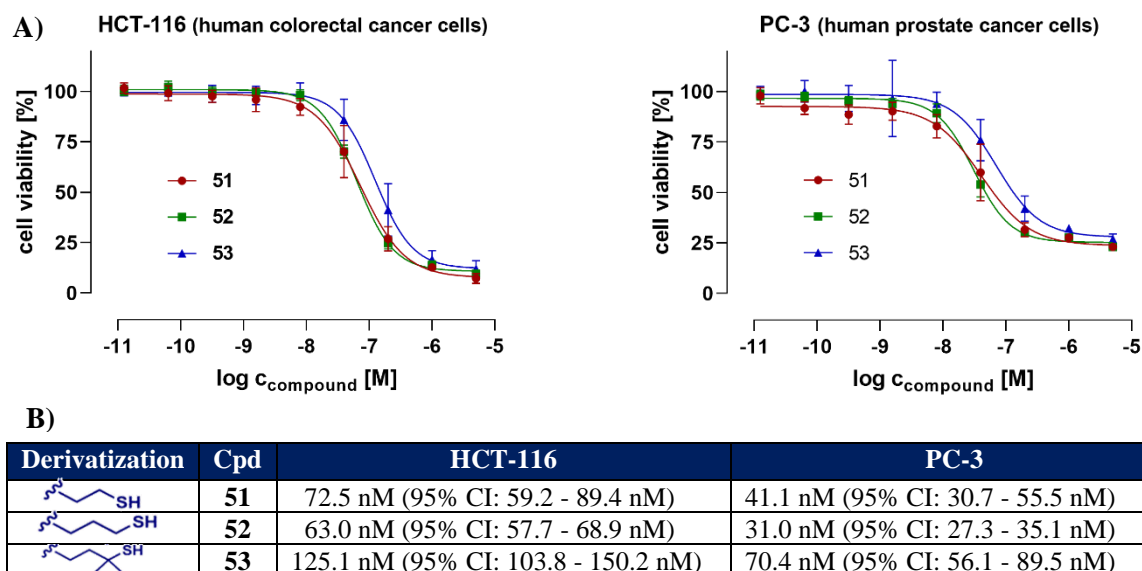

Figure 3.6. Cell-based biological testing of tubugi derivatives with *N*-side chain functionalized with amino groups. **(A)** Cell viability of human HCT-116 colon and PC-3 prostate cancer cells, as determined by resazurin-based fluorometric assay after 48 h treatment. **(B)** Calculated IC_{50} values.

Derivatization	Cpd	HCT-116	PC-3
$\sim$NH$_2$	39	64.6 nM (95% CI: 49.0 - 87.5 nM)	33.3 nM (95% CI: 24.0 - 46.8 nM)
$\sim$NH$_2$	40	241.5 nM (95% CI: 194.1 - 1,310 nM)	72.7 nM (95% CI: 49.9 - 109.8 nM)
$\sim$NH$_2$	41	124.7 nM (95% CI: 107.7 - 143.7 nM)	73.7 nM (95% CI: 62.5 - 86.1 nM)
$\sim$NH$_2$	42	156.1 nM (95% CI: 129.4 - 185.8 nM)	116.2 nM (95% CI: 101.5 - 133.1 nM)
$\sim$NH$_2$	43	69.8 nM (95% CI: 57.1 - 83.8 nM)	52.6 nM (95% CI: 43.5 - 64.7 nM)

3.3.2. Synthesis and cytotoxic activity of tubugis with carboxylic acids at the *N*-side chain

Linkages via the carboxylic acid group at the *C*-terminus have been the pioneer options of using tubulysins as payloads in ADCs and PDCs.[40] This functional group serves as a precursor of a variety of chemical connections explored in conjugation, e. g., amide, ester, and hydrazide.[41] Interestingly, the only example so far of using tubugis as the payload is based on the connection of the tubugi *C*-terminus through an amide bond to a peptide carrier.[18] Despite its extensive usage, the compromise of this functional group in a non-hydrolyzable bond usually leads to mayor decrease of its anticancer activity, thus suggesting that shifting the linkage to another tubugi position could be advantageous.

 The introduction of carboxylic acids at the *N*-side chain of tubugis would be conceivable using isocyanides containing this functional group orthogonally protected. As depicted in scheme 3.7 A, starting from the simple amino acids glycine and β-alanine, the desired isocyanides can be obtained in three synthetic steps. First, the unprotected amino acid is subjected to a formylation of the amino group by acetic-formic anhydride. Then, for the protection of the carboxylic acid, trimethylsilylethyl (TMSE) ester was used. This protecting group was chosen because it can be quantitatively removed in the final cleavage conditions. Also, its formation can be easily achieved by standard coupling of the corresponding alcohol using carbodiimides. Final dehydration using POCl₃ and Et₃N afforded the corresponding isocyanides in global yields around 65% (experimental part 3.5.3). Following the solid-phase strategy based on the corresponding coupling reactions and using isocyanides **44** and **45** in a multi-component procedure, two new analogs were obtained (experimental part 3.5.7).
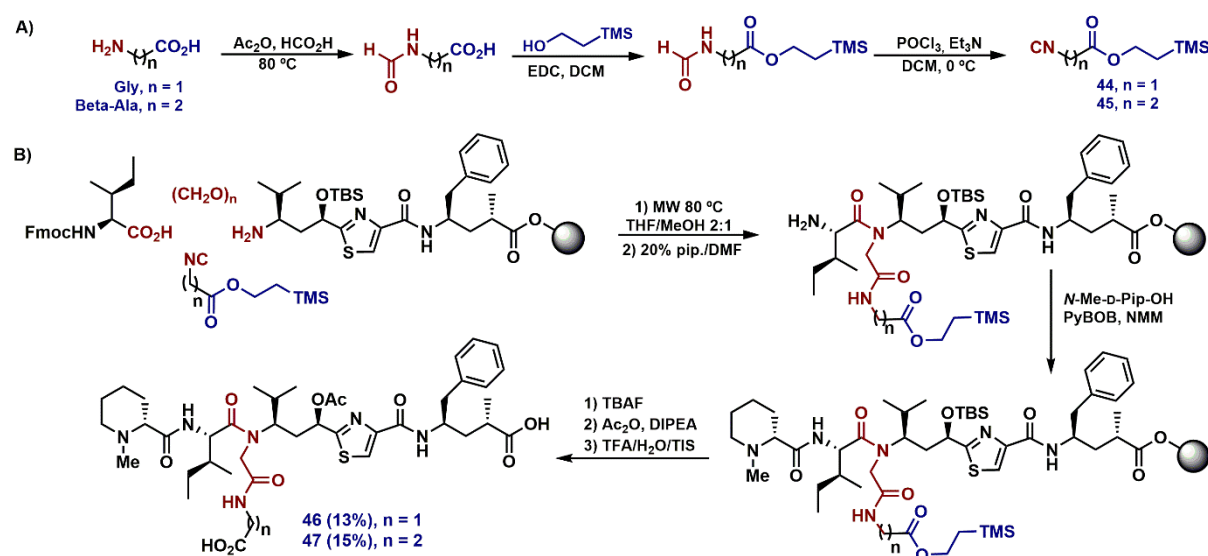
Scheme 3.7. A) Synthesis of isocyanides **44** and **45** containing carboxylic acids protected as TMSE, starting from Gly and β-Ala. **B)** On-resin synthesis of tubugis **46** and **47** containing carboxylic acid groups located at the *N*-side chain.

Final cleavage and purification afforded the tubugis **46** and **47**, both having an additional carboxylic acid group located at the tertiary amide residue and therefore potential candidates to be considered as payloads.

Derivatization	Cpd	HCT-116	PC-3
⌇⌇CO₂H	**46**	509.3 nM (95% CI: 444.9 - 579.8 nM)	376.2 nM (95% CI: 304.1 - 441.3 nM)
⌇⌇CO₂H	**47**	> 1,000 nM	249.1 nM (95% CI: 188.1 - 437.6 nM)
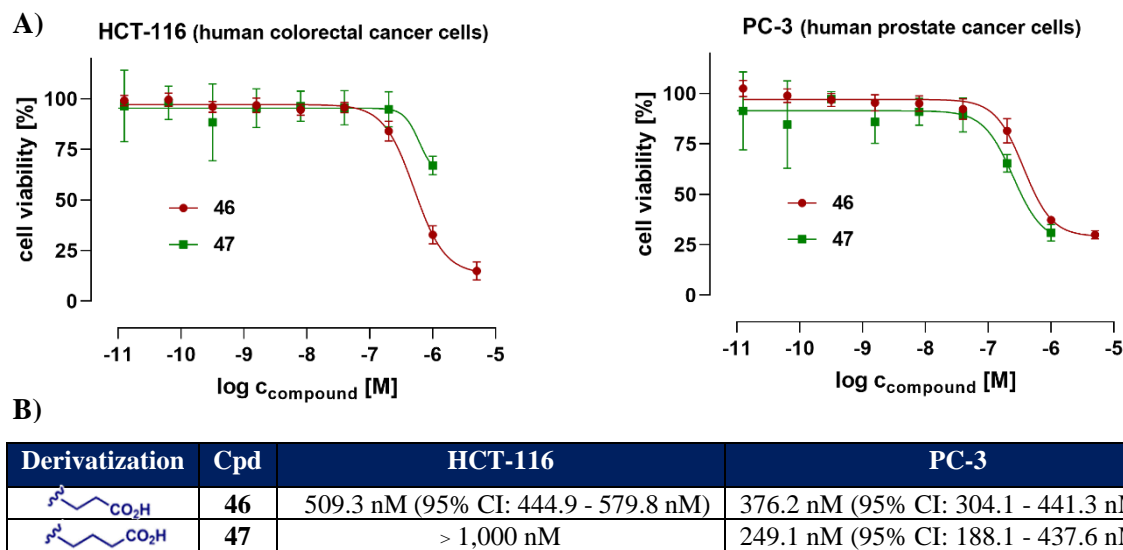
Figure 3.7. Cell-based biological testing of tubugi derivatives with *N*-side chain functionalized with carboxylic acids. (A) Cell viability of human PC-3 prostate and HCT-116 colon cancer cells, as determined by resazurin-based fluorometric assay after 48 h treatment. (B) Calculated IC_{50} values.

Evaluation of anticancer activities

As shown in figure 3.7, for the two tubugis functionalized with carboxylic acids in the *N*-side chain, **46** and **47**, the worst anticancer activity values were obtained. The IC_{50} values are still in the nanomolar range but, compared to the other compounds, these are closer to the micromolar range. This is not unexpected, as negatively charged molecules show bad cell penetration usually, and polar side chains worse activity in tubugis in general.

3.3.3. Synthesis and anticancer activity of tubugis with thiol groups at the *N*-side chain

Disulfide bond-based linkages were one of the earliest linker strategies in ADCs.[26][27] While linking drugs via an amino group requires the combination of several moieties responsible for a specific function, such as connection to the carrier, traceless release of the drug, or the enzymatic cleavage; disulfide conjugation by itself comprise all these requirements and is

therefore superior in terms of atom economy and ease of cleavage.[79] However, the major disadvantage of disulfide conjugation is that it is not directly applicable to most common anticancer drugs as they do not possess a thiol functional group. Also, in some cases preliminary cleavage in the body, e.g., by disulfide reduction or interchange with glutathione. Accordingly, a strategy is proposed for the easy modification of tubugis using thiolalkyl groups at the *N*-side chain, which can serve as substrate for further conjugation reactions such as disulfide formation. Modification around the thiol or disulfide can be used to finetune the cleavage sensitivity. For that, synthesis of isocyanides bearing a protected thiol is necessary, for which the trityl group was chosen.
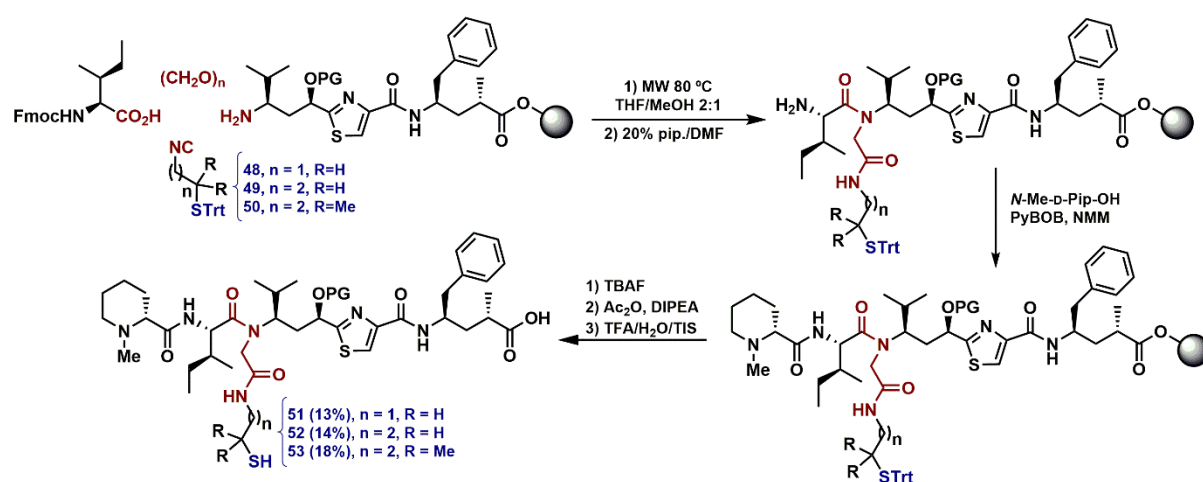
Scheme 3.8. On-resin synthesis of tubugis **51-53** having thiol groups located at the *N*-side chain.

As shown in scheme 3.8, three thiol-isocyanides **48**-**50** were synthesized and incorporated in the on-resin multicomponent synthesis. Tubugi **53** is especially attractive since its sterically protected sulfide guarantees the modular stability of any subsequent disulfide bond (experimental part 3.5.8).

Evaluation of anticancer activities

The compounds modified with non-ionizable functional groups (such as thiol groups **51**-**53**) happened to the be most active ones and therefore are the most promising candidates of the

series (Figure 3.8). Bearing in mind the immense wealth of thiol based selective conjugations and the progress related to the specific cleavage of disulfide bridges inside cancer cells, all the thiol-functionalized tubugis were considered for further peptide-based conjugation strategies (Chapter 4).

Figure 3.8. Cell-based biological testing of tubugi derivatives with *N*-side chain functionalized with thiol groups. **(A)** Cell viability of human HCT-116 colon and PC-3 prostate cancer cells, as determined by resazurin-based fluorometric assay after 48 h treatment. **(B)** Calculated IC_{50} values.

3.4. Conclusions

The solid-phase methodology proved to be capable of the parallel construction of large compound libraries, which is very demanding and tedious using classic solution-phase synthesis. The multicomponent reaction permitted the unprecedented incorporation of biologically significant moieties like lipids, steroids, fluorescent labels, MPEG chains, aminoalkyl, carboxyalkyl, and alkylthiol groups. The anticancer activities of the tubugi derivatives showed a broad-spectrum of activity, obtaining IC_{50} values mostly in the lower nanomolar range. This is remarkably influenced by the balance of polarity and hydrophobicity of the residues introduced at the *N*-tertiary amide, with short and very long alkyl chains being beneficial, while polar groups of any type worsen the activity in the order SH $< NH_3^+ << CO_2^-$,

the latter being the worst. The developed synthetic strategy opens new opportunities for the conjugation of tubugis by linking the special targeting functionalization to the *N*-tertiary amide, with the thiols being the best option of the derivatives tested.

3.5. Experimental Section
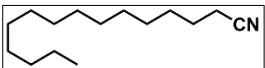
3.5.1. Synthesis of lipid isocyanides

Compounds **34**, **35**, **48,** and **49** were acquired from the laboratory stock. Their synthesis can be found in previous publications from our group.[73,80]

3.5.1.1. 1-Isocyanodecane (24)

 n-Decylamine (5.7 g, 0.038 mol) is quantitatively formylated by refluxing it in ethyl formate (30 mL) for 12 h. After removing the volatiles in a rotary evaporator, the product is placed in high vacuum for 24 h for draying. The pure formamide (6.0 g, 0.038 mol) is dissolved in 20 mL of dry THF and mixed with Et$_3$N (19.4 mL, 0.14 mol). The solution is cooled tounder 0 °C, and under N$_2$ (g) atmosphere a solution of POCl$_3$ (4.3 mL, 0.046 mol) in 10 mL of THF is added dropwise during 30 min. The resulting reaction mixture is stirred at 0 °C for 1 h, then allowed to reach room temperature and stirred for 2 h. The reaction is quenched with 20 mL of aqueous Na$_2$CO$_3$ solution (10 %) and extracted with EtOAc (2×20 mL). The organic phases are combined, washed with brine (10 mL), dried over anh. Na$_2$SO$_4$, and concentrated under reduced pressure in a rotary evaporator to afford after column chromatography (DCM) the pure 1-isocyanodecane (**24**) (5.2 g, 82%) as a pale-yellow oil. R_f = 0.81 (DCM). IR (KBr, cm^{-1}): 2923.1, 2854.3, 2145.6. ^{1}H NMR (400 MHz, CDCl$_3$) δ 3.44 – 3.34 (m, 2H), 1.73 – 1.62 (m, 2H), 1.49 – 1.37 (m, 2H), 1.35 – 1.24 (m, 12H), 0.89 (d, *J* = 6.4 Hz, 3H). ^{13}C NMR (101 MHz, cdcl$_3$) δ 155.6, 41.7, 31.9, 29.6, 29.5, 29.4, 29.2, 28.8, 26.4, 22.8, 14.2.

3.5.1.2. 1-Isocyanotetradecane (25)

 n-Tetradecylamine (5 g, 0.023 mol) is formylated and dehydrated according to the procedure described above to afford column chromatography (DCM) the pure 1-isocyanotetradecane (**25**) (4.6 g, 88%) as pale a yellow oil. R_f = 0.71 (*n*-hex/EtOAc 6:1). IR

(KBr, cm^{-1}): 2921.4, 2852.3, 2145.3. ^{1}H NMR (400 MHz, CDCl$_3$) δ 3.41 – 3.34 (m, 2H), 1.70 – 1.68 (m, 2H), 1.43 (p, J = 7.0 Hz, 2H), 1.32 (s, 20H), 0.88 (t, J = 6.8 Hz, 3H). ^{13}C NMR (101 MHz, cdcl$_3$) δ 155.60, 155.54, 155.49, 41.60, 41.54, 41.47, 31.89, 29.67, 29.64, 29.61, 29.57, 29.48, 29.34, 29.32, 29.10, 28.68, 26.30, 22.66, 14.09.

3.5.1.3. 1-Isocyanooctadecane (26)
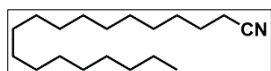
 n-Octadecylamine (5 g, 0.019 mol) is formylated and dehydrated according to the procedure descrived above to afford column chromatography (DCM) the pure 1-isocyanooctadecane (**26**) (3.9 g, 79%) as pale-yellow oil. R_f = 0.82 (*n*-hex/EtOAc 6:1). IR (KBr, cm^{-1}): 2914.5, 2848.1, 2147.5. ^{1}H NMR (400 MHz, CDCl$_3$) δ 3.42 – 3.34 (m, 2H), 1.70 – 1.68 (m, 2H), 1.42 (q, J = 7.1 Hz, 2H), 1.26 (s, 28H), 0.91 – 0.84 (m, 3H). ^{13}C NMR (101 MHz, CDCl$_3$) δ 155.6, 155.6, 155.5, 41.6, 41.5, 41.5, 31.9, 29.7, 29.6, 29.6, 29.6, 29.5, 29.4, 29.1, 28.7, 26.30, 22.7, 14.0.

3.5.1.4. MeO-PEG₄-NC (30)
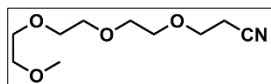
 MeO-PEG$_4$-NH$_2$ (1 g, 4.8 mmol) is formylated by refluxing in ethyl formate for 24 h. Then, all the volatiles are removed under reduced pressure in a rotary evaporator and the product is left under a high vacuum for 24 h, Then, the formamide (1.13 g, 4.8 mmol) is dissolved in 30 mL of dry THF and mixed with Et$_3$N (3.4 mL, 19.2 mmol). The solution is cooled to 0 °C and under N$_2$ (g) atmosphere, a solution of POCl$_3$ (0.58 mL, 6.2 mmol) in 15 mL of THF is added dropwise during 30 min. The resulting reaction mixture is stirred at 0 °C for 1 h, then allowed to reach room temperature and stirred for 2 h more. The reaction is quenched with 50 mL of Na$_2$CO$_3$ (10 %) and extracted with EtOAc (2×30 mL). The combined organic phases are combined, washed with brine (20 mL), dried over anh. Na$_2$SO$_4$, and concentrated under reduced pressure in a rotary evaporator to dryness to afford after column chromatography (DCM/EtOAc 4:1) the pure MeO-PEG$_4$-NC **30** (0.63 g, 60%) as

a pale-yellow oil. R_f = 0.4 (DCM/EtOAc 4:1). ^{1}H NMR (400 MHz, CDCl$_3$), δ = 3.74 – 3.63 (m, 12H), 3.60 – 3.54 (m, 4H), 3.38 (s, 3H). ^{13}C NMR (101 MHz, CDCl$_3$), δ = 157.21, 157.16, 157.10, 71.85, 70.78, 70.57, 70.51, 70.43, 68.59, 58.94, 53.37, 41.74, 41.67, 41.60.

3.5.2. Synthesis of isocyanide containing protected amines
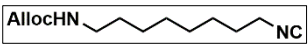
3.5.2.1. General synthesis of allyl ω-isocyanoalkylcarbamates

The Alloc-mono protection of diamines is performed similarly to the procedure described by Gilon and co-workers for smaller diamines.[1] To a solution of the diamine (0.1 mol) in CHCl$_3$ (200 mL) at 0 °C, allyl chloroformate (2.21 mL, 20 mmol) is slowly added. The reaction is allowed to reach room temperature and stirred overnight. The next day, the reaction mixture is filtered and the filtrate is washed with water (4×100 mL) and brine (2×50 mL). This washing eliminates most of the excess of starting material, although for the 1,12-diaminododecane a considerable amount remained. The resulting crude mixture is dissolved in ethyl formate and stirred to reflux for 12 h. Then, it is concentrated under reduced pressure in a rotary evaporator and purified by column chromatography (DCM/MeOH 50:1) to afford the pure formylated and alloc protected diamine in 60 to 65% yield. The pure formamide obtained is dissolved together with DIPEA (4 equiv) in dry THF (mL). It is cooled to 0 °C and under an N$_2$ (g) atmosphere a solution of POCl$_3$ (1.3 equiv) in THF (cooled to 0 °C) is added dropwise during 30 minutes. The resulting mixture is stirred at 0 °C for 3 h, then allowed to reach room temperature and stirred for an additional 30 min. The reaction mixture is quenched with 50 mL of 10 % aqueous solution of Na$_2$CO$_3$ and extracted with EtOAc (2×50 mL). The combined organic phases are washed with brine (20 mL), dried over anhydrous Na$_2$SO$_4$, and concentrated under reduced pressure in a rotary evaporator to dryness. The crude product is purified by column

---
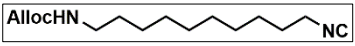
[1] Hurevich, M.; Tal-Gan, Y., Klein, S.; Barda, Y.; Levitski, A.; Gilon, C. *J. Pept. Sci.* **2010**, *16*, 178.

chromatography (DCM/EtOAc 20:1) to afford pure allyl ω-isocyanoalkylcarbamate as a pale-yellow oil.

3.5.2.2. Allyl 8-isocyanooctylcarbamate (36)

 1,8-Diaminooctane (1 g, 6.7 mmol) is mono-alloc protected, formylated and dehydrated following the general procedure given above, to afford after purification by column chromatography the pure allyl 8-isocyanooctylcarbamate **36** (2.14 g, 75%) as a pale/yellow oil. R_f = 0.66 (DCM/EtOAc 10:1). IR (KBr, cm^{-1}): υ_{max} = 3337, 2929, 2857, 2147, 1698. ^{1}H NMR (400 MHz, CDCl$_3$): δ = 5.99 – 5.85 (m, 1H), 5.30 (dq, J = 17.3, 1.7 Hz, 1H), 5.21 (dd, J = 10.5, 1.5 Hz, 1H), 4.74 (s, 1H), 4.56 (d, J = 5.7 Hz, 2H), 3.42 – 3.34 (m, 2H), 3.22 – 3.12 (m, 2H), 1.72 – 1.65 (m, 2H), 1.55 – 1.45 (m, 2H), 1.48 – 1.38 (m, 1H), 1.32 (m, 6H). ^{13}C NMR (101 MHz, CDCl$_3$): δ = 156.2, 155.6, 133.0, 117.5, 65.4, 41.5, 40.9, 29.9, 29.0, 28.9, 28.5, 26.5, 26.2.

3.5.2.3. Allyl 10-isocyanodecylcarbamate (37)

 1,10-Diaminodecane (1.3 g, 7.3 mmol) is mono-alloc protected, formylated and dehydrated following the general procedure given above, to afford after purification by column chromatography the pure allyl 10-isocyanodecylcarbamate **37** (2.5 g, 78%) as a pale-yellow oil. R_f = 0.73 (DCM/EtOAc 10:1). IR (KBr, cm^{-1}): υ_{max} = 3338, 2926, 2855, 2147, 1698. ^{1}H NMR (400 MHz, CDCl$_3$): δ = 5.99 – 5.86 (m, 1H), 5.30 (dd, J = 17.1, 1.8 Hz, 1H), 5.21 (d, J = 10.4 Hz, 1H), 4.73 (s, 1H), 4.56 (d, J = 5.7 Hz, 2H), 3.42 – 3.33 (m, 2H), 3.17 (q, J = 6.7 Hz, 2H), 1.72 – 1.64 (m, 2H), 1.53 – 1.39 (m, 4H), 1.30 (10H). ^{13}C NMR (101 MHz, CDCl$_3$): δ = 156.2, 155.6, 133.0, 117.5, 65.34, 41.5, 41.0, 29.91, 29.3, 29.2, 29.1, 29.0, 28.6, 26.6, 26.2.

3.5.2.4. Allyl 12-isocyanododecylcarbamate (38)
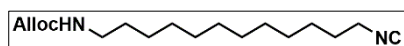
 1,12-diaminododecane (1.2 g, 6.2 mmol) is mono-alloc protected, formylated and dehydrated following the general procedure given above, to afford after purification by column chromatography the pure allyl 12-isocyanododecylcarbamate **38** (2.64 g, 69%) as a pale yellow oil. R_f = 0.78 (DCM/EtOAc 10:1). IR (KBr, cm^{-1}): υ_{max} = 3339, 2924, 2854, 2146, 1698. ^{1}H NMR (400 MHz, CDCl$_3$): δ = 5.92 (ddt, J = 16.4, 10.9, 5.6 Hz, 1H), 5.30 (d, J = 17.2 Hz, 1H), 5.21 (d, J = 10.4 Hz, 1H), 4.72 (s, 1H), 4.56 (d, J = 5.6 Hz, 2H), 3.42 – 3.32 (m, 2H), 3.17 (q, J = 6.7 Hz, 2H), 1.71 – 1.63 (m, 2H), 1.53 – 1.39 (m, 4H), 1.33 – 1.26 (m, 14H). ^{13}C NMR (101 MHz, CDCl$_3$) δ = 156.2, 155.6, 133.0, 117.5, 65.3, 41.5, 41.0, 29.9, 29.4, 29.4, 29.3, 29.2, 29.1, 28.6, 26.7, 26.3.

3.5.3. Synthesis of isocyanides containing protected carboxylic acids

3.5.3.1. (2-Trimethylsilyl) ethyl 3-isocyanopropionate (44)
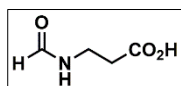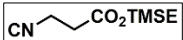
 A mixture of acetic anhydride (54 mL, 0.56 mol) and formic acid (28 mL, 0.84 mol) is stirred at 60 °C for 3 h. This mixture is cooled to room temperature, 40 mL of THF are added, and β-alanine (5.1 g, 0.056 mol) is added in portions. The reaction mixture is stirred at room temperature overnight and then concentrated in a rotary evaporator under reduced pressure to dryness. The product is precipitated with cold ether at 0ºC, washed two times, and finally placed in a high vacuum to afford the pure formylated β-alanine (6.2 g, 92%) as a white solid.
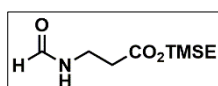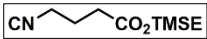
 The formylated β-alanine (5.0 g, 0.043 mol) is dissolved in DCM (20 mL) cooled to 0ºC, DMAP (0.61 g, 5 mmol), DIPEA (6.13 mL, 0.051 mol), and EDCI (9.8 g, 0.051 mol) are added and the system is stirred for 15 min. Trimethylsilylethanol (6.72 mL, 0.047 mol) is slowly added and the reaction mixture is stirred overnight at room temperature. Then, the DCM is evaporated at reduced pressure, EtOAc (60 mL) is added and

the mixture is washed with aq. NaHCO$_3$ (2×20 mL) and brine (2×20 mL), dried over anh. Na$_2$SO$_4$, concentrated under reduced pressure in a rotary evaporator to dryness and left in high vacuum for 24 h.

CN ⌒ CO$_2$TMSE   In a three-necked flask, the crude formamide is dissolved in 40 mL of dry THF and mixed with Et$_3$N (22.7 mL, 0.13 mol). The solution is cooled to 0 °C and under N$_2$ (g) atmosphere, a solution of POCl$_3$ (3.7 mL, 0.043 mol) in 15 mL of THF is added dropwise during 30 min. The resulting reaction mixture is stirred at 0 °C for 1 h, then allowed to reach room temperature and stirred for 2 h more. The reaction is quenched with 50 mL of Na$_2$CO$_3$ (10 %) and extracted with EtOAc (2×30 mL). The combined organic phases are combined, washed with brine (20 mL), dried over anh. Na$_2$SO$_4$, and concentrated under reduced pressure in a rotary evaporator to dryness to afford after column chromatography (*n*-hexane/EtOAc 4:1) the pure trimethylsilyl) ethyl 3-isocyanopropionate (**44**) (4.7 g, 65%) as pale-yellow oil. R_f = 0.62 (DCM). IR (KBr, cm^{-1}): 2955.1, 2899.0, 2149.0, 1731.7. ^{1}H NMR (400 MHz, CDCl$_3$) δ 4.23 (dd, J = 9.4, 7.7 Hz, 2H), 3.72 – 3.65 (m, 2H), 2.73 – 2.66 (m, 2H), 1.04 – 0.97 (m, 2H), 0.04 (s, 9H). ^{13}C NMR (101 MHz, cdcl$_3$) δ 169.5, 157.5, 157.4, 63.7, 37.2, 37.2, 37.1, 34.3, 17.3, -1.56.

3.5.3.2. 2-(Trimethylsilyl) ethyl 4-isocyanobutyrate (45)

CN ⌒⌒ CO$_2$TMSE   GABA (5.8 g, 0.056 mol) was subject to formylation as described above to afford the desired pure formylated GABA (5.0 g, 68%) as a pure white solid. Following the same procedure described above, trimethylsilyl) ethyl was coupled to the formylated GABA (3.9 g, 0.03 mol) and the resulting formamide was finally dehydrated to afford after column chromatography the pure 2-(trimethylsilyl)ethyl 4-isocyanobutyate (**45**) (4.5 g, 70%) as pale yellow oil. R_f = 0.69 (DCM). IR (KBr, cm^{-1}): 2954.3, 2898.3, 2147.2, 1728.2. ^{1}H NMR (400 MHz, CDCl$_3$) δ 4.24 – 4.14 (m, 2H), 3.50 (tt, J = 6.6, 1.9 Hz, 2H), 2.48 (t, J = 7.1 Hz, 2H),

2.06 – 1.93 (m, 2H), 1.04 – 0.95 (m, 2H), 0.05 (s, 9H). ^{13}C NMR (101 MHz, cdcl$_3$) δ 172.19, 156.79, 156.73, 156.68, 62.99, 40.84, 40.78, 40.71, 30.54, 24.31, 17.30, -1.54.

3.5.4. Synthesis of isocyanides containing a thiol group

9-((4-Isocyano-2-methylbutan-2-yl)thio)-9H-xanthene (50)
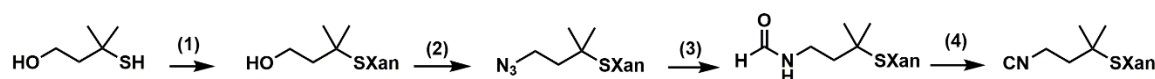
3.5.4.1. Xanthene thioether formation (50a)
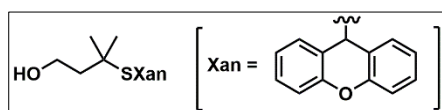
3-mercapto-3-methylbutan-1-ol (1 g, 8.3 mmol) and Xanthidrol (1.8 g, 9.1 mmol, 1.1 eq) are dissolved in 20 mL of DCM at room temperature. Under N$_2$ (g) atmoshere, TFA (0.4 mL, resulting in 2% solution) is slowly added and the reaction mixture is let to stir over night. The volatiles are removed under reduced pressure in a rotary evaporator and the crude is purified by column chromatography (n-hex/EtOAc 4:1) to afford the pure 3-((9H-xanthen-9-yl)thio)-3-methylbutan-1-ol (**50a**) (1.7 g, 68%) as colorless viscous oil. Rf (n-hex/EtOAc 4:1) = 0.28. ^{1}H NMR (500 MHz, CDCl$_3$) δ 7.52 – 7.46 (m, 2H), 7.27 – 7.20 (m, 2H), 7.11 (t, J = 7.2 Hz, 4H), 5.37 (s, 1H), 3.60 (t, J = 6.9 Hz, 2H), 1.67 (t, J = 6.9 Hz, 2H), 1.20 (s, 6H). ^{13}C NMR (126 MHz, CDCl$_3$) δ 152.48, 129.38, 128.45, 123.44, 123.42, 116.76, 59.88, 47.98, 44.72, 41.85, 30.18.

3.5.4.2. Azide formation from 50a (50b)
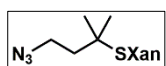
To a mixture of 3-((9H-xanthen-9-yl)thio)-3-methylbutanol (1.7 g, 5.7 mmol) and Et$_3$N (1.2 mL, 8.55 mmol) at 0 °C in DCM (20 mL), MsCl (0.53 mL, 6.8 mmol) is added dropwise for 20 min. The system is allowed to reach room temperature, stirred for 2 h and then diluted with 50 ml of CHCl$_3$ and washed with sat. solution of NaHCO$_3$ (2×20 mL) and brine (2×20 mL). The organic layer is dried oved anh. Na$_2$SO$_4$ and concentrated at reduced pressure.

The crude mesilate is dissolved in dry DMSO (20 mL) and NaN$_3$ (0.7 g, 11.4 mmol, 2 eq) is added. The mixture is stirred at 60ºC for 16 h, then is diluted with EtOAc (50 mL), extensively washed with brine and is dried oved anh. Na$_2$SO$_4$. After removing all volatiles, the crude is purified by column chromatography (n-hex/DCM 3:1) to afford the pure 9-((4-azido-2-methylbutan-2-yl)thio)-9H-xanthene (50b) (1.3 g, 71%). Rf (n-hex/DCM 1:1) = 0.47. ^{1}H NMR (400 MHz, CDCl$_3$) δ = 7.46 (d, J = 7.4 Hz, 2H), 7.30 – 7.21 (m, 2H), 7.11 (t, J = 7.5 Hz, 4H), 5.33 (s, 1H), 3.18 – 3.09 (m, 2H), 1.65 – 1.59 (m, 2H), 1.18 (s, 6H). ^{13}C NMR (101 MHz, CDCl$_3$) δ = 152.4, 129.3, 128.6, 123.5, 123.2, 116.8, 47.76, 47.6, 41.9, 40.9, 29.9.

3.5.4.3. Azide reduction and amine formylation of 50b (50c)
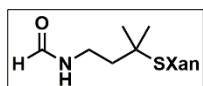
9-((4-azido-2-methylbutan-2-yl)thio)-9H-xanthene (1.1 g, 3.38 mmol) is dissolved in THF (15 mL) and a solution of Et$_3$P in THF (17 mL, 17 mmol, 1M) is added dropwise for 10 min at 0 °C. The system is allowed to reach room temperature and stirred until completion is checked by TLC (around 1h). Then, a solution NaOH (17 mL, 1M) is added and the system is stirred for an additional hour at room temperature. The reaction mixture is diluted with water (30 mL) and extracted with CHCl$_3$ (2×20 mL). The organic phases are combined, washed with brine (2×15 mL), and dried over anh. Na$_2$SO$_4$. The solvent is removed under reduced pressure in a rotary evaporator and the amine obtained is dissolved in ethyl formate (40 mL) and the solution is refluxed for 12 h. The volatiles are removed under reduced pressure in a rotary evaporator and the crude formamide is purified by column chromatography (DCM/EtOAc 6:1) to afford the pure *N*-(3-((9H-xanthen-9-yl)thio)-3-methylbutyl)formamide (**50c**) (0.71 g 64%) as a colorless viscous oil. Rf (DCM/EtOAc 5:1) = 0.51. ^{1}H NMR (400 MHz, CDCl$_3$): δ = 7.97 (d, J = 1.7 Hz, 1H), 7.53 – 7.47 (m, 2H), 7.30 – 7.24 (m, 2H), 7.11 (td, J = 7.2, 4.1 Hz, 4H), 5.37 (s, 1H), 3.22 – 3.15 (m, 2H), 1.56 – 1.48 (m, 2H), 1.14 (s, 6H). ^{13}C NMR (101 MHz, CDCl$_3$): δ = 164.2, 160.8, 152.4, 129.6, 129.5, 128.7,

128.5, 123.5, 123.5, 123.2, 122.9, 116.8, 116.7, 48.2, 47.65, 43.39, 42.22, 41.9, 41.3, 38.2, 34.63, 30.1, 29.9.

3.5.4.4. Formamide dehydration of 50c (50d)
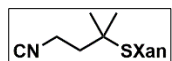
 N-(3-((9H-Xanthen-9-yl)thio)-3-methylbutyl)formamide (0.69 g, 2.1 mmol) is dissolved in 20 mL of dry DCM and mixed with NMM (0.61 mL, 5.5 mmol). The solution is cooled to -50 °C and under N_2 (g) atmosphere a solution of triphosgene (0.31 g, 1.05 mmol) in 5 mL of dry DCM is added dropwise during 10 min. The resulting reaction mixture is stirred at -50 °C for 2 h and then allowed to reach room temperature, quenched with 20 mL of a Na_2CO_3 (10 %) and extracted with $CHCl_3$ (2×20 mL). The combined organic phases are washed with brine (10 mL), dried over anh. Na_2SO_4, and concentrated under reduced pressure in a rotary evaporator to afford after column chromatography (n-hex/DCM 2:1) the pure 9-((4-isocyano-2-methylbutan-2-yl)thio)-9H-xanthene (**50 d**) (0.41 g, 63%) as pale yellow oil. R*f* (n-hex/DCM 2:1) = 0.52. IR (KBr, cm^{-1}): υ_{max} = 3041, 2962, 2917, 2862, 2147, 1658, 1601, 1577. ^{1}H NMR (500 MHz, CDCl$_3$) δ 7.52 – 7.46 (m, 2H), 7.27 – 7.20 (m, 2H), 7.11 (t, *J* = 7.2 Hz, 4H), 5.37 (s, 1H), 3.60 (t, *J* = 6.9 Hz, 2H), 1.67 (t, *J* = 6.9 Hz, 2H), 1.20 (s, 6H). ^{13}C NMR (101 MHz, CDCl$_3$): δ = 155.9, 129.2, 128.8, 123.7, 122.7, 116.9, 47.6, 42.2, 41.6, 37.9, 29.7.

3.5.5. Synthesis of lipid-tubugis, steroid-tubugi, and PEG-tubugi

3.5.5.1. Tubugi 27
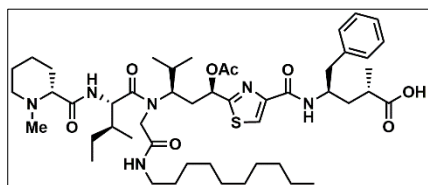
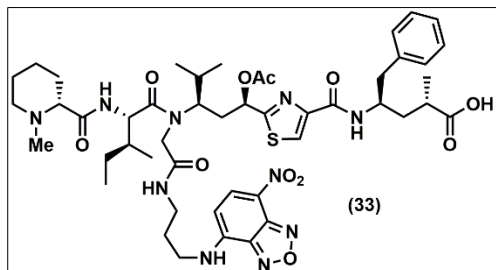 Starting from Fmoc-Tup-Wang resin (100 mg, 0.03 mmol), Fmoc-Tuv(OTBS)-OH (26.1 mg, 0.045 mmol) is coupled following the general method given in epigraph 2.5.3. After removing the Fmoc protecting group, an aminocatalysis-mediated Ugi reaction is performed using Fmoc-Ile-OH (41 mg, 0.12 mmol), paraformaldehyde (3.6 mg, 0.12 mmol), and *n*-decylisocyanide (**24**, 20 mg, 0.12 mmol) as described above. RP-HPLC analysis after mini-

cleavage showed total transformation of starting materials after performing the reaction two times, giving mainly the Ugi product but also some 10% of the undesired direct coupling product. The Fmoc protecting group is removed and *N*-Me-D-Pip-OH (17 mg, 0.12 mmol) is coupled using PyBOP (63 mg, 0.12 mmol) and NMM (27 µL, 0.12 mmol) in DMF for 2 h. The tubugi-bound resin is subjected to TBS deprotection and the subsequent acetylation. The crude peptide is finally cleaved from the resin and purified by preparative RP-HPLC to afford the pure Tubugi **27** (6.7 mg, 25%) as a white solid. R_t = 15.0 min. HR-MS *m/z*: 911.5680 [M+H]$^+$, calcd. for $C_{49}H_{79}N_6O_8S$: 911.5680. NMR data can be found in the Annexes.
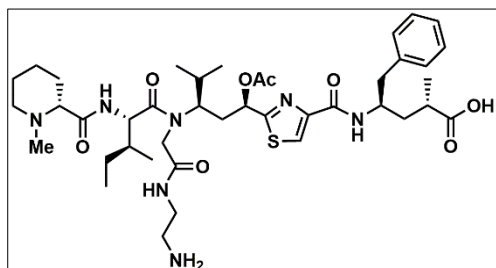
3.5.5.2. Tubugi 28
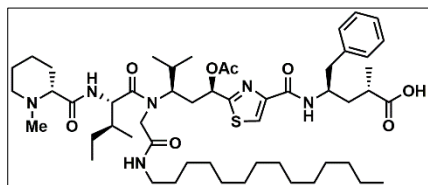
Starting from Fmoc-Tup-Wang resin (100 mg, 0.03 mmol), Fmoc-Tuv(OTBS)-OH (26.1 mg, 0.045 mmol) is coupled following the general method given in epigraph 2.5.3. After removing the Fmoc protecting group, an aminocatalysis-mediated Ugi reaction is performed using Fmoc-Ile-OH (41 mg, 0.12 mmol), paraformaldehyde (3.6 mg, 0.12 mmol), and *n*-tetradecylisocyanide (**25**, 27 mg, 0.12 mmol) as described above. RP-HPLC analysis after mini-cleavage showed that after performing the reaction two times, the total transformation of the starting material mainly in the Ugi product and also the undesired product of direct coupling in about 10%. Then, Fmoc protecting group is removed and *N*-Me-D-Pip-OH (17 mg, 0.12 mmol) is coupled using PyBOP (63 mg, 0.12 mmol) and NMM (27 µL, 0.12 mmol) in DMF for 2 h. The tubugi-bound resin is subjected to TBS deprotection and the subsequent acetylation. The crude peptide is finally cleaved from the resin and purified by preparative RP-HPLC to afford the pure Tubugi **28** (6.9 mg, 24%) as a white solid. R_t = 17.8 min. HR-MS *m/z*: 967.6329 [M+H]$^+$, calcd. for $C_{53}H_{87}N_6O_8S$: 967.6306. NMR data can be found in the Annexes.
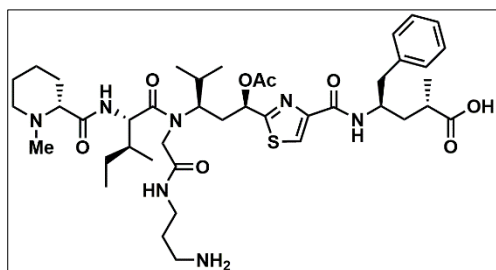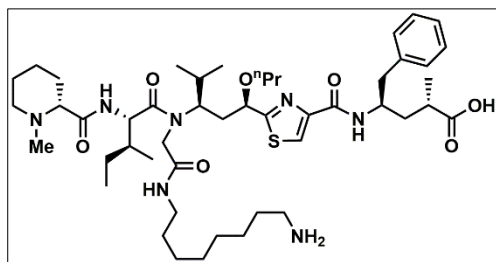
3.5.5.3. Tubugi 29
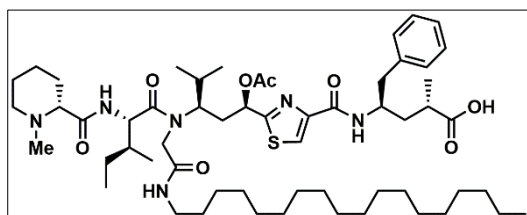
Starting from Fmoc-Tup-Wang resin (100 mg, 0.03 mmol), Fmoc-Tuv(OTBS)-OH (26.1 mg, 0.045 mmol) is coupled following the general method given in epigraph 2.5.3. After removing the Fmoc protecting group, an aminocatalysis-mediated Ugi reaction is performed using Fmoc-Ile-OH (41 mg, 0.12 mmol), paraformaldehyde (3.6 mg, 0.12 mmol), and *n*-octadecylisocyanide (**26**, 33 mg, 0.12 mmol) as described above. RP-HPLC analysis after mini-cleavage showed total transformation of starting materials after performing the reaction two times, giving mainly the Ugi product but also some 10% of the undesired direct coupling product. The Fmoc protecting group is removed and *N*-Me-D-Pip-OH (17 mg, 0.12 mmol) is coupled using PyBOP (63 mg, 0.12 mmol) and NMM (27 μL, 0.12 mmol) in DMF for 2 h. The tubugi-bound resin is subjected to TBS deprotection and the subsequent acetylation. The crude peptide is finally cleaved from the resin and purified by preparative RP-HPLC to afford the pure Tubugi **29** (6.6 mg, 22%) as a white solid. R_t = 20.9 min. HR-MS *m/z*: 1023.6925 [M+H]$^+$, calcd. for $C_{57}H_{95}N_6O_8S$: 10023.6932. NMR data can be found in the Annexes.

3.5.5.4. PEG-tubugi 31
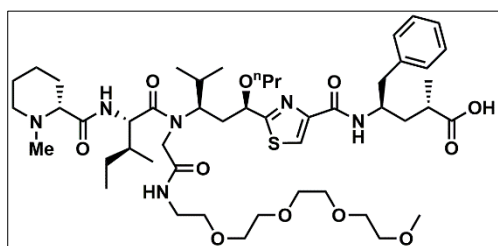
Starting from Fmoc-Tup-Wang resin **18** (100 mg, 0.03 mmol), Fmoc-Tuv(O^{n}Pr)-OH **13** (26.1 mg, 0.045 mmol) is coupled following the general method given in epigraph 2.5.3. After removing the Fmoc protecting group, an aminocatalysis-mediated Ugi reaction is performed using Fmoc-Ile-OH (41 mg, 0.12 mmol), paraformaldehyde (3.6 mg, 0.12 mmol), and MeO-PEG$_4$-NC (**30**, 26 mg, 0.12 mmol) as described above. RP-HPLC analysis after mini-cleavage showed total transformation of starting materials after performing the reaction two times, giving mainly the

Ugi product but also some 10% of the undesired direct coupling product. Then, Fmoc protecting group is removed and *N*-Me-D-Pip-OH (17 mg, 0.12 mmol) is coupled using PyBOP (63 mg, 0.12 mmol) and NMM (27 µL, 0.12 mmol) in DMF for 2 h. The crude peptide is finally cleaved from the resin and purified by preparative RP-HPLC to afford the pure Tubugi **31** (6.0 mg, 21%) as a white amorphous solid. R_t = 11.9 min. HR-MS *m/z*: 961.5703 [M+H]$^+$, calcd. for $C_{49}H_{81}N_6O_{11}S$: 961.5684. NMR data can be found in the Annexes.
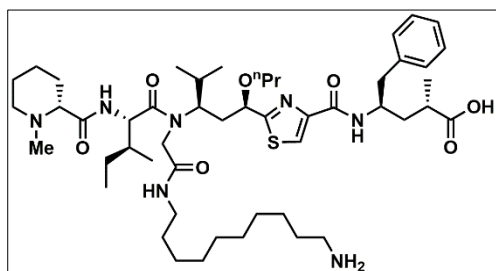
3.5.5.5. Tubugi 32

Starting from Fmoc-Tup-Wang resin (100 mg, 0.03 mmol), Fmoc-Tuv(OTBS)-OH (26.1 mg,
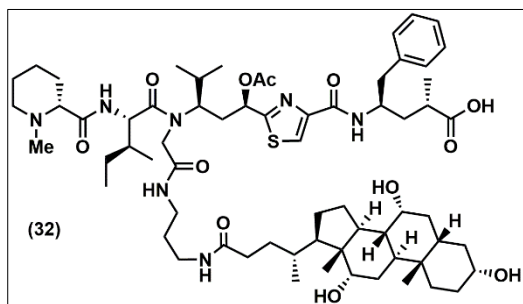
0.045 mmol) is coupled following the general method given in epigraph 2.5.3. After removing the Fmoc protecting group, an aminocatalysis-mediated Ugi reaction is performed using Fmoc-Ile-OH (41 mg, 0.12 mmol), paraformaldehyde (3.6 mg, 0.12 mmol), and Allyl 2-isocyanoethylcarbamate (19 mg, 0.12 mmol) as described above. RP-HPLC analysis after mini-cleavage showed total transformation of starting materials after performing the reaction two times, giving mainly the Ugi product but also some 10% of the undesired direct coupling product. The Fmoc protecting group is removed and *N*-Me-D-Pip-OH (17 mg, 0.12 mmol) is coupled using PyBOP (63 mg, 0.12 mmol) and NMM (27 µL, 0.12 mmol) in DMF for 2 h. Alloc protecting group is removed by washing the resin with dry DCM (2×2 min) under a stream of nitrogen. A solution of phenylsilane (20 equiv) in dry DCM and tetrakis(triphenylphosphine) palladium(0) (0.2 equiv) are added to the resin under a continuous stream of nitrogen. The reaction mixture is stirred in the dark for 15 min, and the procedure is repeated once and then washed with 0.5% of sodium diethyldithiocarbamate trihydrate in DMF (5×2 min) and DCM (2×2 min). Cholic acid (49 mg, 0.12 mmol) is coupled using PyBOP (63 mg, 0.12 mmol) and NMM (27 µL, 0.12 mmol) in DMF for 2 h. The crude peptide is finally cleaved from the resin and purified by preparative

RP-HPLC to afford the pure Tubugi **32** (8.3 mg, 23%) as a white solid. HR-MS *m/z*: 609.9969 $[M+2H]^{2+}$, calcd. for $C_{67}H_{109}N_7O_{11}S$: 609.8952. NMR data can be found in the Annexes.
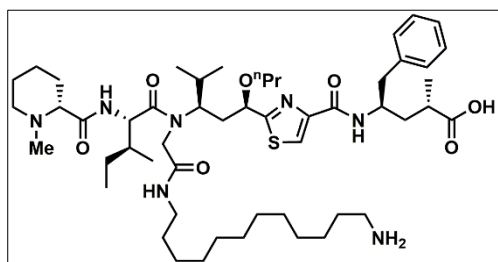
3.5.5.6. Tubugis 33

Starting from Fmoc-Tup-Wang resin (100 mg, 0.03 mmol), Fmoc-Tuv(OTBS)-OH (26.1 mg, 0.045 mmol) is coupled following the general method given in epigraph 2.5.3. After removing the Fmoc protecting group, an aminocatalysis-mediated Ugi reaction is performed using Fmoc-Ile-OH (41 mg, 0.12 mmol), paraformaldehyde (3.6 mg, 0.12 mmol), and Allyl 3-isocyanoproylcarbamate (20 mg, 0.12 mmol) as described above. RP-HPLC analysis after mini-cleavage showed total transformation of starting materials after performing the reaction two times, giving mainly the Ugi product but also some 10% of the undesired direct coupling product. The Fmoc protecting group is removed and *N*-Me-D-Pip-OH (17 mg, 0.12 mmol) is coupled using PyBOP (63 mg, 0.12 mmol) and NMM (27 µL, 0.12 mmol) in DMF for 2 h. The tubugi-bound resin is subjected to TBS deprotection and the subsequent acetylation. Alloc protecting group is removed by treating the resin with a solution of phenylsilane (20 equiv) in dry DCM and tetrakis(triphenylphosphine) palladium (0) (0.2 equiv) under a continuous stream of nitrogen. The reaction mixture is stirred in the dark for 15 min, and the procedure is repeated once, then washed with 0.5% of sodium diethyldithiocarbamate trihydrate in DMF (5×2 min) and DCM (2×2 min). 4-Chloro-7-nitrobenzofurazan (24 mg, 0.12 mmol) is attached to the peptide by adding it mixed with NMM (27 µL, 0.12 mmol) in DMF for 12 h. The crude peptide is finally cleaved from the resin and purified by preparative RP-HPLC to afford the pure Tubugi **33** (6.6 mg, 21%) as a white solid. R_t = 10.3 min. HR-MS *m/z*: 991.4749 $[M+H]^+$, calcd. for $C_{49}H_{71}N_{10}O_{10}S$: 991.4711. NMR data can be found in the Annexes.

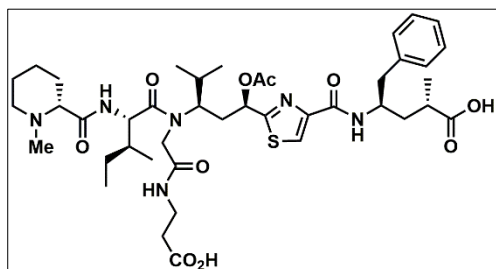### 3.5.6. Synthesis of amino tubugis

3.5.6.1. Tubugi 39

Starting from Fmoc-Tup-Wang resin (100 mg, 0.03 mmol), Fmoc-Tuv(On-Pr)-OH (22.9 mg, 0.045 mmol) is coupled following the general method given in epigraph 2.5.3. After removing the Fmoc protecting group, an aminocatalysis-mediated Ugi reaction is performed using Fmoc-Ile-OH (41 mg, 0.12 mmol), paraformaldehyde (3.6 mg, 0.12 mmol), and *t*-butyl 2-isocyanoethylcarbamate (**34**, 20 mg, 0.12 mmol) as described above. RP-HPLC analysis after mini-cleavage showed total transformation of starting materials after performing the reaction two times, giving mainly the Ugi product but also some 10% of the undesired direct coupling product. The Fmoc protecting group is removed and *N*-Me-D-Pip-OH (17 mg, 0.12 mmol) is coupled using PyBOP (63 mg, 0.12 mmol) and NMM (27 µL, 0.12 mmol) in DMF for 2 h. The crude peptide is finally cleaved from the resin and purified by preparative RP-HPLC to afford the pure Tubugi **39** (4.0 mg, 16%) as a white solid. R_t = 11.6 min. HR-MS *m/z*: 407.7516 $[M+2H]^{2+}$, calcd. for $C_{42}H_{69}N_7O_7S$: 407.7490. NMR data can be found in the Annexes.
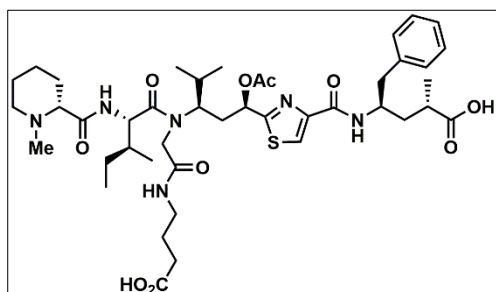
3.5.6.2. Tubugi 40

Starting from Fmoc-Tup-Wang resin (100 mg, 0.03 mmol), Fmoc-Tuv(OTBS)-OH (26.1 mg, 0.045 mmol) is coupled following the general method given in epigraph 2.5.3. After removing the Fmoc protecting group, an aminocatalysis-mediated Ugi reaction is performed using Fmoc-Ile-OH (41 mg, 0.12 mmol), paraformaldehyde (3.6 mg, 0.12 mmol), and *t*-Butyl 3-isocyanopropylcarbamate (**35**, 22 mg, 0.12 mmol) as described above. RP-HPLC analysis after

mini-cleavage showed total transformation of starting materials after performing the reaction two times, giving mainly the Ugi product but also some 10% of the undesired direct coupling product. The Fmoc protecting group is removed and *N*-Me-D-Pip-OH (17 mg, 0.12 mmol) is coupled using PyBOP (63 mg, 0.12 mmol) and NMM (27 μL, 0.12 mmol) in DMF for 2 h. The tubugi-bound resin is subjected to TBS deprotection and the subsequent acetylation. The crude peptide is finally cleaved from the resin and purified by preparative RP-HPLC to afford the pure Tubugi **40** (4.3 mg, 17%) as a white solid. R_t = 11.9 min. HR-MS *m/z*: 414.7412 $[M+2H]^{2+}$, calcd. for $C_{42}H_{67}N_7O_8S$: 414.7386. NMR data can be found in the Annexes.
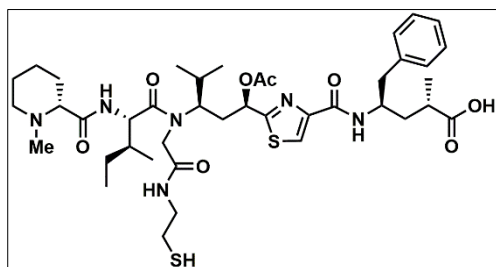
3.5.6.3. Tubugi 41

Starting from Fmoc-Tup-Wang resin (100 mg, 0.03 mmol), Fmoc-Tuv(OnPr)-OH (22.9 mg, 0.045 mmol) is coupled following the general method given in epigraph 2.5.3. After removing the Fmoc protecting group, an aminocatalysis-mediated Ugi reaction is performed using Fmoc-Ile-OH (41 mg, 0.12 mmol), paraformaldehyde (3.6 mg, 0.12 mmol), and Allyl 8-isocyanooctylcarbamate (**36**, 27 mg, 0.12 mmol) as described above. RP-HPLC analysis after mini-cleavage showed total transformation of starting materials after performing the reaction two times, giving mainly the Ugi product but also some 10% of the undesired direct coupling product. The Fmoc protecting group is removed and *N*-Me-D-Pip-OH (17 mg, 0.12 mmol) is coupled using PyBOP (63 mg, 0.12 mmol) and NMM (27 μL, 0.12 mmol) in DMF for 2 h. Alloc protecting group is removed by adding a solution of phenylsilane (20 equiv) in dry DCM and tetrakis(triphenylphosphine)palladium (0) (0.2 equiv) to the resin under a continuous stream of nitrogen. The reaction mixture is stirred in the dark for 15 min, and the procedure is repeated once again and then washed with 0.5% of sodium diethyldithiocarbamate trihydrate in DMF (5×2 min) and DCM (2×2 min). The crude peptide is finally cleaved from the resin and purified

by preparative RP-HPLC to afford the pure Tubugi **41** (5.6 mg, 21%) as a white solid. $R_t = 10.3$, 10.9 min. HR-MS *m/z*: 449.7978 $[M+2H]^{2+}$, calcd. for $C_{48}H_{79}N_7O_7S$: 449.7959. NMR data can be found in the Annexes.
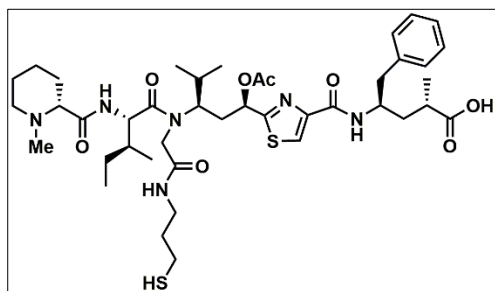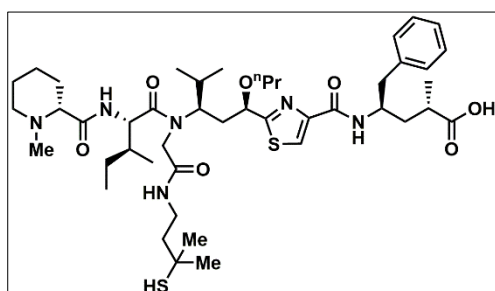
3.5.6.4. Tubugi 42

Starting from Fmoc-Tup-Wang resin (100 mg, 0.03 mmol), Fmoc-Tuv(O^{n}Pr)-OH (22.9 mg, 0.045 mmol) is coupled following the general method given in epigraph 2.5.3. After removing the Fmoc protecting group, an aminocatalysis-mediated Ugi reaction is performed using Fmoc-Ile-OH (41 mg, 0.12 mmol), paraformaldehyde (3.6 mg, 0.12 mmol) and Allyl 10-isocyanodecylcarbamate (**37**, 30 mg, 0.12 mmol) as described above. RP-HPLC analysis after mini-cleavage showed total transformation of starting materials after performing the reaction two times, giving mainly the Ugi product but also some 10% of the undesired direct coupling product. The Fmoc protecting group is removed and *N*-Me-D-Pip-OH (17 mg, 0.12 mmol) is coupled using PyBOP (63 mg, 0.12 mmol) and NMM (27 μL, 0.12 mmol) in DMF for 2 h. The alloc protecting group is removed by adding a solution of phenylsilane (20 equiv) in dry DCM and tetrakis(triphenylphosphine) palladium(0) (0.2 equiv) to the resin under a continuous stream of nitrogen. The reaction mixture is stirred in the dark for 15 min, and the procedure is repeated once again and then washed with 0.5% of sodium diethyldithiocarbamate trihydrate in DMF (5×2 min) and DCM (2×2 min). The crude peptide is finally cleaved from the resin and purified by preparative RP-HPLC to afford the pure Tubugi **42** (7.8 mg, 28%) as a white solid. $R_t = 10.6$, 11.6 min. HR-MS *m/z*: 463,8136 $[M+2H]^{2+}$, calcd. for $C_{50}H_{85}N_7O_7S$: 463.8116. NMR data can be found in the Annexes.

3.5.6.5. Tubugi 43

Starting from Fmoc-Tup-Wang resin (100 mg, 0.03 mmol), Fmoc-Tuv(O^{n}Pr)-OH (22.9 mg, 0.045 mmol) is coupled following the general method given in epigraph 2.5.3. After removing the Fmoc protecting group, an aminocatalysis-mediated Ugi reaction is performed using Fmoc-Ile-OH (41 mg, 0.12 mmol), paraformaldehyde (3.6 mg, 0.12 mmol), and Allyl 12-isocyanododecylcarbamate (**38**, 34 mg, 0.12 mmol) as described above. RP-HPLC analysis after mini-cleavage showed total transformation of starting materials after performing the reaction two times, giving mainly the Ugi product but also some 10% of the undesired direct coupling product. The Fmoc protecting group is removed and *N*-Me-D-Pip-OH (17 mg, 0.12 mmol) is coupled using PyBOP (63 mg, 0.12 mmol) and NMM (27 µL, 0.12 mmol) in DMF for 2 h. Alloc protecting group is removed by adding a solution of phenylsilane (20 equiv) in dry DCM and tetrakis(triphenylphosphine)palladium(0) (0.2 equiv) to the resin under a continuous stream of nitrogen. The reaction mixture is stirred in the dark for 15 min, and the procedure is repeated once again and then washed with 0.5% of sodium diethyldithiocarbamate trihydrate in DMF (5×2 min) and DCM (2×2 min). The crude peptide is finally cleaved from the resin and purified by preparative RP-HPLC to afford the pure Tubugi **43** (8.6 mg, 30%) as a white solid. R$_t$ = 11.1, 11.9 min. HR-MS *m/z*: 477.8336 [M+2H]$^{2+}$, calcd. for C$_{52}$H$_{89}$N$_7$O$_7$S: 477.8272. NMR data can be found in the Annexes.

3.5.7. Synthesis of carboxylic acids tubugis

3.5.7.1. Tubugi 46

Starting from Fmoc-Tup-Wang resin (100 mg, 0.03 mmol), Fmoc-Tuv(O^{n}Pr)-OH (22.9 mg, 0.045 mmol) is coupled following the general method given in epigraph 2.5.3. After removing the Fmoc protecting group, an aminocatalysis-mediated Ugi reaction is performed using Fmoc-Ile-OH (41 mg, 0.12 mmol), paraformaldehyde (3.6 mg, 0.12 mmol) and 2-(trimethylsilyl)ethyl 3-isocyanopropionate (**44**, 24 mg, 0.12 mmol) as described above. RP-HPLC analysis after mini-cleavage showed total transformation of starting materials after performing the reaction two times, giving mainly the Ugi product but also some 10% of the undesired direct coupling product. The Fmoc protecting group is removed and *N*-Me-D-Pip-OH (17 mg, 0.12 mmol) is coupled using PyBOP (63 mg, 0.12 mmol) and NMM (27 µL, 0.12 mmol) in DMF for 2 h. The crude peptide is finally cleaved from the resin and purified by preparative RP-HPLC to afford the pure Tubugi **46** (3.4 mg, 13%) as a white solid. R_t = 11.8, 13.0 min. HR-MS *m/z*: 843.4637 [M+H]$^+$, calcd. for C$_{43}$H$_{67}$N$_6$O$_9$S: 843.4690. NMR data can be found in the Annexes.

3.5.7.2. Tubugi 47

Starting from Fmoc-Tup-Wang resin (100 mg, 0.03 mmol), Fmoc-Tuv(OTBS)-OH (26.1 mg, 0.045 mmol) is coupled following the general method given in epigraph 2.5.3. After removing the Fmoc protecting group, an aminocatalysis-mediated Ugi reaction is performed using Fmoc-Ile-OH (41 mg, 0.12 mmol), paraformaldehyde (3.6 mg, 0.12 mmol), and 2-(trimethylsilyl)ethyl 4-isocyanobutyate (**45**, 26 mg, 0.12 mmol) as described

above. RP-HPLC analysis after mini-cleavage showed total transformation of starting materials after performing the reaction two times, giving mainly the Ugi product but also some 10% of the undesired direct coupling product. The Fmoc protecting group is removed and *N*-Me-D-Pip-OH (17 mg, 0.12 mmol) is coupled using PyBOP (63 mg, 0.12 mmol) and NMM (27 μL, 0.12 mmol) in DMF for 2 h. The tubugi-bound resin is subjected to TBS deprotection and the subsequent acetylation. The crude peptide is finally cleaved from the resin and purified by preparative RP-HPLC to afford the pure Tubugi **47** (3.9 mg, 15%) as a white solid. $R_t = 12.0$ min. HR-MS *m/z*: 857.4593 $[M+H]^+$, calcd. for $C_{43}H_{65}N_6O_{10}S$: 857.4483. NMR data can be found in the Annexes.

3.5.8. Synthesis of thiol tubugis

3.5.8.1. Tubugi 51

tarting from Fmoc-Tup-Wang resin (100 mg, 0.03 mmol), Fmoc-Tuv(O^{n}Pr)-OH (22.9 mg, 0.045 mmol) is coupled following the general method given in epigraph 2.5.3. After removing the Fmoc protecting group, an aminocatalysis-mediated Ugi reaction is performed using Fmoc-Ile-OH (41 mg, 0.12 mmol), paraformaldehyde (3.6 mg, 0.12 mmol), and 2-(tritylthio)ethylisocyanide (39 mg, 0.12 mmol) as described above. RP-HPLC analysis after mini-cleavage showed total transformation of starting materials after performing the reaction two times, giving mainly the Ugi product but also some 10% of the undesired direct coupling product. The Fmoc protecting group is removed and *N*-Me-D-Pip-OH (17 mg, 0.12 mmol) is coupled using PyBOP (63 mg, 0.12 mmol) and NMM (27 μL, 0.12 mmol) in DMF for 2 h. The crude peptide is finally cleaved from the resin with TFA/TIPS/EDT/H$_2$O 91.3:3:3 and purified by preparative RP-HPLC to afford the pure Tubugi **51** (3.2 mg, 13%) as a white solid. $R_t = 12.6$, 13.3 min. HR-MS *m/z*: 831.4546 $[M+H]^+$, calcd. for $C_{42}H_{67}N_6O_7S_2$: 831.4512. NMR data can be found in the Annexes.

3.5.8.2. Tubugi 52

Starting from Fmoc-Tup-Wang resin (100 mg, 0.03 mmol), Fmoc-Tuv(O^{n}Pr)-OH (22.9 mg, 0.045 mmol) is coupled following the general method given in epigraph 2.5.3. After removing the Fmoc protecting group, an aminocatalysis-mediated Ugi reaction is performed using Fmoc-Ile-OH (41 mg, 0.12 mmol), paraformaldehyde (3.6 mg, 0.12 mmol), and 3-(tritylthio)propylisocyanide (43 mg, 0.12 mmol) as described above. RP-HPLC analysis after mini-cleavage showed total transformation of starting materials after performing the reaction two times, giving mainly the Ugi product but also some 10% of the undesired direct coupling product. The Fmoc protecting group is removed and *N*-Me-D-Pip-OH (17 mg, 0.12 mmol) is coupled using PyBOP (63 mg, 0.12 mmol) and NMM (27 µL, 0.12 mmol) in DMF for 2 h. The crude peptide is finally cleaved from the resin with TFA/TIPS/EDT/H$_2$O 91.3:3:3 and purified by preparative RP-HPLC to afford the pure Tubugi **52** (3.5 mg, 14%) as a white solid. R_t = 12.4, 13.2 min. HR-MS *m/z*: 845.4605 [M+H]$^+$, calcd. for C$_{43}$H$_{69}$N$_6$O$_7$S$_2$: 845.4669. NMR data can be found in the Annexes.

3.5.8.3. Tubugi 53

Starting from Fmoc-Tup-Wang resin (100 mg, 0.03 mmol), Fmoc-Tuv(O^{n}Pr)-OH (22.9 mg, 0.045 mmol) is coupled following the general method given in epigraph 2.5.3. After removing the Fmoc protecting group, an aminocatalysis-mediated Ugi reaction is performed using Fmoc-Ile-OH (41 mg, 0.12 mmol), paraformaldehyde (3.6 mg, 0.12 mmol), and 3-(tritylthio)propylisocyanide (**50**, 43 mg, 0.12 mmol) as described above. RP-HPLC analysis after mini-cleavage showed total transformation of starting materials after performing the reaction two times, giving mainly the Ugi product but also some 10% of the undesired direct coupling product. The Fmoc protecting

group is removed and *N*-Me-D-Pip-OH (17 mg, 0.12 mmol) is coupled using PyBOP (63 mg, 0.12 mmol) and NMM (27 µL, 0.12 mmol) in DMF for 2 h. The crude peptide is finally cleaved from the resin with TFA/TIPS/EDT/H_2O 91.3:3:3 and purified by preparative RP-HPLC to afford the pure Tubugi **53** (4.7 mg, 18%) as a white solid. R_t = 13.5, 14.7 min.HR-MS *m/z*: 873.5013 $[M+H]^+$, calcd. for $C_{45}H_{72}N_6O_7S_2$: 873.4982. NMR data can be found in the Annexes.

3.5.9. *In vitro* cell-based assays

The tubugi derivatives were tested in three different *in vitro* cell-based assays, namely cell viability assays for IC_{50} value determination, fluorescence microscopic inspection, and flow cytometric investigations for deeper insights into the mode of the tubugis' internalization inside the cancer cells. For these experiments, two human cancer cell lines were used, namely PC-3 and HCT-116.

The prostate cancer cell line PC-3 was cultured in RPMI 1640 medium supplemented with 10% heat-inactivated FCS and 2 mM L-glutamine. HCT-116 colorectal cancer cells were cultured in DMEM supplemented with 10% not heat-inactivated FCS and 2 mM L-glutamine. All cells were routinely cultured in T-75 flasks in a humidified atmosphere with 5% CO_2 at 37°C to reach subconfluency (~ 70-80%) prior to subsequent sub-culturing or assay usage. The adherent cells were rinsed with PBS and detached using trypsin/EDTA (0.05% in PBS) prior to cell passaging and seeding [R1]. Both human cancer cell lines were purchased from ATCC (Manassas, USA). Media and supplements for cell culturing were purchased from Capricorn Scientific GmbH (Ebsdorfergrund, Germany). All cell culture plastics were purchased from TPP (Trasadingen, Switzerland) or Greiner Bio-One GmbH (Frickenhausen, Germany).

3.5.9.1 *In vitro* cell viability assay

Anti-proliferative and cytotoxic effects of the tubulysin derivatives were investigated using a fluorometric resazurin-based cell viability assay [R2]. Resazurin, purchased from Sigma-Aldrich (Taufkirchen, Germany), was prepared as 50x (2.5 mM) stock solution in sterile filtered aqua bidest. and stored at 4°C with light protection. To assay the test items, human prostate PC-3 and colorectal HCT-116 cancer cells were seeded in low densities into 96-well plates (4,000 – 6,000 cells per well; seeding confluency ~ 10%), and were allowed to adhere for 24 h. Subsequently, the compounds – diluted to appropriate concentration series covering the pico- and nanomolar range using the respective culture media – were added to the cells (100 µL/96-well) for a 48h treatment under standard growth conditions. There should be mentioned, that at very high dilutions, lipophilic compounds can be absorbed to lipophilic (plastic) vial walls and thus distort measurements (causing higher than real IC_{50} values to be measured). For control measures, cells were treated in parallel with 0.5% (*v/v*) DMSO (negative control, representing the DMSO content of the highest test item concentration; Duchefa Biochemie, Haarlem, The Netherlands) and 100 µM digitonin (positive control, for data normalization set to 0% cell viability; Sigma-Aldrich, Taufkirchen, Germany), both in standard growth medium. After 48 h cell treatment, the incubation medium was discarded, and cells were rinsed once with PBS (100 µL/96-well). A 1X (50 µM) resazurin working solution was prepared freshly in basal culture medium, added to the treated cells (100 µL/96-well) that were subsequently incubated for further 2 h under standard growth conditions. Each data point was determined in technical triplicates and at least 3-4 biological replicates. The conversion of resazurin to resorufin by the remaining portion of viable, metabolically active cells was fluorometrically measured (exc.: 540 nm/em.: 590 nm) using a SpectraMax M5 multiwell plate reader (Molecular Devices, San Jose, USA). For non-linear regression analyses of the data GraphPad Prism 8.0.2 software was used to calculate IC_{50} values.

3.5.9.2 *Fluorescence Microscopic Inspection of Tubugi Internalization*

Fluorescence microscopy photographs were taken to visualize the cancer cell internalization of the NBD-labeled Tubugi **33**. For that purpose, PC-3 cancer cells – grown in T-75 flasks to reach subconfluency, as described above – were harvested and seeded with 10,000 cells/well in 8-well chamber slides (ibidi GmbH, Gräfelfing, Germany). When reaching ~80% cell confluency, the PC-3 cells were treated with 10 µM of Tubugi **33** (in basal RPMI 1640 medium without supplements and without phenol red) for several incubation durations, namely 1 min, 20 min, 40 min, 1h, 1.5 h, and 2h. Whereby the 1 min incubation was intended as a "treated but no internalization" control and reference. During Tubugi **33** incubation, the cells were maintained under standard growth conditions in the incubator. 10 min prior to the end of the incubation period the cells' nuclei were stained by adding Hoechst 33342 dye (1:100 *v/v*; final concentration 5 µg/mL). In case of the 1min incubation, the nuclei staining was done before adding Tubugi **33**. As soon as the incubation periods were finished, the incubation solutions were discarded and the PC-3 cells were washed once with ice-cold PC-3 complete medium. Subsequently, ice-cold 0.1% Trypan Blue solution (1:5 *v/v*; Sigma-Aldrich, Taufkirchen, Germany) was added to each well in order to quench extracellular NBD fluorescence. After 3 min the Trypan Blue quenching solution was discarded again, and the cells were washed once again with basal RPMI 1640 medium without supplements and without phenol red. The following fluorescence microscopic inspection was done under the same medium using an EVOS® FL Auto Imaging System (Thermo Fisher Scientific/Life Technologies, Carlsbad, USA) with GFP filter cube for NBD imaging and DAPI filter cube for Hoechst 33342 imaging.

3.5.9.3 Flow Cytometric Investigation of Tubugi Internalization

The cellular internalization of the NBD-labeled Tubugi **33** was analyzed in more detail by conducting flow cytometric analyses. In this sense, experiments varying the application time and the concentration of Tubugi **33** as well as the temperature of cell treatment were executed.

For that purpose, PC-3 cancer cells – grown in T-75 flasks to reach subconfluency, as described above – were harvested and seeded with 25,000 cells/well in 24-well plates. When reaching ~ 60% cell confluency, the PC-3 cells were treated with 1 µM, 5 µM and 10 µM, respectively, of Tubugi **33** (in basal RPMI 1640 medium without supplements and without phenol red) at 37 °C for 1 min, 30 min, 1 h, 2 h, and 3 h (the 1 min treatment was intended as a "treated but no internalization" control). This experiment setup allowed for both the investigation of the concentration and time dependency of the internalization process. Furthermore, a comparable study was done maintaining the cells during the whole incubation phase at 4°C instead of 37°C, in order to investigate the temperature – and consequently energy – dependency of the internalization of Tubugi **33**. As soon as the desired incubation time was finished, the incubation medium was discarded, and the cells were very gently washed once with the basal cell medium RPMI 1640 without any supplements and without phenol red. Afterwards, the cells were detached from the 24-well plate using trypsin/EDTA (0.05% in PBS), and carefully resuspended in ice-cold RPMI 1640 complete medium, including 10% FCS to stop the trypsin activity. All samples were hold on ice until measurement. Directly prior the flow cytometric measurement each sample was mixed with ice-cold trypan blue solution (in RPMI 1640 basal medium; final concentration of 0.1% *v/v* per sample) to quench NBD fluorescence of not internalized Tubugi **33** that might remain unspecifically bound to the outer surface of the cell membrane. The flow cytometric measurement was done using a FACSAria^{TM} III device (Becton Dickinson GmbH, Heidelberg, Germany) analyzing 10,000 cells per sample. Data analyses were done using Cyflogic software version 1.2.1.

Chapter 4

Design and synthesis of novel PDCs based on the conjugation of bombesin analogs with *N*-functionalized tubugis
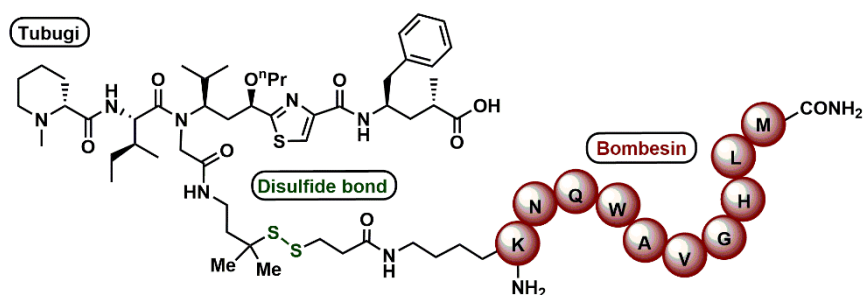
Abstract

Recently, peptide–drug conjugates (PDCs) have attracted increased attention in targeted delivery therapeutics. The accumulated experience shows favorable pharmacokinetic properties, lower-cost production, and in general a lower antigenicity (immune reaction) and more defined chemical composition when compared with antibody-drug conjugates (ADCs), among other factors, explains the rapidly rising interest and demand. Here, we designed and synthesized novel PDCs based on the conjugation of especially functionalized tubugis to Bombesin, a targeting peptide with important applications in cancer treatment. Using disulfide-based linker chemistry with proven stability, and selective cleavage properties, three different Bombesin-tubugi conjugates were obtained. The cell proliferation profiles of these new PDCs were investigated in in vitro experiments. They showed notable selectivity and high cytotoxic activity, which converts them into motivating candidates for further anticancer studies.

4.1. Introduction

In the last decades, peptide-drug conjugates (PDCs) are experiencing increased attention in anticancer research.[8][9] PDCs are advantageous in comparison with ADCs considering the well-defined and homogenous structure, low immunogenicity, and better performance regarding efficient distribution due to the smaller size.[81][9] Additionally, the well-established peptide synthesis is less time consuming, cheaper, pyrogen free and without animal requirements. All this is a tremendous advantage in PDCs regarding regulatory demands for registration and further drug manufacture. Peptides used in PDCs target. e.g., receptors overexpressed on cancer cell surfaces ideally with high affinity.[82] Some examples include Somatostatin, Gonadotropin-releasing hormone, Gastrin-releasing peptide (GRP), neuropeptide Y, RGD-peptides, etc.[83,84]

Among of the different receptor families, G-protein-coupled receptors (GPCRs) are among the most prominent therapeutic targets in cancers. Activation of GPCRs of tumor cells can have prominent growth effects, and GPCRs are frequently over-/ectopically expressed and thus can be used for targeted therapy. An important peptide that has shown an intensive request for targeting cancer cells in the last decades is Bombesin (BBN), a 14-residue neuropeptide with a high affinity for GRP receptors (GRPRs).[85][86] Bombesin is a natural peptide isolated from the skin of the *Bombina bombina* frog in 1972, extensively applied for tumor imaging and treatment. [20][87][88] The high cancer receptor specificity suggests that it could be advantageous in the efficient delivery of drugs into cancer cells. One of the major requirements in choosing the best drug candidate is a low IC$_{50}$, typically below the nanomolar range. Tubulysins, and per consequence their derivatives, the more easily and stable tubugis, are considered some of the most potent anticancer compounds and therefore highly promising for targeted delivery.[67] Here, we aim at design and synthesis of novel PDCs, based on the combination of Bombesin

peptide with tubugis. The construction is based on the use of the best candidates functionalized with thiol groups through the *N*-side chain (tertiary amide) of the tubugis and Bombesin.

4.2. Synthesis of Bombesin peptide bearing a thiol-functionalized linker

Toth and co-workers demonstrated that the first nine amino acids from the *C*-terminus of Bombesin peptide (Asn-Gln-Trp-Ala-Val-Gly-His-Leu-Met) are sufficient to reproduce the ability of the natural peptide to target GRPRs.[7] A truncated version of bombesin (BBN (6-14) -NH$_2$), was designed with an additional Lys residue at the *N*-terminus to facilitate further functionalization. Using the amino group of the Lys-side chain, in a simple amide coupling, they were able to introduce a fluorescent label that allowed the visualization of its binding to different cancer cell lines.[86]These data suggest that the truncated BBN (6–14) peptide, owing to its shorter sequence, would be preferable for incorporation into GRPR-based targeted drug delivery systems.

Taking advantage of the proposed model, we planned synthesizing a Lys-BBN (6-14)-NH$_2$ bearing an additional linker connected to the Lys-side chain. The chosen linker would be responsible for the connection between the drug and the peptide, in a way that it will foster the specific cleavage inside the cell. Among all the functionalized tubugis described in the present document, the thiol-modified ones certainly stand out due to their higher activity compared to most other examples. Moreover, the thiol group offers the possibility of applying the classic disulfide-bond chemistry for conjugation, a very straightforward and one of the most recurrent strategies in the creation of either ADCs or PDCs. Consequently, the envisioned bifunctional linker would require the presence of a thiol group and an additional carboxylic acid for the linkage to the Lys side chain at the *N*-terminus of the bombesin sequence.

As shown in scheme 4.1, following a reported strategy[89], linker **54** was synthesized starting from 3-mercaptopropionic acid in one single step. As thiol-protecting group, 2-pyridine-disulfide was chosen because it will not only ensure the (pH-dependent) stability of the thiol group upon peptide coupling and cleavage, but it also serves as an electrophilic activator of the disulfide bond as required in the further conjugation strategy.
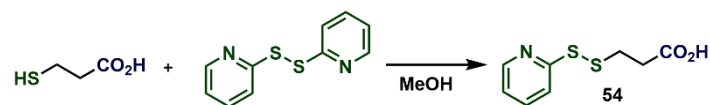
Scheme 4.1. Synthesis of a bifunctional linker having a protected thiol-group and a carboxylic acid.

The Bombesin assembly was performed automatically in an Intavis SL synthesizer, using Fmoc/tBu strategy on TG-S-RAM resin on a 0.05 mmol scale. As shown in scheme 4.2, two different Bombesin derivatives were synthesized. Bombesin **56,** was obtained by introducing the linker **54** via direct coupling using DIC as an activating agent. On the other hand, the incorporation of the linker in the Bombesin derivative **57**, was achieved following a more elaborated strategy. Here, we took advantage of our experience in multicomponent reactions and implemented the simultaneous incorporation of the desired linker and an additional lipid tail. The presence of the lipid moiety is anticipated to improve cell membrane permeabilization compared with bombesin derivative **56**. It also can be used to control the redox properties and sensitivity of disulfide cleavage. As previously detailed, the Ugi-4CR was executed in two stages: first, the imine was formed via an organocatalysis-based process, and later the linker **54** (carboxylic acid component) and the lipid-isocyanide were added. This mixture was left to react for 48 h at room temperature. Final cleavage using the standard acid cocktail TFA/TIS/H_2O (94:3:3 *v/v/v*) afforded the final bombesin candidates. Analytic RP-HPLC showed a sufficiently good purity (84 %) for Bombesin **56** and therefore it was used in the conjugation experiments without additional purification.
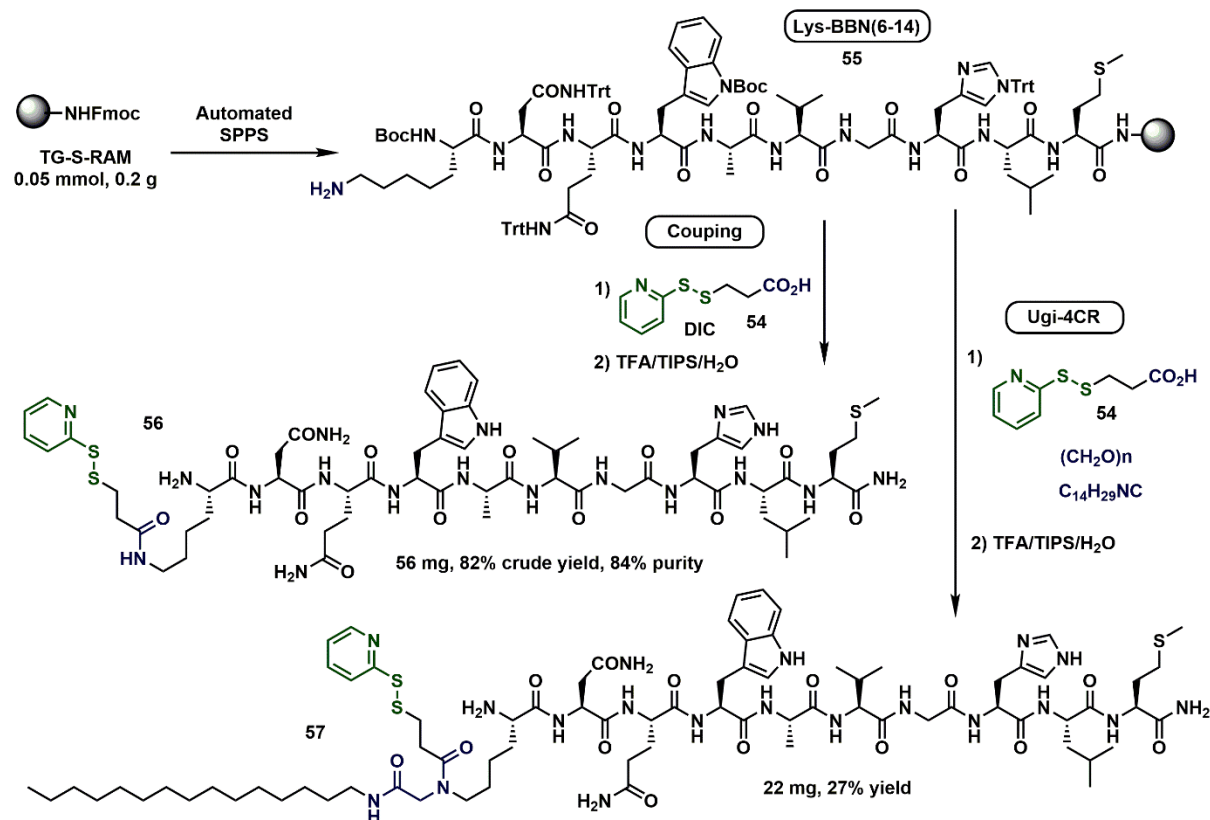
Scheme 4.2. Solid-phase synthesis of Bombesin peptides **56** and **57** having a linker functionalized with a thiol group, and in **57** additionally with a variable alkyl-amide side chain.

However, for Bombesin **57** with its more complex synthesis an additional preparative RP-HPLC purification was required, affording the compound **57** in 27% final yield and purity over 90% (Figure 4.1).
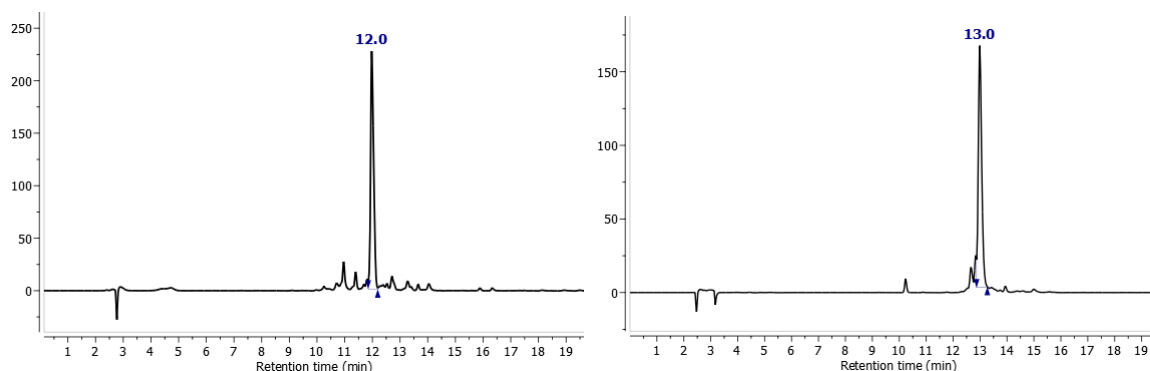
Figure 4.1. A) RP-HPLC trace of crude Bombesin peptide **56** after cleavage. **B)** RP-HPLC trace of pure Bombesin peptide **57** after RP-HPLC purification.

4.3. Synthesis of Bombesin-tubugi conjugates based on disulfide bond

The chemistry of disulfide bonds is well understood in the peptide field, especially for processes of symmetric dimerization or intramolecular cyclization involving Cys residues.[29][26] For these purposes, usually, the thiol-containing substrate is subjected to an oxidation condition that will enable the formation of the S-S bond. However, in the formation of asymmetric disulfides, as required for the conjugation of two different molecules, a common strategy is the thiol exchange on electro deficient disulfides, where especially Ellman's reagent and 2-pyridyl disulfides find important applications.[28][27]
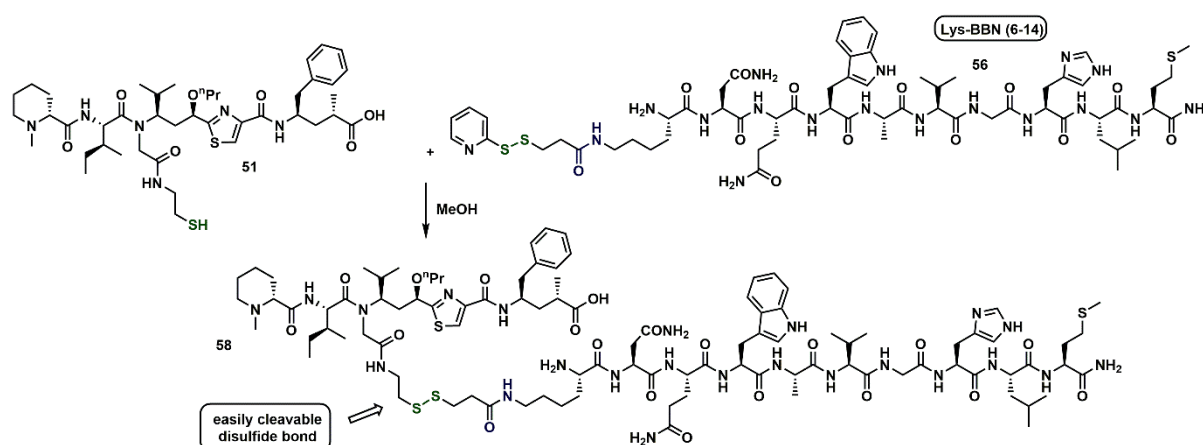
Scheme 4.3. Synthesis of conjugate **58**, by combining Bombesin peptide **56** with Tubugi **51**.

Thus, having a Bombesin peptide with an asymmetrically activatable pyridyl disulfide linker allows the combination with a thiol-functionalized tubugi in a very direct process. Thus, as shown in scheme 4.3, Bombesin derivative **56** in methanol (5 mL) is simply mixed with the thiol-containing Tubugi **51** in close to equimolar quantities (20% excess of bombesin peptide) and in the presence of DIPEA. Analysis by ESI-MS proved that after two hours of reaction, the starting material was consumed and the first example of a Bombesin-tubugi conjugate **58** is obtained in 46% after RP-PHPLC purification.

Even when conjugate **58** already constitutes an important result, the lack of methyl groups in the alpha position to the disulfide bridge may have a negative effect on its reactivity – it may cleave too fast. Therefore, a conjugate in which the disulfide bond is sterically more hindered and therefore less reactive was envisioned. For that purpose, Tubugi **53** constitutes indeed a privileged candidate, supported by the potent activity and the presence of a thiol group dimethylated in alpha-Position. Consequently, Tubugi **53** was conjugated to bombesin **56** following the same procedure, affording conjugate **59** in 52% yield.
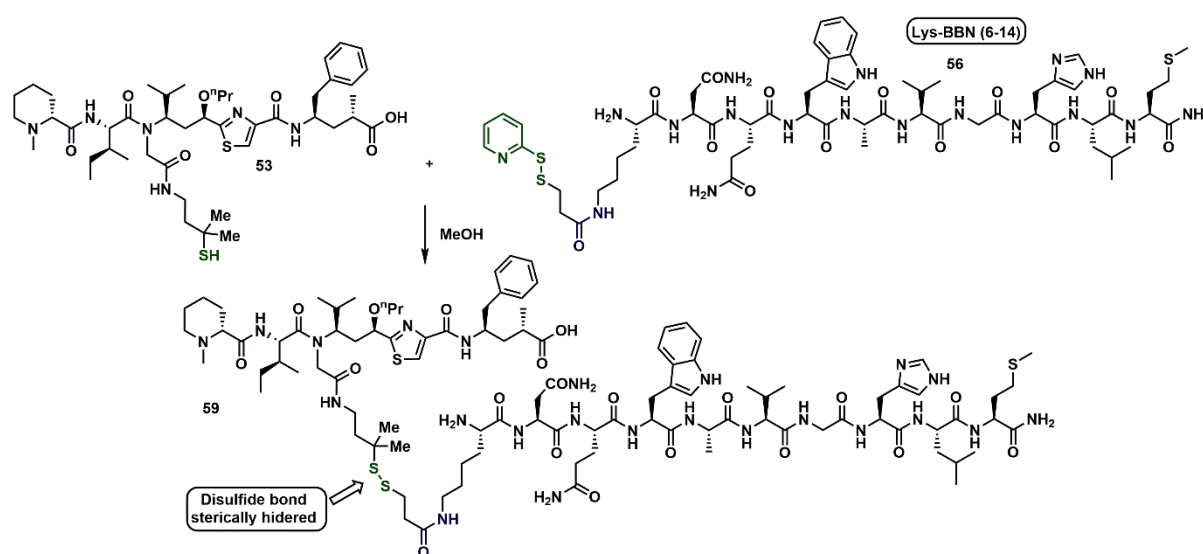
Scheme 4.4. Synthesis of conjugate **59**, by combining Bombesin peptide **56** with Tubugi **53**.

Beyond the tunable stability of the conjugate, another important parameter that was taken into consideration in the design of the PDCs was the cell membrane permeability. It is well known that the introduction of lipid units in peptides and proteins helps these molecules to cross bilipid membranes. Therefore, an improved PDC was constructed by combining the Tubugi **53** and the Bombesin lipopeptide **57**, superior components featuring not only enhanced stability but also membrane permeability.
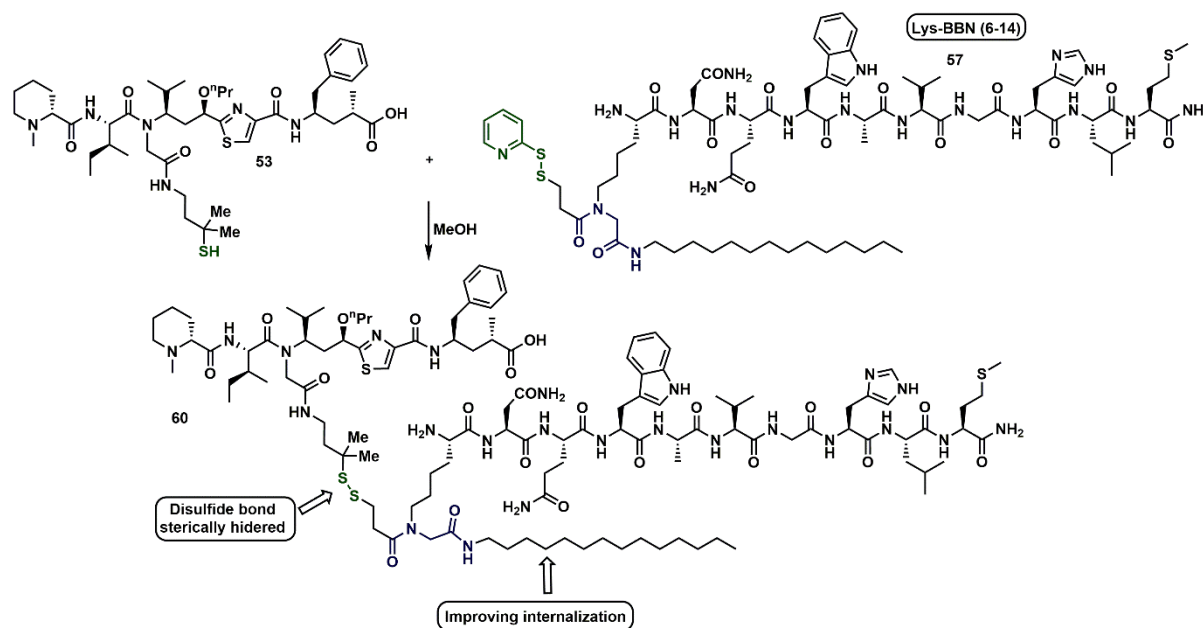
Scheme 4.5. Synthesis of conjugate **60**, by combining Bombesin peptide **57** with Tubugi **53.**

As shown in scheme 4.5, this conjugate was prepared by the direct combination of its precursors, letting them react overnight at room temperature. Purification by RP-HPLC afforded the conjugate **60** in 41% yield.

4.4. Biological evaluations of the Bombesin-tubugi conjugates

The Bombesin-tubugi conjugates **58**, **59**, and **60** were tested on cancer cell lines representing various receptor levels of expression of bombesin receptor type 2, also called gastrin-releasing peptide receptor (GRPR). The goal was to investigate a supposed correlation between the anti-proliferative efficacies of the conjugates and the GRPR levels of the cancer cells. For that purpose, the human cancer cell lines used in the experiments were T-47D (HR+ breast cancer), MDA-MB-231 (TNBC), PC-3 (prostate), MCF-10A (breast epithelial), and HCT-116 (colon). According to expression databases, e.g., Genevestigator's cell lines data selection mRNA-Seq Gene Level *Homo sapiens* (ref. Ensembl 97, GRCh38.p12) (HS_mRNASeq_HUMAN), T-47D has been reported with relatively highest, MDA-MB-231 and PC-3 with medium, and HCT-116 and MCF-10A with relatively low GRPR expression levels (decreasing in the order of that list), respectively.

Table 4.1. Genevestigator's cell lines data selection mRNA-Seq Gene Level Homo sapiens
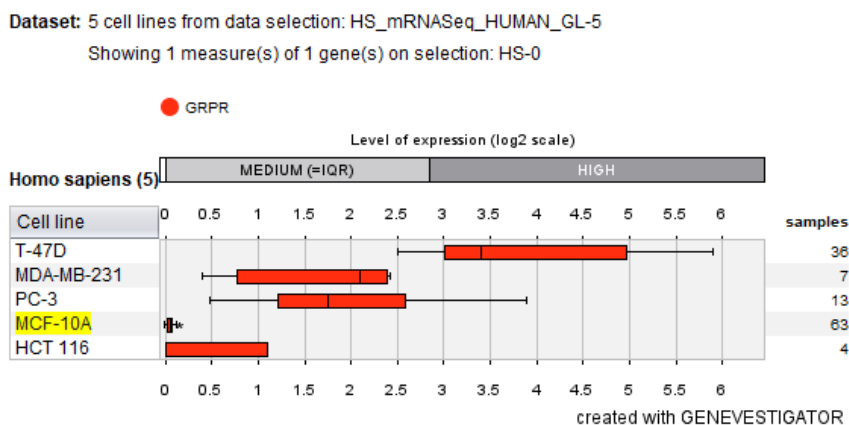
All cell viability tests on selected tumor cell lines were carried out and reproduced in at least triplicate and analyzed by a resazurin-based fluorometric assay. Based on the IC$_{50}$ values presented in former works, concentrations for the dilution series of testing compounds were chosen. Additionally, to the general dependence of the activity on the expression level of the receptors, the incubation time was also investigated. Thus, the cancer cells were exposed to the conjugates for 6 h and 48 h. Irrespective of the initial incubation time, the cells were allowed to grow for 72 h after treatment initialization until cell viability was determined. For that purpose, after ending of the initial 6 h or 48 h treatment period, the incubation solutions containing the test compounds were discarded, cells were washed and then allowed to grow on in fresh, compound-free culture medium until measurement after 72 h.

In figures 4.1 to 4.3, the bioassays revealed the cytotoxic activity of all Bombesin-tubugi conjugates (**58**, **59**, and **60**) against the cell lines under investigation. Looking at figure 4.1 A, the cell viability tested after 6h initial incubation showed conjugate **58** had a strong impact and selective affinity to GRPR. A direct correlation between the GRPR expression levels (as reported in public databases, see Table 4.1) and the efficacy of conjugate **58** was obvious. Thus, IC$_{50}$ values obtained for conjugate **58** in those cell lines with the higher GRPR expression (T-47D, MDA-MB-231, and PC-3) was detected in a nanomolar range, whereas in the case of lower receptor levels (HCT-116 and the healthy breast cell line MCF-10A), the IC$_{50}$ values

were found to be in the micromolar range. After 48 h of incubation, a similar correlation between the GRPR expression levels and the anti-proliferative efficacy of conjugate **58** was observed. Worth highlighting that after an initial cell treatment for 48 h the cytotoxic activity of **58** increased significantly for all the cell lines. That means, all the IC_{50} values obtained were now in the nanomolar range. As a conclusion for conjugate **58**, the IC_{50} values showed that the longer the cancer cells were exposed to the conjugate the higher but also less selective is its anti-proliferative effect – which is expected. However, the correlation to the cells' GRPR expression levels even remained, albeit with lower selectivity factor, for long term treatment.
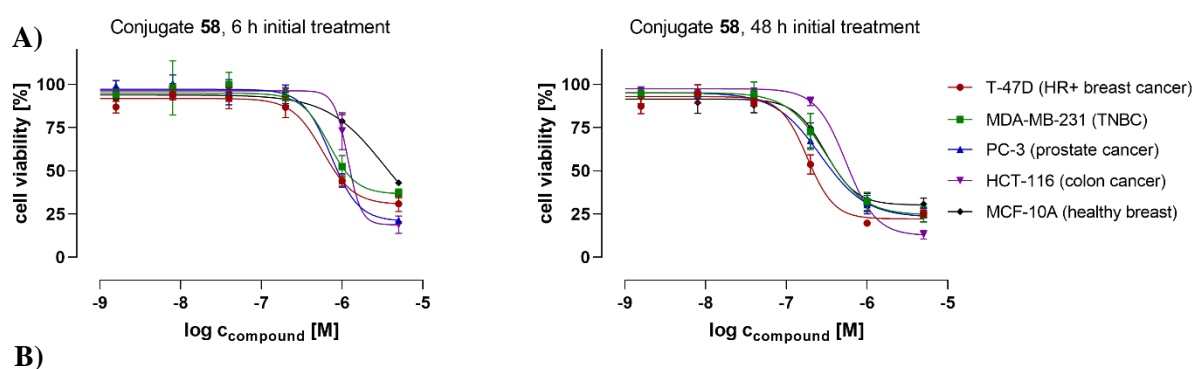
Cell line	6 h	48 h
T-47D	576.6 nM (95% CI: 414.7 - n.d. nM)	182.3 nM (95% CI:155.3 - 203.4 nM)
MDA-MB-231	682.7 nM (95% CI: 432.5 - n.d. nM)	307.8 nM (95% CI: n.d. - 422.6 nM)
PC-3	724.7 nM (95% CI: 569.5 - n.d. nM)	264.1 nM (95% CI: 231.5 - 305.8 nM)
HCT-116	1,173 nM (95% CI: n.d.)	550.0 nM (95% CI: 504.5 - 598.2 nM)
MCF-10A	≈3000 nM (95% CI: n.d.)	303.9 nM (95% CI: n.d. - 367.4 nM)

Figure 4.1. Cell-based biological testing of Bombesin-tubugi conjugates **58**. **(A)** Cell viability of human T-47D (HR+ breast cancer), MDA-MB-231 (TNBC), PC-3 (prostate), and HCT-116 (colon) cancer cells, as well as healthy MCF-10A breast epithelial cells as determined by resazurin-based fluorometric assay after an initial treatment of 6 h and 48 h and subsequent proliferation until 72 h. **(B)** Calculated IC_{50} values.

Figure 4.2 A shows the viability of the cells after treatment with conjugate **59**. After 6 h initial incubation treatment, conjugate **59** also had a strong impact and selective affinity to GRPR. Except for T-47D, there is a correlation between the GRPR expression levels and the efficacy of conjugate **59**. For the three cell lines with the highest GRPR levels (T-47D, MDA-MB-231, and PC-3) an IC_{50} value in the nanomolar range was detected, whereas those cell lines with the

lower receptor expression levels the calculated IC_{50} values were found in the micromolar range. Expectedly, after 48 h incubation treatment, the cytotoxic activity increased significantly in all cell lines, and all the IC_{50} values obtained were in the nanomolar range. As a non-surprising conclusion for conjugate **59**, the IC_{50} values showed that the longer the cancer cells were exposed to the conjugate the higher the efficacy but also less selective is its anti-proliferative effect.
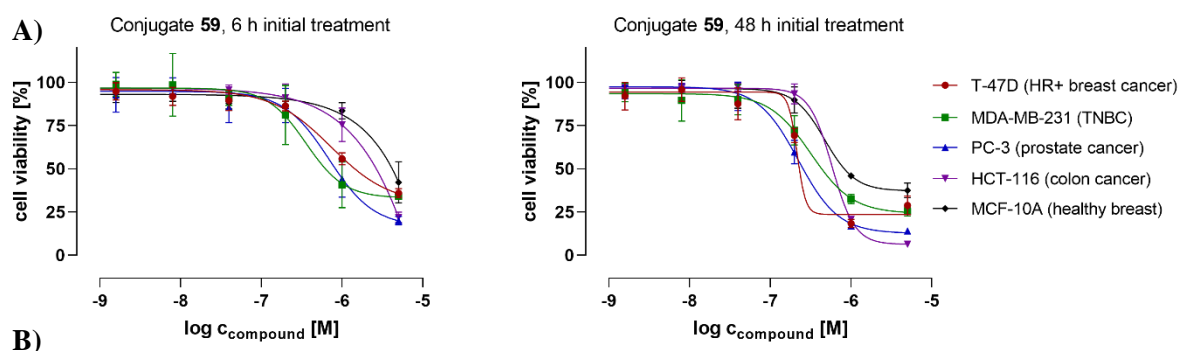
Cell line	6 h	48 h
T-47D	731.3 nM (95% CI: 513.5 - 2,440 nM)	214.9 nM (95% CI: n.d.)
MDA-MB-231	356.9 nM (95% CI: n.d. - 573.3 nM)	318.2 nM (95% CI: n.d. - 447.9 nM)
PC-3	687.2 nM (95% CI: 501.6 - 1,137 nM)	222.3 nM (95% CI: 199.9 - 250.0 nM)
HCT-116	≈2000 nM (95% CI: n.d.)	582.3 nM (95% CI: 516.0 - 720.7 nM)
MCF-10A	≈4000 nM (95% CI: n.d.)	474.1 nM (95% CI: 357.7 - 613.6 nM)

Figure 4.2. Cell-based biological testing of Bombesin-tubugi conjugates **59**. **(A)** Cell viability of human T-47D (HR+ breast cancer), MDA-MB-231 (TNBC), PC-3 (prostate), and HCT-116 (colon) cancer cells, as well as healthy MCF-10A breast epithelial cells as determined by resazurin-based fluorometric assay after an initial treatment of 6 h and 48 h and subsequent proliferation until 72 h. **(B)** Calculated IC_{50} values.

In general, conjugates **58** and **59** are quite similar, both with respect to activity (IC_{50} values) and selectivity. Therefore, the intended stabilization of the disulfide bridge by the methylations has no significant effect on the PDC's activity, at least in vitro. However, there could be indeed a more obvious difference and an advantage for **59** over **58** when applying these PDCs in vivo since the disulfide bridge will be much more stressed in vivo than in vitro, and then better protection of the disulfide could be necessary.

In figure 4.3, the cell viability tested after 6 h initial cell incubation with conjugate **60** showed no direct correlation between the GRPR expression levels (as reported in expression databases) and the anti-proliferative effect of the conjugate. The IC_{50} values obtained after an initial cell treatment for 6 h with conjugate **60** in the cell lines T-47D, MDA-MB-23, and PC-3 were very similar, in the nanomolar range. Interestingly, the IC_{50} values showed also no big difference after a far longer incubation for 48 h. This observation might be attributed to the fact that Bonbesin-tubugi **60** is a lipidated peptide conjugate. Not just specific binding to the GRPR receptor but also unspecific interactions with the cells' plasma membrane might lead to enhanced but also inselective internalization of conjugate **60** in all the cell lines tested.

Cell line	6 h	48 h
T-47D	90.1 nM (95% CI: 58.6 - 139.0 nM)	77.8 nM (95% CI: 52.3 - 119.4 nM)
MDA-MB-231	92.8 nM (95% CI: 71.7 - 120.5 nM)	94.5 nM (95% CI: 73.1 - 125.2 nM)
PC-3	119.5 nM (95% CI: 91.5 - 158.6 nM)	86.1 nM (95% CI: 73.6 - 101.0 nM)
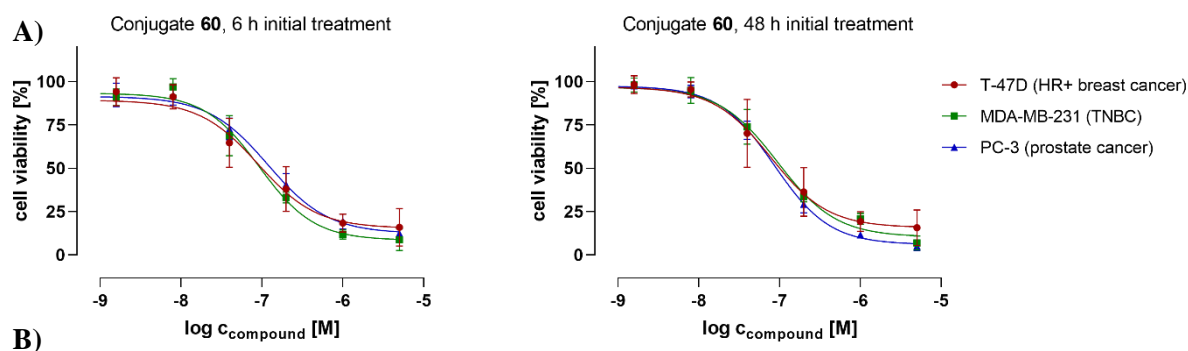
Figure 4.3. Cell-based biological testing of Bombesin-tubugi conjugates **60**. **(A)** Cell viability of human T-47D (HR+ breast cancer), MDA-MB-231 (TNBC), PC-3 (prostate), and HCT-116 (colon) cancer cells, as well as healthy MCF-10A breast epithelial cells as determined by resazurin-based fluorometric assay after an initial treatment of 6 h and 48 h and subsequent proliferation until 72 h. **(B)** Calculated IC_{50} values.

4.5. Conclusions

Here we showed for the first time the possibility of tubulysin conjugation at the *N*-tertiary amide side chain, the most variable and expandable residue of their complex structure. A result that undoubtedly opens new possibilities for applications in payload research. Our study included the design and the solid-phase synthesis of two different Bombesin peptide analogs

containing already the linker that enables the final disulfide-based conjugation. Taking advantage of the established Ugi-multicomponent protocol, the best bombesin candidate was synthesized bearing the desired linker together with an additional lipid moiety inflicting enhanced cell membrane permeability. Differently protected disulfide linkages were introduced to evaluate the balance between stability and cleavability, obtaining as expected, slightly superior results when using alpha dimethylated thiol groups. The *in vitro* proliferative screening of the Bombesin-tubugi conjugates, showed notably high activity and selectivity, offering significant potential for further anticancer studies.

4.6. Experimental Section

4.6.1. 3-(Pyridin-2-yldisulfaneyl) propanoic acid
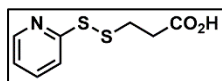
3-Mercaptopropanoic acid (5 g, 0.047 mol) is reacted with 1,2-di(pyridin-2-yl)disulfane (20.6 g, 0.094 mol) in MeOH (40 mL), according to the method reported in the literature[90] to afford after column chromatography (DCM/MeCN 8:1), 3-(pyridin-2-yldisulfanyl)propanoic acid (**54**, 7.6 g, 75%) as a white solid. $R_f = 0.6$ (DCM/MeCN 5:1). ^{1}H NMR (400 MHz, CDCl$_3$) δ 8.49 (dt, J = 4.9, 1.4 Hz, 1H), 7.72 – 7.63 (m, 2H), 7.15 (ddd, J = 6.0, 5.0, 2.5 Hz, 1H), 3.07 (t, J = 6.8 Hz, 2H), 2.81 (t, J = 6.8 Hz, 2H). ^{13}C NMR (101 MHz, CDCl$_3$) δ 175.7, 149.4, 137.4, 121.2, 120.5, 34.1, 33.8.

4.6.2. Synthesis of bombesin derivatives

The peptide sequence of Bombesin derivatives was assembled automatically on an INTAVIS ResPepSL peptide synthesizer by a stepwise Fmoc/*t*Bu strategy using TG-S-RAM resin (Iris Biotech) at 0.05 mmol scale. Coupling reactions (unless specified) were accomplished in DMF using a 5-fold excess of the amino acid residue and PyBOP and a 10-fold excess of NMM. *Fmoc removal*: The resin is treated with a solution of 20% piperidine in DMF (2×10 min), then washed with DCM (3×1 min) and DMF (2×1 min). *Aminocatalysis-mediated Ugi reaction*: The free *N*-terminal resin-bound peptide is subjected to imine formation by treating the resin beads with a suspension of paraformaldehyde (4 equiv) and pyrrolidine (4 equiv) in THF/MeOH (1:1) for 30 min. Excess of reagents is removed by washing the beads with THF (3×1min). The resin is transferred to a 5 mL MW tube and a solution of the Fmoc-protected amino acid (4 equiv) in 1 mL of THF/MeOH (1:1) and another of the isocyanide (4.0 equiv) in 1 mL of THF/MeOH (1:1) are added to the resin and the mixture is stirred at room temperature for 48 h. Completion is indicated by ESI-MS and RP-HPLC monitoring after mini-cleavages and if it was necessary the reaction is performed again for 24 h. Finally, the resin is washed

with DCM (3×1 min) and DMF (2×1 min). Final cleavage is performed by mixing the resin

with the cocktail TFA/TIS/H$_2$O (95:2.5:2.5). The crude peptide was precipitated from diethyl

ether (-20 ºC), then taken up in 1:2 acetonitrile/water and lyophilized.

4.6.2.1. Bombesin peptide 56
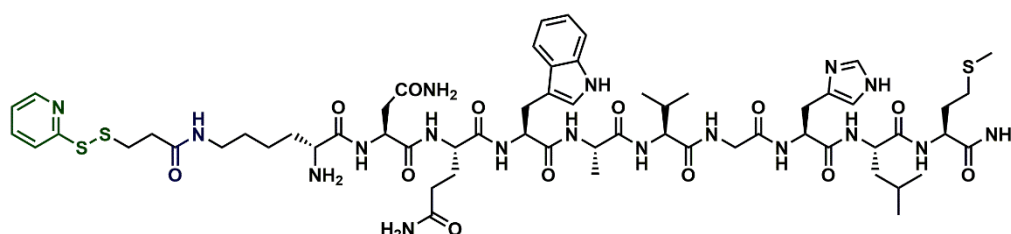
Bombesin (6-14) was synthesized automatically on an INTAVIS ResPepSL peptide

synthesizer using TG-S-RAM resin (Iris-Biotech, 0.05 mmol, 0.24 mmol/g) by sequential

coupling of Fmoc-Met-OH, Fmoc-Leu-OH, Fmoc-His (Trt)-OH, Fmoc-Gly-OH, Fmoc-Val-

OH, Fmoc-Ala-OH, Fmoc-Trp(Boc)-OH, Fmoc-Gln(Trt)-OH, Fmoc-Asn(Trt)-OH and Boc-

Lys(Fmoc)-OH. Then, the Fmoc of the Lys side chain is removed and 3-(pyridin-2-

yldisulfanyl)propanoic (43 mg, 0.2 mmol) is manually coupled using DIC (31 µL, 0.2 mmol)

in DMF for 2 h. The peptide is cleaved from the resin with the cocktail TFA/TIPS/H$_2$O

(95:2.5:2.5), the filtrate is precipitated from cold (-20°C) diethyl ether, then taken up in

acetonitrile/water 1:2 (*v/v*) and lyophilized to afford the crude peptide **56** (56 mg, 82% crude

yield, 84% purity) as a white solid. R$_t$ = 12.0 min. HR-MS m/z: 690.3215 [M+2H]$^{2+}$, calcd. for

C$_{61}$H$_{92}$N$_{18}$O$_{13}$S$_3$: 690.3127.

4.6.2.2. Bombesin peptide 57
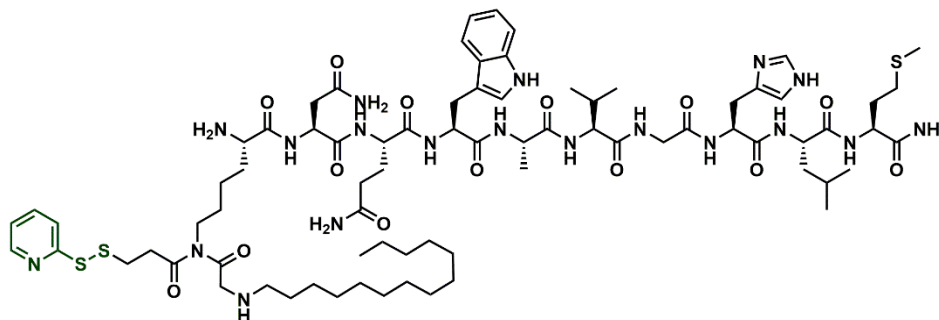
Resin-bound bombesin (6-14) was synthesized automatically on an INTAVIS ResPepSL peptide synthesizer using TG-S-RAM resin (Iris-Biotech, 0.05 mmol, 0.24 mmol/g) by sequential coupling of Fmoc-Met-OH, Fmoc-Leu-OH, Fmoc-His(Trt)-OH, Fmoc-Gly-OH, Fmoc-Val-OH, Fmoc-Ala-OH, Fmoc-Trp(Boc)-OH, Fmoc-Gln(Trt)-OH, Fmoc-Asn(Trt)-OH and Boc-Lys(Fmoc)-OH. Then, the Fmoc of the Lys side chain is removed and an aminocatalysis-mediated Ugi reaction is performed by combining paraformaldehyde (0.6 mg, 0.2 mmol), 1-isocyanotetradecane (45 mg, 0.2 mmol), and 3-(pyridin-2-yldisulfaneyl)propanoic (43 mg, 0.2 mmol) following the general procedure detailed before. The peptide is cleaved from the resin with the cocktail TFA/TIPS/H_2O (95:2.5:2.5), the filtrate is precipitated from cold (-20°C) diethyl ether, then taken up in acetonitrile/water 1:2 (*v/v*), lyophilized and purified by RP-HPLC to afford the crude peptide 57 (22 mg, 27 % yield) as a white solid. R_t = 13.0 min. HR-MS m/z: 816.9276 $[M+2H]^{2+}$, calcd. for $C_{77}H_{123}N_{19}O_{14}S_3$: 816.9329.

4.6.3. Synthesis of tubugi-bombesin conjugates

4.6.3.1. Conjugate 58
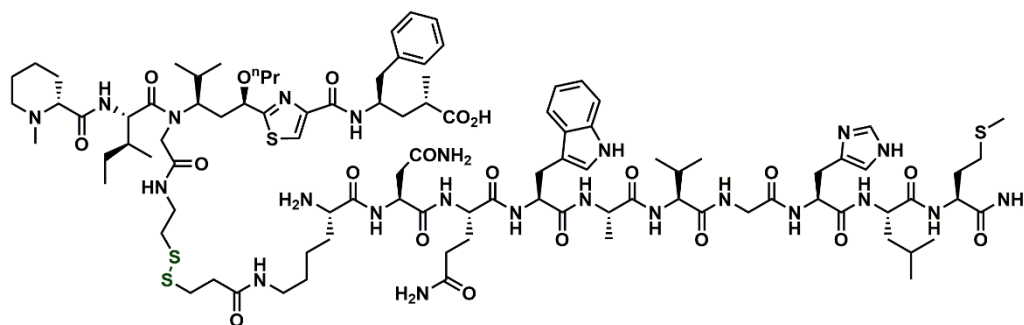
In a 2 mL vial containing Bombesin peptide **56** (2.4 mg, 1.74 µmol) in MeOH (1 mL), DIPEA (1 µL) and Tubugi **51** (1.2 mg, 1.45 µmol) are added and the mixture is stirred for 2 h and finally purified by preparative RP-HPLC to afford the conjugate **58** (1.4 mg, 46%) as a white

amorphous solid. R_t = 12.8 min. HR-MS *m/z*: 700.3626 $[M+3H]^{3+}$, calcd. for $C_{98}H_{154}N_{23}O_{20}S_4$: 700.3541.

4.6.3.2. Conjugate 59
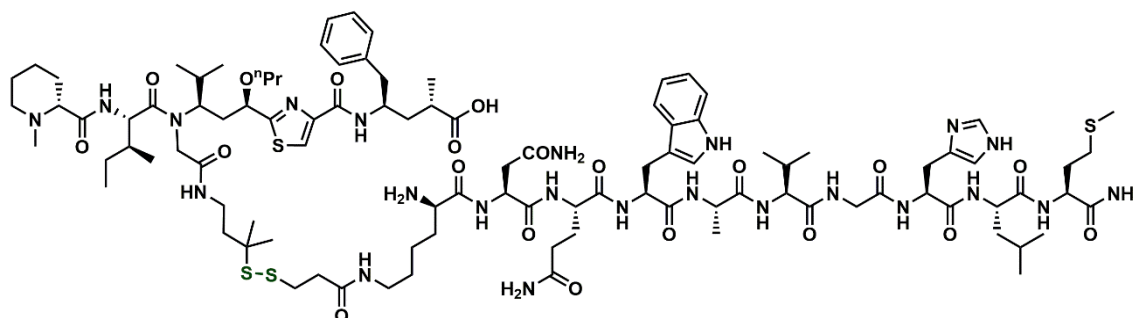
In a 2 mL vial containing Bombesin peptide **56** (3.3 mg, 2.4 µmol) in MeOH (1 mL), DIPEA (1 µL) and Tubugi **53** (1.75 mg, 2.0 µmol) are added and the mixture is stirred for 2 h and finally purified by preparative RP-HPLC to afford the conjugate **59** (2.2 mg, 52%) as a white amorphous solid. R_t = 13.2, 13.6 min. HR-MS *m/z*: 714.3661 $[M+3H]^{3+}$, calcd. for $C_{101}H_{160}N_{23}O_{20}S_4$: 714.3693.

4.6.3.3. Conjugate 60
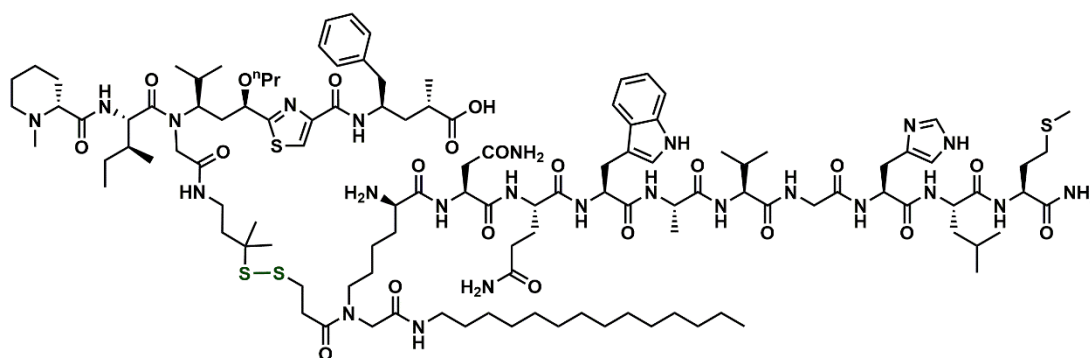
In a 2 mL vial containing Bombesin peptide **57** (5.9 mg, 3.6 µmol) in MeOH (1 mL), DIPEA (1 µL) and Tubugi **53** (2.6 mg, 3.0 µmol) are added and the mixture is stirred for 4 h and finally purified by preparative RP-HPLC to afford the conjugate **60** (3.0 mg, 41%) as a white amorphous solid. R_t = 12.9 min. HR-MS *m/z*: 798.7791 $[M+3H]^{3+}$, calcd. for $C_{115}H_{187}N_{24}O_{21}S_4$: 798.7833.

4.6.4. *In vitro* cell-based assays

The tubugi-bombesin conjugates were tested in four human cancer cell lines – namely PC-3, HCT-116, T-47D and MDA-MB-231 cells – and a healthy, non tumorigenic breast epithelial cell line, MCF-10A, using *in vitro* cell viability assays for IC_{50} value determination.

The prostate cancer cell line PC-3 was cultured in RPMI 1640 medium supplemented with 10% heat-inactivated FCS and 2 mM L-glutamine. The same medium, however, additionally supplemented with 0.2 U/mL of human insulin, was used for the cultivation of both breast cancer cell lines T-47D (hormone receptors-positive BC) and MDA-MB-231 (triple-negative BC). HCT-116 colorectal cancer cell were cultured in DMEM supplemented with 10% not heat-inactivated FCS and 2 mM L-glutamine. MCF-10A cells were cultured using PAN Biotech's Endopan 3 medium and supplements kit.

All cells were routinely cultured in T-75 flasks in a humidified atmosphere with 5% CO2 at 37°C to reach subconfluency (~ 70-80%) prior to subsequent sub-culturing or assay usage. The adherent cells were rinsed with PBS and detached using trypsin/EDTA (0.05% in PBS) prior to cell passaging and seeding [R1]. All cell lines were purchased from ATCC (Manassas, USA). Media and supplements for cell culturing were purchased from Capricorn Scientific GmbH (Ebsdorfergrund, Germany). Human insulin and the Endopan 3 medium kit for MCF-10A cells were from PAN Biotech (Aidenbach, Germany). All cell culture plastics were purchased from TPP (Trasadingen, Switzerland) and Greiner Bio-One GmbH (Frickenhausen, Germany), respectively.

4.6.4.1 *In vitro* cell viability assay

Anti-proliferative and cytotoxic effects, respectively, of the tubugi-bombesin conjugates were investigated using a fluorometric resazurin-based cell viability assay [R2]. Resazurin, purchased from Sigma-Aldrich (Taufkirchen, Germany), was prepared as 50X (2.5 mM) stock

solution in sterile filtered aqua bidest. and stored at 4°C under light protection. To assay the test items, human prostate PC-3, colorectal HCT-116, breast T-47D and MDA-MB-231 cancer cells, as well as the healthy breast epithelial cell line MCF-10A were seeded in low densities into 96-well plates (3,000 – 8,000 cells per well; seeding confluency ~ 10%), and were allowed to adhere overnight. Subsequently, the compounds – diluted to appropriate concentration series covering the pico- to low micromolar range using the respective culture media – were added to the cells (100 µL/96-well) for an initial treatment lasting 6 h, and 48 h, respectively, under standard growth conditions. For control measures, cells were treated in parallel with 1.0 % (*v/v*) DMSO (negative control, representing the DMSO content of the highest test item concentration; Duchefa Biochemie, Haarlem, The Netherlands) and 100 µM digitonin (positive control, for data normalization set to 0% cell viability; Sigma-Aldrich, Taufkirchen, Germany), both in standard growth medium. As soon as the desired initial treatment time was finished, the incubation media containing the peptide-toxin conjugates were removed, the cells were very carefully rinsed with medium and subsequently provided with 100 µL/well of fresh cell line-specific culture medium. Afterwards, the cells were cultured under standard growth conditions to finalize a 72 h proliferation period post start of treatment. After 72 h, a 6X (300 µM) resazurin working solution was prepared freshly in basal culture medium, and 20 µL of that 6X resazurin solution were added to each well resulting in a final volume of 120 µL/96-well including 1X resazurin (50 µM). Subsequently, the cells were incubated for the metabolic dye reaction (resazurin reduction) for further 2 h under standard growth conditions. Each data point was determined and reproduced in at least triplicate. The conversion of resazurin to resorufin by the remaining portion of viable, metabolically active cells was fluorometrically measured (exc.: 540 nm/em.: 590 nm) using a SpectraMax M5 multiwell plate reader (Molecular Devices, San Jose, USA). For non-linear regression analyses of the data GraphPad Prism 8.0.2 software was used to calculate IC_{50} values.

REFERENCES

[1]   H. Sung, J. Ferlay, R. L. Siegel, M. Laversanne, I. Soerjomataram, A. Jemal, F. Bray, *CA Cancer J.Clin.* **2021**, *71*, 209–249.

[2]   S. Cazzamalli, A. D. Corso, D. Neri, *Chimia (Aarau).* **2017**, *71*, 712–715.

[3]   F. Kratz, I. A. Müller, C. Ryppa, A. Warnecke, *ChemMedChem* **2008**, *3*, 20–53.

[4]   R. G. Panchal, *Biochem. Pharmacol.* **1998**, *55*, 247–252.

[5]   K. C. Nicolaou, S. Rigol, *Angew. Chem. Int. Ed.* **2019**, *58*, 11206–11241.

[6]   J. A. Francisco, C. G. Cerveny, D. L. Meyer, B. J. Mixan, K. Klussman, D. F. Chace, S. X. Rejniak, K. A. Gordon, R. DeBlanc, B. E. Toki, C. L. Law, S. O. Doronina, C. B. Siegall, P. D. Senter, A. F. Wahl, *Blood* **2003**, *102*, 1458–1465.

[7]   U. Hafeez, S. Parakh, H. K. Gan, A. M. Scott, *Molecules* **2020**, *25*, 4764.

[8]   R. He, B. Finan, J. P. Mayer, R. D. Dimarchi, *Molecules* **2019**, *24*, 1855.

[9]   P. Hoppenz, S. Els-Heindl, A. G. Beck-Sickinger, *Front. Chem.* **2020**, *8*, 571.

[10]   U.S. Food and Drug Administration, "FDA approves lutetium Lu 177 dotatate for treatment of GEP-NETS, https://www.fda.gov/drugs/resources-information-approved-drugs/fda-approves-lutetium-lu-177-dotatate-treatment-gep-nets, accessed 23 November **2021**," n.d.

[11]   Y. Wang, A. G. Cheetham, G. Angacian, H. Su, L. Xie, H. Cui, *Adv. Drug Deliv. Rev.* **2017**, *110–111*, 112–126.

[12]   V. M. Ahrens, A. G. Beck-sickinger, *Futur. Med. Chem.* **2012**, *4*, 1567–1586.

[13]   O. Keskin, S. Yalcin, *Onco. Targets. Ther.* **2013**, *6*, 471–483.

[14]   M. A. Schwartz, M. D. Schaller, M. H. Ginsberg, *Annu. Rev. Cell Dev. Biol.* **1995**, *11*,

549–599.

[15]   C. Ryppa, H. Mann-Steinberg, M. L. Biniossek, R. Satchi-Fainaro, F. Kratz, *Int. J. Pharm.* **2009**, *368*, 89–97.

[16]   H. Ruan, X. Chen, C. Xie, B. Li, M. Ying, Y. Liu, M. Zhang, X. Zhang, C. Zhan, W. Lu, W. Lu, *ACS Appl. Mater. Interfaces* **2017**, *9*, 17745–17756.

[17]   H. Gicquiaux, S. Lecat, M. Gaire, A. Dieterlen, Y. Mély, K. Takeda, B. Bucher, J. L. Galzi, *J. Biol. Chem.* **2002**, *277*, 6645–6655.

[18]   R. Kufka, R. Rennert, G. N. Kalu, L. Weber, W. Richter, L. A. Wessjohann, *Beilstein J. Org. Chem.* **2019**, *15*, 96–105.

[19]   P. Moreno, I. Ramos-Álvarez, T. W. Moody, R. T. Jensen, *Expert Opin. Ther. Targets* **2016**, *20*, 1055–1073.

[20]   A. Anastasi, V. Erspamer, M. Bucci, *Arch. Biochem. Biophys.* **1972**, *148*, 443–446.

[21]   A. Beck, L. Goetsch, C. Dumontet, N. Corvaïa, *Nat. Rev. Drug Discov.* **2017**, *16*, 315–337.

[22]   B. Wei, J. Gunzner-Toste, H. Yao, T. Wang, J. Wang, Z. Xu, J. Chen, J. Wai, J. Nonomiya, S. P. Tsai, J. Chuh, K. R. Kozak, Y. Liu, S. F. Yu, J. Lau, G. Li, G. D. Phillips, D. Leipold, A. Kamath, D. Su, K. Xu, C. Eigenbrot, S. Steinbacher, R. Ohri, H. Raab, L. R. Staben, G. Zhao, J. A. Flygare, T. H. Pillow, V. Verma, L. A. Masterson, P. W. Howard, B. Safina, *J. Med. Chem.* **2018**, *61*, 989–1000.

[23]   A. D. Corso, L. Pignataro, L. Belvisi, C. Gennari, *Chem. Eur. J.* **2019**, *25*, 14740–14757.

[24]   L. Ducry, B. Stump, *Bioconjugate Chem.* **2010**, *21*, 5–13.

[25]   J. D. Bargh, A. Isidro-Llobet, J. S. Parker, D. R. Spring, *Chem. Soc. Rev.* **2019**, *48*, 4361–4374.

[26] M. Danial, A. Postma, *Ther. Deliv* **2017**, *8*, 359–362.

[27] G. J. L. Bernardes, G. Casi, S. Trüssel, I. Hartmann, K. Schwager, J. Scheuermann, D. Neri, *Angew. Chemie - Int. Ed.* **2012**, *51*, 941–944.

[28] T. H. Pillow, J. D. Sadowsky, D. Zhang, S. F. Yu, G. Del Rosario, K. Xu, J. He, S. Bhakta, R. Ohri, K. R. Kozak, E. Ha, J. R. Junutula, J. A. Flygare, *Chem. Sci.* **2016**, *8*, 366–370.

[29] Z. Deng, J. Hu, S. Liu, *Macromol. Rapid Commun.* **2020**, *41*, 1–14.

[30] W. C. Widdison, S. D. Wilhelm, E. E. Cavanagh, K. R. Whiteman, B. A. Leece, Y. Kovtun, V. S. Goldmacher, H. Xie, R. M. Steeves, R. J. Lutz, R. Zhao, L. Wang, W. A. Bla, *J. Med. Chem.* **2006**, *49*, 4392–4408.

[31] T. H. Pillow, *Pharm. Pat. Anal.* **2017**, *6*, 25–33.

[32] G. R. Pettit, Y. Kamano, C. L. Herald, Y. Fujii, H. Kizu, M. R. Boyd, F. E. Boettner, D. L. Doubek, J. M. Schmidt, J. C. Chapuis, C. Michel, *Tetrahedron* **1993**, *49*, 9151–9170.

[33] P. Zhao, Y. Zhang, W. Li, C. Jeanty, G. Xiang, Y. Dong, *Acta Pharm. Sin.* **2020**, *10*, 1589–1600.

[34] F. Sasse, H. Steinmetz, J. Heil, G. Hofle, H. Reichenbach, *J. Antibiot. (Tokyo).* **2000**, *53*, 879–885.

[35] H. M. Peltier, J. P. Mcmahon, A. W. Patterson, J. A. Ellman, *JACS* **2006**, *128*, 16018–16019.

[36] B. C. Murray, M. T. Peterson, R. A. Fecik, *Nat. Prod. Rep.* **2015**, *32*, 654.

[37] J. R. Junutula, H. P. Gerber, *ACS Med. Chem. Lett.* **2016**, *7*, 972–973.

[38] K. C. Nicolaou, J. Yin, D. Mandal, R. D. Erande, P. Klahn, M. Jin, M. Aujay, J. Sandoval, J. Gavrilyuk, D. Vourloumis, *J. Am. Chem. Soc* **2016**, *138*, 1698–1708.

[39]   C. A. Leverett, S. C. K. Sukuru, B. C. Vetelino, S. Musto, K. Parris, F. Loganzo, A. H. Varghese, G. Bai, B. Liu, D. Liu, S. Hudson, R. Doppalapudi, J. R. Stock, C. J. O. Donnell, C. Subramanyam, C. A. Leverett, S. C. K. Sukuru, B. C. Vetelino, S. Musto, K. Parris, *ACS Med. Chem. Lett.* **2016**, *7*, 999–1004.

[40]   R. Cohen, D. J. Vugts, G. W. M. Visser, M. S. Walsum, M. Bolijn, M. Spiga, P. Lazzari, S. Shankar, M. Sani, M. Zanda, G. A. M. S. van Dongen, *Cancer Res* **2014**, *74*, 5700–5710.

[41]   M. Kaake, M. Srinivasarao, P. S. Low, *Bioconjugate Chem.* **2018**, *29*, 2208–2214.

[42]   J. A. Reddy, R. Dorton, A. Bloomfield, M. Nelson, C. Dircksen, M. Vetzel, P. Kleindl, H. Santhapuram, I. R. Vlahov, C. P. Leamon, *Sci. Rep.* **2018**, *8*, 8943.

[43]   J. Y. Li, S. R. Perry, V. Muniz-Medina, R. Dixit, J. K. Osbourn, S. R. Coats, *Cancer Cell* **2016**, *29*, 117–129.

[44]   J. S. Parker, M. McCormick, D. W. Anderson, B. A. Maltman, L. Gingipalli, D. Toader, *Org. Process Res. Dev.* **2017**, *21*, 1602–1609.

[45]   L. Nathan Tumey, C. A. Leverett, B. Vetelino, F. Li, B. Rago, X. Han, F. Loganzo, S. Musto, G. Bai, S. C. K. Sukuru, E. I. Graziani, S. Puthenveetil, J. Casavant, A. Ratnayake, K. Marquette, S. Hudson, V. R. Doppalapudi, J. Stock, L. Tchistiakova, A. J. Bessire, T. Clark, J. Lucas, C. Hosselet, C. J. O'Donnell, C. Subramanyam, *ACS Med. Chem. Lett.* **2016**, *7*, 977–982.

[46]   K. C. Nicolaou, S. Pan, K. K. Pulukuri, Q. Ye, S. Rigol, R. D. Erande, D. Vourloumis, B. P. Nocek, S. Munneke, J. Lyssikatos, A. Valdiosera, C. Gu, B. Lin, H. Sarvaiaya, J. Trinidad, J. Sandoval, C. Lee, M. Hammond, M. Aujay, N. Taylor, M. Pysz, J. W. Purcell, J. Gavrilyuk, *J. Org. Chem.* **2021**, *86*, 3377–3421.

[47]   D. Lipovšek, I. Carvajal, A. J. Allentoff, A. Barros, J. Brailsford, Q. Cong, P. Cotter, S.

Gangwar, C. Hollander, V. Lafont, W. L. Lau, W. Li, M. Moreta, S. O'Neil, J. Pinckney, M. J. Smith, J. Su, C. Terragni, M. A. Wallace, L. Wang, M. Wright, H. N. Marsh, J. W. Bryson, *Protein Eng. Des. Sel.* **2018**, *31*, 159–171.

[48] T. Rodrigues, G. J. L. Bernardes, *Nat. Chem.* **2016**, *8*, 1088–1090.

[49] L. R. Staben, S. G. Koenig, S. M. Lehar, R. Vandlen, D. Zhang, J. Chuh, S. Yu, C. Ng, J. Guo, Y. Liu, A. F. Donohue, M. Go, X. Linghu, N. L. Segraves, T. Wang, J. Chen, B. Wei, G. D. L. Phillips, K. Xu, K. R. Kozak, S. Mariathasan, J. A. Flygare, T. H. Pillow, *Nat. Chem.* **2016**, *8*, 1112–1119.

[50] P. J. Burke, J. Z. Hamilton, T. A. Pires, J. R. Setter, J. H. Hunter, J. H. Cochran, A. B. Waight, K. A. Gordon, B. E. Toki, K. K. Emmerton, W. Zeng, I. J. Stone, P. D. Senter, R. P. Lyon, S. C. Jeffrey, *Mol. Cancer Ther.* **2016**, *15*, 938–945.

[51] P. Wipf, T. Takada, M. J. Rishel, *Org. Lett.* **2004**, *6*, 4057–4060.

[52] D. Neri, G. Fossati, M. Zanda, *ChemMedChem* **2006**, *1*, 175–180.

[53] A. W. Patterson, H. M. Peltier, J. A. Ellman, *J. Org. Chem.* **2008**, *73*, 4362–4369.

[54] R. Balasubramanian, B. Raghavan, A. Begaye, D. L. Sackett, R. A. Fecik, *J. Med. Chem.* **2009**, *52*, 238–240.

[55] K. C. Nicolaou, R. D. Erande, J. Yin, D. Vourloumis, M. Aujay, J. Sandoval, S. Munneke, J. Gavrilyuk, *J. Am. Chem. Soc.* **2018**, *140*, 3690–3711.

[56] W. Tao, W. Zhou, Z. Zhou, C. Si, X. Sun, B. Wei, *Tetrahedron* **2016**, 5928–5933.

[57] X. M. Wang, Y. W. Liu, Q. E. Wang, Z. Zhou, C. M. Si, B. G. Wei, *Tetrahedron* **2019**, *75*, 260–268.

[58] S. P. Shankar, M. Jagodzinska, L. Malpezzi, L. Paolo, I. Manca, I. R. Greig, M. Zanda, *Org. Biomol. Chem.* **2013**, *11*, 2273–2287.

References

[59] D. G. Rivera, M. G. Ricardo, A. V. Vasco, L. A. Wessjohann, E. V. Van der Eycken, *Nat. Protoc.* **2021**, *16*, 561–578.

[60] A. Aletras, K. Barlos, D. Gatos, S. Koutsogianni, P. Mamos, *Int. J. Pept. Protein Res.* **1995**, *45*, 488–496.

[61] Dorin Toader, F. Wang, L. Gingipalli, M. Vasbinder, M. Roth, S. Mao, M. Block, J. Harper, S. Thota, M. Su, J. Ma, V. Bedian, A. Kamal, **2016**, *59*, 10781–10787.

[62] A. Dömling, I. Ugi, *Angew. Chem. Int. Ed.* **2000**, *39*, 3168–3210.

[63] B. Ganem, *Acc. Chem. Res.* **2009**, *42*, 463–472.

[64] L. Reguera, D. G. Rivera, *Chem. Rev.* **2019**, *17*, 9836–9860.

[65] E. Ruijter, R. Scheffelaar, R. V. A. Orru, *Angew. Chem. Int. Ed.* **2011**, *50*, 6234–6246.

[66] T. M. Vishwanatha, B. Giepmans, S. K. Goda, A. Dömling, *Org. Lett.* **2020**, *22*, 5396−5400.

[67] O. Pando, S. Stark, A. Denkert, A. Porzel, R. Preusentanz, L. A. Wessjohann, *J. Am. Chem. Soc* **2011**, *133*, 7692–7695.

[68] H. Chen, Z. Lin, K. E. Arnst, D. D. Miller, W. Li, *Molecules* **2017**, *22*, 1281.

[69] O. Pando, S. Dörner, R. Preusentanz, A. Denkert, A. Porzel, W. Richter, L. Wessjohann, *Org. Lett.* **2009**, *24*, 5567–5569.

[70] G. Bhalay, A. R. Dunstan, *Tetrahedron Lett.* **1998**, *39*, 7803–7806.

[71] É. Lévesque, S. T. Laporte, A. B. Charette, *Angew. Chem. Int. Ed.* **2017**, *56*, 837–841.

[72] F. E. Morales, H. E. Garay, D. F. Muñoz, Y. E. Augusto, A. J. Otero-González, O. Reyes Acosta, D. G. Rivera, *Org. Lett.* **2015**, *17*, 2728–2731.

[73] M. G. Ricardo, A. V. Vasco, D. G. Rivera, L. A. Wessjohann, *Org. Lett.* **2019**, *21*, 7307–

7310.

[74] M. Sani, P. Lazzari, M. Folini, M. Spiga, V. Zuco, M. De Cesare, I. Manca, S. Dall'Angelo, M. Frigerio, I. Usai, A. Testa, N. Zaffaroni, M. Zanda, *Chem. - A Eur. J.* **2017**, *23*, 5842–5850.

[75] L. R. Staben, S. Yu, J. Chen, G. Yan, Z. Xu, T. Lau, L. Liu, J. Guo, B. Zheng, J. Cruz-chuh, B. Lee, R. Ohri, W. Cai, H. Zhou, K. R. Kozak, K. Xu, G. D. L. Phillips, J. Lu, J. Wai, A. G. Polson, T. H. Pillow, *ACS Med. Chem. Lett.* **2017**, *8*, 1037–1041.

[76] N. Nischan, C. P. R. Hackenberger, *J. Org. Chem.* **2014**, *79*, 10727–10733.

[77] G. Pasut, A. Guiotto, F. M. Veronese, *Expert Opin. Ther. Pat.* **2004**, *14*, 859–894.

[78] B. Heyne, C. Beddie, J. C. Scaiano, *Org. Biomol. Chem.* **2007**, *5*, 1454–1458.

[79] P. Ochtrop, C. P. R. Hackenberger, *Curr. Opin. Chem. Biol.* **2020**, *58*, 28–36.

[80] M. G. Ricardo, J. F. Marrero, O. Valdes, D. G. Rivera, L. A. Wessjohann, *Chem. - A Eur. J.* **2018**, *25*, 769–774.

[81] B. M. Cooper, J. Iegre, D. H. O'Donovan, M. Ölwegård Halvarsson, D. R. Spring, *Chem. Soc. Rev.* **2021**, *50*, 1480–1494.

[82] R. T. Dorsam, J. S. Gutkind, *Nat. Rev. Cancer* **2007**, *7*, 79–94.

[83] M. Roveri, M. Bernasconi, J. Leroux, P. Luciani, *J. Mater. Chem. Mater. Chem. B* **2017**, *5*, 4348–4364.

[84] O. E. Vercillo, C. K. Z. Andrade, L. A. Wessjohann, *Org. Lett.* **2008**, *10*, 205–208.

[85] H. Ohki-Hamazaki, M. Iwabuchi, F. Maekawa, *Int. J. Dev. Biol.* **2005**, *49*, 293–300.

[86] A. A. Begum, P. M. Moyle, I. Toth, *Bioorg. Med. Chem.* **2016**, *24*, 5834–5841.

[87] B. L. Faintuch, R. Teodoro, A. Duatti, E. Muramoto, S. Faintuch, C. J. Smith, *Nucl.*

Med. Biol. **2008**, *35*, 401–411.

[88]   H. Chen, S. Wan, F. Zhu, C. Wang, S. Cui, C. Dua, Y. Maa, Y. Gua, *Contrast Media Mol. Imaging* **2014**, *9*, 122–134.

[89]   W. A. Henne, D. D. Doorneweerd, A. R. Hilgenbrink, S. A. Kularatne, P. S. Low, *Bioorganic Med. Chem. Lett.* **2006**, *16*, 5350–5355.

[90]   Y. Koh, J. K. Sung, J. Park, C. Park, S. Cho, H. G. Woo, C. K. Young, H. Sohn, *BKCS* **2007**, *28*, 2083–2088.

Annexes

Table of contents

A.1. IR and NMR data of isocyanides

1-Isocyanodecane **24**

Figure A1. Infrared spectrum of 1-isocyanodecane **24**.
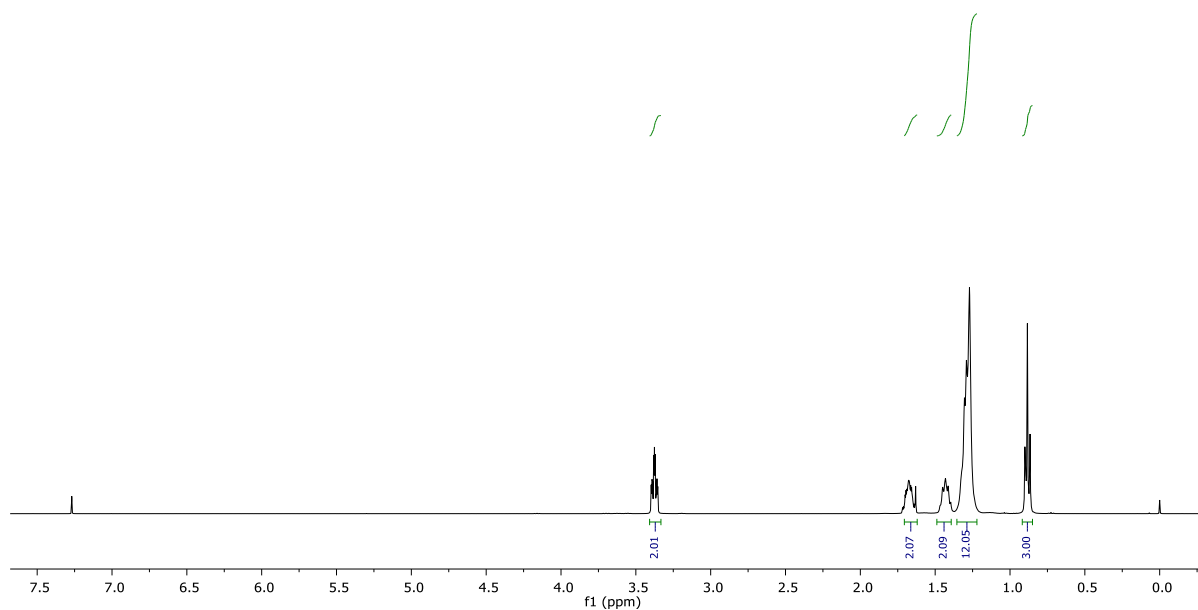
Figure A2. ^{1}H NMR (400 MHz, CDCl$_3$) spectrum of 1-isocyanodecane **24**.
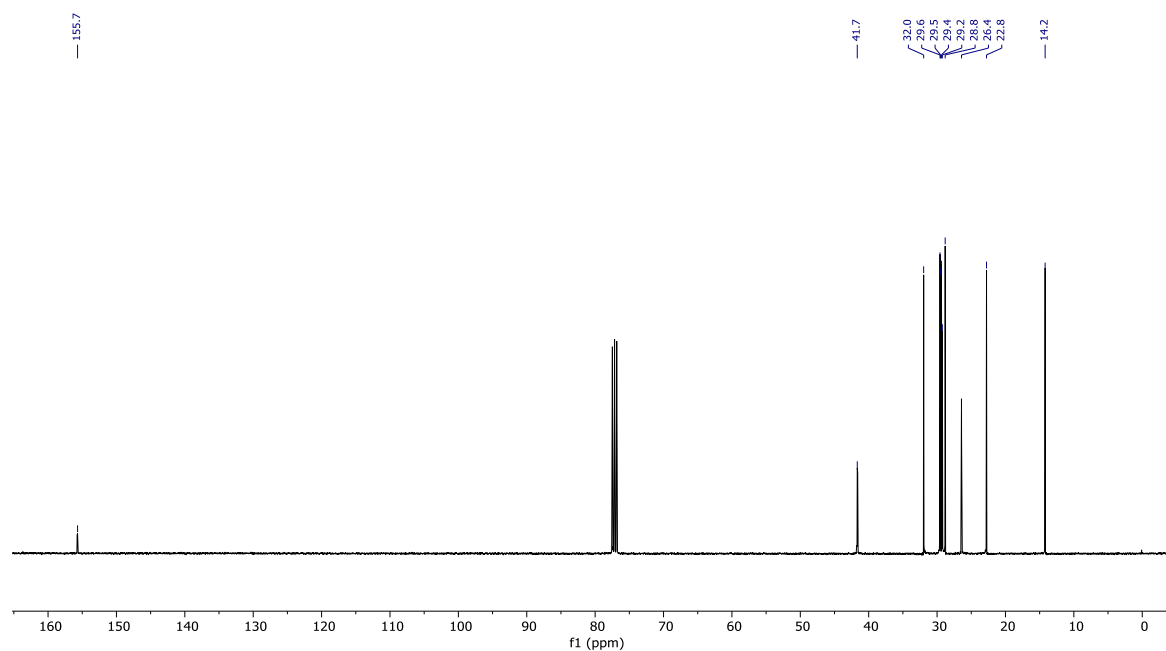
Figure A3. ^{13}C NMR (101 MHz, CDCl$_3$) of 1-isocyanodecane **24**.

1-isocyanotetradecane **25**
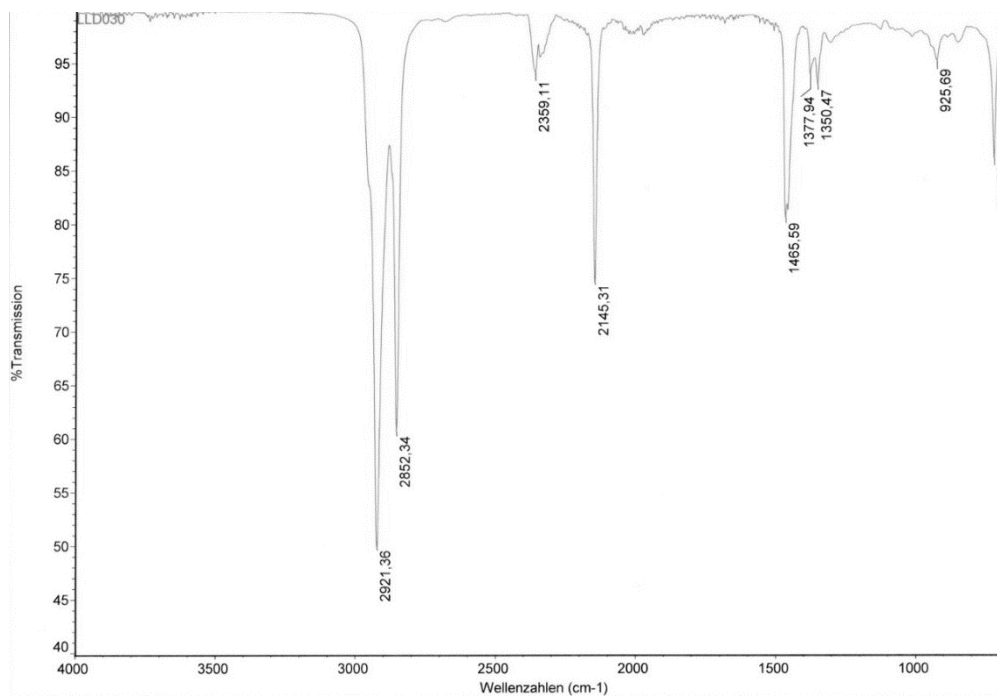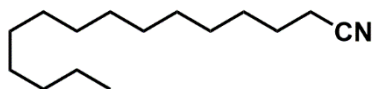
Figure A4. Infrared spectrum of 1-isocyanotetradecane **25**.
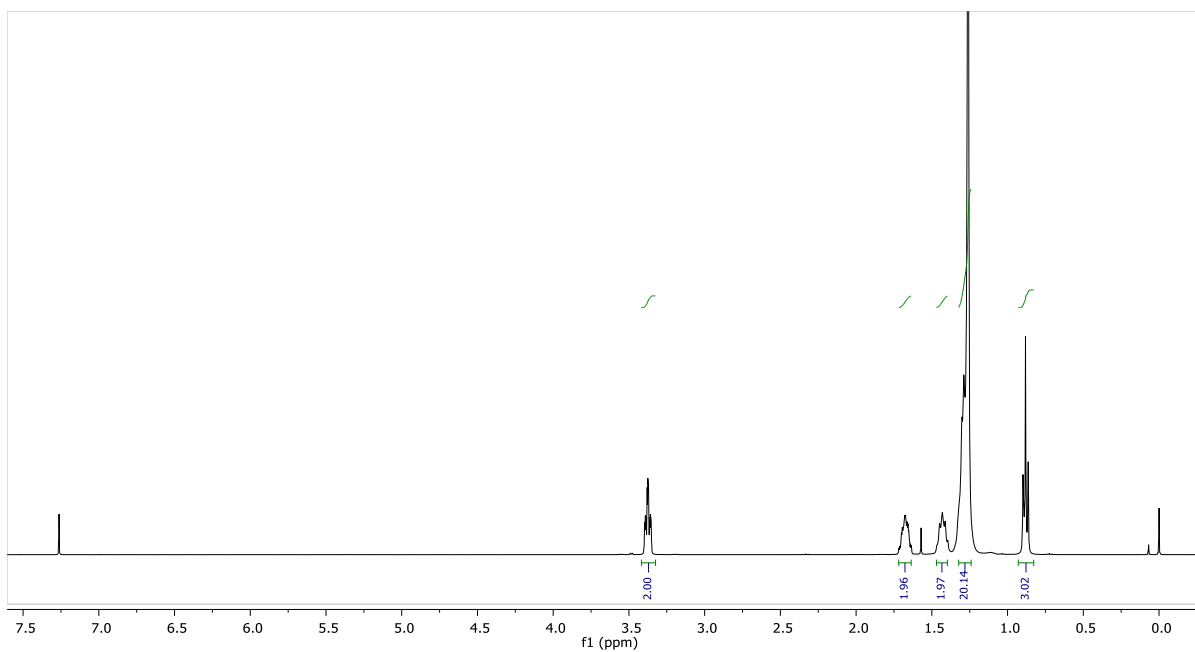
Figure A5. ^{1}H NMR (400 MHz, CDCl$_3$) spectrum of 1-isocyanotetradecane **25**.
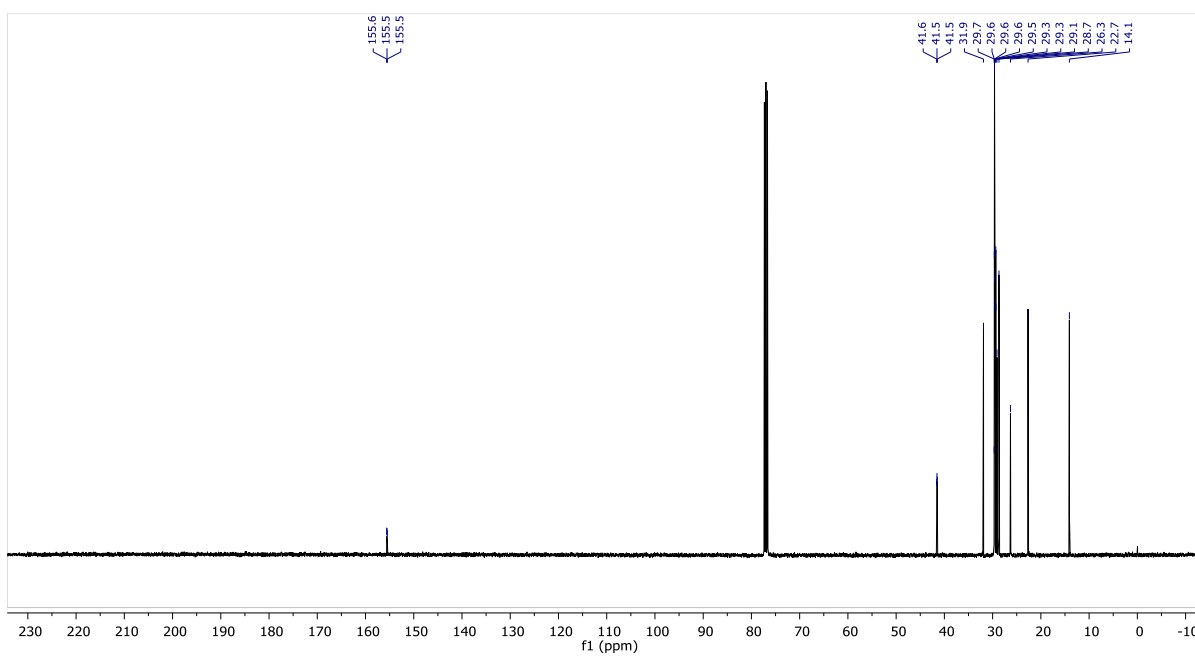
Figure A6. ^{13}C NMR (101 MHz, CDCl$_3$) spectrum of 1-isocyanotetradecane **25**.

1-isocyanooctadecane **26**
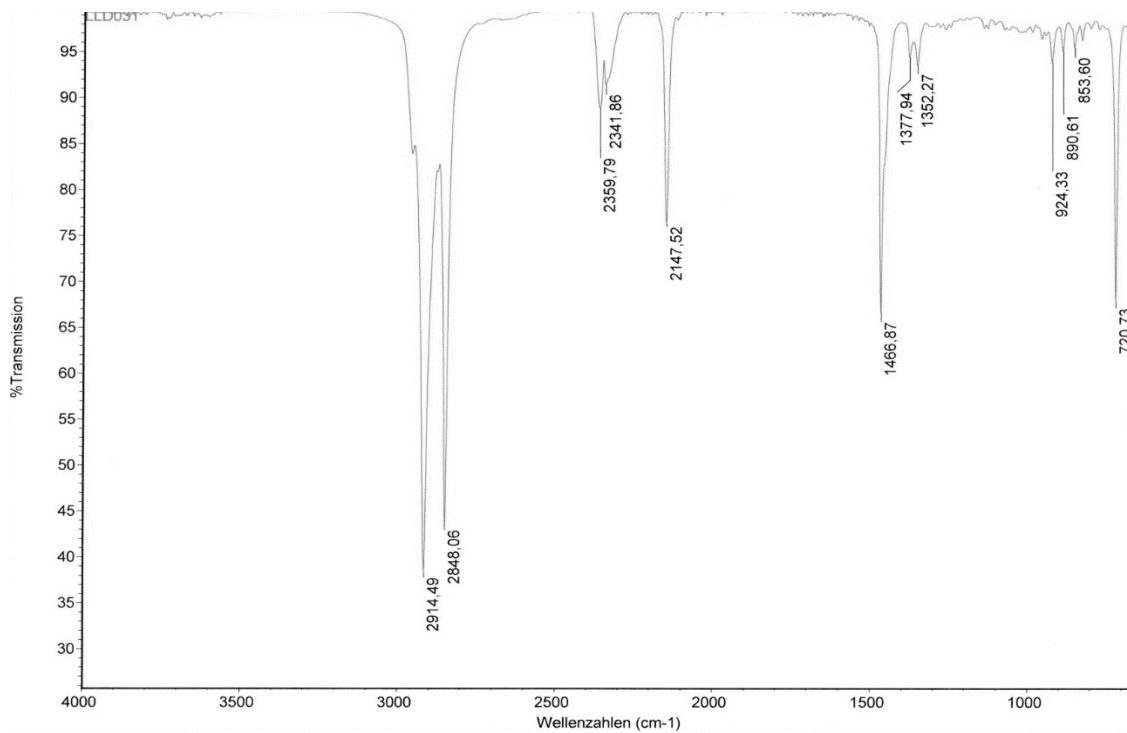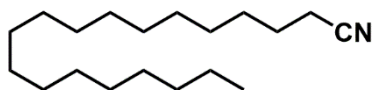
Figure A7. Infrared spectrum of 1-isocyanooctadecane **26**.
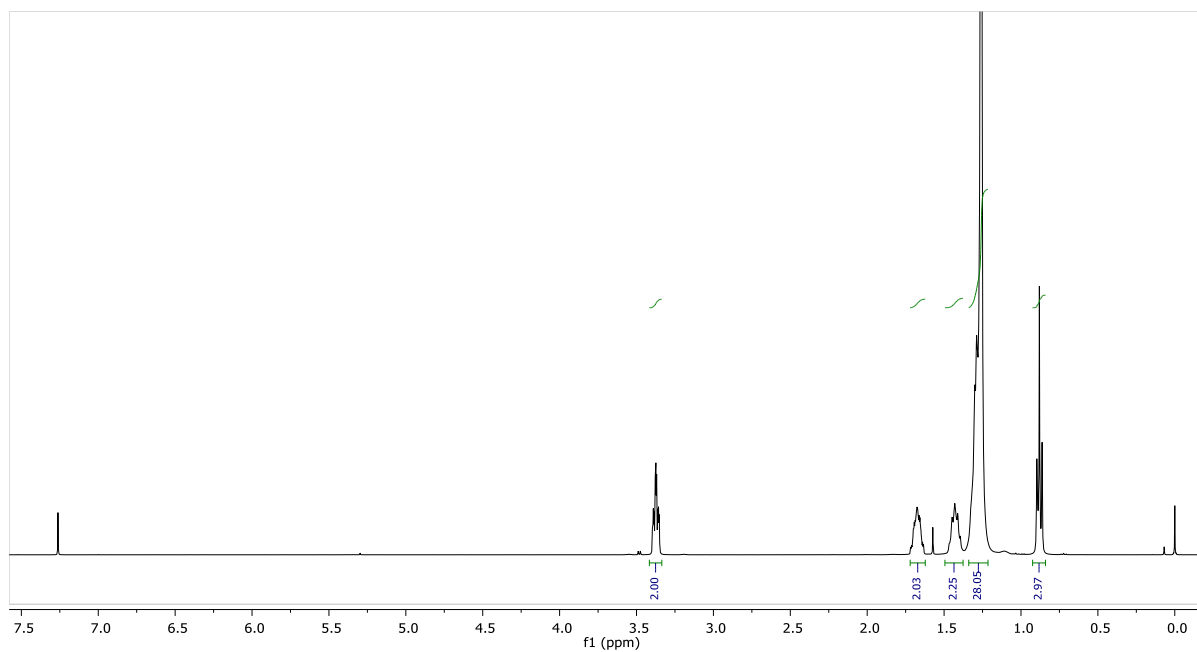
Figure A8. ^{1}H NMR (400 MHz, CDCl$_3$) spectrum of 1-isocyanooctadecane **26**.
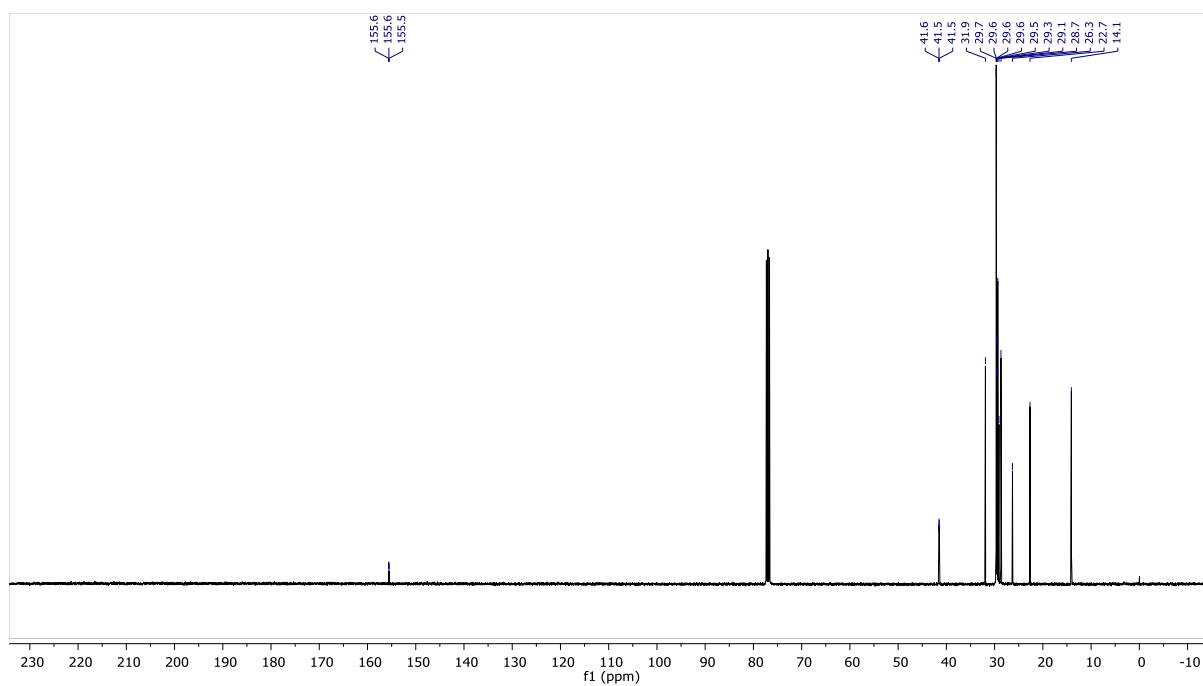
Figure A9. ^{13}C NMR (101 MHz, CDCl$_3$) spectrum of 1-isocyanooctadecane **26**.

MeO-PEG$_4$-NC **30**
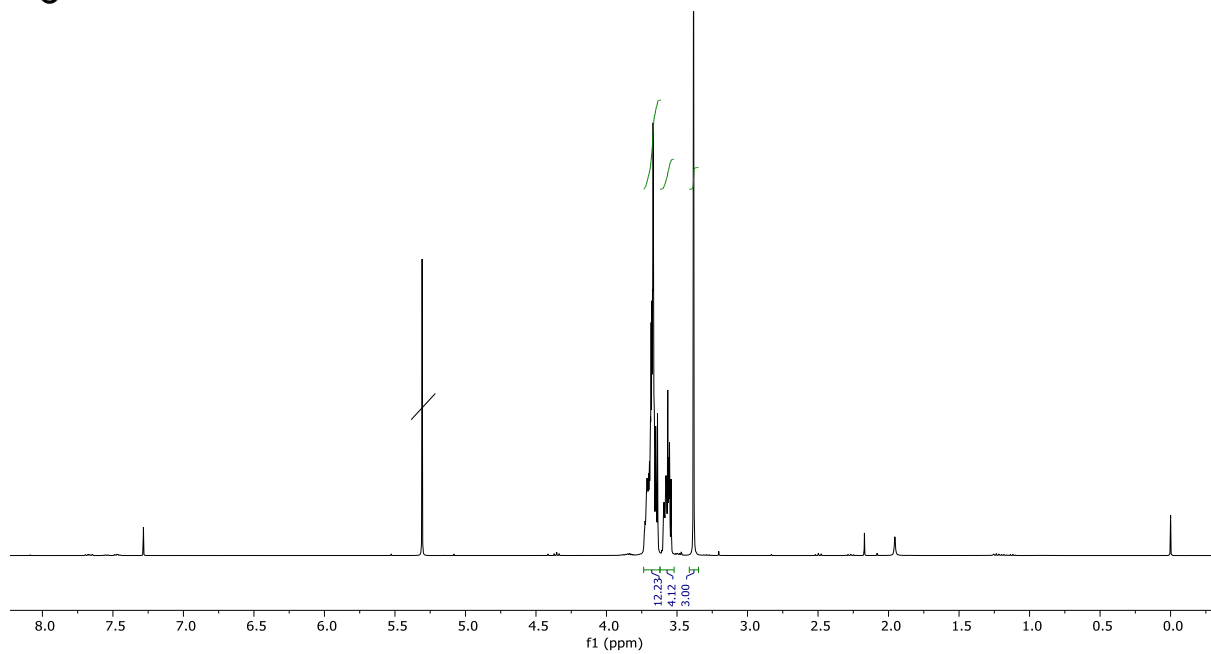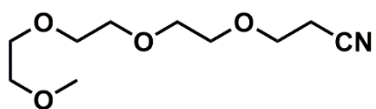
Figure A10. ^{1}H NMR (400 MHz, CDCl$_3$) spectrum of MeO-PEG$_4$-NC **30**.
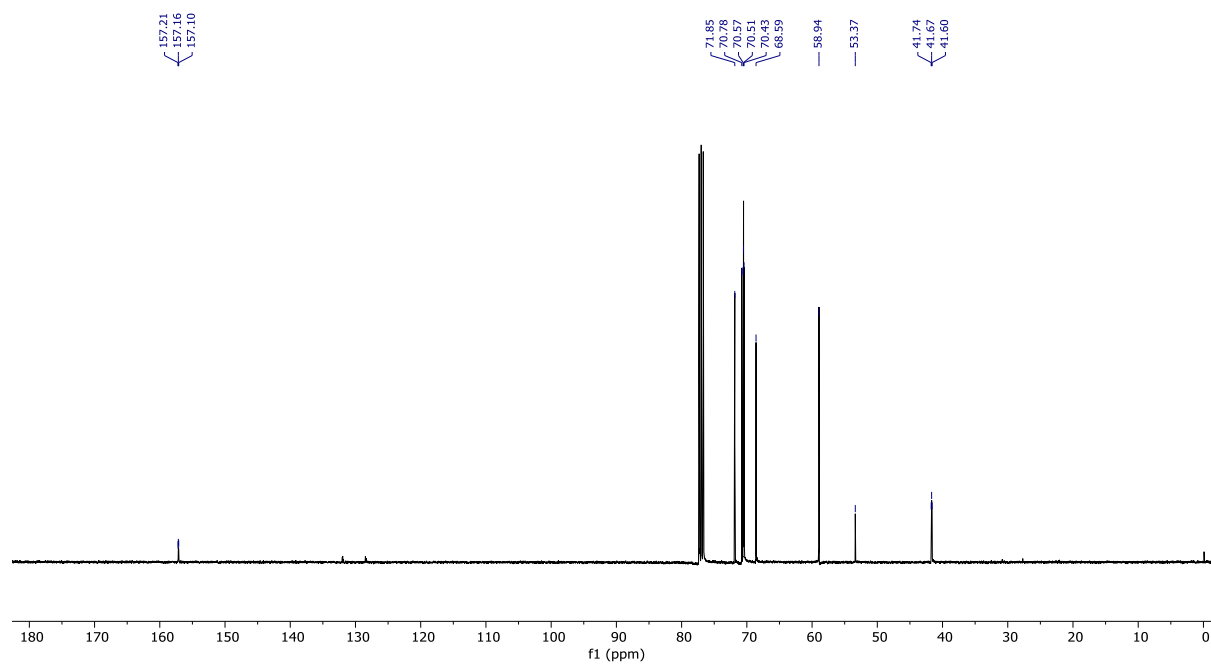
Figure A11. ^{13}C NMR (101 MHz, CDCl$_3$) spectrum of MeO-PEG$_4$-NC **30**.

Allyl 8-isocyanooctylcarbamate **36**
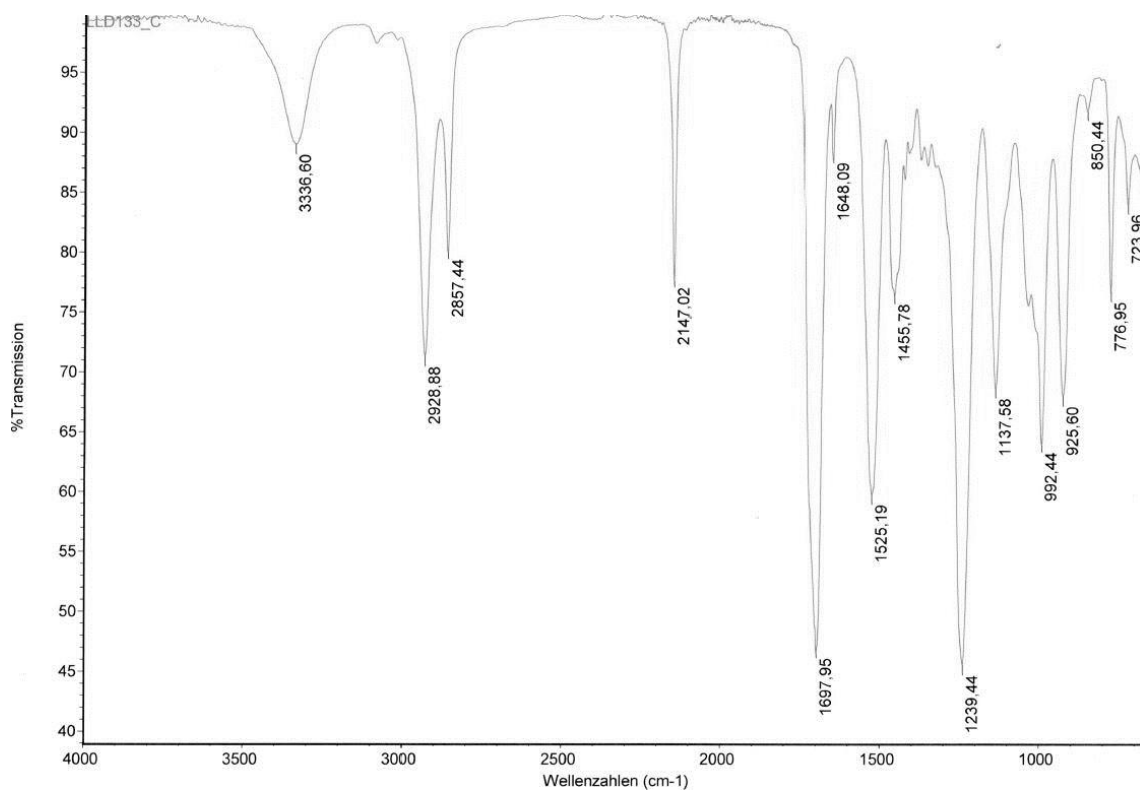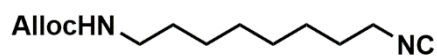
Figure A12. Infrared spectrum of Allyl 8-isocyanooctylcarbamate **36**.
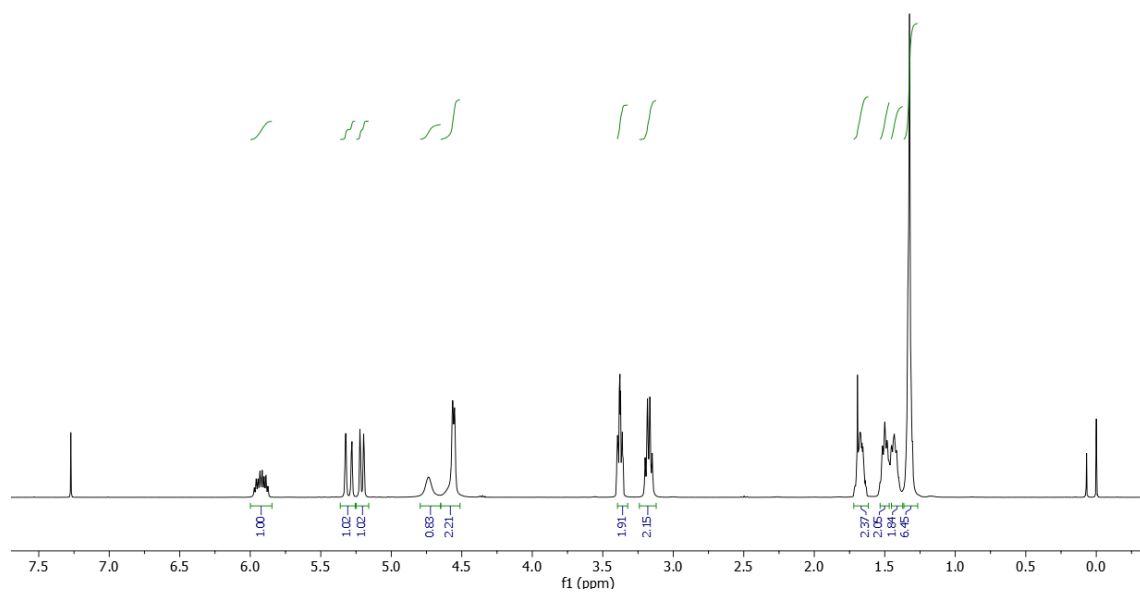
Figure A13. ^{1}H NMR (400 MHz, CDCl$_3$) spectrum of Allyl 8-isocyanooctylcarbamate **36**.
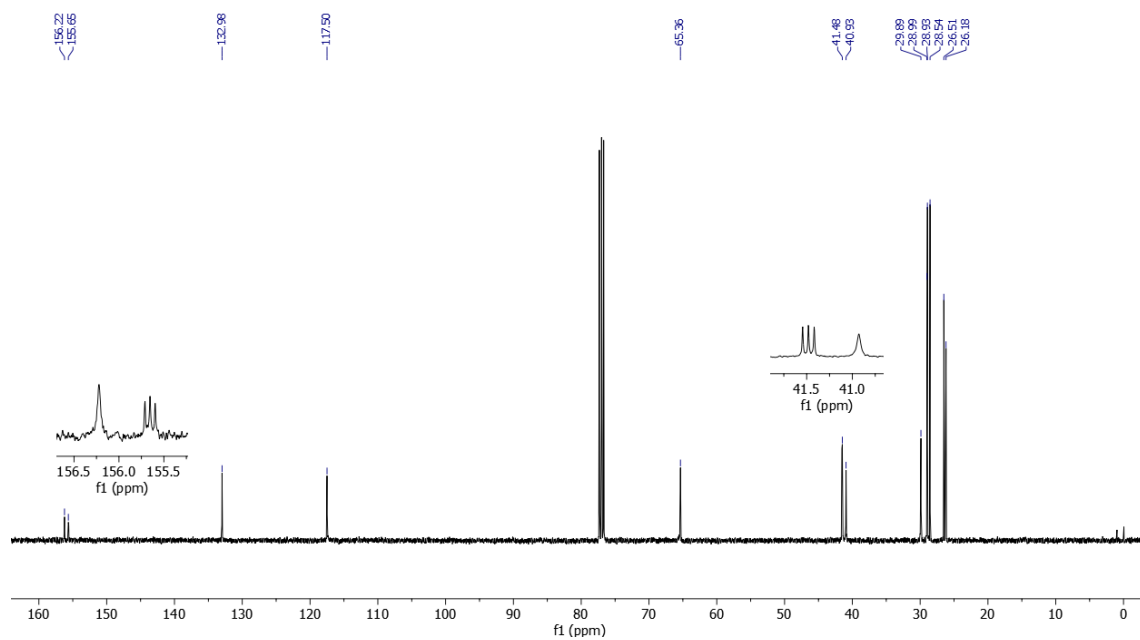
Figure A14. ^{13}C NMR (100 MHz, CDCl$_3$) spectrum of Allyl 8-isocyanooctylcarbamate **36**.

Allyl 10-isocyanodecylcarbamate **37**
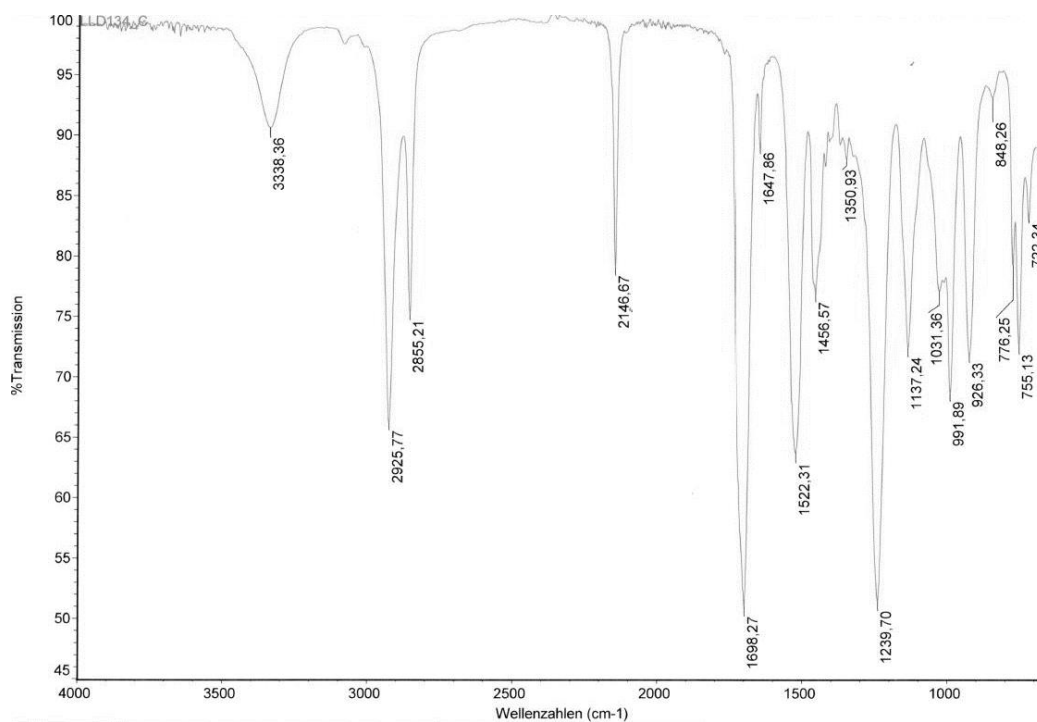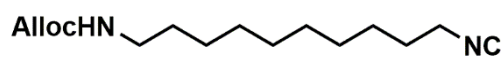
Figure A15. Infrared spectrum of Allyl 10-isocyanodecylcarbamate **37**.
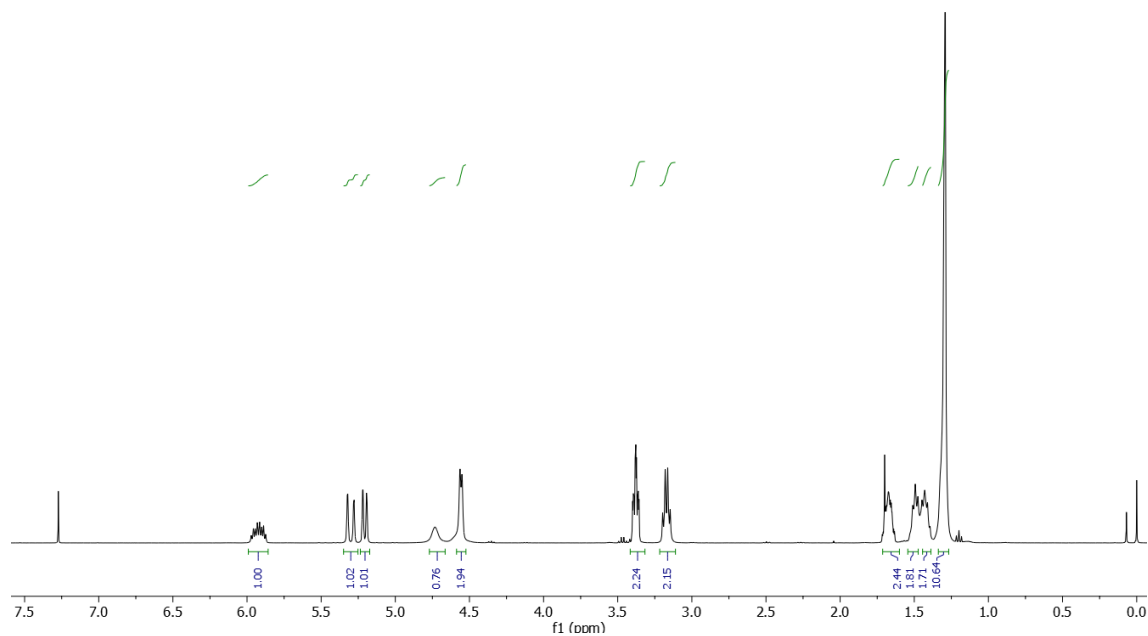
Figure A16. ^{1}H NMR (400 MHz, CDCl$_3$) spectrum of Allyl 10-isocyanodecylcarbamate **37**.
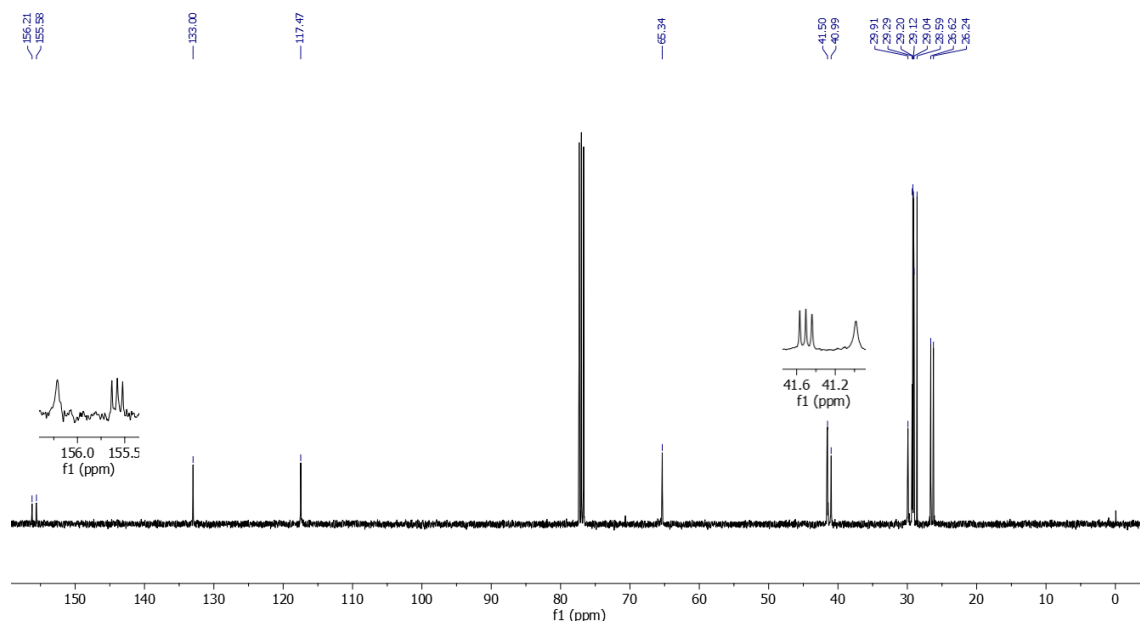
Figure A17. ^{13}C NMR (100 MHz, CDCl$_3$) spectrum of Allyl 10-isocyanodecylcarbamate **37**.

Allyl 12-isocyanododecylcarbamate **38**
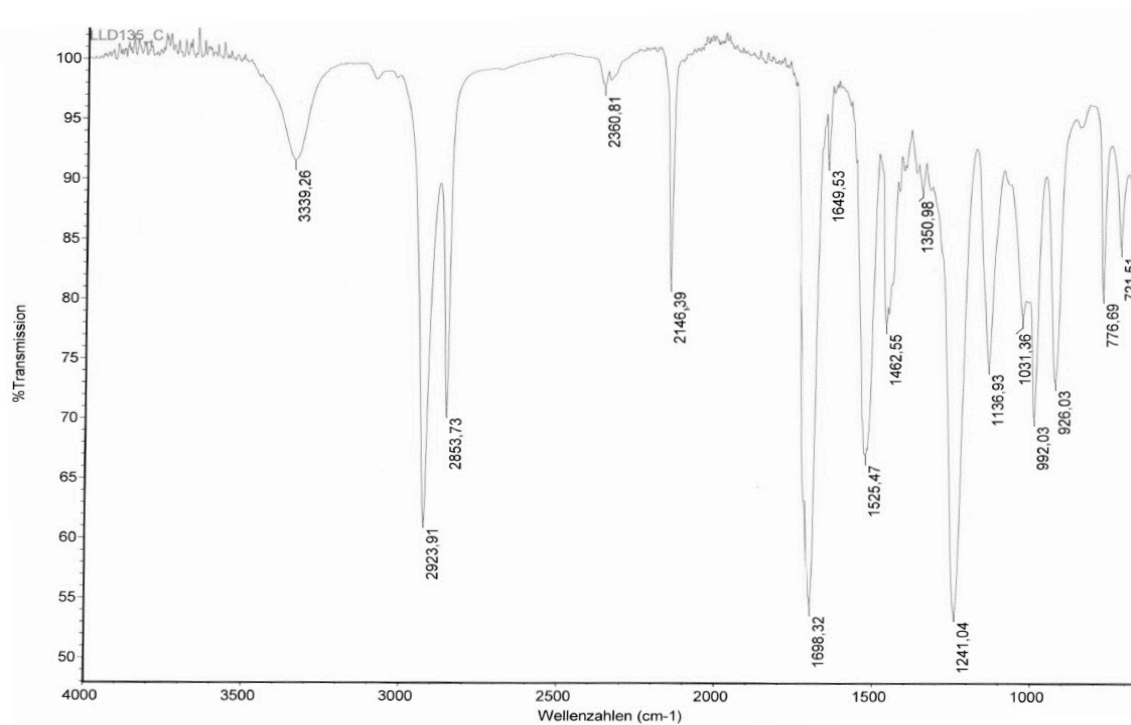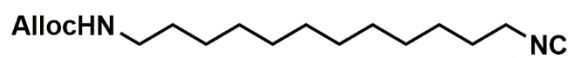
Figure A18. Infrared spectrum of Allyl 12-isocyanododecylcarbamate **38**.
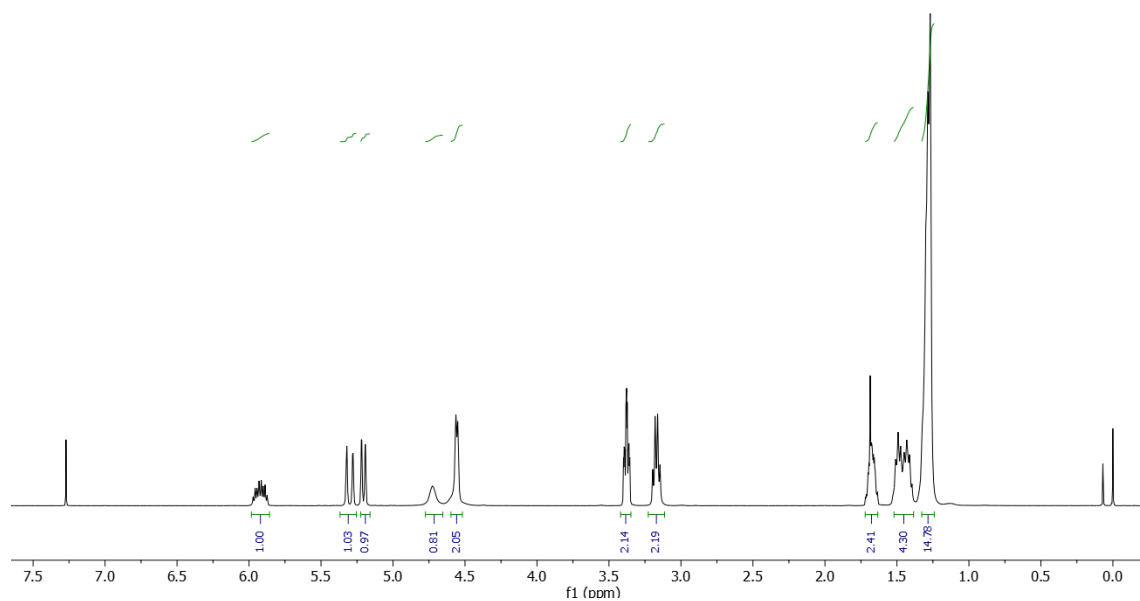
Figure A19. ^{1}H NMR (400 MHz, CDCl$_3$) spectrum of Allyl 12-isocyanododecylcarbamate **38**.
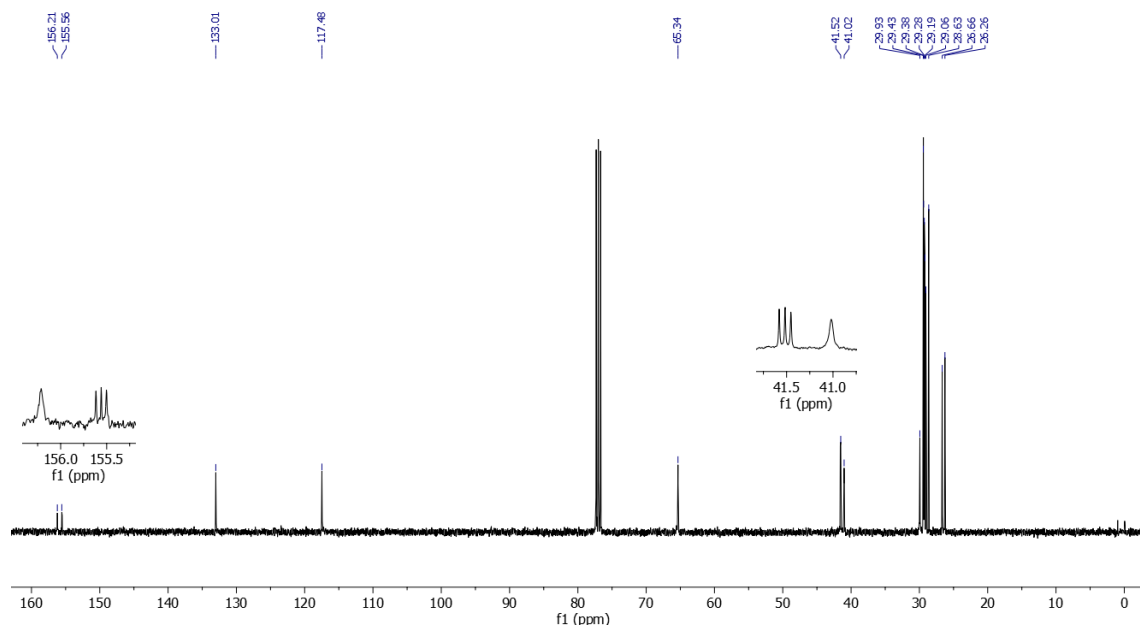
Figure A20. ^{13}C NMR (100 MHz, CDCl$_3$) spectrum of Allyl 12-isocyanododecylcarbamate **38**.

(2-trimethylsilyl)ethyl 3-isocyanopropionate **44**
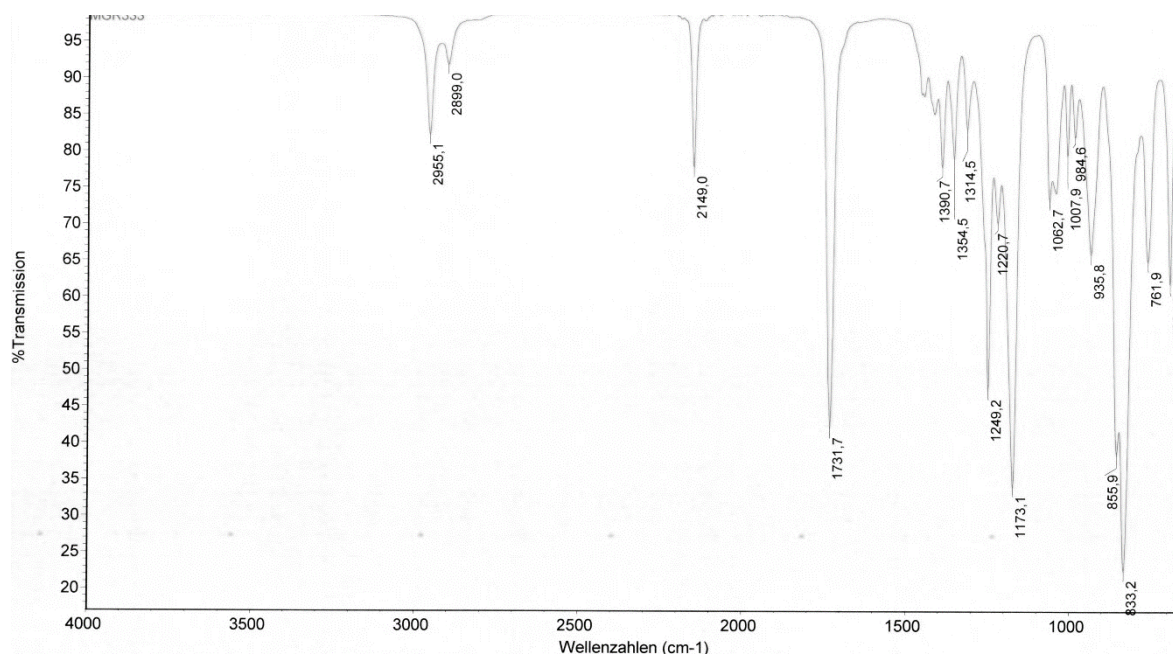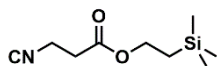
Figure A21. Infrared spectrum of 2-(trimethylsilyl) ethyl 3-isocyanopropionate **44**.
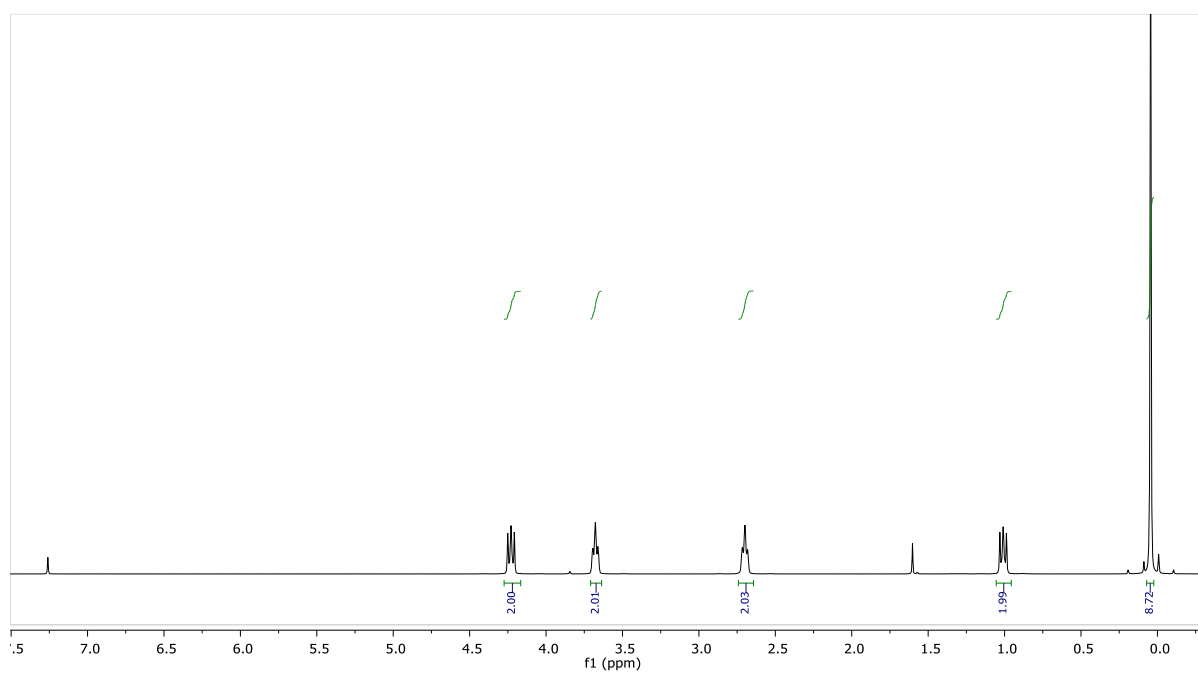
Figure A22. ^{1}H NMR (400 MHz, CDCl$_3$) spectrum of 2-(trimethylsilyl) ethyl 3-isocyanopropionate **44**.
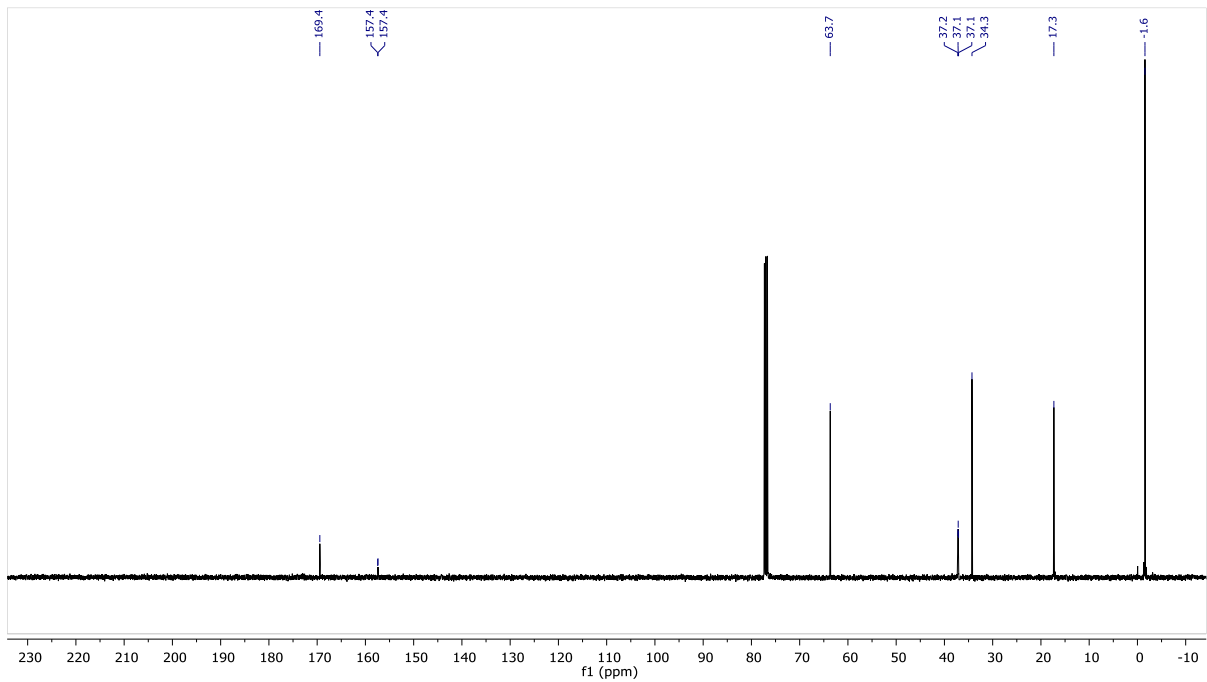
Figure A23. ^{13}C NMR (101 MHz, CDCl[3]) spectrum of 2-(trimethylsilyl)ethyl 3-isocyanopropionate **44**.

2-(trimethylsilyl)ethyl 4-isocyanobutyrate **45**
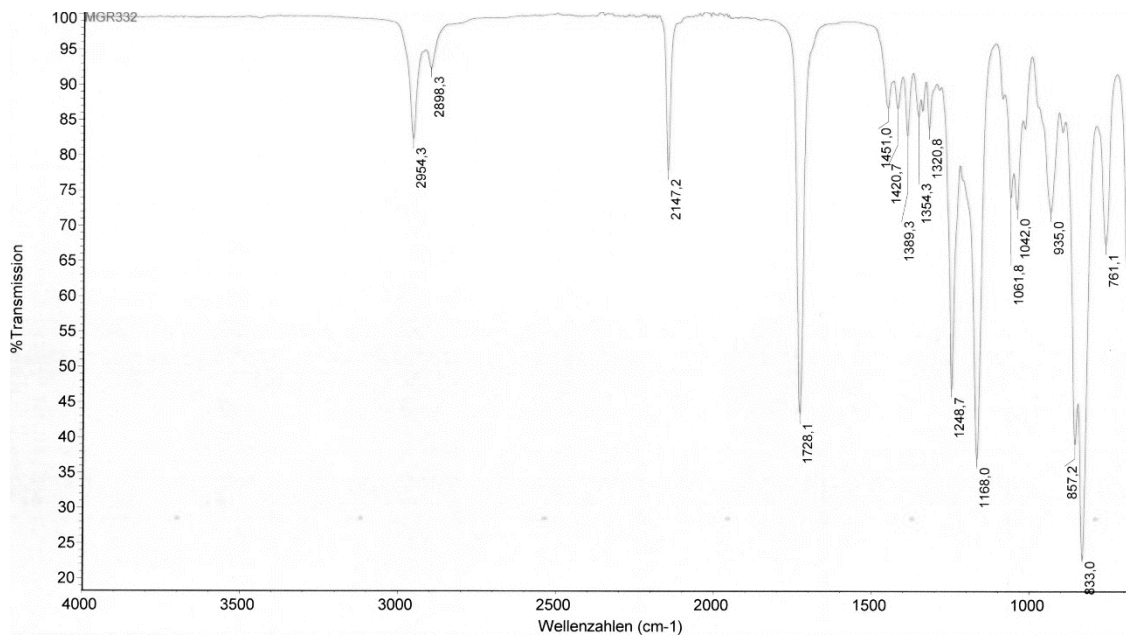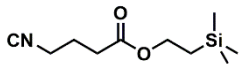
Figure A24. Infrared spectrum of 2-(trimethylsilyl) ethyl 4-isocyanobutyate **45**.
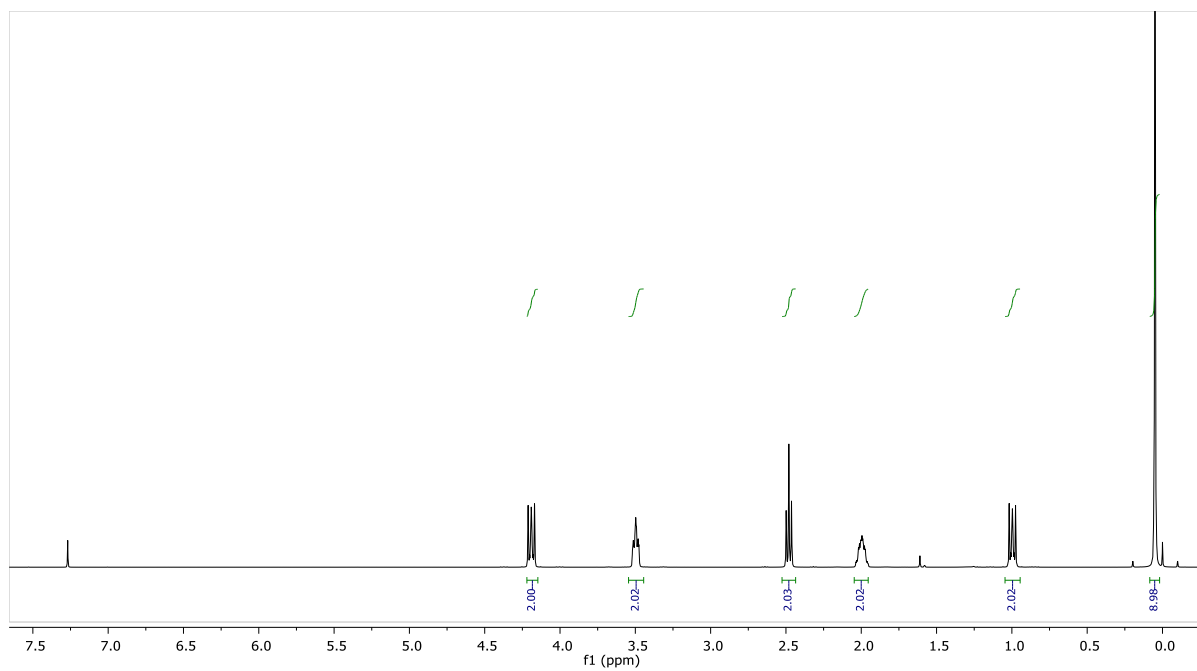
Figure A25. ^{1}H NMR (400 MHz, CDCl$_3$) spectrum of 2-(trimethylsilyl) ethyl 4-isocyanobutyate **45**.
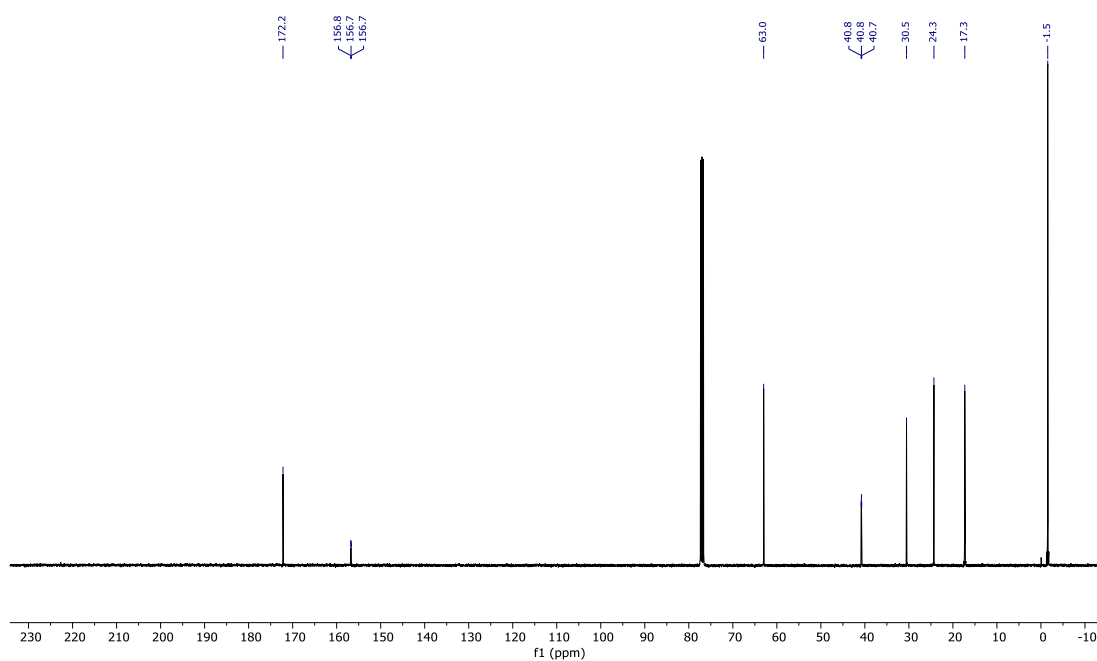
Figure A26. ^{13}C NMR (101 MHz, CDCl$_3$) spectrum of 2-(trimethylsilyl)ethyl 4-isocyanobutyate **45**.

9-((4-isocyano-2-methylbutan-2-yl)thio)-9H-xanthene **50**
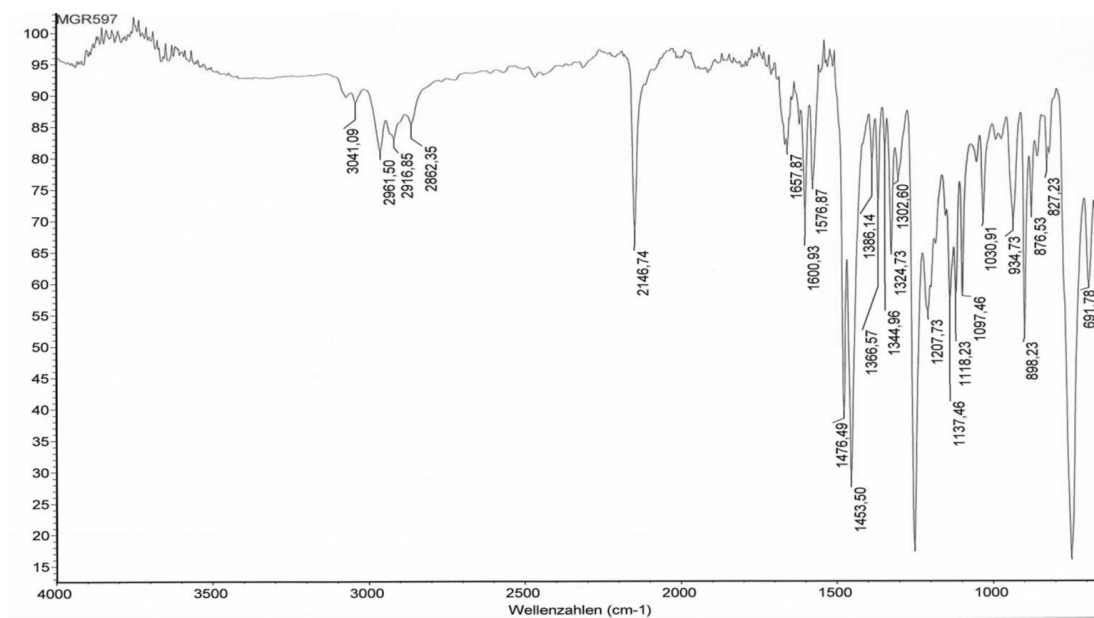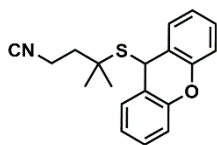
Figure A27. Infrared spectrum of 9-((4-isocyano-2-methylbutan-2-yl)thio)-9H-xanthene **50**.
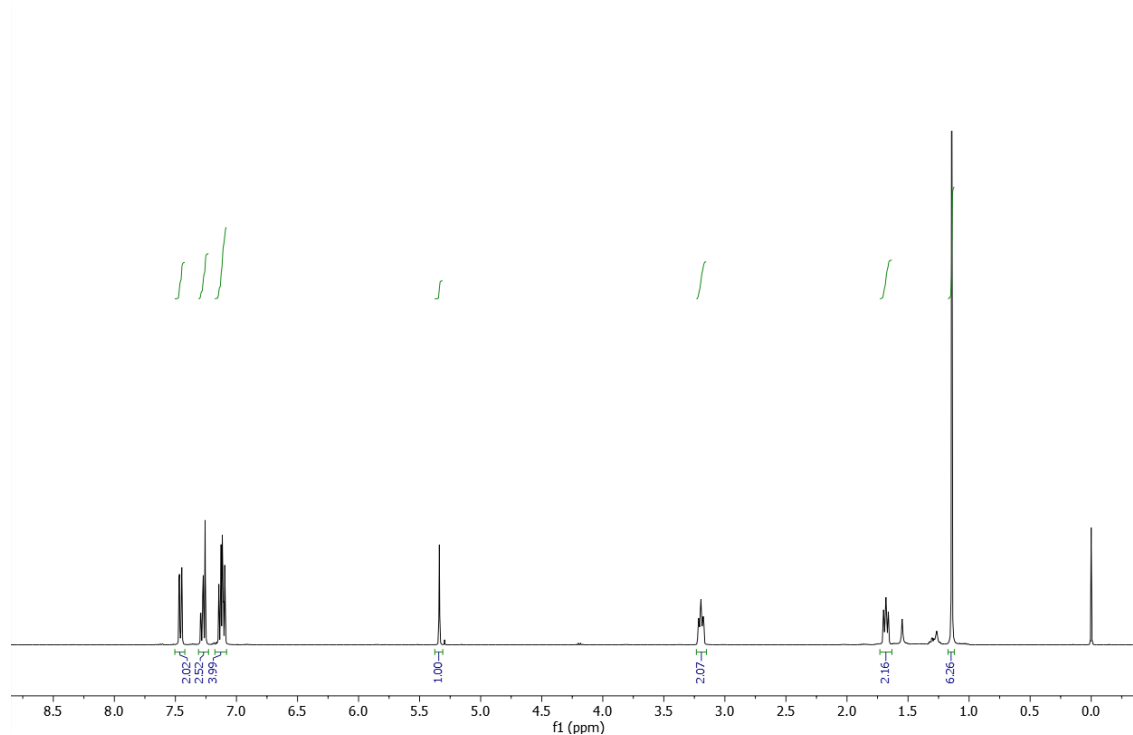
Figure A28. ^{1}H NMR (400 MHz, CDCl$_3$) spectrum of 9-((4-isocyano-2-methylbutan-2-yl)thio)-9H-xanthene **50**.
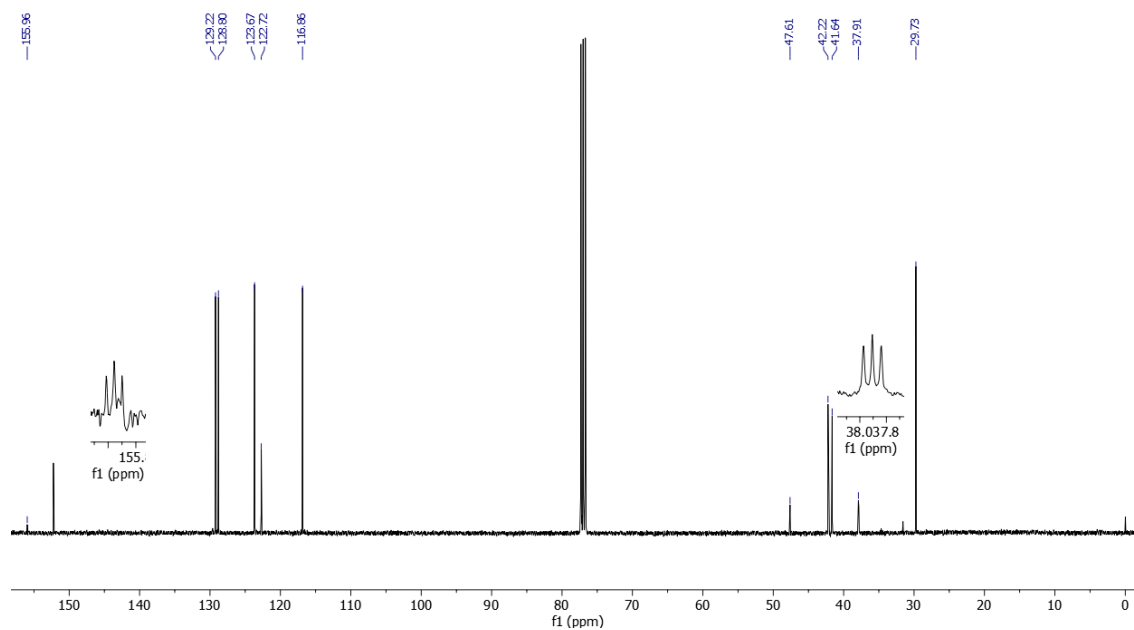
Figure A29. ^{13}C NMR (101 MHz, CDCl$_3$) spectrum of 9-((4-isocyano-2-methylbutan-2-yl)thio)-9H-xanthene **50**.

A.2. HR-MS and NMR data of tubugis

Tubugi **23**
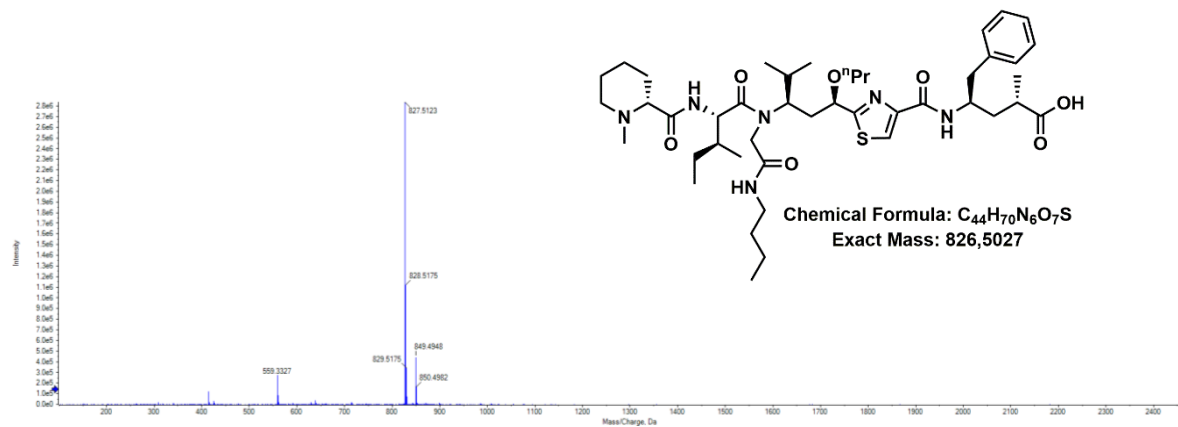
Figure A30. ESI-HRMS of Tubugi **23**.
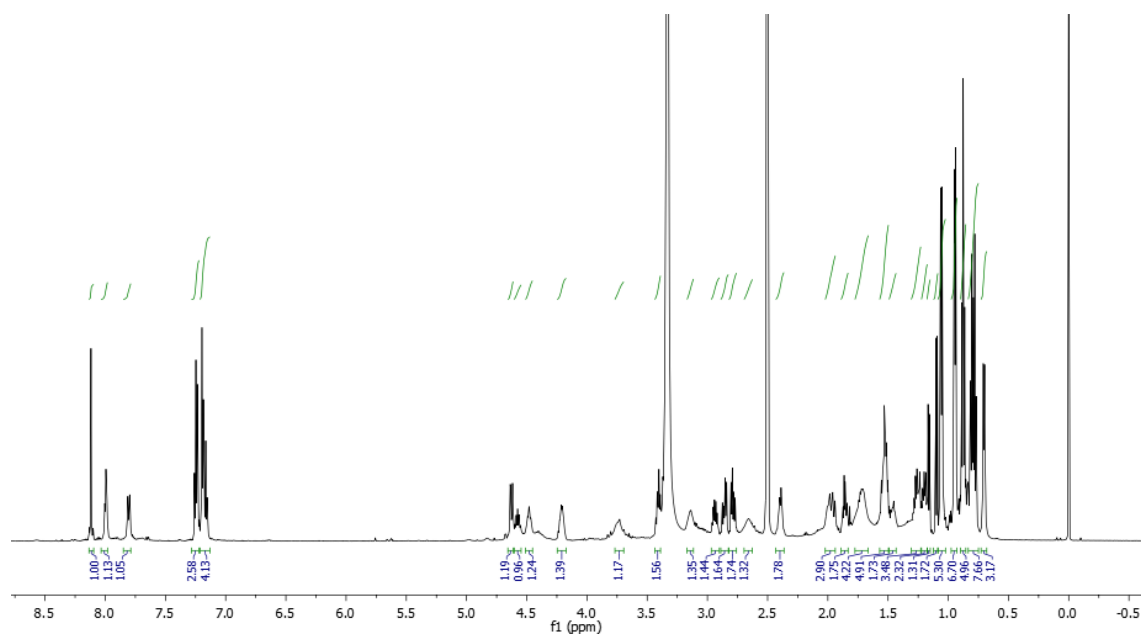
Figure A31. ^{1}H NMR (400 MHz, DMSO-*d*6) spectrum of Tubugi **23**.

Tubugi **27**

Chemical Formula: C₄₉H₇₈N₆O₈S
Exact Mass: 910,5602
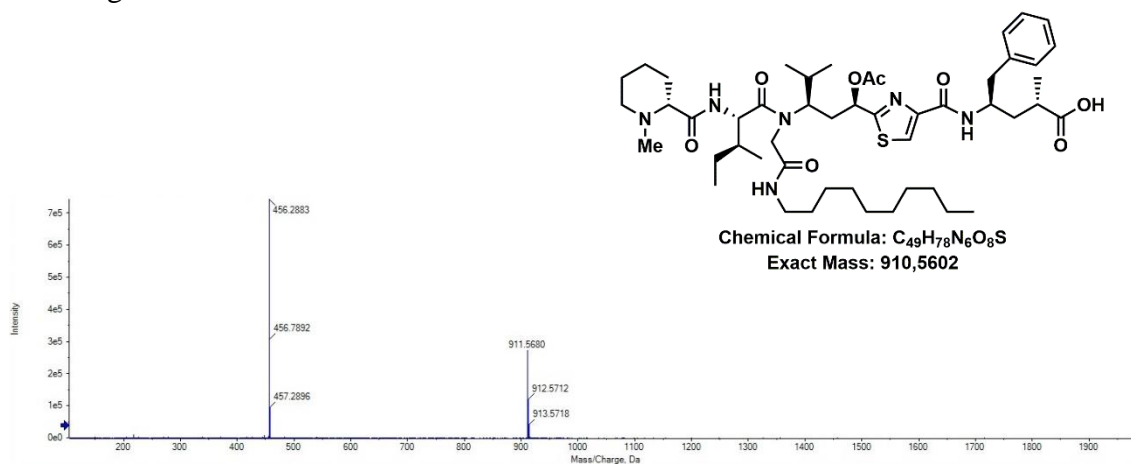
Figure A32. ESI-HRMS of Tubugi **27**.
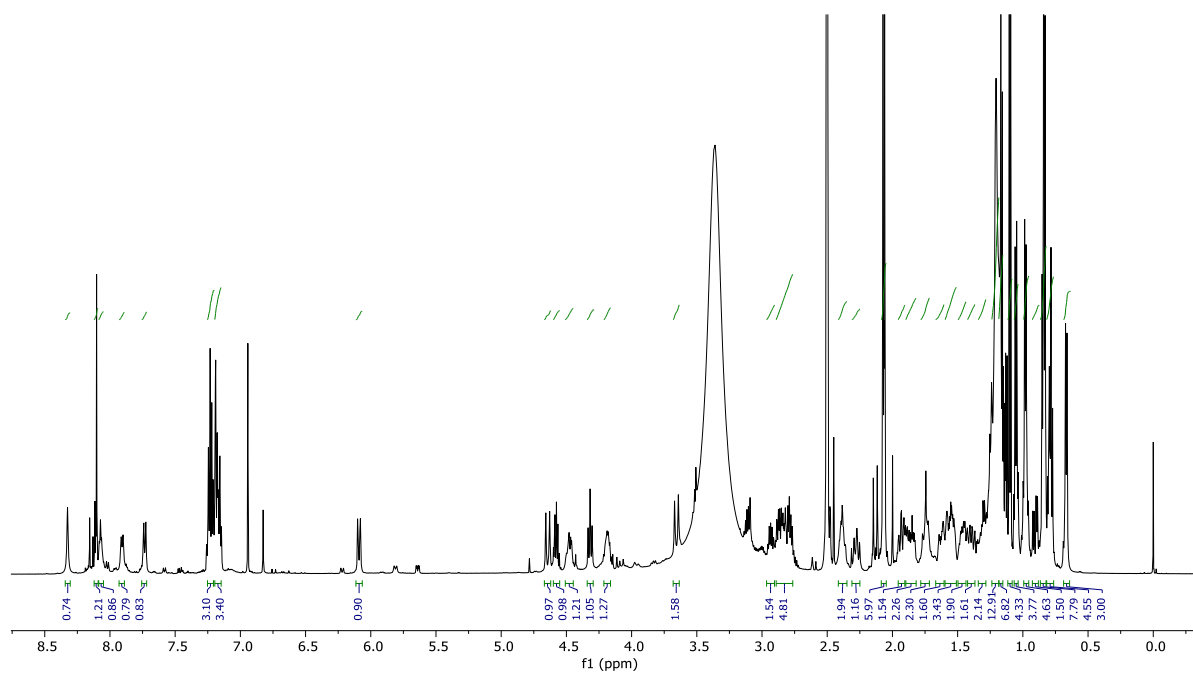
Figure A33. ¹H NMR (400 MHz, DMSO-*d*6) spectrum of Tubugi **27**.

Tubugi **28**
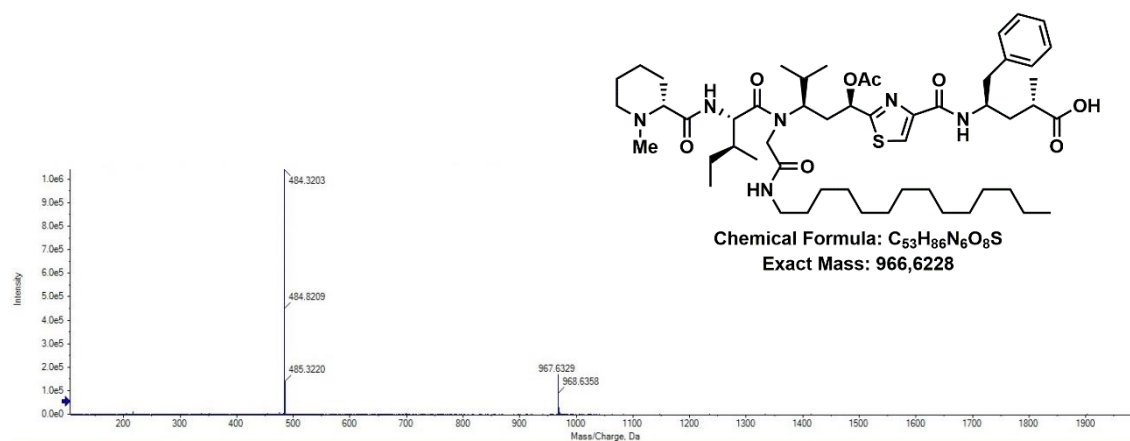
Figure A34. ESI-HRMS of Tubugi **28**.
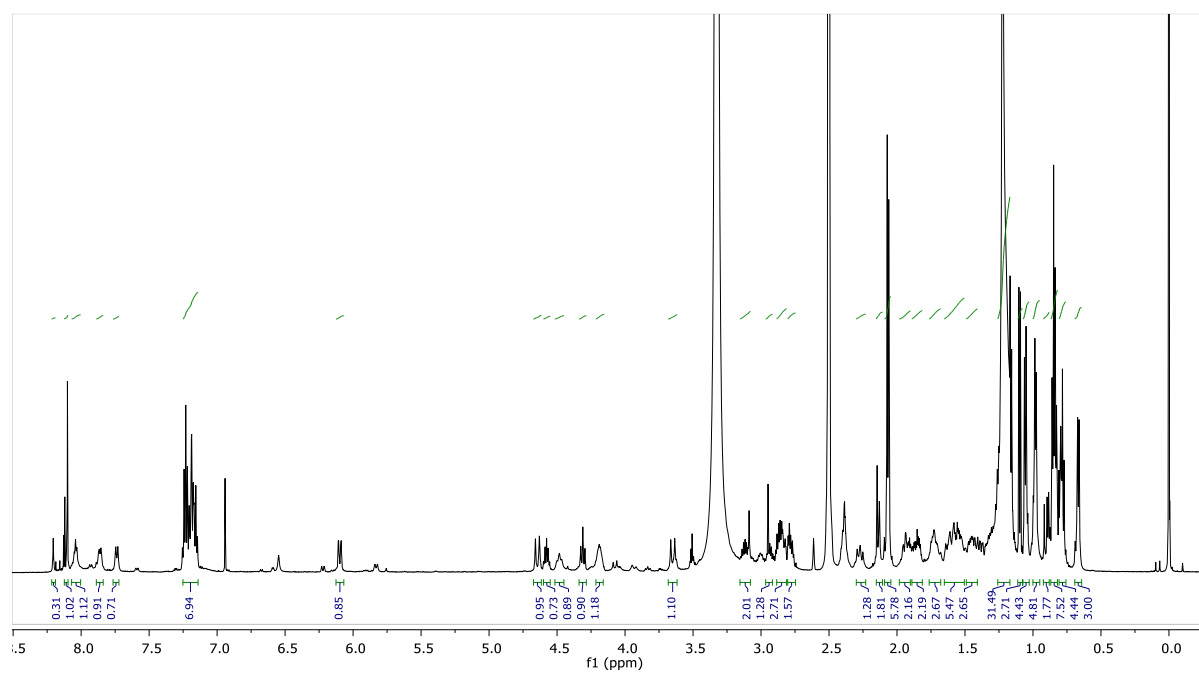
Figure A35. ^{1}H NMR (400 MHz, DMSO-*d*6) spectrum of Tubugi **28**.

Tubugi **29**
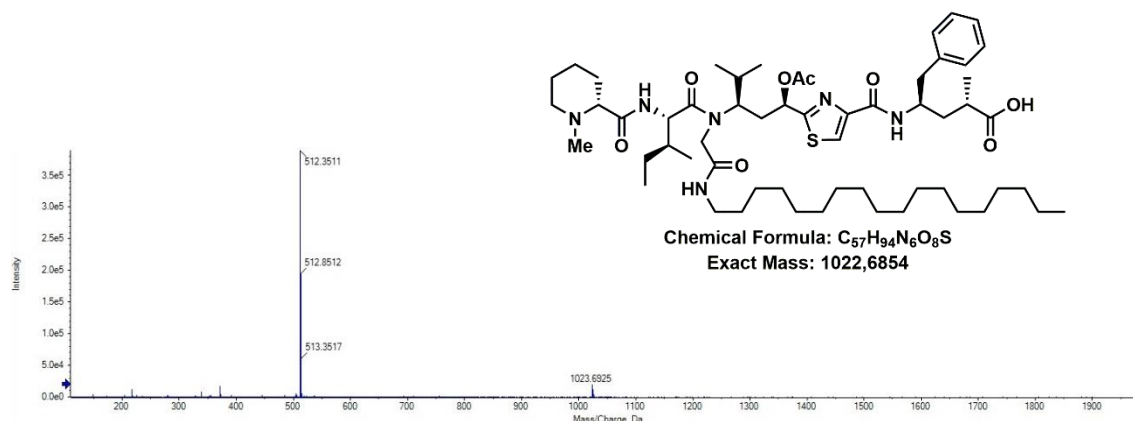
Figure A36. ESI-HRMS of Tubugi **29**.
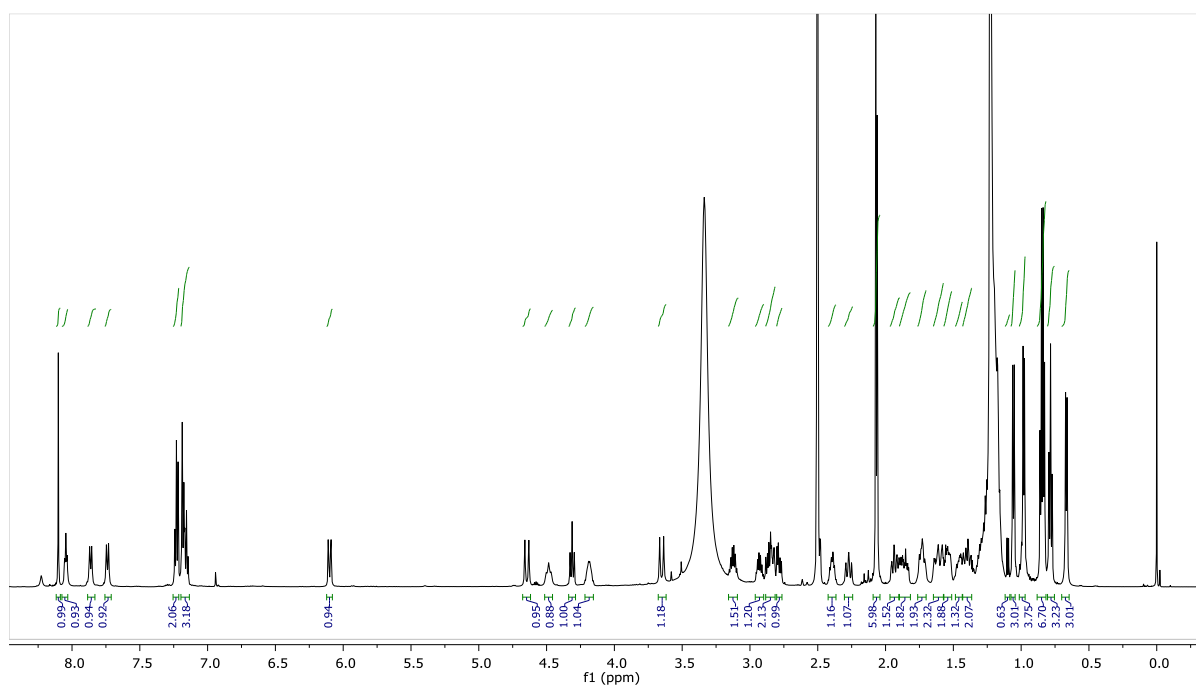
Figure A37. ¹H NMR (400 MHz, DMSO-*d*6) spectrum of Tubugi **29**.

Tubugi **31**
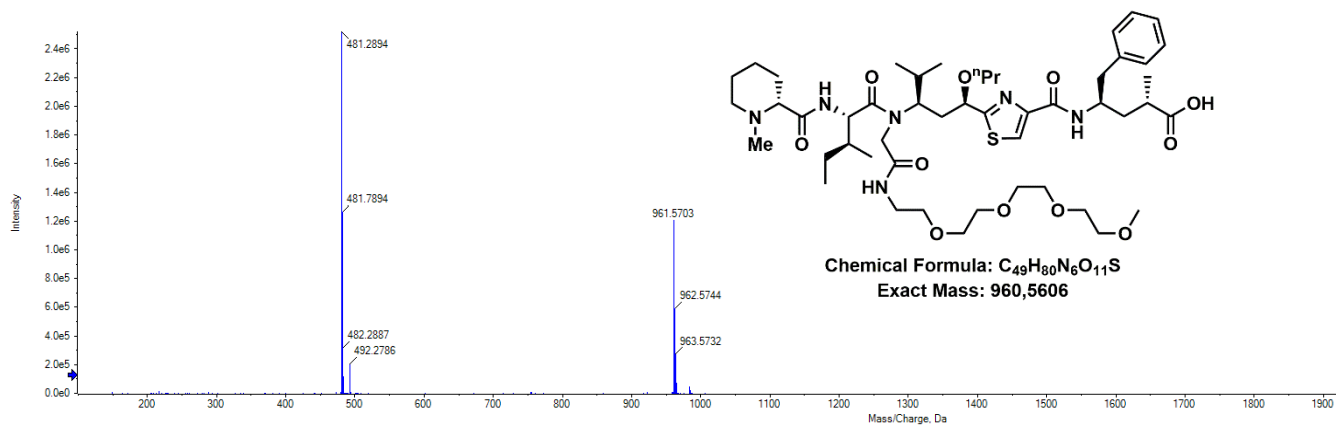
Figure A38. ESI-HRMS of Tubugi **31**.
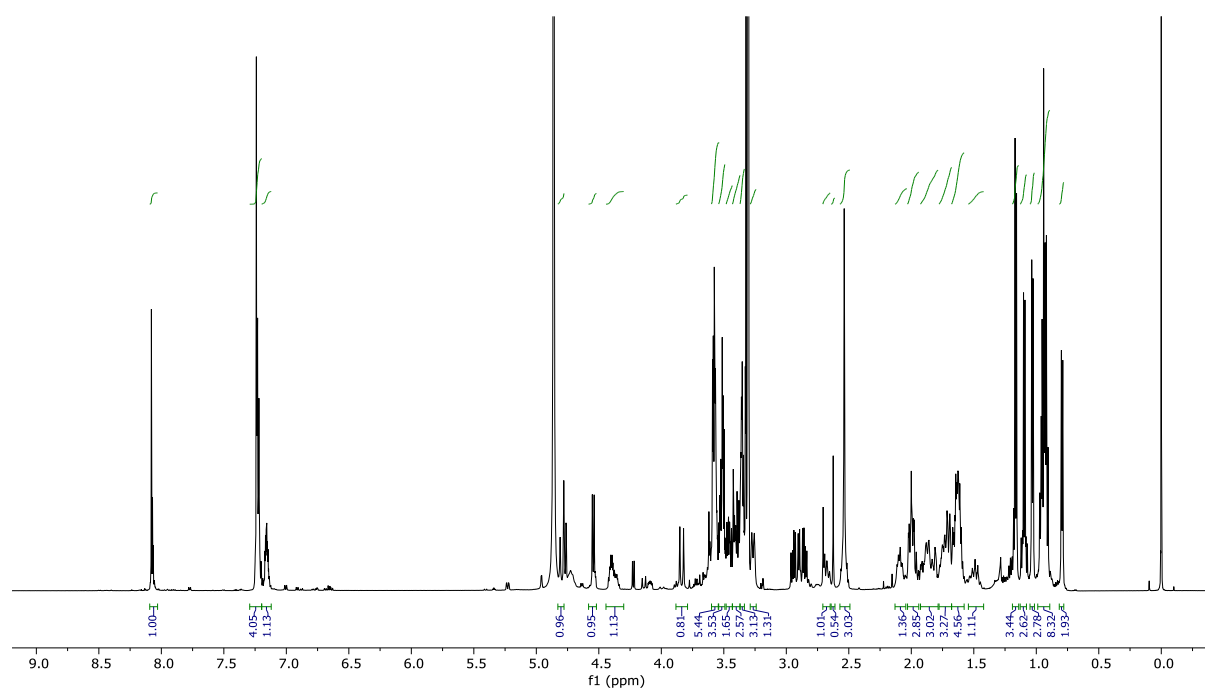
Figure A39. ^{1}H NMR (400 MHz, DMSO-*d*6) spectrum of Tubugi **31**.

Tubugi **32**
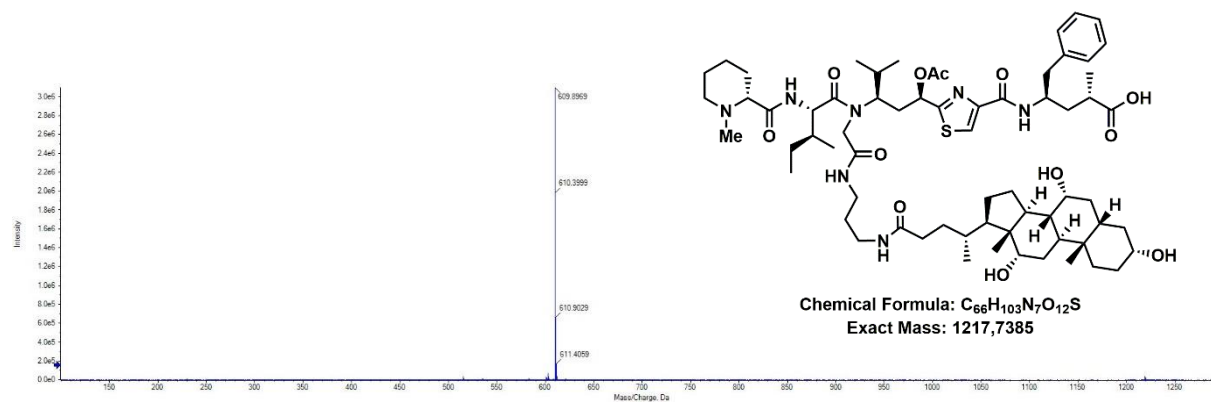
FigureA40. ESI-HRMS of Tubugi **32**.
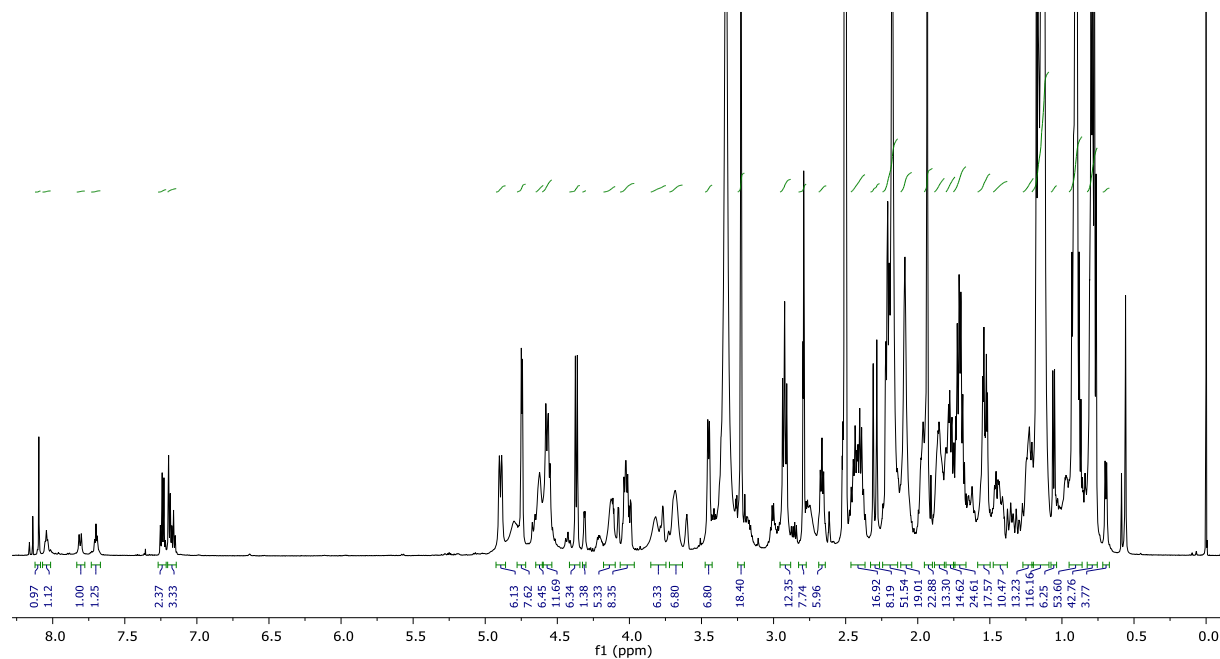
Figure A41. ^{1}H NMR (400 MHz, DMSO-*d*6) spectrum of Tubugi **32**.

Tubugi **33**
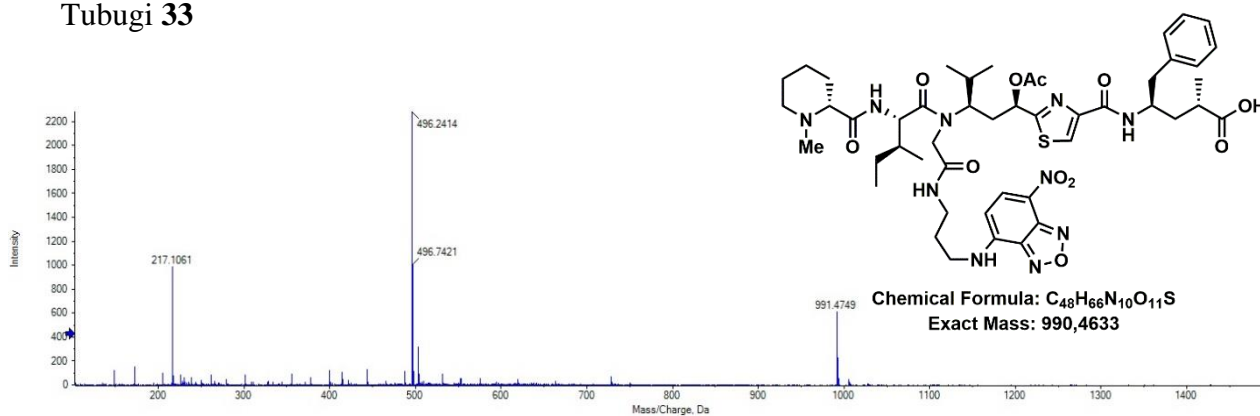
Figure A42. ESI-HRMS of Tubugi **33**.
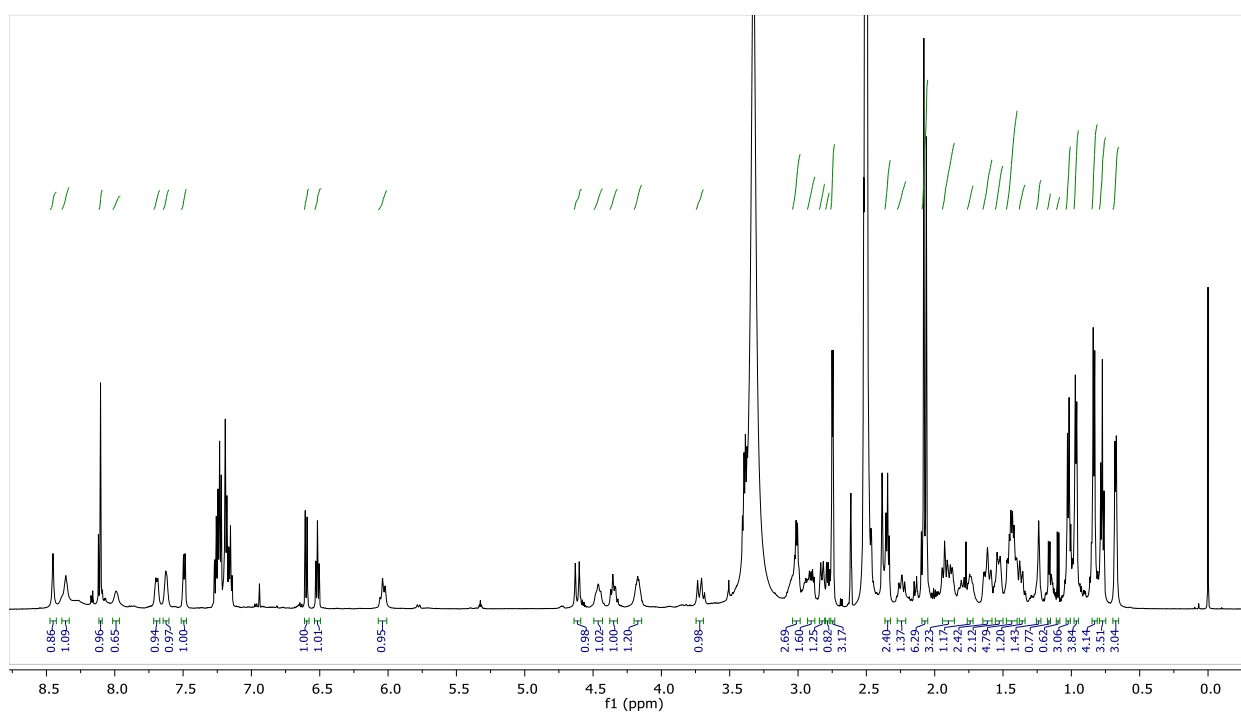
Figure A43. ^{1}H NMR (400 MHz, DMSO-*d*6) spectrum of Tubugi **33**.

Tubugi **39**
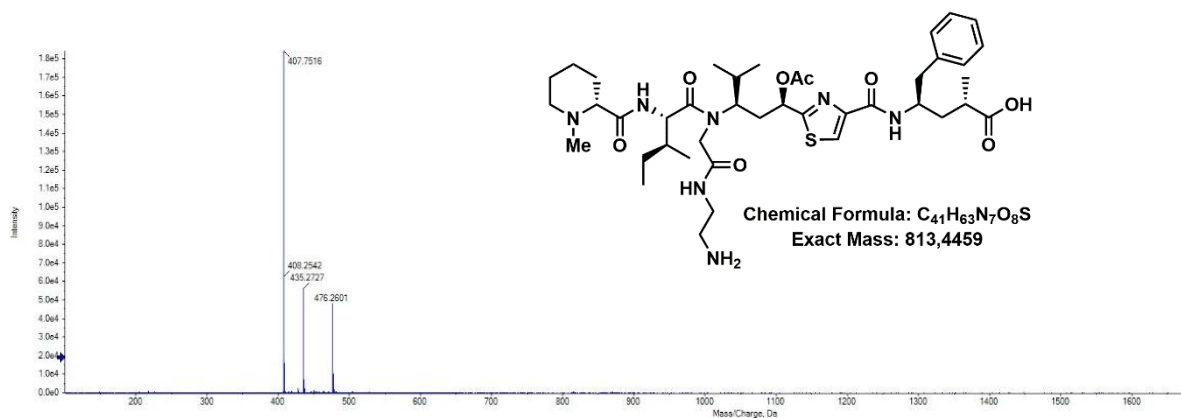
Figure A44. ESI-HRMS of Tubugi **39**.
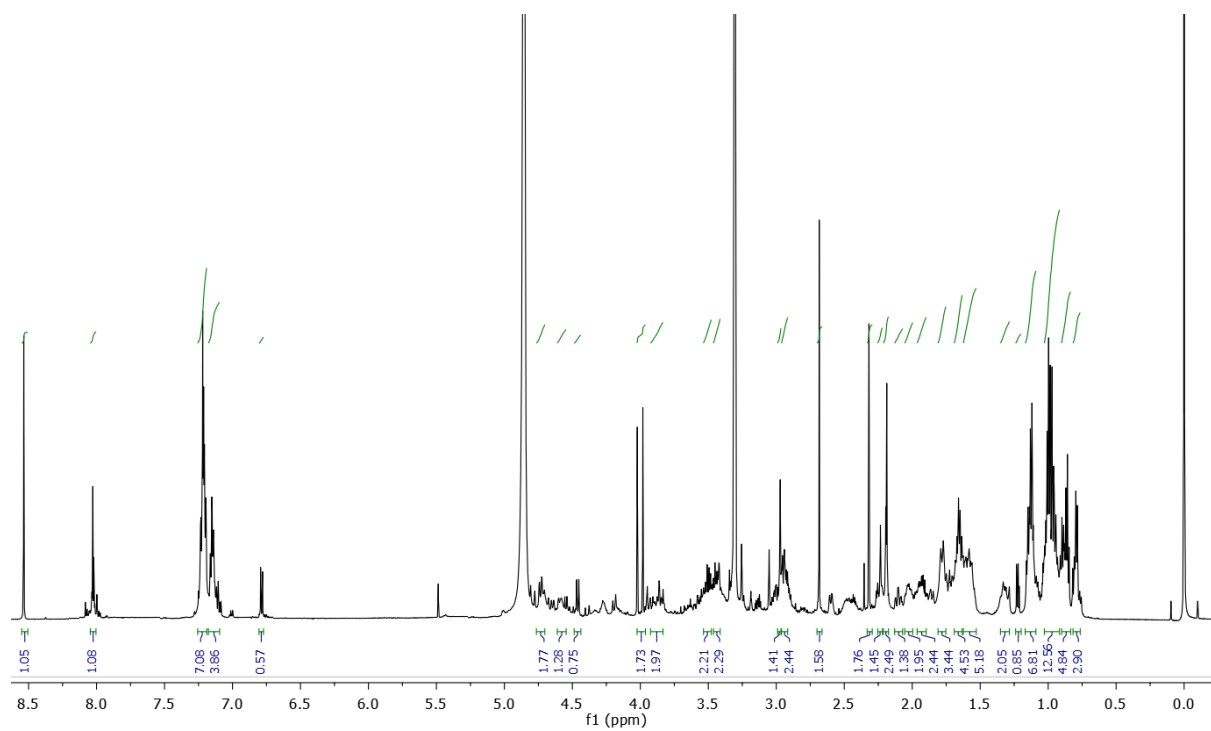
Figure A45. ^{1}H NMR (400 MHz, DMSO-*d*6) spectrum of Tubugi **39**.

Tubugi **40**
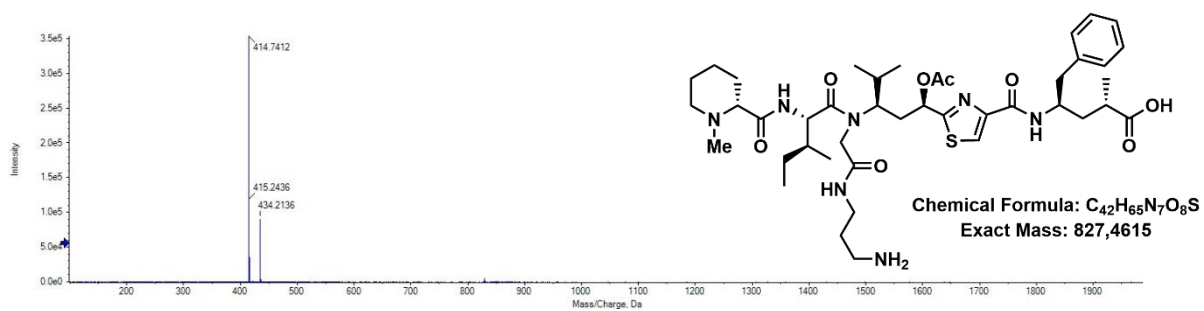
Figure A46. ESI-HRMS of Tubugi **40**.
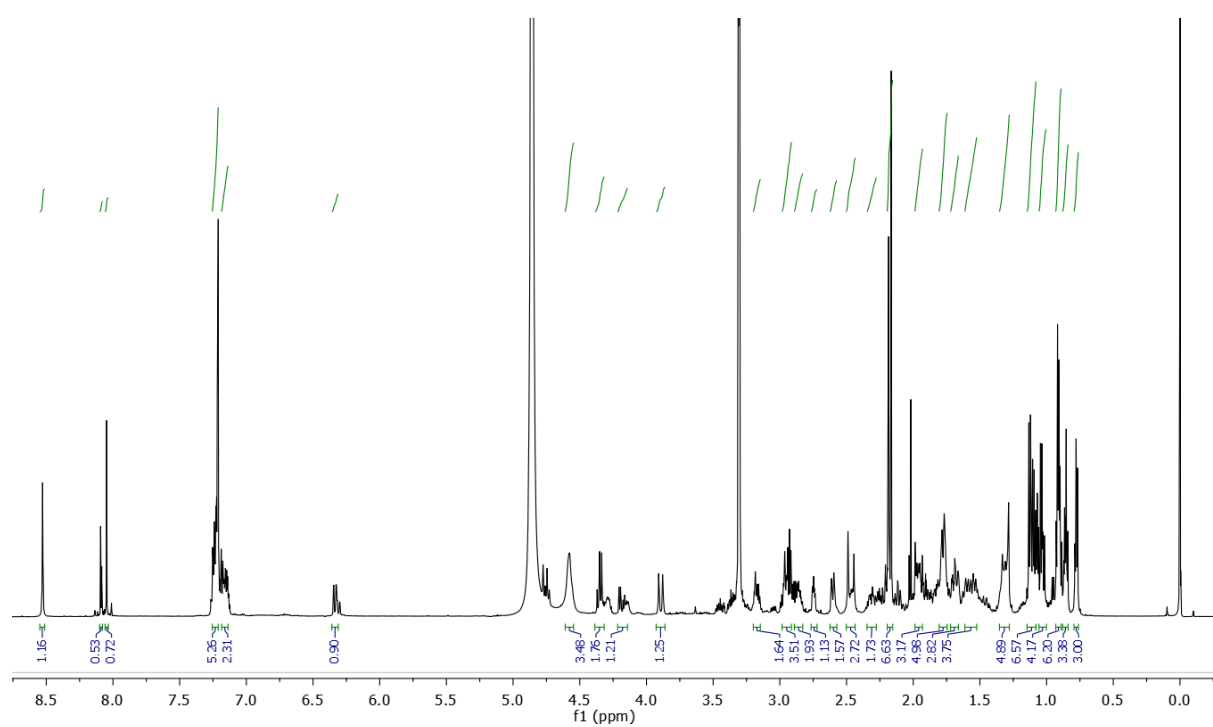
Figure A47. ¹H NMR (400 MHz, DMSO-*d*6) spectrum of Tubugi **40**.

Tubugi **41**
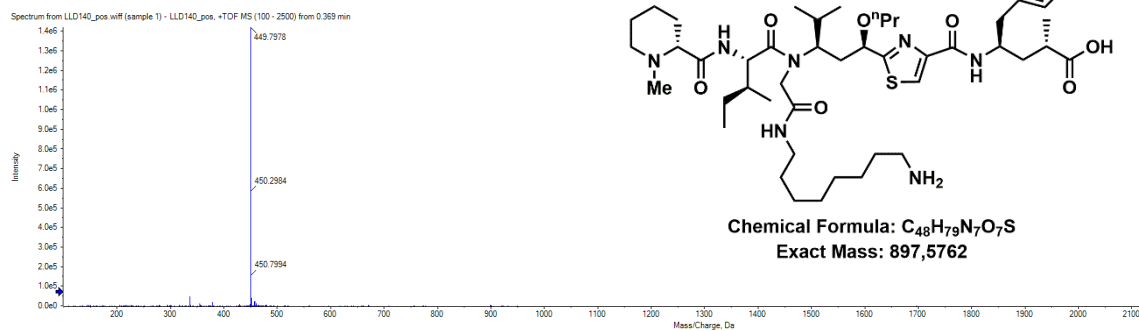
Figure A48. ESI-HRMS of Tubugi **41**.
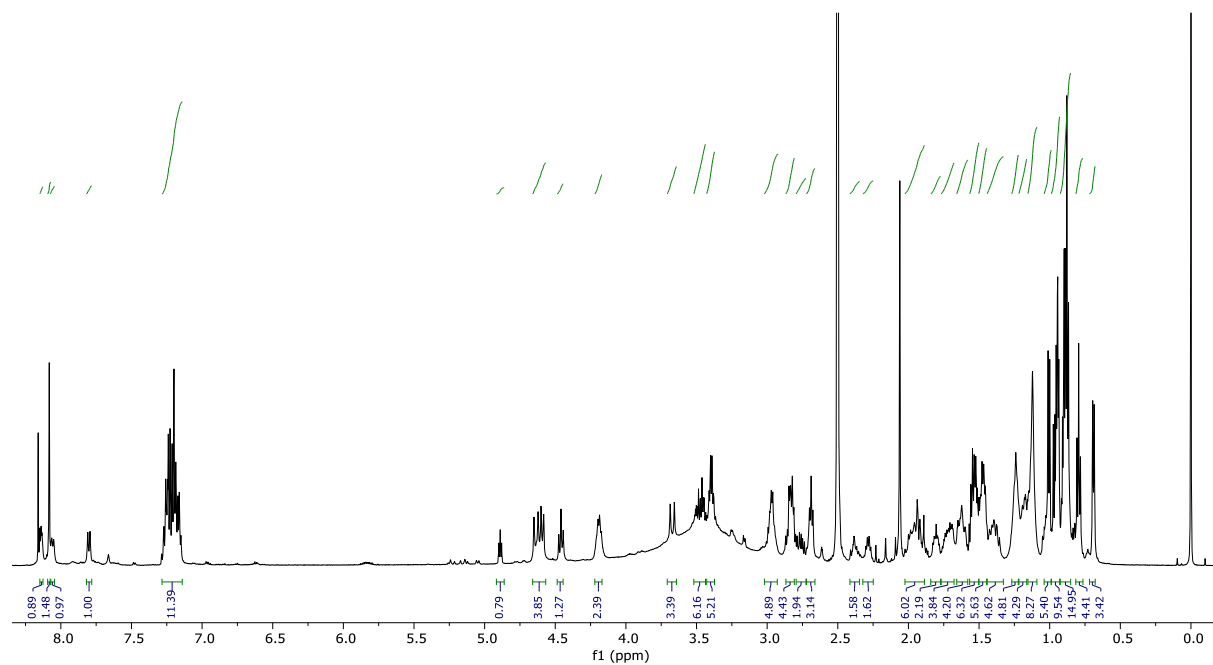
Figure A49. ^{1}H NMR (400 MHz, DMSO-d6) spectrum of Tubugi **41**.

Tubugi **42**
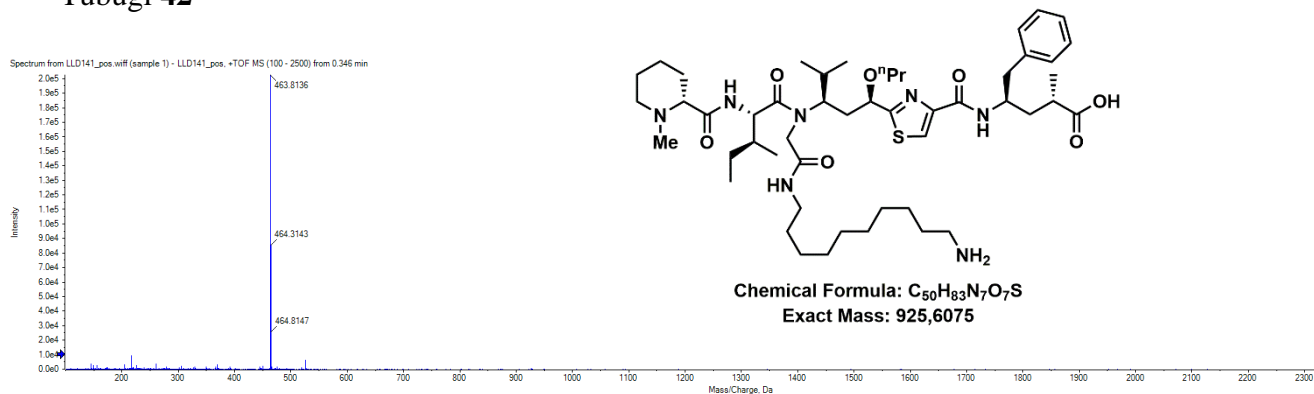
Figure A50. ESI-HRMS of Tubugi **42.**
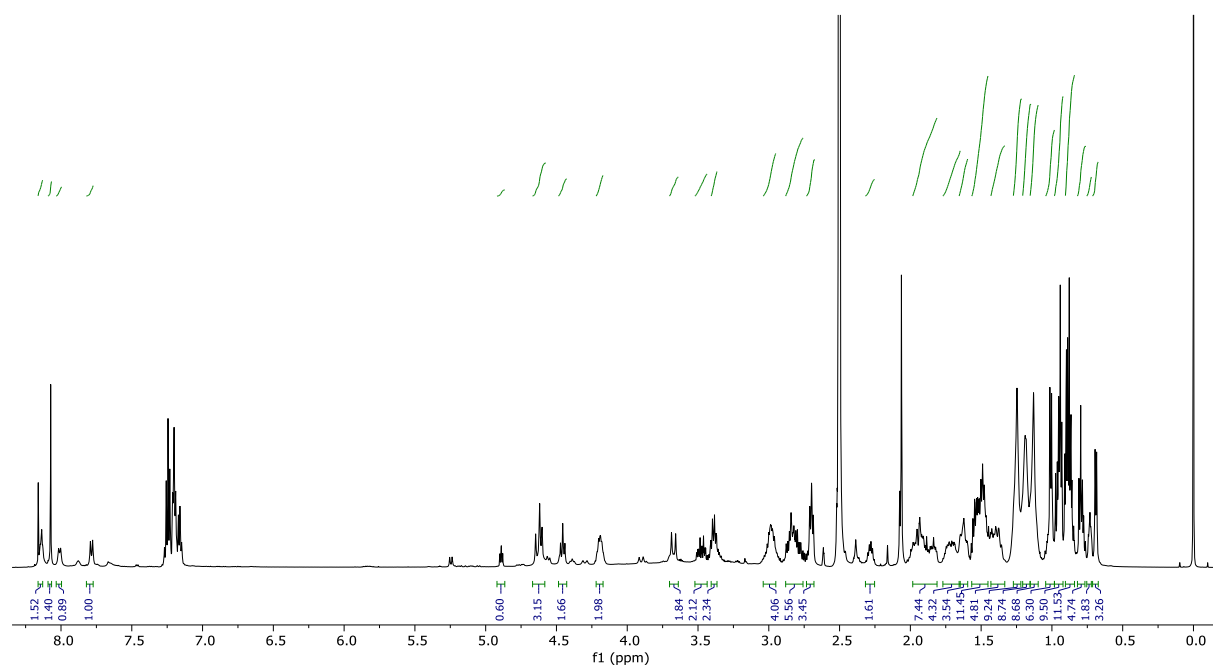
Figure A51. ^{1}H NMR (400 MHz, DMSO-*d*6) spectrum of Tubugi **42**.

Tubugi **43**
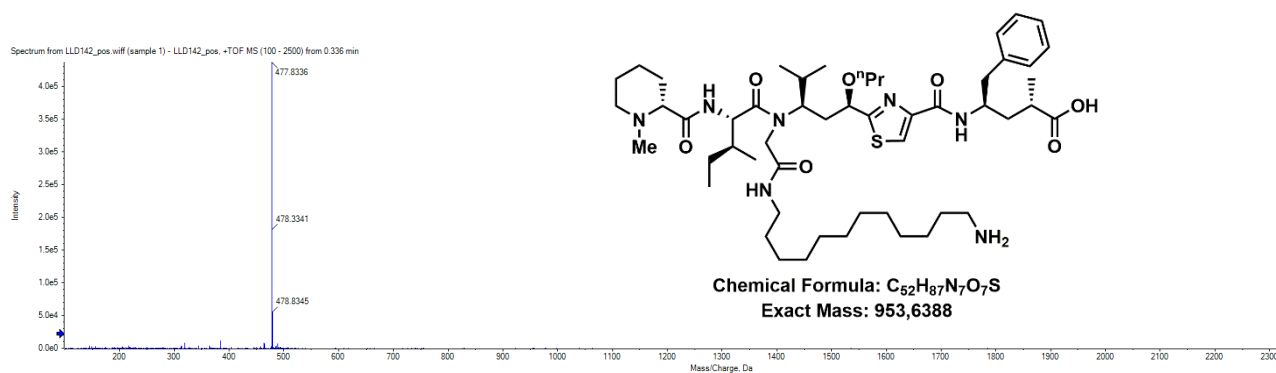
Figure A52. ESI-HRMS of Tubugi **43**.
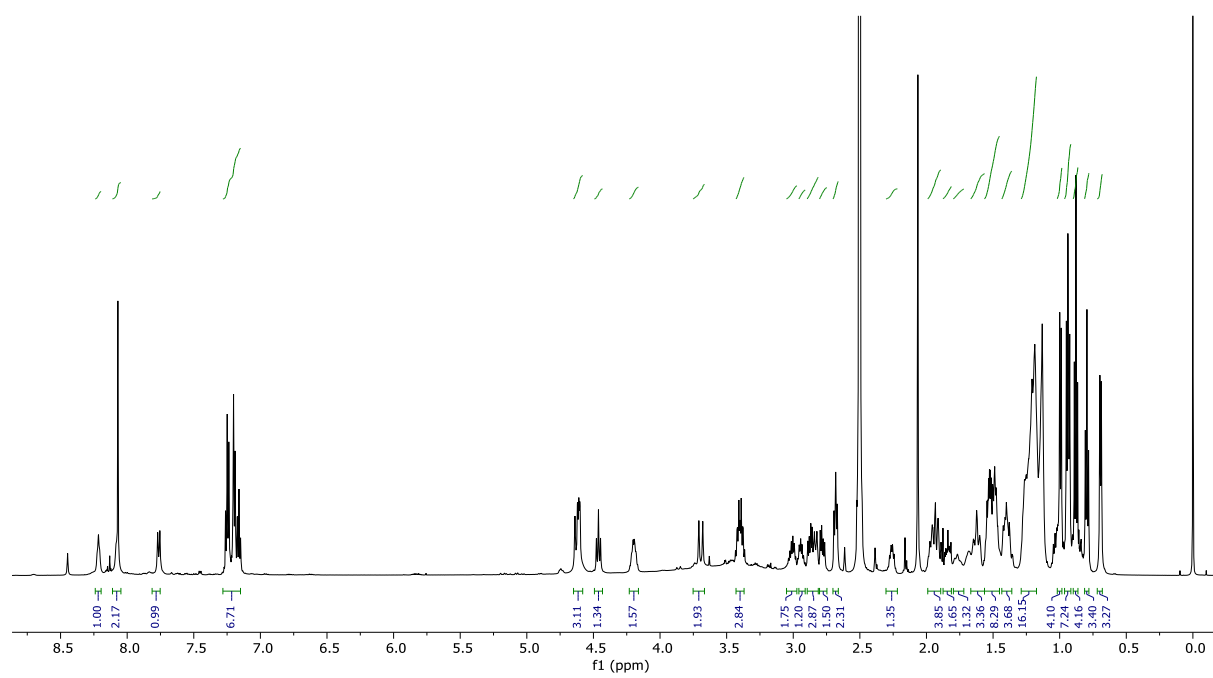
Figure A53. ^{1}H NMR (400 MHz, DMSO-*d*6) spectrum of Tubugi **43**.

Tubugi **46**
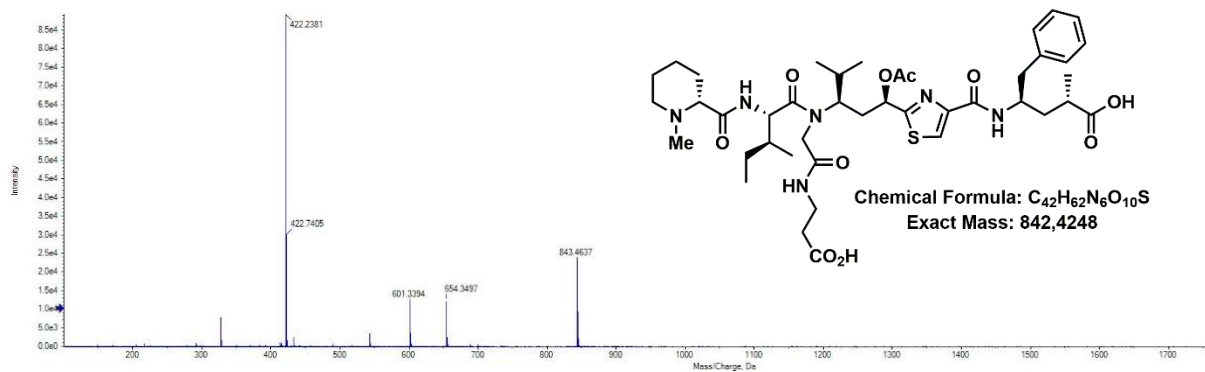
Figure A54. ESI-HRMS of Tubugi **46**.
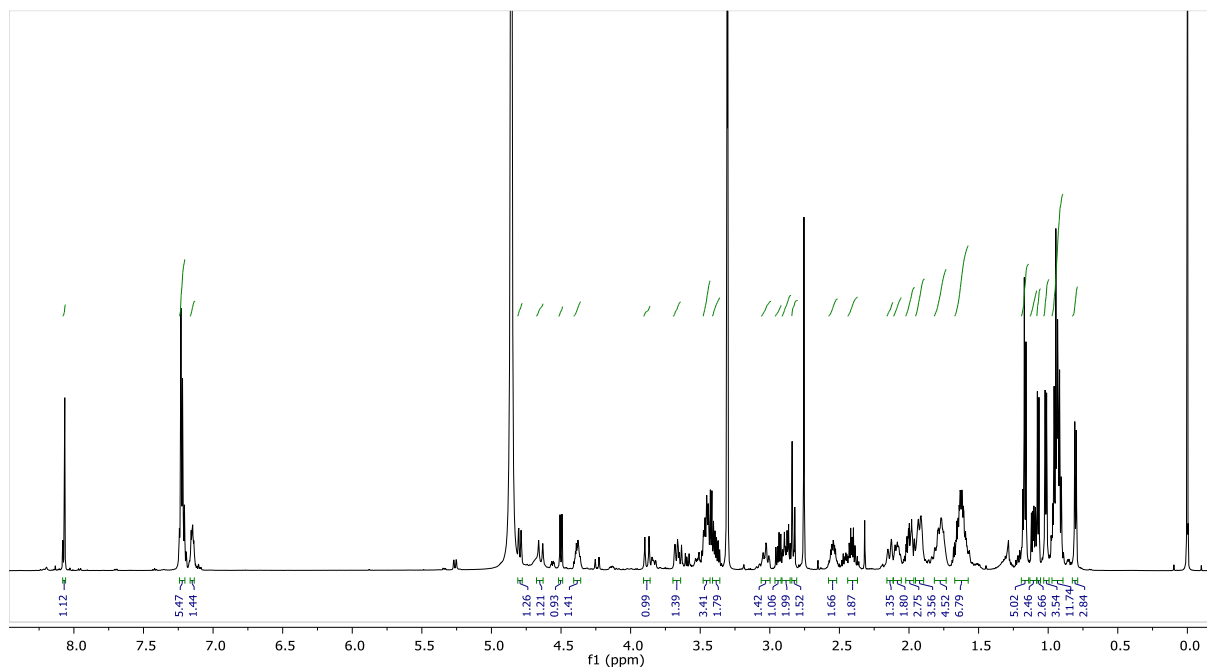
Figure A55. ^{1}H NMR (400 MHz, DMSO-*d*6) spectrum of Tubugi **46.**

Tubugi **47**
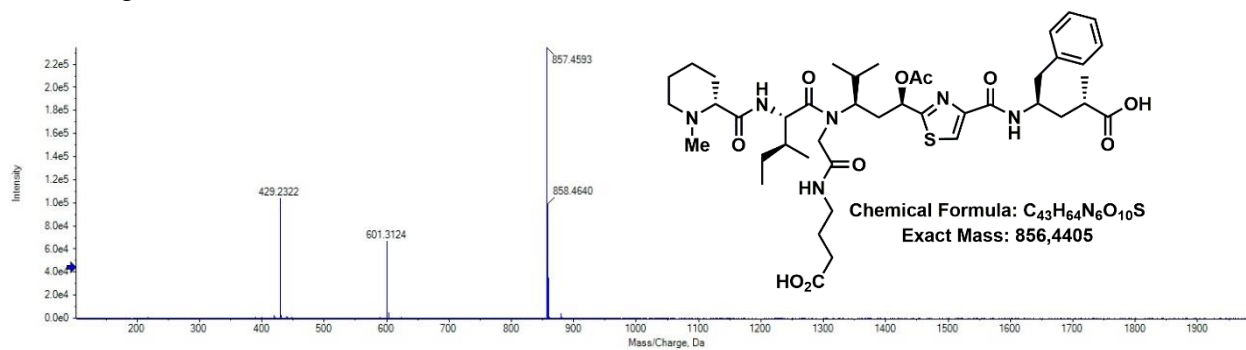
Figure 56. ESI-HRMS of Tubugi **47**.
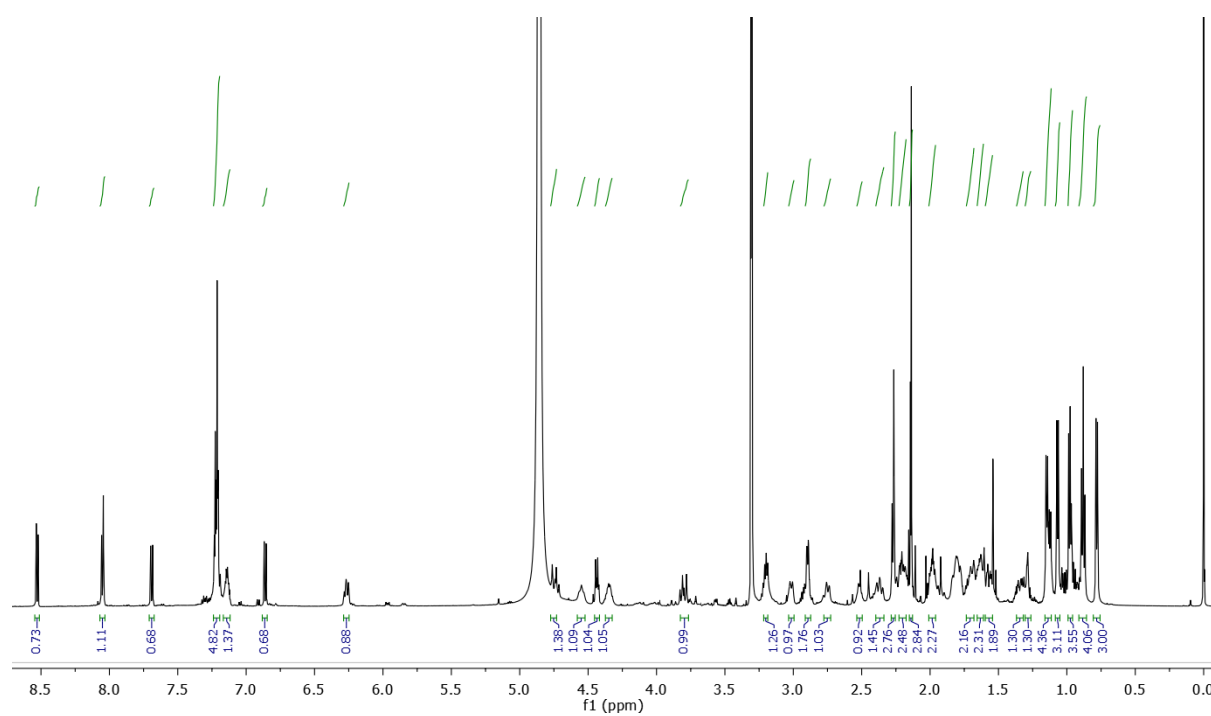
Figure A57. ^{1}H NMR (400 MHz, DMSO-*d*6) spectrum of Tubugi **47**.

Tubugi **51**
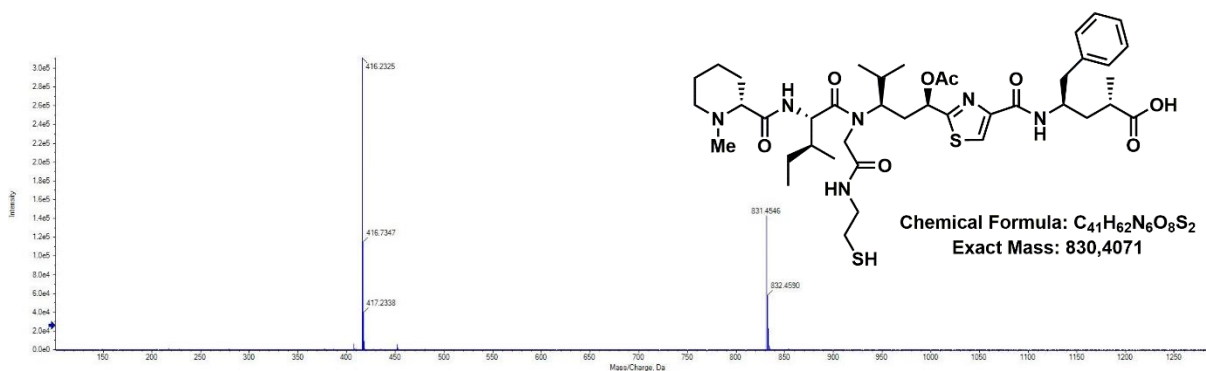
Figure A58. ESI-HRMS of Tubugi **51**.
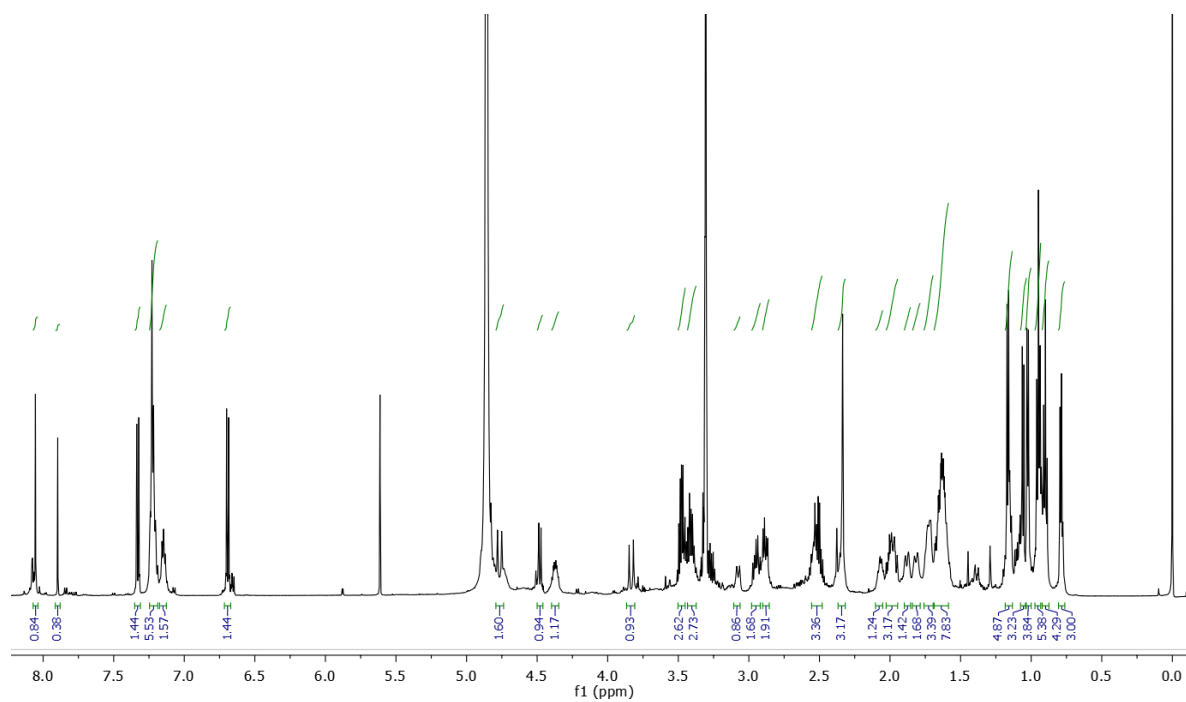
Figure A59. ¹H NMR (400 MHz, DMSO-*d*6) spectrum of Tubugi **51**.

Tubugi **52**
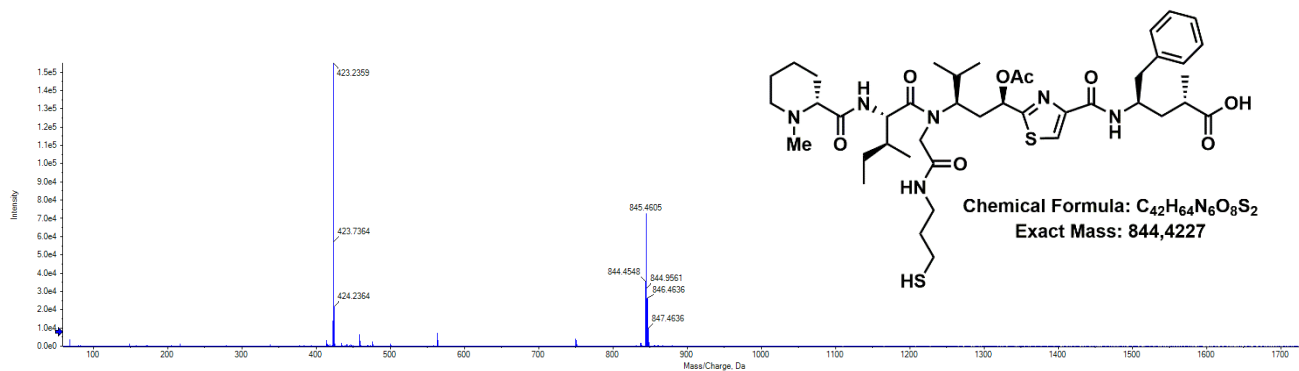
Figure A60. ESI-HRMS of Tubugi **52**.
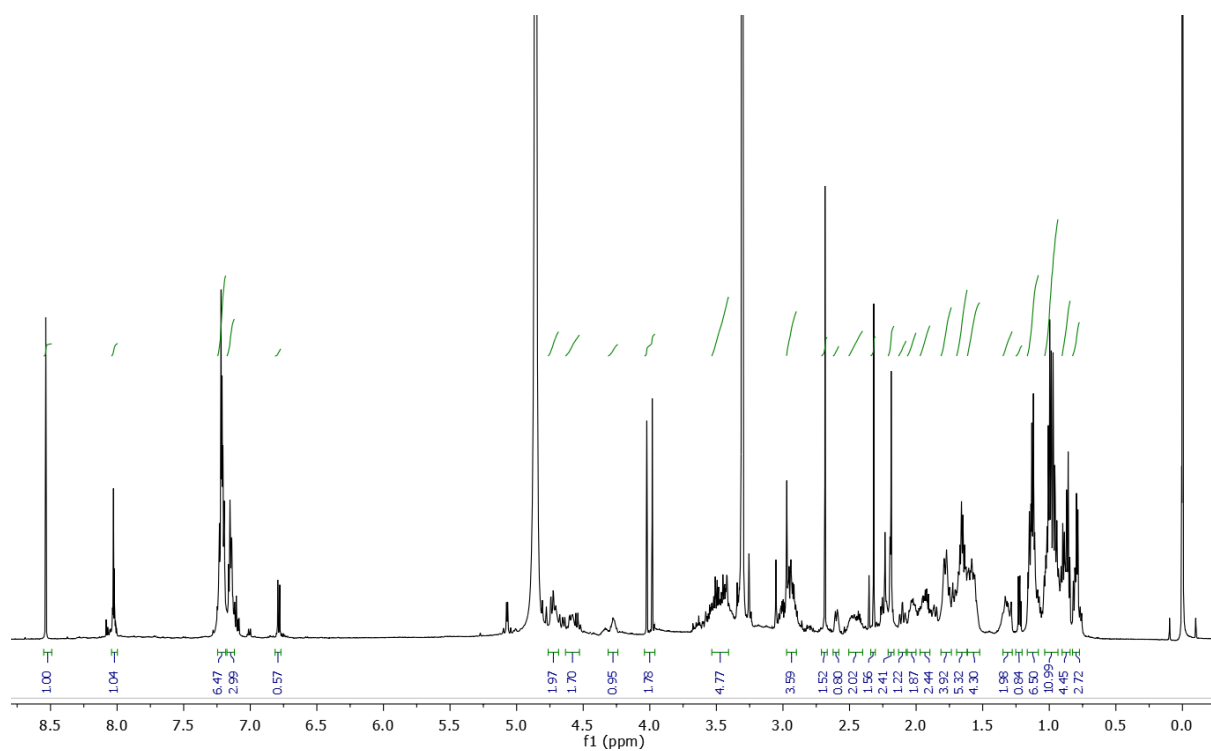
Figure A61. ^{1}H NMR (400 MHz, DMSO-*d*6) spectrum of Tubugi **52**.

Tubugi **53**

Figure A62. ESI-HRMS of Tubugi **53**.

Figure A63. ^{1}H NMR (400 MHz, DMSO-*d*6) spectrum of Tubugi **53**.

A3. RP-HPLC trace and HR-MS spectrum of Bombesin peptides and conjugates

Bombesin peptide **56**

Chemical Formula: $C_{61}H_{90}N_{18}O_{13}S_3$
Exact Mass: 1378,6097
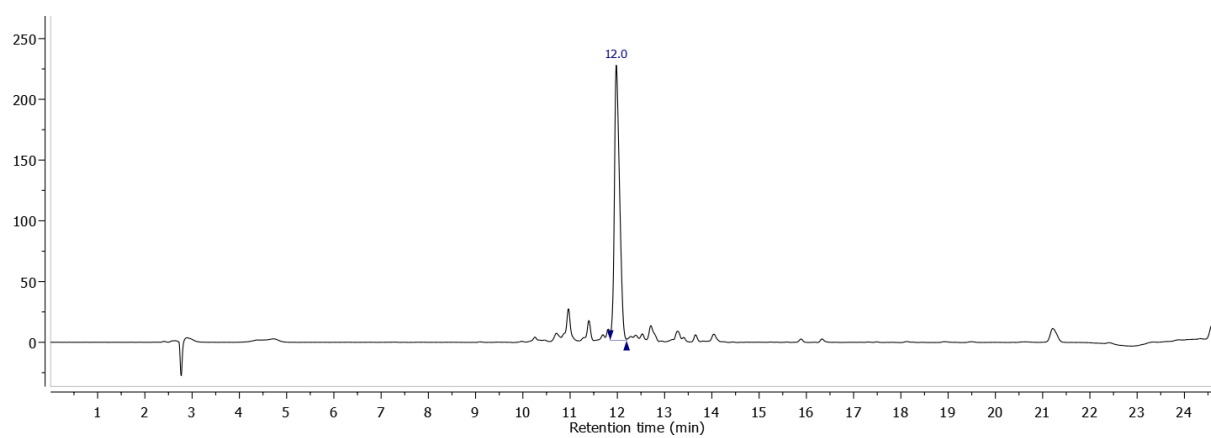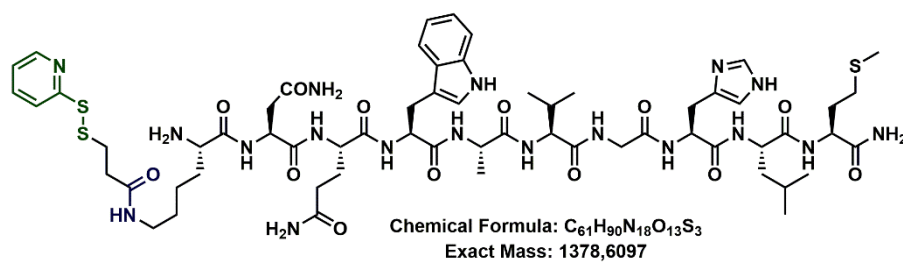
Figure A64. RP-HPLC trace of crude Bombesin peptide **56**.
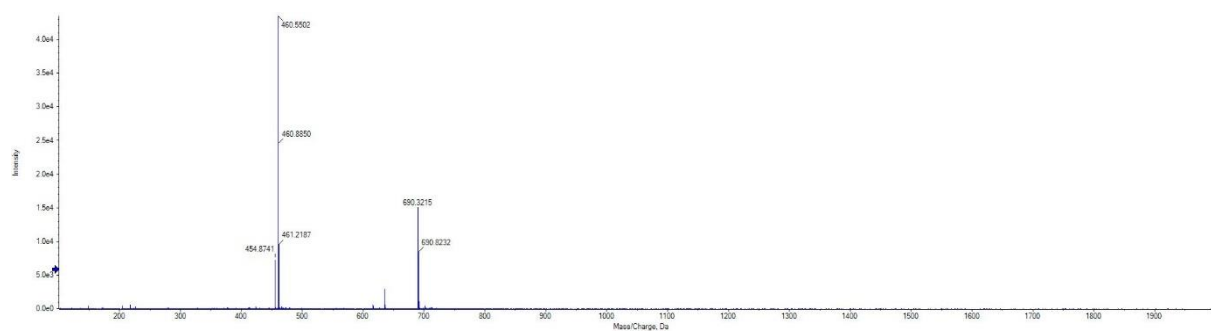
Figure A65. ESI-HRMS of Bombesin peptide **56**.

XXXIV

Bombesin peptide **57**

Chemical Formula: $C_{78}H_{123}N_{19}O_{14}S_3$
Exact Mass: 1645,8659
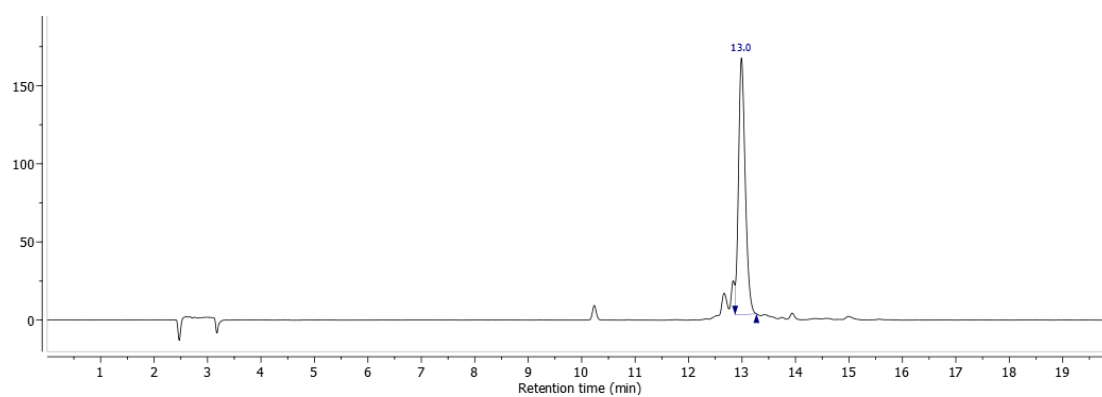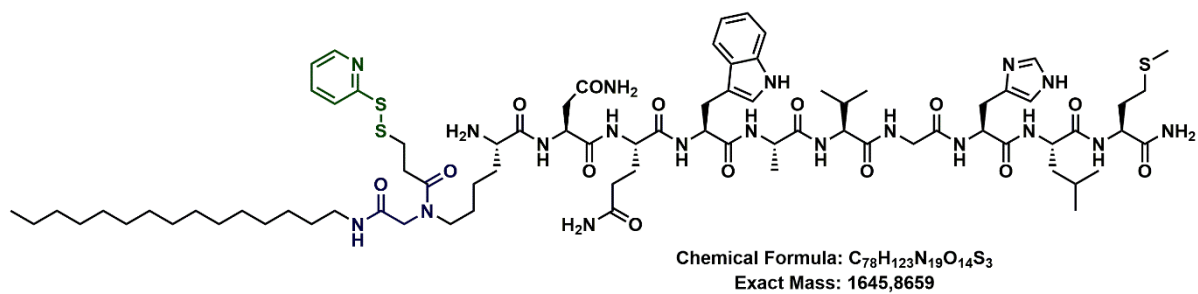
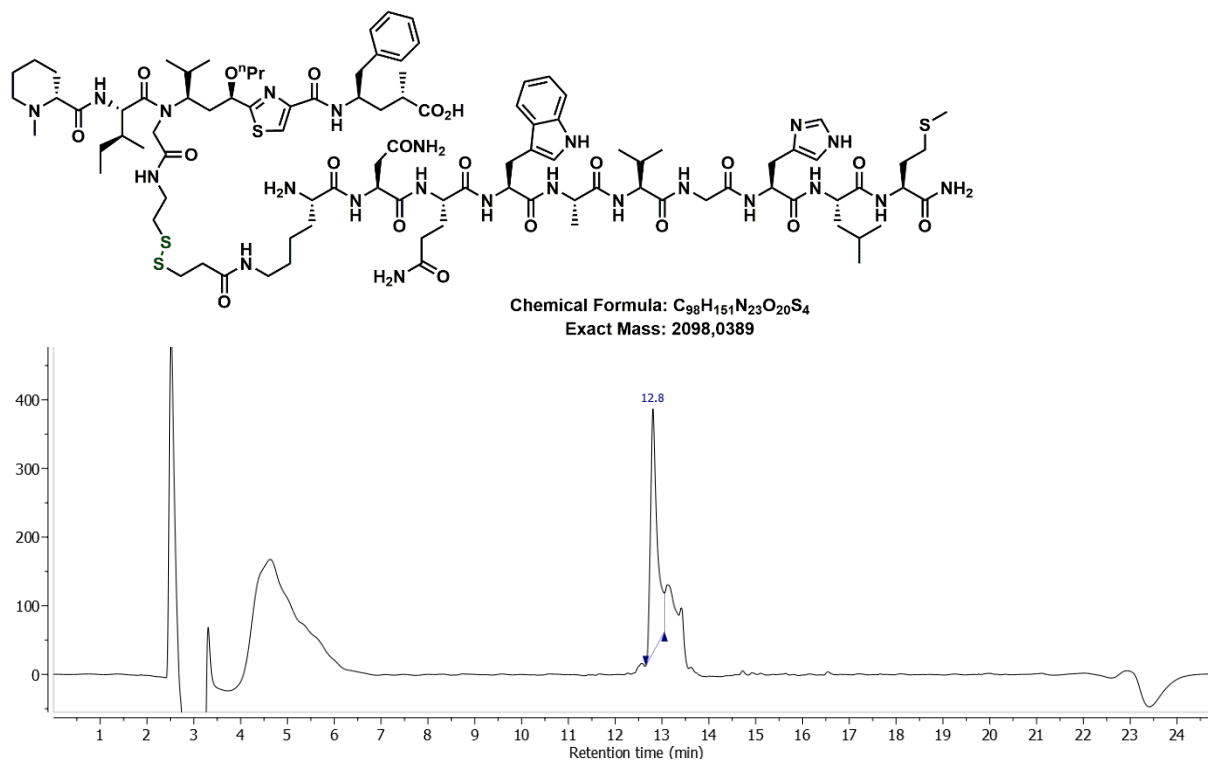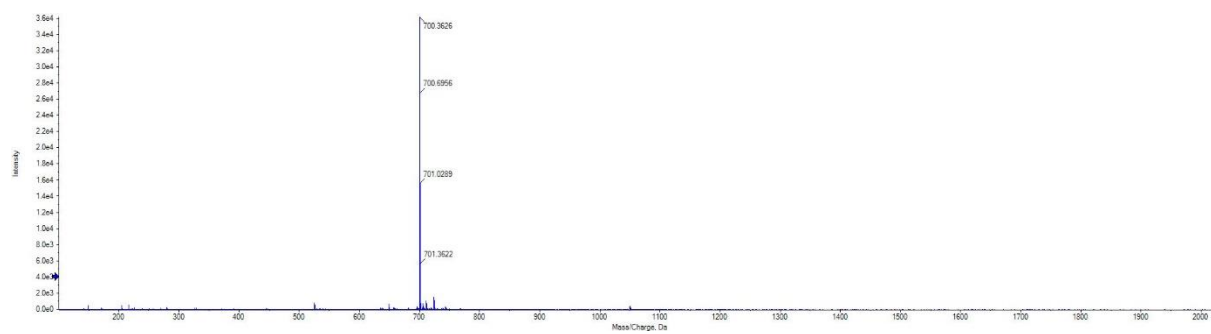**Figure A66**. RP-HPLC trace of the pure bombesin peptide **57**.
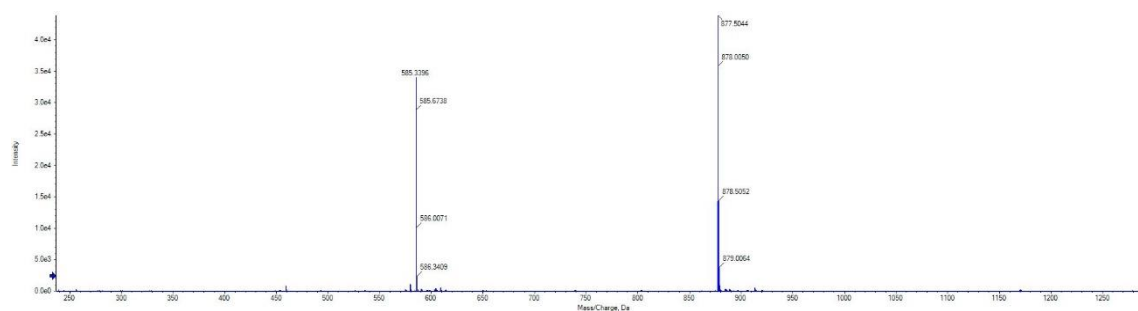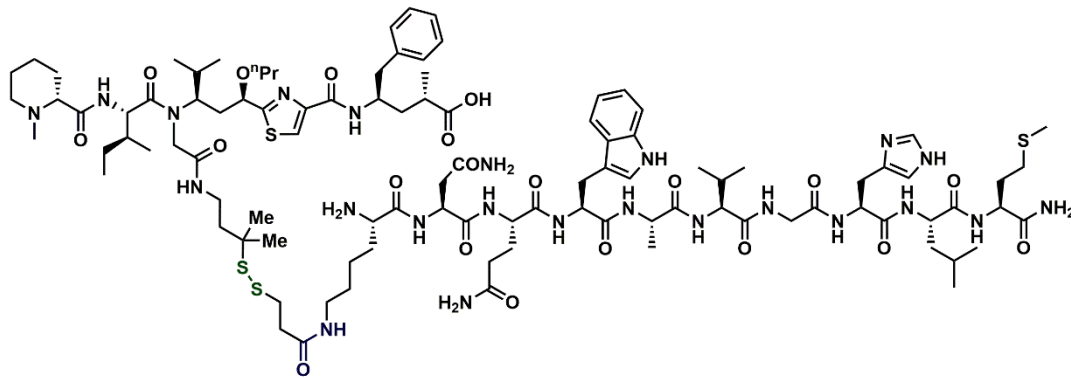

Figure A67. ESI-HRMS of Bombesin peptide **5**7.

Conjugate **58**

Figure A68. RP-HPLC trace of the pure bombesin peptide **58**.

Figure A69. ESI-HRMS of Bombesin peptide **58**.

Conjugate **59**

Chemical Formula: $C_{101}H_{157}N_{23}O_{20}S_4$
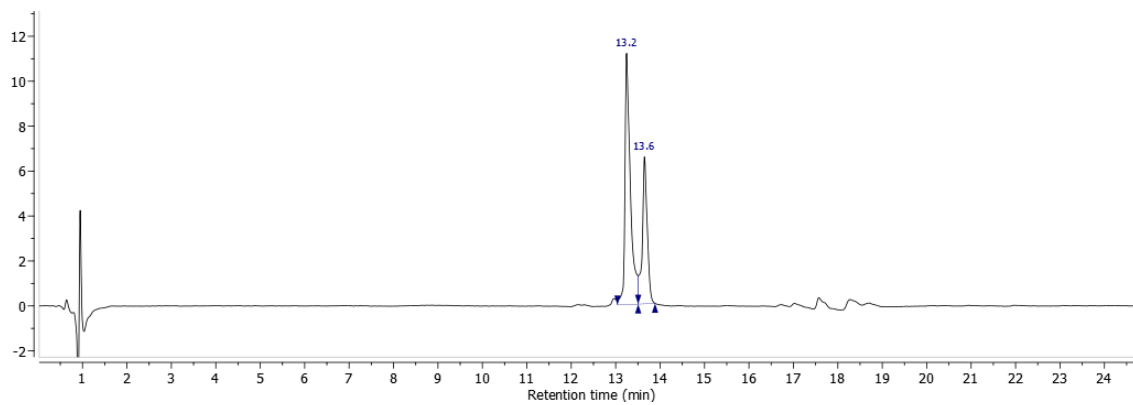**Exact Mass:** 2140,0858

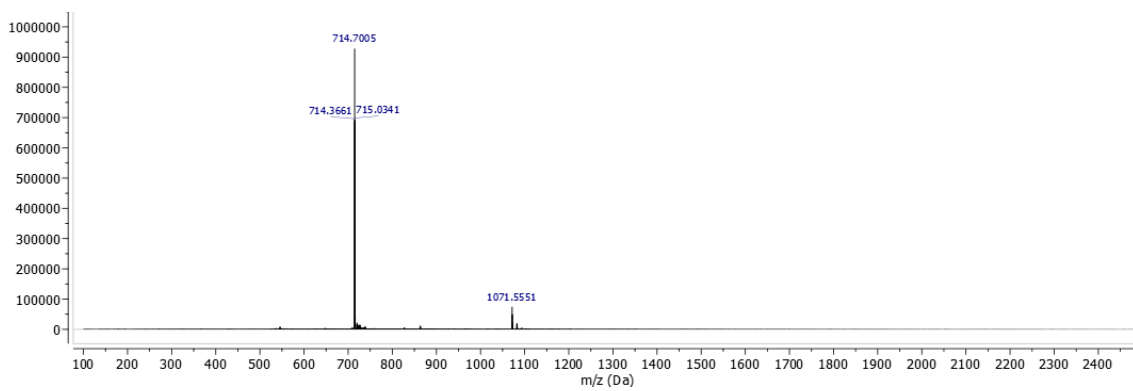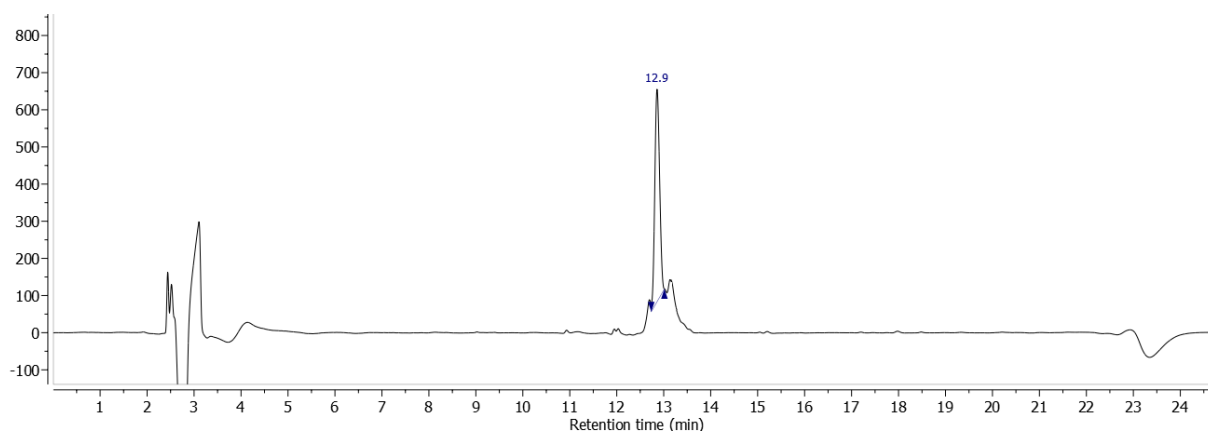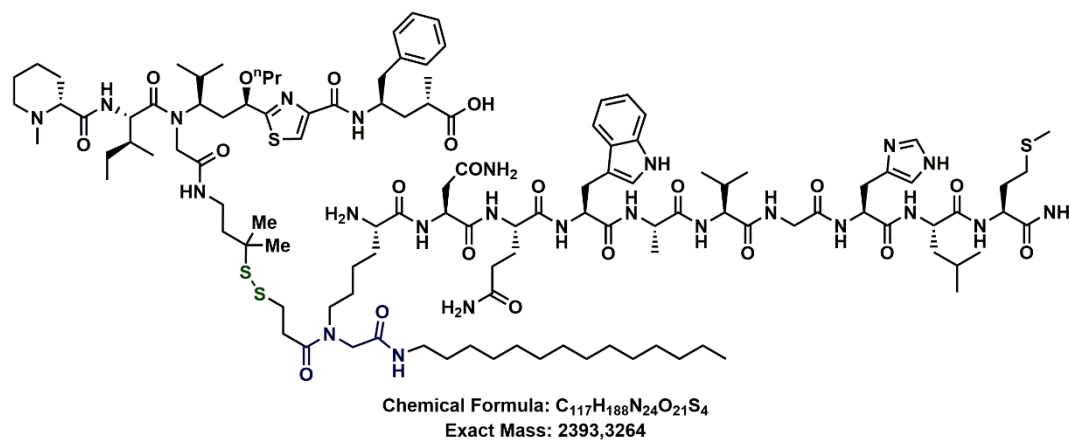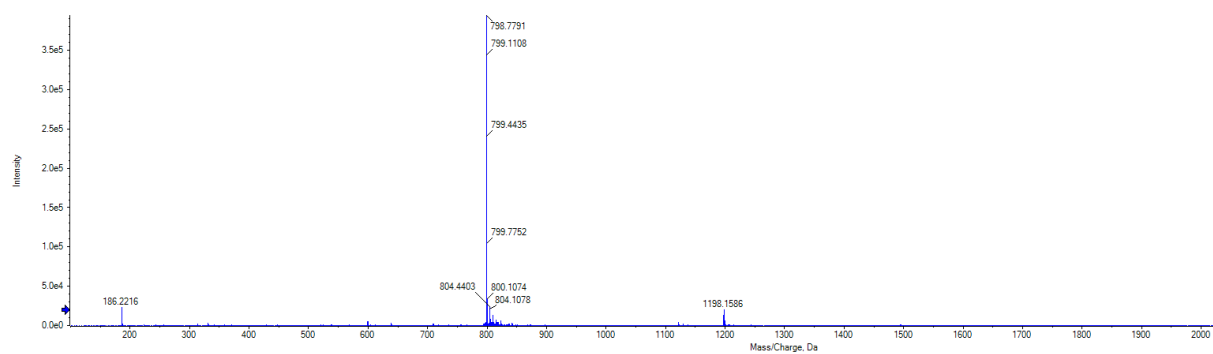**Figure A70**. RP-HPLC trace of the pure bombesin peptide **59**.

FigureA71. ESI-HRMS of tubugi-bombesin conjugate **59**.

Conjugate **60**

Chemical Formula: $C_{117}H_{188}N_{24}O_{21}S_4$
Exact Mass: 2393,3264

Figure A72. RP-HPLC trace of the pure bombesin peptide **60**.

Figure A73. ESI-HRMS of tubugi-bombesin conjugate **60**.

DAYMA LLANES MARTINEZ

Date and place of birth: June 18, 1991. Havana, Cuba
Nationality: Cuban
Email: daymallanes@gmail.com

EDUCATIONAL BACKGROUND

09.2018-10.2022
PhD student

Leibniz-Institut für Pflanzenbiochemie, Halle, Germany

Supervisor: Prof. Dr. Ludger Wessjohann

Project: Synthesis, conjugation, and biological evaluation of new N-functionalized tubugis

02.2015-06.2017
Master

Faculty of Chemistry, University of Havana, Cuba

Supervisor: Prof. Dr. Leslie Reguera Núñez

Project: Synthesis and structural characterization of hexacyanuroferrates (III) mixed

with potential applications in electrochemical biosensors

09.2009-06.2014
Diploma
(BSc+MSc)

Faculty of Chemistry, University of Havana, Cuba

Supervisors: Dr. Pedro Ortíz del Toro

Project: Synthesis of potential liquid crystals based on the Naphtylazobencene system

WORKING EXPERIENCE

09.2018-10.2022
PhD student

Leibniz-Institut für Pflanzenbiochemie - IPB Halle, Germany

Main activities developed:

1- Retrosynthetic analysis and synthetic design of natural molecules

2- Automated and manual solid-phase peptide synthesis

3- Combinatorial chemistry

4- Peptide derivatization by multicomponent and cross-coupling reactions (e. g. Ugi-4CR, Click and Sonogashira)

5-Characterization and structural analysis by HPLC, MS, IR, and NMR

6-Analysis and interpretation of biological assays (anticancer and antimicrobial)

7-Proficient skills in MestreNova, Chemdraw, Origin, and SigmaPlot softwares

8- Scientific writing of projects, reports and articles

04.2015-02.2017

SolMed Laboratories Company, BioCubaFarma. Havana, Cuba.

Specialist A on Industrial Processes for generic drug manufacturing.

Main activities developed:

1- Process validation in accordance with regulatory and GMP guidelines

2- Access to a robust system to manage the product lifecycle

	3- Seamless execution for right-the-first-time delivery
	4- Quality management
09.2014-03.2015	**SolMed Laboratories Company, BioCubaFarma. Havana, Cuba**
	Training as Type A Specialist on Industrial Processes for Generic Drug Manufacturing
01.2011-06.2011	**Finlay Institute of Vaccines, BioCubaFarma. Havana, Cuba**
	Internship in Cuban Biotechnological Industry

PUBLICATIONS

▪ Dube, M.; **Llanes, D**.; (…); Arnold, A. Albatrellus confluens (Alb. & Schwein.) Kotl. & Pouz.: Natural Fungal Compounds and Synthetic Derivatives with In Vitro Anthelmintic Activities and Antiproliferative Effects against Two Human Cancer Cell Lines. *Molecules*. **2022**, 27, 2950-2966

▪ Peralta, Y. M.; **Llanes, D**.; Reguera, L.; (…); Antuch, M. "Mixed $Ni2^+Co^{2+}$ Transition Metal Nitroprusside: Determination of Its Electrochemical Behavior and Electrocatalytic Activity towards the Oxidation of Phenylhydrazine". *ChemistrySelect*. **2022**, 7, 1-11

▪ Ricardo, M. G.; Schwark, M.; **Llanes, D.;** Niedermeyer, T. H. J.; Westerman, B. "Total Synthesis of Aetokthonotoxin, the Cyanobacterial Neurotoxin Causing Vacuolar Myelinopathy" *Chem. Eur. J*. **2021**, 27, 12032 –12035

▪ Ricardo, M. G.; **Llanes, D**.; Wessjohann, L. A. and Rivera, D. G. "Introducing the Petasis Reaction for the Late-Stage Multicomponent Diversification, Labeling, and Stapling of Peptides". *Angew. Chem Int. Ed*., **2019**, 58, 2700-2704

▪ Antuch, M.; Peralta, Y. M.; **Llanes, D**.; Reguera, L. "Bimetallic Co^{2+} and Mn^{2+} Hexacyanoferrate for Hydrogen Peroxide Electrooxidation and Its Application in a Highly Sensitive Cholesterol Biosensor". *ChemElectroChem*. **2019**. 6, 1567–1573